

CHARACTERIZATION OF LEISHMANIA RNA VIRUS INFECTED  
*LEISHMANIA MAJOR* EXOSOMES AND EVALUATION OF THE IMPACT OF  
CYTOSOLIC DNA SENSING RELATED PATHWAYS IN *L. MAJOR*  
INFECTION

A THESIS SUBMITTED TO  
THE GRADUATE SCHOOL OF NATURAL AND APPLIED SCIENCES  
OF  
MIDDLE EAST TECHNICAL UNIVERSITY

BY

İSMAİL CEM YILMAZ

IN PARTIAL FULFILLMENT OF THE REQUIREMENTS  
FOR  
THE DEGREE OF DOCTOR OF PHILOSOPHY  
IN  
BIOLOGY

JANUARY 2020



Approval of the thesis:

**CHARACTERIZATION OF LEISHMANIA RNA VIRUS INFECTED  
LEISHMANIA MAJOR EXOSOMES AND EVALUATION OF THE  
IMPACT OF CYTOSOLIC DNA SENSING RELATED PATHWAYS IN L.  
MAJOR INFECTION**

submitted by **İSMAİL CEM YILMAZ** in partial fulfillment of the requirements for the degree of **Doctor of Philosophy in Biology Department, Middle East Technical University** by,

Prof. Dr. Halil Kalıpçılar  
Dean, Graduate School of **Natural and Applied Sciences**

\_\_\_\_\_

Prof. Dr. Ayşegül Gözen  
Head of Department, **Biology**

\_\_\_\_\_

Prof. Dr. Mayda Gürsel  
Supervisor, **Biology, METU**

\_\_\_\_\_

\_\_\_\_\_

**Examining Committee Members:**

Prof. Dr. Mesut Muyan  
Biological Sciences, METU

\_\_\_\_\_

Prof. Dr. Mayda Gürsel  
Biology, METU

\_\_\_\_\_

Prof. Dr. Ayşen Tezcaner  
Faculty of Engineering, METU

\_\_\_\_\_

Assist. Prof. Dr. Serkan Belkaya  
Molecular Biology and Genetics, Bilkent University

\_\_\_\_\_

Assoc. Prof. Dr. Yasemin Özsürekcı  
Infectious Diseases, Hacettepe University

\_\_\_\_\_

Date: 31.01.2020

**I hereby declare that all information in this document has been obtained and presented in accordance with academic rules and ethical conduct. I also declare that, as required by these rules and conduct, I have fully cited and referenced all material and results that are not original to this work.**

Name, Surname: İsmail Cem Yılmaz

Signature:

## ABSTRACT

### **CHARACTERIZATION OF LEISHMANIA RNA VIRUS INFECTED *LEISHMANIA MAJOR* EXOSOMES AND EVALUATION OF THE IMPACT OF CYTOSOLIC DNA SENSING RELATED PATHWAYS IN *L.* *MAJOR* INFECTION**

Yılmaz, İsmail Cem  
Doctor of Philosophy, Biology  
Supervisor: Prof. Dr. Mayda Gürsel

January 2020, 161 pages

Leishmaniasis is a neglected infectious disease caused by *Leishmania* parasite. The disease represents a significant health problem, necessitating urgent development of effective treatment strategies. New World *Leishmania* species harboring Leishmania RNA virus (LRV) cause severe, metastatic disease. In this thesis, we compared LRV2-1 deficient and proficient Old World *L. major* strains in terms of their exosomal content and infectivity. PCR and mass spectrometry based analysis revealed that virus infected *Leishmania* exosomes contained at least 64% of the viral RNA but not the viral proteins. LRV2-1 positive and negative *L. major* strains had similar infectivity in macrophages, the positive strain exhibited delayed infection in a cutaneous leishmaniasis model in mice. Next, we aimed to investigate the role of cGAS-STING DNA sensing pathway in *Leishmania* infection. Infection rates in STING and TBK-1 knockout cell lines were significantly lower than wild type THP-1 cells and this difference was related to decreased phagocytic capacities of the knockout lines. Effect of the TBK1 inhibitor amlexanox was investigated in *in vitro* and *in vivo* infection models. The drug blocked parasite phagocytosis in macrophages and delayed footpad swelling in parasite infected mice, suggesting that amlexanox could be of interest as a candidate drug in cutaneous leishmaniasis treatment. We also aimed to determine the

role of ISG15 in *L. major* infection and autophagy by mutating the ISG15 using a LentiCRISPRv2 system. Our findings revealed a pro-parasitic role of ISG15 in early stages of *Leishmania* infection. Furthermore, we found that autophagy was enhanced in ISG15 KO cells, suggesting a regulatory role for ISG15 in autophagy. Collectively, our findings might benefit future work related to *Leishmania* immunity in defining new targets and developing effective treatment strategies.

Keywords: Leishmania RNA virus, Leishmania, amlexanox, ISG15, cGAS, STING, TBK-1, exosome, autophagy

## ÖZ

### **LEISHMANIA RNA VİRUS İLE ENFEKTE *LEISHMANIA MAJOR* EKSOZOMLARININ KARAKTERİZASYONU VE *L. MAJOR* ENFEKSİYONUNDA SİTOSOLİK DNA ALGILAMA İLE ALAKALI YOLAKLARIN ETKİSİNİN DEĞERLENDİRİLMESİ**

Yılmaz, İsmail Cem  
Doktora, Biyoloji  
Tez Danışmanı: Prof. Dr. Mayda Gürsel

Ocak 2020, 161 sayfa

Leishmaniasis, *Leishmania* parazitinin neden olduğu ihmal edilmiş bir bulaşıcı hastalıktır. Hastalık, etkili tedavi stratejilerinin acil olarak geliştirilmesini gerektiren önemli bir sağlık sorununu temsil eder. *Leishmania* RNA virüsü (LRV) barındıran Yeni Dünya *Leishmania* türleri ciddi, metastatik hastalıklara neden olur. Bu tezde, LRV2-1 bulunduran ve bulundurmeyen Eski Dünya *L. major* suşlarını eksozom içeriği ve enfektiviteleri açısından karşılaştırdık. PCR ve kütle spektrometri bazlı analizler, virüs bulaşmış *Leishmania* eksozomlarının viral RNA genomunun en az % 64'ünü içerdiğini, ancak viral proteinleri içermediğini ortaya koydu. LRV2-1 pozitif ve negatif *L. major* suşlarının makrofajlarda benzer enfektivitesi olmasına rağmen pozitif suş, farelerde kutanöz leishmaniasis modelinde gecikmiş enfeksiyon sergiledi. Daha sonra *Leishmania* enfeksiyonunda cGAS-STING DNA algılama yolunun rolünü araştırmayı amaçladık. STING ve TBK-1 nakavt hücre hatlarındaki enfeksiyon oranları, vahşi tip THP-1 hücrelerinden önemli ölçüde daha düşüktü ve bu fark nakavt hücre hatlarının fagositik kapasitelerinin azalmasıyla ilgiliydi. Daha sonra, TBK1 inhibitörü amlexanox'un *in vitro* ve *in vivo* enfeksiyon modellerindeki etkisi araştırıldı. İlaç, makrofajlarda parazit fagositozunu azalttı ve parazit enfekte farelerde ayak pedi şişmesini geciktirdi, bu da amlexanox'un kutanöz leishmaniasis tedavisinde

aday bir ilaç olabileceğini düşündürdü. Ayrıca ISG15'i THP-1 hücrelerinde LentiCRISPRv2 sistemi kullanarak mutasyona uğrattık ve ISG15'in *L. major* enfeksiyonunda ve otofajideki rolünü belirlemeye çalıştık. Bulgularımız *Leishmania* enfeksiyonunun erken evrelerinde ISG15'in parazit için olumlu bir rolü olduğunu ortaya koydu. Ayrıca, otofajinin ISG15 KO hücrelerinde arttığını ve ISG15'in otofajide düzenleyici bir rolü olduğunu ortaya koyduk. Sonuç olarak bulgularımız *Leishmania* enfeksiyonunda faydalanılacak ve ilaç hedefi olarak kullanılacak yeni alanlar belirlemesi açısından gelecekteki çalışmalara ışık tutmaktadır.

Anahtar Kelimeler: *Leishmania* RNA virus, *Leishmania*, amlexanox, ISG15, cGAS, STING, TBK-1, eksozom, otofaji

To my beloved wife

## ACKNOWLEDGEMENTS

First of all, I would like to express my deepest gratitude to my supervisor Prof. Mayda Gürsel for her endless contribution to my scientific curiosity and collective work. At each individual step throughout the presented work, she enlightened and eased the path. Discussing the next step and determining new strategies with her were the most educational and joyful moments of my scientific career.

I also want to thank Prof. İhsan Gürsel for his support and mentorship. His organizational management and experimental support taught me how to be a group leader, by caring for the best about each individual student.

I exclusively want to thank my wife, Naz Yılmaz, who is my life and lab partner. Her endless caring and support was and will be the most precious time of my life. Her intellectual contributions and insights to newly recorded data were our first deductions about the topic which became a ritual for us and I thank her for that.

I want to thank the members of my thesis examining committee; Prof. Mesut Muyan, Prof. Ayşen Tezcaner, Assist. Prof. Serkan Belkaya and Assoc. Prof. Yasemin Özsürekcı for their critics and contributions.

Moreover, I want to show my special gratitude to our laboratory's *Leishmania* team: Emre Dünürođlu, Emre Mert İpekođlu and İhsan Cihan Ayanođlu. Especially, I want to express my special thanks to İhsan Cihan Ayanođlu for his contribution to practical establishment of *Leishmania* work in our laboratory. I also want to thank my lab partners, Esin Alpdündar Bulut, Bařak Kayaođlu, Büşranur Geçkin, Yađmur Aydın and members of I.G. group, specifically Muzaffer Yıldırım for their contributions and friendship.

Lastly, I want to express my life long gratitude and love to my family, Ömer Yılmaz, Hatice Yılmaz, İrem Sevgi Yılmaz, Aysan Canver and Naz Yılmaz, again and again.

## TABLE OF CONTENTS

ABSTRACT .....	v
ÖZ .....	vii
ACKNOWLEDGEMENTS .....	x
TABLE OF CONTENTS .....	xi
LIST OF TABLES .....	xvi
LIST OF FIGURES .....	xvii
CHAPTERS	
1. INTRODUCTION .....	1
1.1. Tropical disease: Leishmaniasis .....	1
1.1.1. Life cycle of <i>Leishmania</i> .....	4
1.1.2. Promastigote versus amastigote transition in <i>Leishmania</i> .....	6
1.2. Immunity to <i>Leishmania</i> .....	7
1.2.1. Innate immunity to <i>Leishmania</i> .....	7
1.2.1.1. The role of the complement system in anti-leishmanial immunity .....	7
1.2.1.2. The role of Toll like receptors in anti-leishmanial immunity .....	9
1.2.1.3. The role of Nod like receptors in anti-leishmanial immunity .....	10
1.2.1.4. The role of cGAS-STING cytosolic DNA sensing pathway in parasitic infections .....	11
1.2.2. Adaptive immunity against <i>Leishmania</i> .....	12
1.3. <i>Leishmania</i> RNA virus (LRV) .....	13
1.4. <i>Leishmania</i> extracellular vesicles .....	15
1.4.1. Extracellular vesicles .....	15

1.4.2. <i>Leishmania</i> exosomes.....	15
1.5. <i>Leishmania</i> and autophagy.....	17
1.5.1. Autophagy.....	17
1.5.2. <i>Leishmania</i> induced autophagy.....	18
1.6. Type I interferons and <i>Leishmania</i> infection.....	19
1.7. Medications used for the treatment of leishmaniasis.....	20
1.8. Aims of the thesis.....	20
2. MATERIALS AND METHODS.....	23
2.1. Parasite Culture and Maintenance.....	23
2.2. Isolation of <i>L. major</i> exosomes from cultured parasites.....	23
2.2.1. Isolation of exosomal RNA.....	24
2.2.2. cDNA synthesis.....	25
2.2.3. PCR amplification of LRV 2-1 specific sequences.....	25
2.2.4. Sequencing of PCR amplified LRV 2-1 specific sequences.....	26
2.3. Generation of EGFP-LUC fusion protein-expressing transgenic parasites....	26
2.3.1. Generation of LRV negative transgenic <i>L. major</i> .....	26
2.3.2. Generation of LRV positive transgenic <i>L. major</i> .....	27
2.4. Generation of THP-1 Dual ISG15 Knock out cell line.....	28
2.4.1. Oligo design and cloning.....	28
2.4.2. Lentiviral vector production.....	29
2.4.3. Lentiviral transduction of THP-1 Dual cells.....	30
2.4.4. Confirmation of <i>ISG15</i> knock out clones.....	30
2.5. <i>In vitro</i> infection with transgenic EGFP-LUC expressing <i>L. major</i> .....	31
2.5.1. Cell culture.....	31

2.5.2. Metacyclic parasite preparation for <i>in vitro</i> infection studies .....	32
2.5.3. Detection of infection rates of THP-1 cell lines .....	32
2.5.4. Western Blotting .....	33
2.6. Comparison of infectivity of LRV+ versus LRV- <i>L. major</i> strains in <i>in vivo</i> mouse infection model .....	33
2.6.1. LRV- and LRV+ <i>L. major</i> virulence comparison .....	34
2.6.1.1. IVIS measurements of parasite loads in footpads .....	34
2.6.2. Amlexanox therapy for the LRV- <i>L. major</i> infected mice .....	34
3. RESULTS & DISCUSSION .....	35
3.1. Detection of the Leishmania RNA virus 2-1 (LRV 2-1) in LRV + <i>L. major</i> exosomes .....	35
3.1.1. Analysis of LRV+ <i>L. major</i> exosomes for the presence of LRV2-1 specific RNA .....	37
3.1.2. Analysis of LRV+ <i>L. major</i> exosomes for the presence of LRV2-1 specific proteins.....	43
3.1.2.1. Mass spectrometric analysis of LRV+ <i>L. major</i> exosomes .....	43
3.2. Generation of EGFP-LUC Expressing Transgenic LRV- and LRV+ <i>L. major</i> Strains.....	48
3.2.1. Generation of EGFP-LUC expressing Transgenic LRV- <i>L. major</i> .....	48
3.2.2. Generation of EGFP-LUC expressing Transgenic LRV+ <i>L. major</i> .....	49
3.3. Generation of THP-1 Dual ISG15 Knock out and THP-1 Dual Lentiviral Control (LVC) Cell lines by LentiCRISPR v2 System.....	52
3.4. Assessment of <i>in vitro</i> infection rates of THP-1 cell lines.....	59
3.4.1. Optimization of <i>in vitro</i> <i>Leishmania</i> infection model .....	59

3.4.2. Comparison of <i>L. major</i> infection rates of WT versus STING or cGAS KO THP-1 cells.....	61
3.4.3. Comparison of <i>in vitro</i> infectivity of LRV- and LRV+ <i>L. major</i> transgenic strains.....	65
3.4.4. Infection of THP-1 WT and THP-1 TBK-1 KO cells with transgenic <i>L. major</i> in the presence and absence of the TBK-1 inhibitor-Amlexanox.....	68
3.4.5. Phagocytosis rates of THP-1 cell lines and the effects of drug treatments on phagocytosis rate .....	71
3.4.6. Comparison of <i>Leishmania</i> infection rates of THP-1 ISG15 KO and THP-1 LVC cells.....	76
3.5. Characterization of autophagic changes in <i>in vitro</i> <i>L. major</i> infection model	80
3.5.1. Characterization of autophagy related changes in THP-1 ISG15 KO cells and THP-1 LVC .....	85
3.6. <i>In vivo</i> infection studies with LRV- and LRV+ <i>L. major</i> strains.....	92
3.7. <i>In vivo</i> amlexanox treatment of LRV- <i>L. major</i> infected BALB/c mice .....	94
4. CONCLUSION AND FUTURE PERSPECTIVES.....	97
REFERENCES .....	103
APPENDICES	
A. Media Recipes .....	125
B. Vector Maps and Sequences.....	129
C. Western blot buffers .....	135
D. Western Blot images .....	137

E. MS full protein list.....	145
F. Representative <i>in vitro</i> infection raw data .....	146
CURRICULUM VITAE .....	161

## LIST OF TABLES

### TABLES

Table 1.1. Taxonomy of <i>Leishmania</i> .....	1
Table 2.1. PCR amplification conditions.....	26
Table 3.1. Most Abundant Proteins of LRV+ <i>L. major</i> Exosomes based on MS Analysis .....	45

## LIST OF FIGURES

### FIGURES

Figure 1.1. <i>Leishmania</i> species and clinical forms of leishmaniasis .....	3
Figure 1.2. The digenic life cycle of <i>Leishmania</i> .....	5
Figure 3.1. Presence of 5241 bp LRV dsRNA genome inside the <i>L. major</i> strain. ....	36
Figure 3.2. Use of J2 antibody on Dot Blot .....	38
Figure 3.3. LRV2-1 dsRNA genomic organization. ....	39
Figure 3.4. Detection of LRV2-1 specific sequence inside the exosomes by primer pair of LRV2-1_Fb and LRV2-1_R. ....	40
Figure 3.5. Detection of LRV2-1 specific sequence inside the exosomes by primer pair of LRV2-1_Fb and LRV2-1_R. ....	41
Figure 3.6. Next-generation sequencing result of 3350 base pair amplified region with the primer pair of LRV2-1_Fa and LRV2-1_R. ....	42
Figure 3.7. PANTHER Protein Class GO term Analysis classification of exosomal proteins. ....	44
Figure 3.8. Fluorescence microscopy images of EGFP-LUC expressing LRV- (A) and LRV+ (B) <i>L. major</i> .....	49
Figure 3.9. Neomycin depletion of LRV2-1 to generate transgenic LRV- <i>L. major</i> strain. ....	50
Figure 3.10. Blasticidin selected transgenic LRV+ <i>L. major</i> . ....	51
Figure 3.11. Confirmation of luciferase expression in transgenic parasites and optimization of injection dose of the <i>L. major</i> into the footpad of mice .....	52
Figure 3.12. Sanger Sequencing of ISG15 oligo pair ligated into the TLCV2 transfer vector. ....	54
Figure 3.13. Monitoring of ISG15 deficient clones by Immunoblotting .....	55
Figure 3.14. Sanger (A) and Next generation (B) sequencing of PAM sequence included region of THP-1 ISG15 KO cell line genome .....	56

Figure 3.15. THP-1 ISG15 KO intracellular staining with PE-conjugated ISG15 flow cytometry antibody .....	58
Figure 3.16. Assessment of <i>in vitro</i> infection rates and parasite loads of wild type THP-1 cells. ....	61
Figure 3.17. Transgenic <i>L. major</i> infection rate of THP-1 cell lines.....	62
Figure 3.18. Western blot analysis of STING activation upon <i>in vitro L. major</i> infection of THP-1 WT cells. ....	64
Figure 3.19. <i>In vitro</i> infection of THP-1 WT cells with LRV+ and LRV- parasites. ....	66
Figure 3.20. <i>In vitro</i> infection of THP-1 WT, cGAS KO and STING KO cells with LRV+ and LRV- parasites.....	67
Figure 3.21. <i>In vitro</i> infection of THP-1 WT, TBK-1 KO cells with transgenic <i>L. major</i> .....	69
Figure 3.22. Infection of THP-1 cell lines with opsonized <i>L. major</i> .....	71
Figure 3.23. Phagocytosis assay with pHrodo green zymosan bioparticles .....	72
Figure 3.24. <i>In vitro</i> infection of THP-1 WT cells with opsonized and unopsonized transgenic <i>L. major</i> .....	74
Figure 3.25. <i>In vitro</i> infection of THP-1 WT cells with opsonized transgenic <i>L. major</i> pretreated or not with Chloroquine or Bafilomycin A1.....	76
Figure 3.26. Phagocytosis assay with pHrodo green zymosan bioparticles .....	77
Figure 3.27. Comparison of <i>L. major</i> infection rates in THP-1 ISG15 KO and THP-1 LVC cells .....	78
Figure 3.28. THP-1 ISG15 KO and THP-1 LVC infection rates with opsonized <i>L. major</i> .....	79
Figure 3.29. Western blot images (A) and densitometric analysis of band intensities (B) of THP-1 WT cells. ....	83
Figure 3.30. Western blot images and densitometric analysis of THP-1 LVC cells infected with <i>L. major</i> for 1 and 6 hours. ....	85
Figure 3.31. Western blot images (A) and densitometric analysis (B) of autophagy marker in THP-1 ISG15 KO and THP-1 LVC cells.....	88

Figure 3.32. Fluorescence microscopy images of LysoTracker Red stained THP-1 ISG15 KO (A) and LVC (B) cells. ....	91
Figure 3.33. Monitoring of parasite loads in mice challenged with LRV- and LRV+ transgenic <i>L. major</i> using <i>in vivo</i> imaging.....	93
Figure 3.34. Monitoring of footpad swelling in LRV- <i>L. major</i> challenged mice during 12 days of amlexanox treatment .....	94
Figure 3.35. Monitoring of parasite loads in LRV- <i>L. major</i> challenged mice using IVIS <i>in vivo</i> imaging. ....	96



## CHAPTER 1

### INTRODUCTION

#### 1.1. Tropical disease: Leishmaniasis

Leishmaniasis are a group of vector-borne diseases caused by intracellular parasites of the genus *Leishmania*. The parasites are transmitted to humans by *Phlebotomus* or *Lutzomyia* sandflies during an infective blood meal. As a tropical and subtropical disease, leishmaniasis can be classified according to the hemisphere in which it occurs. In the Eastern Hemisphere, Old World (OW) leishmaniasis exists and is endemic in Africa, southern Europe and Asia. In the Western Hemisphere, New World (NW) leishmaniasis exists and is endemic in south central Texas to Central and South America except for Chile and Uruguay (Table 1.1.) (Kevric, Cappel, & Keeling, 2015).

Table 1.1. *Taxonomy of Leishmania*

Region	Complex	Species	Clinical Manifestation
<b>Old World</b>	<i>Leishmania donovani</i>	<i>L. donovani</i>	CL, VL, PKLD, ML
		<i>L. infantum</i>	CL, VL, PKLD, ML
		<i>L. chagasi</i>	CL, VL, PKLD, ML
	<i>Leishmania tropica</i>	<i>L. tropica</i>	CL, ML, VL (rare)
		<i>L. major</i>	CL, ML (rare)
		<i>L. aethiopica</i>	CL, DCL
<b>New World</b>	<i>Leishmania mexicana</i>	<i>L. mexicana</i>	CL, DCL (rare)
		<i>L. amazonensis</i>	CL, DCL, ML, VL
	<i>Leishmania (Viannia) braziliensis</i>	<i>L. venezuelensis</i>	CL, DCL
		<i>L. braziliensis</i>	CL, ML, VL
		<i>L. guyanensis</i>	CL, ML
		<i>L. panamensis</i>	CL, ML
	<i>L. peruviana</i>	CL	

CL: cutaneous leishmaniasis, DCL: diffuse CL, ML: mucocutaneous leishmaniasis, VL: visceral leishmaniasis, PKLD: post-kala azar dermal leishmaniasis

Leishmaniasis is a serious world health problem with a broad spectrum of clinical manifestations and one of the seven most important neglected tropical and subtropical diseases (Andrade-Narváez, Vargas-González, Canto-Lara, & Damián-Centeno, 2001). An estimated 12 to 15 million people worldwide are infected with *Leishmania* and 350 million people are at risk of acquiring the disease. 1.5 to 2 million new cases occur each year, causing 70,000 deaths annually (Hoyos et al., 2016; Kevric et al., 2015). The characteristics of the infecting parasite species and the host's immune status determine the clinical features of the disease. Based on this, there are three main clinical forms of the disease: cutaneous (disseminated or localized) (1), mucocutaneous (2) and visceral or kala-azar leishmaniasis (Arenas, Torres-Guerrero, Quintanilla-Cedillo, & Ruiz-Esmenjaud, 2017). Cutaneous leishmaniasis (CL) generally manifests as a localized skin lesion, characterized by reddish brown infiltrative plaques and hard erythematous nodules on the skin (Bailey & Lockwood, 2007). However, in rare cases lesions can also disseminate through blood and lymph to various anatomical regions, including the face, chest and upper limbs (disseminated cutaneous leishmaniasis; DCL). Specific to *Leishmania tropica* infections, recidivans leishmaniasis (RL) is a recurrent form of CL, appearing at the original skin ulcer site, generally within 2 years and often around the edge of the scar (Alvar & Arana, 2018). Parasite species that cause CL are listed in Table 1.1. Mucocutaneous leishmaniasis (MCL) is another form of leishmaniasis in which the nasopharyngeal mucosa is invaded and destroyed by *L. braziliensis*, *L. guyanensis*, or *L. panamensis*, which are the most common species that cause MCL (Davies et al., 2000). Progression of the disease usually takes places through the nasal mucosa to oral and pharynx mucosa and to the skin of the nose and lips. Atrophy of the nasal turbinates and cartilaginous septum destruction can cause death in extreme cases (Lessa et al., 2007). Visceral leishmaniasis (VL) (or kala-azar), is a systemic, severe form of this infectious disease and is caused by *L. donovani*, *L. infantum*, *L. chagasi*, *L. amazonensis* and *L. tropica*. Development of the disease can take months to years and infected macrophages disseminate through the reticuloendothelial system. Fever, weight loss, anorexia, pallor, diarrhea, epistaxis, hepatosplenomegaly and lymphadenopathy are the

common symptoms of VL. This disease can cause death within two years if left untreated (Kevric et al., 2015). Post-kala-azar dermal leishmaniasis (PKDL) is a complication observed in half of the patients successfully treated for VL and is characterized by diffuse hypopigmented macules, malar rash, papules and nodules all-around the body. PKDL is caused by *L. donovani* and it is almost exclusively found in India and East Africa (Berman, 1997). *Leishmania* species and the type of leishmaniasis they cause is Summarized in Figure 1.1.

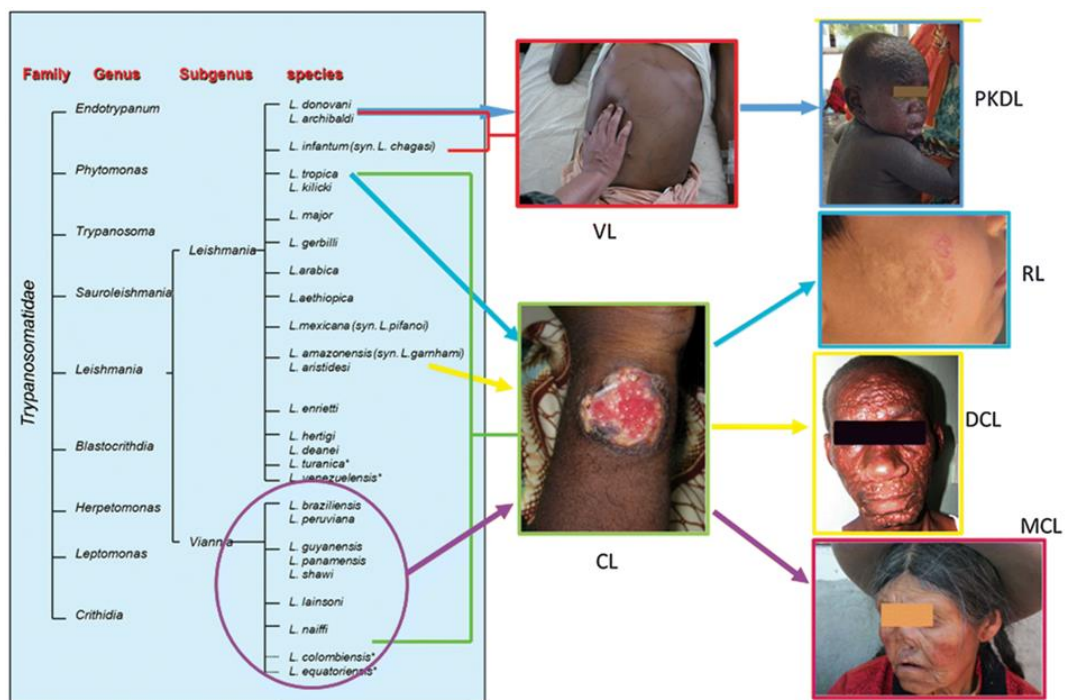


Figure 1.1. *Leishmania* species and clinical forms of leishmaniasis

Adopted from Alvar & Arana, (2018). VL, visceral leishmaniasis; PKDL, post-kala-azar-dermal leishmaniasis; CL, cutaneous leishmaniasis; RL, recidivans leishmaniasis; DCL, disseminated cutaneous leishmaniasis; MCL, mucocutaneous leishmaniasis.

### 1.1.1. Life cycle of *Leishmania*

Genus *Leishmania* belongs to subkingdom Protozoa, order Kinetoplastida and family of Trypanosomatidae. *Leishmania* genus is further divided into two subgenera as *Leishmania* and *Viannia*, based on their location in the vector's intestine (Bañuls, Hide, & Prugnotte, 2007). *Leishmania* parasites have a digenetic life cycle which requires an insect vector and a vertebrate host. Female sandflies (*Phlebotomus* spp. and *Lutzomyia* spp.) carry the flagellated and motile promastigotes which are the extracellular form of *Leishmania*. Infectious form of *Leishmania* is the metacyclic promastigote. Within the insect mid-gut, the parasites undergo several developmental changes and differentiate into this infectious form. Metacyclic promastigotes are disseminated into the mammalian host dermis during a blood meal of the female sand fly and are quickly phagocytosed by mono and polymorphonuclear (PMN) phagocytes. Following their internalization by phagocytosis, the parasites then differentiate into their non-motile amastigote forms and multiply by binary fission. After a sand fly takes another blood meal from the infected host, amastigotes return to the insect vector gut, differentiate into promastigotes, completing the life cycle (Cecilio et al., 2014). The *Leishmania* life cycle is summarized in Figure 1.2.

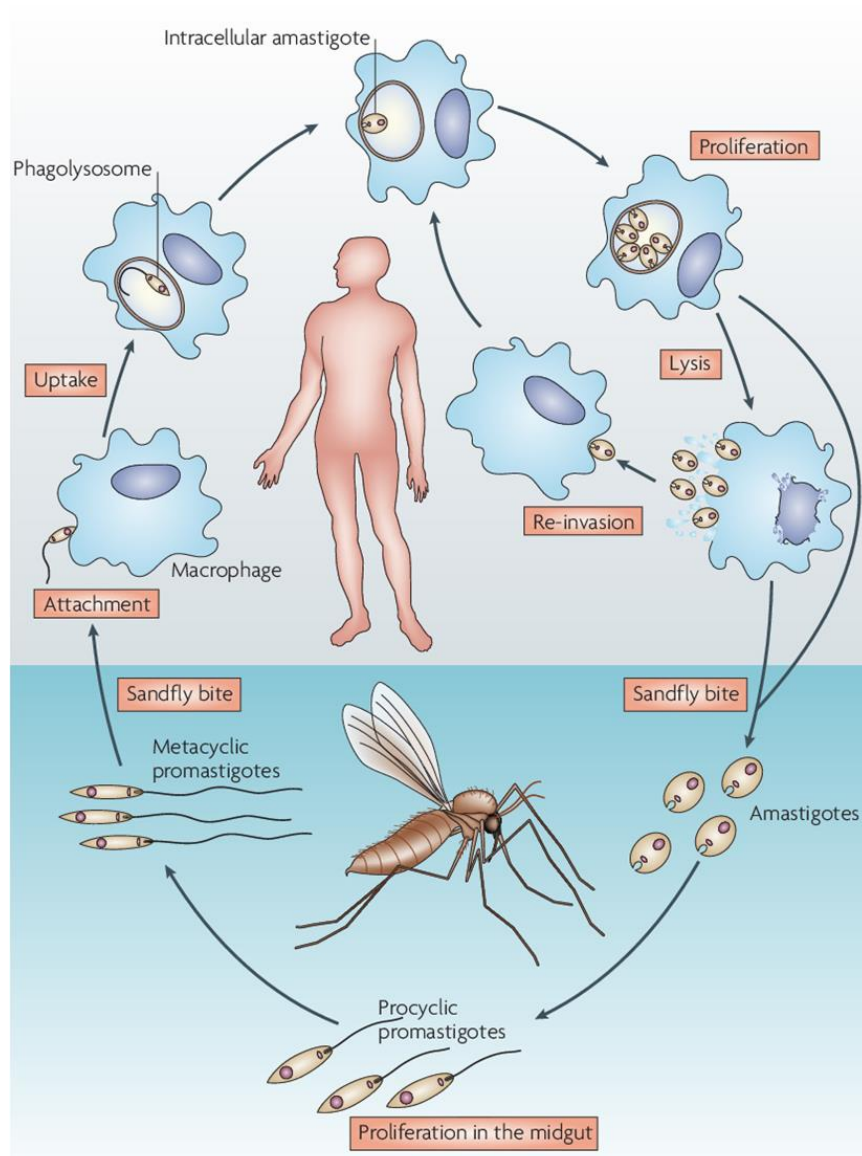


Figure 1.2. The digenic life cycle of *Leishmania*

Adopted from (Chappuis et al., 2007). The Figure summarizes the stages of *Leishmania* lifecycle in sand fly and mammalian host cells

It is worth mentioning that in the mammalian host, neutrophils are the first immune cells that encounter the parasites following their migration to the site of infection. Internalized *Leishmania* then delays neutrophil apoptosis (the 1<sup>st</sup> 24 h of infection), establishing a temporary parasite-safe niche (Aga et al., 2002). Other studies dispute

this claim and suggest that neutrophils undergo rapid apoptosis upon parasite uptake (Ribeiro-Gomes, Peters, Debrabant, & Sacks, 2012). However, as a general strategy for the internalization of parasites by macrophages, infected apoptotic neutrophils release different chemotactic factors to summon macrophages which remove dying neutrophils by phagocytosis and secrete anti-inflammatory cytokine TGF- $\beta$  (van Zandbergen et al., 2004). Moreover, low amounts of interleukin IL-12 and high levels of IL-10 secretion from macrophages upon the internalization of apoptotic neutrophils might also support the silent entry of *Leishmania* into their primary target, the macrophages (Filaridy et al., 2010). Since the parasites arrive at their final destination by manipulating the immune response through neutrophil invasion, their macrophage infection strategy has been named as the “Trojan horse” strategy (John & Hunter, 2008). Skin resident dendritic cells have also been shown to phagocytose the infected apoptotic neutrophils in a mouse model of intradermal *L. major* infection (Ribeiro-Gomes et al., 2012). Other studies also suggest that apoptotic parasites themselves can induce anti-inflammatory cytokine production in immune cells, including TGF- $\beta$  (Ravichandran, 2010). This enables silent entry into macrophages, followed by inhibition of apoptosis (Moore & Matlashewski, 1994).

### **1.1.2. Promastigote versus amastigote transition in *Leishmania***

Promastigote to amastigote transition occurs inside the macrophage. Promastigote parasites have long flagella, elongated cell shapes and are motile. During promastigote to amastigote transition, parasites differentiate into spherical non-flagellated cells (Sunter & Gull, 2017). It is thought that the purpose of this shape change is to reduce the surface area of the parasite to survive inside the parasitophorous vacuole (Antoine, Prina, Jouanne, & Bongrand, 1990). Moreover, these two different life stages have differential surface molecule compositions. Infectious metacyclic promastigotes have a surface glycocalyx which is almost absent in amastigotes (Pimenta, Saraiva, & Sacks, 1991). Surface of promastigotes is mainly covered with lipophosphoglycan (LPG), which is a glycosylphosphatidylinositol (GPI)-anchored molecule. LPG is made of repeating disaccharide units and a phosphate. Moreover, promastigotes have

another important GPI anchored molecule, the major metalloprotease gp63 (Abu-Dayyeh, Hassani, Westra, Mottram, & Olivier, 2010). In contrast, amastigotes express very little LPG and lower amounts of gp63 (McConville & Blackwell, 1991; Schneider, Rosat, Bouvier, Louis, & Bordier, 1992). Amastigote to promastigote transition on the other hand, happens after sand fly digestion of infected macrophages. The cues triggering the differentiation are not clearly explained yet. However, pH and temperature changes are thought to play important roles (Bee et al., 2001). First stage of amastigote to promastigote differentiation is elongation of flagellum, followed by transition into an elongated ovoid shape. Moreover, the neck region of the flagellum becomes visible as opposed to the amastigote phase (Wheeler, Sunter, & Gull, 2016).

## **1.2. Immunity to *Leishmania***

### **1.2.1. Innate immunity to *Leishmania***

#### **1.2.1.1. The role of the complement system in anti-leishmanial immunity**

Elimination of *Leishmania* infection requires coordinated action of multiple immune system effectors. Success of infection depends on the ability of the parasites to evade host immunity. Host reaction to *Leishmania* begins with the complement system. Complement system is a group of 30 different plasma associated proteins which function in clearance of invading pathogens (Dunkelberger & Song, 2010). Three distinct pathways can induce complement activation: the classical, lectin and alternative pathways. Antibody binding to the surface of the invading pathogen activates the classical pathway, whereas binding of ficolins or the mannose binding lectin to pathogen-associated carbohydrates initiates the lectin pathway. However, alternative pathway is directly activated on pathogen surfaces due to a lack of complement regulatory proteins on most pathogens. Activation of C3 convertase which cleaves C3 to generate C3b is common phenomenon in all three pathways. C3b then deposits on the pathogen surface, and following the generation of a C5 convertase, other activated complement members are recruited (C5b-C6-C7-C8-C9) to form the C5b-9 membrane attack complex (MAC). C5b-9 MAC promotes

complement dependent lysis of invading pathogens. Moreover, C3b promotes phagocytosis of pathogens by serving as an opsonin (Gurung & Kanneganti, 2015).

The concentration of activated serum complement components is directly related to complement directed lysis *in vitro* (Moreno et al., 2007). However, *Leishmania* parasites counteract the complement dependent lysis when they are at the metacyclic phase (Stephen M. Puentes, Sacks, Da Silva, & Joiner, 1988). Although the three complement activation pathways play a role in clearance of *Leishmania*, contribution of the alternative pathway is more prominent (Gurung & Kanneganti, 2015). Human serum clearance of parasites is independent of antibodies or C4, the classical complement pathway protein. C5b-9 MAC dependent alternative pathway activated lysis was shown to play an important role. (Hoover & Nacy, 1984; Mosser & Edelson, 1984). Moreover, classical complement pathway targets promastigotes but alternative pathway targets *Leishmania* amastigotes (Hoover, Berger, Nacy, Hockmeyer, & Meltzer, 1984). Resistance mechanism of metacyclic promastigotes to complement dependent lysis depends on the LPG layer interaction with C3b (McConville, Turco, Ferguson, & Sacks, 1992; Stephen M. Puentes et al., 1988). Even though LPG binds to C3b and further recruit the C5b-9 MAC complex, the MAC complex cannot reach the *Leishmania* plasma membrane and hence the complex disseminates (S M Puentes, Da Silva, Sacks, Hammer, & Joiner, 1990). Furthermore, the major virulence factor of *Leishmania*, gp63, inactivates C3b and thereby inhibits the formation of the subsequent C5b-9 MAC complex (Brittingham et al., 1995). Interestingly, gp63 and LPG augment C3b opsonization, which further facilitates parasite phagocytosis through binding to the macrophage C3b receptor, CD11b (N. Ueno, Bratt, Rodriguez, & Wilson, 2009). As a result, *Leishmania* circumvent complement mediated lysis by utilizing LPG and gp63 dependent entry into the host.

### 1.2.1.2. The role of Toll like receptors in anti-leishmanial immunity

Toll like receptors are a family of pattern recognition receptors expressed by immune cells, specialized in detection of damage associated or pathogen associated molecular patterns (DAMPs or PAMPs) (Sato & Akira, 2016). Except for TLR3, all TLRs use the common adaptor protein MyD88 for signal transduction. Whereas TLR3 strictly uses TRIF as an adaptor, TLR4 can use both MyD88 and TRIF. MyD88 deficient mice are susceptible to *L. major* infection, consequent to severely diminished expression of IL-12 (de Veer et al., 2003; Debus, Gläsner, Röllinghoff, & Gessner, 2003; Muraille et al., 2003). Therefore, MyD88 and TLR receptors play important roles in anti-*Leishmania* immunity. Specifically, TLR2 and TLR3 are involved in establishment of a response against *L. donovani* infection of macrophages, through activation of TNF- $\alpha$  and nitric oxide production, which are essential for anti-*Leishmania* immunity (Flandin, Chano, & Descoteaux, 2006). LPG binding directly activates TLR2 and promotes downstream signaling (de Veer et al., 2003). However, studies with LPG-deficient *L. donovani* demonstrated that TLR2 is still activated, suggesting recognition of other phosphoglycan structures through TLR2. Interestingly, TLR2 deficiency results in resistance against *Leishmania* as a consequence of augmented IL-12 secretion. Based on this finding, researchers concluded that through LPG, *Leishmania* uses TLR2 to evade host immunity (Guerra et al., 2010; Vargas-Inchaustegui et al., 2009).

TLR4 is another receptor that was reported to bind to glycoproteins and glycosphingophospholipids of *L. donovani*. TLR4-mediated recognition results in expression of IL-12 and reactive oxygen species (Karmakar, Bhaumik, Paul, & De, 2012; Paul, Karmakar, & De, 2012). TLR4 deficient mice are more susceptible to *Leishmania* infection, and their parasite loads are higher than the wild type mice (P. Kropf et al., 2004; Pascale Kropf et al., 2004). Another TLR that is important against *Leishmania* immunity is TLR9, which recognizes DNA of infecting *Leishmania* and promotes subsequent IL-12 production (Liese, Schleicher, & Bogdan, 2007). TLR9 deficient mice demonstrated increased susceptibility to *Leishmania* infection with

augmented parasite load and footpad lesions (Liese et al., 2007; Weinkopff et al., 2013). Furthermore, whereas TLR3, TLR7, TLR9 single deficient mice demonstrated susceptibility to *Leishmania* infection, triple deficiency severely compromised immunity against parasitic infection and disease severity. Interestingly, progression of infection in this triple TLR deficient mice was even worse than MyD88 deficiency, emphasizing the role of TLR3,7 and 9 in parasite resistance (Schamber-Reis et al., 2013). However, *Leishmania* can also interfere with TLR signaling by inhibiting degradation of TRAF3, an essential molecule involved in TLR4 signaling. Furthermore, *Leishmania* induced degradation of STAT1/STAT2, ERK1/2 and IRF1, and inhibition of serine peptidase 2 was previously reported, collectively leading to inhibition of TLR4 signaling (Faria et al., 2011; P. Gupta et al., 2014; Vargas-Inchaustegui, Xin, & Soong, 2008). Studies conducted with TLR2, TLR4 and TLR9 agonists are in support of the critical role played by TLR signaling in protection against infection with *Leishmania*. Specifically, TLR2, TLR4 or TLR9 agonist administration prior to infection all resulted in significant protection against *Leishmania* (Chandel et al., 2014; Huang, Hinchman, & Mendez, 2015; Raman et al., 2010).

### **1.2.1.3. The role of Nod like receptors in anti-leishmanial immunity**

NLRs are a family of cytoplasmic pattern recognition receptors (PRR) that mediate innate immune responses to cellular injury and stress (Platnich & Muruve, 2019). Some NLR family members form a multi-protein complex known as the inflammasome. Canonical Inflammasomes form a platform to activate the inflammatory caspase 1 through a common adaptor molecule ASC (Evavold & Kagan, 2019; Gurung & Kanneganti, 2015; Kanneganti et al., 2006; Mariathasan et al., 2006; Martinon, Burns, & Tschopp, 2002; Martinon, Pétrilli, Mayor, Tardivel, & Tschopp, 2006). Active caspase-1 then proteolytically cleaves specific substrates, including pro-IL-1 $\beta$ , pro-IL-18 and gasdermin-D, leading to inflammation and a highly inflammatory form of cell death known as pyroptosis (Lieberman, Wu, & Kagan, 2019). The role of inflammasome activation in *Leishmania* infection is not

clear. For example, previous studies demonstrated that, NLRP3 inflammasome controls IL-1 and IL-18 secretion mechanism which collectively advance *Leishmania* proliferation in infection sensitive BALB/c mice but inhibit parasite growth in C57BL/6 mice (Gurung & Kanneganti, 2015). A more recent study demonstrated that *L. infantum* was unable to activate inflammasomes in infected cells (Borim et al., 2020).

#### **1.2.1.4. The role of cGAS-STING cytosolic DNA sensing pathway in parasitic infections**

Emerging evidence suggests that cGAS-STING cytosolic DNA sensing pathway might also play an important role in parasitic infections, including *Leishmania* (Das et al., 2019; Majumdar et al., 2015, 2019). Cytosolic DNA detection and subsequent immune activation against viral or bacterial DNA is coupled to several signaling molecules in the cytosol. Early identified sensors like DAI, IFI16, and DDX41, as well as the more recently discovered cyclic GMP-AMP synthase (cGAS), facilitate the production of type I interferons (IFNs) upon sensing of cytosolic DNA (Paludan & Bowie, 2013). Another type of cytosolic DNA sensor is the PYHIN protein family member absent in melanoma 2 (AIM2), which directly binds to DNA, leading to caspase-1 dependent inflammasome activation and subsequent IL-1 $\beta$  production and secretion. While DAI and IFI16 is dispensable for cytosolic DNA-mediated type I IFN production, cGAS was shown to be indispensable for cytosolic DNA mediated interferon expression (Chen, Sun, & Chen, 2016). Following binding to host or pathogen-derived cytosolic DNA, cGAS synthesizes the second messenger cyclic GMP-AMP (cGAMP), which in turn binds and activates the ER-resident adapter molecule stimulator of interferon genes (STING) (Lijun Sun, Wu, Du, Chen, & Chen, 2013). STING exists as a homodimer, anchored to the ER at its amino terminus and undergoes conformational change after encountering its ligand cGAMP. Between the mammalian and bacterial isoforms of cGAMP, the mammalian isoform (2'3'cGAMP) binds to STING with higher affinity, resulting in robust type I IFN production (Xu Zhang et al., 2013). Conformational change in STING upon its activation, leads to the

recruitment of the TANK-binding kinase 1 (TBK1) which phosphorylates STING at serine and tyrosine residues, enabling the recruitment of interferon regulatory factor 3 (IRF3) (Liu et al., 2015). The transcription factor IRF3 is also phosphorylated by TBK1, leading to its dimerization and translocation into the nucleus, where it initiates transcription of type I IFN expression (Tanaka & Chen, 2012). Since type I IFNs are able to interfere with viral replication machinery, they are essential in the defense against viral infections. However, whether or not the cGAS/STING dependent central cytosolic DNA sensing pathway modulates anti-leishmanial immunity, is not known. To date, only one study demonstrated that *L. donovani* DNA transfection resulted in cGAS/STING-mediated recognition, culminating in increased type I IFN production and enhanced parasite loads (Das et al., 2019).

### **1.2.2. Adaptive immunity against *Leishmania***

T cells are considered as major players in establishing protective immunity against *Leishmania*. T helper type I (Th1) cells that produce IFN- $\gamma$  are important for the resolution of *L. major* infections because they can induce nitric oxide production in macrophages, which aids parasite clearance. Conversely, production of IL-4 and IL-13 cytokines by T helper type II (Th2) cells is associated with susceptibility to *Leishmania*. Historically, *L. major* infection resistance versus susceptibility in C57BL/6 versus BALB/c mice has been linked to their Th1 versus Th2 cytokine dominated genotypes, respectively (G. Gupta, Oghumu, & Satoskar, 2013). It was previously reported that in visceral leishmaniasis, IFN- $\gamma$  producing Th1 cells provided protection against infection in both mice and humans (Kushawaha, Gupta, Sundar, Sahasrabudhe, & Dube, 2011). Moreover, IFN- $\gamma$ -producing CD8<sup>+</sup> T cells (cytotoxic T cells) contribute to disease resolution in cutaneous leishmaniasis (Rostami et al., 2010). The other adaptive immune cell type that plays an important role in infection with the parasites are B cells, which interestingly, have a pro-parasitic role. B cell deficient mice have reduced parasite burdens (Smelt, Cotterell, Engwerda, & Kaye, 2000). Mechanistically, marginal zone B cells were shown to suppress antigen specific CD8 T cell cytotoxic activity and the frequency of IFN- $\gamma$  producing

CD4<sup>+</sup> T cells (Bankoti, Gupta, Levchenko, & Stäger, 2012). Various types of cytokines and chemokines can modulate immunity to *Leishmania* infection. Cytokines are secreted from infected or immune cells and activate other cells. Cytokine-activated immune cells then release molecules that either favor or inhibit *Leishmania* infection (G. Gupta et al., 2013). Some of these cytokines and chemokines might lead to activation of immune cells critical in parasite clearance (IL-12, IFN- $\gamma$ -, TNF- $\alpha$ ), whereas others (IL-10, IL-4, IL-13, TGF- $\beta$ ) might promote the persistence of parasites (Kopf et al., 1996; Mattner et al., 1996).

### **1.3. Leishmania RNA virus (LRV)**

Leishmania RNA virus infection of *Leishmania* (*L. guyanensis*) was first recorded in 1988 (Tarr et al., 1988). LRVs are classified under *Totiviridae* family and are non-enveloped, icosahedral dsRNA viruses, capable of infecting protozoa (Weeks, Aline, Myler, & Stuart, 1992). LRV viral particles are generally 40 nm, containing a non-segmented dsRNA genome (4 to 8 kilo base). The dsRNA genome encodes two proteins: the major capsid protein and a capsid-RNA dependent RNA polymerase (RDRP) fusion protein which is necessary for virus replication. However, RDRP protein might also be independent of the capsid protein, such as the case in LRV2-1 (Hartley, Ronet, Zangger, Beverley, & Fasel, 2012). After its initial discovery in *L. guyanensis*, presence of LRV was also described in *L. braziliensis* (Salinas, Zamora, Stuart, & Saravia, 1996). The only reported LRV outside of the *Viannia* (Table 1.1.) was identified in *L. major* and was named as LRV2-1 (Scheffter, Ro, Chung, & Patterson, 1995). LRV 2-1 was more recently identified in other Old World species, including, *L. aethiopica* and *L. infantum* (Hajjarian et al., 2016; Kleschenko et al., 2019; Nalçacı et al., 2019; Zangger et al., 2014). New World *Viannia* infecting viruses on the other hand, are named as LRV1. Genetic studies on LRVs demonstrated that the genetic distance between LRV1 and LRV2 are similar to the genetic distance between the hosts that are infected with the specific LRV (Giovanni Widmer & Dooley, 1995). Therefore, LRVs seem to co-evolved with their host which was present prior to New and Old World divergence of the parasites.

LRV possesses a 5.3 kb dsRNA inside a capsid which serves as a plus stranded mRNA for viral protein synthesis (Weeks et al., 1992). LRV1 and LRV2 dsRNA genomes show less than 40% homology. Therefore, it is safe to say that these two types of LRVs are highly divergent (Scheffter et al., 1995). There are 3 open reading frames (ORF) identified in the dsRNA genome of the LRV1-1, while 4 ORFs are present in the LRV1-4 genome that infects *L. guyanensis* strains. However, in both LRVs, ORF 2 and 3 encode the major capsid protein and the capsid-RDRP fusion protein. In addition, capsid-RDRP fusion protein is formed by +1 ribosomal frameshift in LRV1 (Lee, Suh, Scheffter, Patterson, & Chung, 1996; Maga, Widmer, & LeBowitz, 1995; Y T Ro, Scheffter, & Patterson, 1997b). In contrast, for LRV2, RDRP encoding site (ORF3) does not overlap with capsid (ORF2) and therefore, RDRP could be encoded as an independent protein. RDRP translation in LRV-2 is not fully understood but according to one hypothesis, the presence of an additional ribosomal entry site upstream of ORF3 and/or a pseudoknot structure participating in ribosomal hopping might account for translation of RDRP (Scheffter et al., 1995).

The clinical impact of LRV1 presence on the pathogenesis of *Leishmania* has been studied extensively. However, there are no reports on the effect of LRV2-1 in clinical progression of disease caused by infected old world strains (Hartley et al., 2012). Presence of LRV in *L. guyanensis* was previously shown to exacerbate inflammation and this property of LRV has been linked to the metastatic potential of LRV infected *L. (Viannia)* parasites (Ives et al., 2011; Ronet, Beverley, & Fasel, 2011). Even though metastatic parasites generally bear LRV virus such as in the case of metastatic *L. braziliensis* and *L. guyanensis*, metastasis can also occur in LRV free *L. panamensis* (Hartley et al., 2012). How LRV is preserved and transmitted is not known. However, other viruses of the Totiviridae family are transmitted either vertically (mother to daughter) or horizontally (cell fusion and hyphal anastomosis in fungi) (Dalzoto et al., 2006). In addition, infection of virus negative *Leishmania* parasites with LRV is only transient or does not take place at all (Armstrong, Keenan, Widmer, & Patterson, 1993). LRV exerts its disease worsening phenotype through TLR3, which recognizes

dsRNA. TLR3-deficient mice do not exhibit LRV-induced exacerbation of leishmanial disease (Ives et al., 2011). Lastly, a recent study suggests that LRV1 transmission is exosome-mediated, which also augments the infectivity of *Leishmania* in the mammalian host, leading to severe leishmaniasis (Atayde et al., 2019).

#### **1.4. *Leishmania* extracellular vesicles**

##### **1.4.1. Extracellular vesicles**

From prokaryotes to highly evolved eukaryotes, extracellular vesicle (EV) secretion is a common phenomenon observed in almost all cellular life forms (Yáñez-Mó et al., 2015). EVs are membranous structures which can be further classified into exosomes, microvesicles and apoptotic bodies, according to their biogenesis (Colombo, Raposo, & Théry, 2014). Fusion of multivesicular bodies with early endosomes forms exosomes, while microvesicle biogenesis happens through budding of the outer cell membrane. Apoptotic bodies on the other hand, disseminate from apoptotic cells (Colombo et al., 2014). Exosomes play important roles in intercellular communication. EVs carry multiple messengers, including proteins, lipids, nucleic acids and sugars. Depending on their content, they modulate the biological function of the target cells that internalize the EVs (Yáñez-Mó et al., 2015). Interestingly, pathogen-derived EVs are also internalized by the host cells, and this process often actively modulates the immune responses of the host in favor of the pathogen (Gomez et al., 2009). Exosomes are single membrane, small (30-200 nm) and secreted vesicular organelles that are enriched in proteins, lipids, nucleic acids and glycoconjugates. Exosome sizes differ profoundly even for the single cell that secrete them (Keller, Sanderson, Stoeck, & Altevogt, 2006).

##### **1.4.2. *Leishmania* exosomes**

*Leishmania* species secretes extracellular vesicles that share nearly 50% protein content similarity with mammalian exosomes and morphologically, mammalian and *Leishmania* exosomes are identical (Maxwell et al., 2008; Simpson, Lim, Moritz, & Mathivanan, 2009). Various studies demonstrated that several *Leishmania* specific

proteins utilize the exosomal system as a noncanonical protein secretion system (Dong, Filho, & Olivier, 2019; Pérez-Cabezas et al., 2019). Cargo of *Leishmania* exosomes includes various proteins, small non coding guide RNAs and tRNAs, which collectively contribute to immunomodulation of host cells (Lambertz et al., 2012). *Leishmania* exosomes are also enriched in parasite virulence factors. Upon entry into the mammalian host, parasites are exposed to acidic environment and undergo heat shock (shift to 37C), which collectively contribute to augmented secretion of EVs (Hassani, Antoniak, Jardim, & Olivier, 2011). Moreover, studies indicate that temperature shift leads to enrichment in Kinase Activity related proteins and pH shift result in enrichment in Phosphatase Activity related proteins (J. M. Silverman, Clos, De'Oliveira, et al., 2010). Delivery of GP63, heat shock protein 10 (HSP10) to macrophages by *Leishmania* exosomes was also reported previously. GP63 is a major virulence factor of *Leishmania* which was observed in the macrophage cytoplasm upon parasite infection and similarly upon incubation of parasite free culture supernatant with macrophages. In both occasions, GP63 localize to the same subcellular compartment (Gomez et al., 2009). Exosomes are also released from promastigotes and perform an infection-enhancing role, following their co-injection into the host during sand-fly's blood meal (Atayde et al., 2015). Specifically, immediately following entry into the host, these promastigote-derived exosomes trigger IL-8 production, leading to early recruitment of neutrophils to the infection site (Peters et al., 2008; Peters & Sacks, 2009). This in turn, facilitates the "Trojan Horse" entry of *Leishmania* into the macrophages. (van Zandbergen et al., 2004). *Leishmania* exosomes have also been implicated in blunting of the effects of IFN- $\gamma$ -treatment on macrophages. Macrophages pretreated with exosomes responded poorly to IFN- $\gamma$ -treatment in *Leishmania* infected cells when compared to exosome untreated macrophages (J. M. Silverman, Clos, Horakova, et al., 2010). Furthermore, exosome pretreatment of macrophages induced IL-10 production, a potent anti-inflammatory cytokine, inducing immune suppression upon *Leishmania* infection (J. M. Silverman & Reiner, 2011). Collectively, evidence suggests that the parasites secrete exosomes to modulate the immune response in their favor.

## **1.5. *Leishmania* and autophagy**

### **1.5.1. Autophagy**

Cellular autophagy is the keeper of cellular homeostasis and normal physiology of cells under stress conditions and is a conserved catabolic process (Cooper, 2018). Infectious, carcinogenic, degenerative and deleterious agents are overcome by autophagy. Therefore, dysfunctional autophagic pathway can result in multiple human diseases (Mizushima, 2007; Z. Yang & Klionsky, 2010). Autophagy is activated by stress conditions like starvation or rapamycin treatment and it can lead to selective or non-selective lysosomal degradation of cellular components (Füllgrabe, Ghislat, Cho, & Rubinsztein, 2016; Z. J. Yang, Chee, Huang, & Sinicrope, 2011). In mammalian cells, three main types of autophagy have been defined: microautophagy, macroautophagy and chaperone-mediated autophagy (CMA) (Mizushima, Levine, Cuervo, & Klionsky, 2008). In macroautophagy (also called as autophagy), large portions of cellular content and cytoplasm, including long lived proteins, damaged organelles, intracellular pathogens and aggregated proteins are engulfed into a double membraned autophagosome vacuole. Then, the autophagosome fuses with lysosomes to form the autolysosome, in which autophagic contents are degraded and recycled for cellular reuse (Kunzt, Schwarz, & Mayer, 2004; Li, Li, & Bao, 2012; T. Ueno & Komatsu, 2017). Microautophagy on the other hand, refers to direct lysosomal engulfment and digestion of small cytosolic substrates (Nagar, 2017; Paolini et al., 2018). CMA pathway brings target proteins into the lysosomal lumen in a vesicular trafficking-independent manner, through a translocation complex containing the lysosome associated membrane protein type 2A (LAMP-2A) (Campbell, Morris, & Schapira, 2018; Kunzt et al., 2004). Autophagic degradation can be selective or non-selective. In selective autophagy, particular ubiquitinated substrates are recognized by specific receptors, sequestered, and degraded by autophagosomes. Conversely, in non-selective autophagy, all types of substrates are indiscriminately degraded in autolysosomes (Kiššova et al., 2007; Zaffagnini & Martens, 2016).

Mechanistically, the earliest step of autophagy involves the assembly of the unc-51-like kinase (ULK) complex, which activates phosphatidylinositol 3-kinase (PI3K) by phosphorylating Beclin 1-regulated autophagy protein 1 (AMBRA1) (Mercer, Gubas, & Tooze, 2018; Yu et al., 2010). Beclin 1 and PI3K are known to mediate membrane nucleation, while Class III PI3K participates in membrane trafficking events. Autophagy protein (Atg) 5-12-16 complex is then recruited to the pre-autophagosomal structure. Atg 5-12-16 complex associates with phagophore's outer membrane, in order to prevent premature fusion with lysosomes and vesicles (Kaur & Debnath, 2015). Upon maturation of the autophagosome, phosphatidylethanolamine (PE) and Atg8/microtubule associated protein 1 light chain (LC3) are bound, a process, stimulated with second ubiquitin like system. LC3 has a high affinity to phagosome and lysosome complex (LAPosome), therefore, ingested pathogens or cargoes are degraded at a higher rate (Herb, Gluschko, & Schramm, 2019). LC3 conversion to LC3-II is a molecular marker for autophagosomes and involves processing by Atg4, Atg7, and Atg3 (Glick, Barth, & Macleod, 2010). LC3-II is present on both the inner and the outer surface of the autophagosome and this phenomenon is important for the completion of the autophagic membrane. After autophagosomal closure, Atg5-12-16 complex detach from the autophagosome (Bader, Shandala, Ng, Johnson, & Brooks, 2015). Autophagosome then fuses with lysosomes to form autolysosome, where autophagic cargo is degraded with hydrolytic enzymes (Khandia et al., 2019).

### **1.5.2. *Leishmania* induced autophagy**

Autophagic induction upon *Leishmania* infection was reported in several studies (Cyrino, Araújo, Joazeiro, Vicente, & Giorgio, 2012; Franco et al., 2017; Frank et al., 2015; S. A. Thomas, Nandan, Kass, & Reiner, 2018). However, it was also reported that *L. major* directs LC3 phagosome to apoptotic parasites rather than viable ones to escape the LC3-associated phagocytosis (LAP) in a gp63 dependent manner (Crauwels et al., 2015). Therefore, it appears that parasites have evolved some strategies to escape LC3 labelling of the parasitophorous vacuole to escape elimination by autophagy. Even though some reports claimed that increased autophagy may

benefit *L. major* intracellular survival, contradictory results about *Leishmania* and autophagy interplay necessitate further research to elaborate this phenomenon.

### **1.6. Type I interferons and *Leishmania* infection**

There are several reports that claim that type I interferon stimulation may increase parasite load or disease severity (Das et al., 2019; Rossi et al., 2017). *ISG15* is one of the most upregulated interferon stimulated genes (ISGs) subsequent to type I interferon signaling. To date, only a single study reported on *L. braziliensis* infection-induced upregulation of ISG15 in dendritic cells (Vargas-Inchaustegui et al., 2008). Whether ISG15 is also upregulated in cells infected with Old World *Leishmania* species or how its expression impacts anti-parasite immunity is not known. Viral infections in mammals induce the production and secretion of type I interferons (IFN $\alpha/\beta$ ) which interferes with viral replication. Type I IFN release results in the upregulation of interferon stimulated genes (ISGs). One ISG is the 15kDa antiviral protein ISG15. ISG15 is a member of the ubiquitin protein family and like ubiquitin, ISG15 is able to covalently bind to target proteins and thereby alter their functions. The covalent conjugation of ISG15 is termed ISGylation and involves a series of reversible enzymatic reactions (Loeb & Haas, 1992). There are numerous intracellular targets of ISG15 including, certain enzymes that are bound and inhibited by ISG15 (Okumura, Pitha, & Harty, 2008). ISG15 also targets ubiquitin-binding sites on proteins, preventing their degradation. Furthermore, this antiviral protein is capable of acting as a cytokine following its release, where it is able to recruit neutrophils to the site of infection or injury (Owhashi et al., 2003), promote the maturation of dendritic cells (DCs) (Padovan et al., 2002), and induce the expression of IFN- $\gamma$  (Bogunovic et al., 2012). The means of ISG15 release from cells remains to be resolved, but there is a study suggesting that ISG15 is carried inside of exosomes (Li Sun et al., 2016). The deconjugation of ISG15 is mediated by Ubl carboxy-terminal hydrolase 18 (USP18) (Malakhov, Malakhova, Il Kim, Ritchie, & Zhang, 2002). Another target of USP18 is the interferon  $\alpha/\beta$  receptor 2 (IFNAR) complex, which leads to the downregulation of IFN signaling (Malakhova et al., 2006). Interestingly, free ISG15 is involved in the

stabilization of USP18, thereby regulating interferon signal transduction (Xianqin Zhang et al., 2015). Based on both *in vitro* and *in vivo* studies, ISG15 was suggested to exert an anti-viral effect since ISG15 deficient cells or mice showed increased viral loads. However, ISG15 deficient human patients are not susceptible to viral infections, suggesting that in humans and mice, ISG15 and ISGylation may mediate separate functions (Xianqin Zhang et al., 2015). ISG15 may interact with other unidentified intracellular proteins and may regulate additional cellular processes (Perng & Lenschow, 2018; Werneke et al., 2011). Future work should unravel the many-faceted role of this protein in immunity to parasites.

### **1.7. Medications used for the treatment of leishmaniasis**

Pentavalent antimonies are the first line of drugs used for the treatment of leishmaniasis. However, increasing resistance to the drug and toxicity associated with its use, have diminished their suitability (Sundar, 2001). Pentamidine and amphotericin are the second line of drugs. Emerging resistance and toxicity has ended the use of pentamidine and high cost and acute toxicity of amphotericin has terminated its usage (Croft & Coombs, 2003). Chemotherapy is the most effective and practical drug treatment for all three major types of leishmaniasis. However, high toxicity, long-term treatment schedule and high cost of the current drugs necessitates investigators to seek for other effective alternatives (Savoia, 2015). Miltefosine, as a third line treatment, is another chemotherapeutic drug that was registered for VL and CL therapy. Short course of treatment and oral efficacy are the advantages of the drug, but teratogenic effects and long duration use related resistance are the drawbacks of Miltefosine (Dorlo et al., 2014). Reported adverse effects of current anti-leishmanial drugs are hepatitis, cardiac arrhythmia, thrombophlebitis and renal dysfunction (Jain & Jain, 2015).

### **1.8. Aims of the thesis**

Leishmaniasis is considered as one of the deadliest neglected tropical infectious diseases. The cost of medications used in treatment, their toxicity and absence of

effective vaccines, hampers elimination efforts. Turkey is one of the endemic countries and the number of *Leishmania* infected individuals is on the rise. To better understand processes involved in immunity to *Leishmania*, we carried out experiments to address questions related to different aspects of this parasitic infection. Our specific aims were as follows:

Aims 1, 2 and 3: Many species of *Leishmania* are stably infected with a dsRNA virus known as the Leishmania RNA virus (LRV). For new world *Leishmania* species, presence of LRV was associated with a more aggressive disease phenotype. Old world *Leishmania* also harbors a different variant of the virus (LRV-2). Whether or not virus infected strains cause severe disease is not known. Furthermore, how LRV is maintained and transmitted in *Leishmania* is not clear. In this thesis, we first hypothesized that the Old World *Leishmania* infecting virus LRV2-1 or its genetic material could be found in exosomes secreted from infected *L. major* parasites, might further modulate immune cells or contribute to virus transmission between parasites. Therefore, we aimed to determine the presence of virus derived signatures within exosomes purified from LRV infected *L. major*.

To address whether LRV-2 infected *Leishmania* exacerbated disease progression, we aimed to compare the infectivity of LRV+ and LRV cured *L. major* strains both in *in vitro* and in *in vivo* experiments. To our knowledge, both of these aims have not been previously addressed for *L. major*.

To be able to compare the infectivity of the virus infected and cleared cells, we required a tool to accurately detect infection rates in our *in vitro* and *in vivo* models. For this, we aimed to generate enhanced green fluorescent protein-luciferase (EGFP-LUC) fusion protein expressing LRV+ and LRV- transgenic strains to be employed in infection models.

Aim 4: cGAS/STING cytosolic nucleic acid pathway plays a prominent role in resistance to various pathogens. Our laboratory's previous work identified that *Leishmania* kinetoplast DNA increased the parasite loads in *Leishmania* infected cells

upon delivery to the cytosol (PhD thesis of Ihsan Cihan Ayanoglu, 2019). Since this data suggested involvement of cGAS/STING signaling pathway, we aimed to carry out infection studies in cGAS, STING and TBK1 knockout cell lines and also tested the activity of a TBK1 inhibitor (Amlexanox) in our *in vitro* and *in vivo* infection models.

Aim 5: Several reports indicate a possible deleterious effect of type I interferon signaling in *Leishmania* infections production (Das et al., 2019; Rossi et al., 2017). ISG15 is one of the most significantly upregulated proteins in response to type I interferon signaling and a central player in the host anti-pathogen immunity. Therefore, we aimed to determine the outcome of *Leishmania* infection in macrophages in which the ISG15 gene was knocked out. To achieve this, we used the LentiCRISPRv2 system and mutated the ISG15 gene in the THP-1 human monocytic cell line genome. Using our *in vitro* infection model, we compared the infection rates in lentivirus control and ISG15 KO cell lines.

During our experiments, we also aimed to investigate important cellular processes involved in *Leishmania* infection, such as parasite phagocytosis studies and assays to reveal autophagic changes taking place in infected cells.

## CHAPTER 2

### MATERIALS AND METHODS

#### 2.1. Parasite Culture and Maintenance

*Leishmania* RNA virus (LRV) positive (+) and negative (-) *Leishmania major* (*L. major*) promastigote parasites were kindly provided by Prof. Ahmet Özbilgin from the Department of Molecular Parasitology at Celal Bayar University, in two separate *Leishmania* growth media (Table A.1., A.2., Appendix A). Plug sealed tissue culture flasks (SPL, South Korea) were used to culture promastigote parasites at 26°C without CO<sub>2</sub>. Parasites were diluted to early-log phase ( $5 \times 10^6$ /ml) every 2-3 days upon reaching late-log phase ( $25 \times 10^6$ /ml). The parasite growth curves were established in previous studies in our laboratory (Ayanoglu, 2019). Parasites were quantified on a Novocyte 2060R flow cytometer (ACEA Biosciences, U.S.A.) based on forward and side scatter gated parasite numbers per acquired volume. Cryopreservation of parasites was achieved by mixing the mid-log phase parasite suspension (in null RPMI-1640 medium) with an equivalent volume of *Leishmania* freezing medium (Table A.3., Appendix A). One ml cell suspension was then transferred into 2 ml cryogenic vials (Corning, U.S.A.) and the parasites were frozen at -80°C overnight in a Mr. Frosty™ freezing container (Thermo Fisher Scientific, U.S.A.) The next day, cryovials were transferred to a liquid nitrogen tank for long term storage. Frozen parasite stabilates were thawed at 37°C and re-suspended in *Leishmania* growth medium for in vitro and in vivo experiments.

#### 2.2. Isolation of *L. major* exosomes from cultured parasites

To isolate *L. major* exosomes, we modified our laboratory's former exosome isolation procedure (Ayanoglu, 2019) and exosome isolation procedures used in several other studies (Hassani et al., 2011; J. M. Silverman, Clos, De'Oliveira, et al., 2010; Woalder,

2017). First, since FBS supplementation in *Leishmania* growth medium would also contain exosomes originating from the serum, FBS was centrifuged at 100,000g for 3 hours at 4°C to obtain exosome-free FBS. Then, late-log phase *L. major* promastigotes were washed with DPBS and resuspended at a neutral pH in RPMI-1640 supplemented with 1% (v/v) exosome-free FBS, 1% (w/v) D-glucose, 1% (v/v) penicillin-streptomycin, 20 mM HEPES at a concentration of 10<sup>8</sup> promastigotes/ml in T-75 flasks with a ventilated cap (Sarstedt, Germany) and incubated for 12 hours at 37°C (Barbosa et al., 2018). While axenic parasites were cultured and maintained at 26°C, for exosome isolation, *Leishmania* were subjected to a temperature switch to 37°C in order to increase exosome release *in vitro* (Hassani et al., 2011; J. M. Silverman, Clos, De'Oliveira, et al., 2010). Following the completion of incubation period, exosomes were precipitated at 1,500g for 10 minutes. Next, the samples were spun at 15,000g for 30 minutes at 4°C to remove debris and small components other than exosomes in an ultra-centrifuge (Hitachi, Japan). Then, the supernatant was filtered through a 0.22 µm syringe filter (Jet-Biofill, China) to eliminate remaining cellular debris. Subsequently, exosomes were precipitated at 100,000g for 1.5 hours at 4°C. The pellet was re-suspended in DPBS (20ml) and centrifuged again at 100,000g for 1.5 hours at 4°C. For some experiments related to RNA isolation from exosomes, the exosomal pellet was treated with 100 µg/ml Proteinase K for 30 minutes at 37°C for degradation of bound proteins. Then the volume was increased to 20 ml with DPBS and the sample was centrifuged again at 100,000g for 1.5 hours at 4°C. Final exosomal pellets were resuspended in DPBS (100 µl), and from this point on, the exosome suspension was ready for quantification with Qubit™ Protein Assay Kit (Invitrogen, U.S.A.) or subjected to RNA isolation.

### **2.2.1. Isolation of exosomal RNA**

The exosome suspension was treated with 50 µg/ml RNase A for 20 minutes at room temperature (RT) before lysis with TRIzol reagent (Thermo Fisher Scientific, U.S.A.). The aqueous phase containing exosomal RNA was obtained according to the manufacturer's instructions. RNA clean and concentrator kit (Zymo Research, U.S.A.)

was used for the isolation of exosomal RNA from the aqueous phase according to the manufacturer's recommendations. The same protocol was utilized for RNA isolation from *L. major* LRV + and LRV – strains, as a control.

### **2.2.2. cDNA synthesis**

cDNA synthesis was performed using ProtoScript® First Strand cDNA Synthesis Kit (New England BioLabs, U.S.A). 4.8 µl exosomal RNA was mixed with 1.2 µl DMSO (final 15% v/v) and 2 µl random primer mix (6 µM final concentration) and incubated at 94°C for 8 minutes in order to denature any dsRNA of LRV origin that might be present in exosomes collected from LRV+ strain (Mijatovic-Rustempasic et al., 2013). Subsequently, PCR tubes were rapidly placed on ice in order to minimize the formation of secondary structures. After this step, 10 µl of M-MuLV Reaction Mix and 2 µl of M-MuLV Enzyme Mix were added into the previously prepared mixture. Negative control was prepared by adding 2 µl dH<sub>2</sub>O instead of the M-MuLV Enzyme Mix to 10 µl of M-MuLV Reaction Mix. Mixtures were incubated for 5 minutes at RT and then at 42°C for 1 hour. Reverse transcriptase was inactivated by incubation at 80°C for 5 minutes

### **2.2.3. PCR amplification of LRV 2-1 specific sequences.**

Two primer pairs were designed to detect LRV 2-1 specific sequences: LRV2-1\_Fa: 5'-TGTTGAGGCTGCACTACCAG-3' and LRV2-1\_R: 5'-CCGCTGTGGCAAACATTTCA-3' which amplify 3350 base pairs of LRV2-1 genome; LRV2-1\_Fb: 5'-TCACAGCACTCACTAGCTGC-3' and LRV2-1\_R: 5'-CCGCTGTGGCAAACATTTCA-3' which amplify 757 base pairs of LRV2-1 genome from exosomal cDNA. Q5® Hot Start High-Fidelity 2X Master Mix (New England BioLabs, U.S.A) was used to detect 3350 and 757 base pairs of LRV2-1 genome according to the manufacturer's instructions. PCR amplification steps are summarized in Table 2.1.

Table 2.1. PCR amplification conditions

temperature (°C)	duration	
98	4 minutes	35 cycles
98	25 seconds	
68	25 seconds	
72	30 seconds	

#### 2.2.4. Sequencing of PCR amplified LRV 2-1 specific sequences

The 3350 bp PCR amplified fragment of the LRV2-1 genome was sequenced by next-generation sequencing using Miseq System (Illumina, USA) via the service of Sentegen (Turkey).

### 2.3. Generation of EGFP-LUC fusion protein-expressing transgenic parasites

A custom vector was previously designed and synthesized to encode for the EGFP-LUC fusion protein in our lab (Ayanoglu, PhD thesis, 2019). Transgenic strains of LRV- or LRV+ *L. major* were generated separately using two different strategies based on their restricted antibiotic selection requirements as described below.

#### 2.3.1. Generation of LRV negative transgenic *L. major*

Plasmid pLEXSY-neo2.1 (Jena Biosciences, Germany) was custom-designed to encode EGFP-LUCIFERASE (LUC) fusion sequence that was not a ligation product. The chemically synthesized vector was codon-optimized for *L. major* protein expression by Jena Biosciences (<https://www.jenabioscience.com/images/103bb272b3/EGE-273.txt>).

Codon optimized EGFP-LUC fusion sequence and vector map are listed in Appendix B. After the pLEXSY vector is linearized and transfected into the parasites, it integrates into the chromosomal 18S sRNA locus through homologous recombination, where constitutive mRNA transcription takes place (Bolhassani et al., 2011). The plasmid was expanded in and isolated from *E. coli* DH5 $\alpha$  using Qiagen Midi Plasmid isolation

kit according to the manufacturer's instructions. A minimum of 5 µg plasmid was linearized with the restriction enzyme *SwaI* (New England Biolabs, U.S.A.). After successful linearization, the expression cassette was detected using agarose gel electrophoresis. Linearized DNA was electroporated inside the parasites using the Gene Pulser® II Electroporation System (Biorad, U.S.A.). Mid-log phase parasites (~15x10<sup>6</sup> parasites/ml) were pelleted at 1,500g for 10 minutes at RT and re-suspended in the electroporation buffer at a concentration of 10<sup>8</sup> promastigotes/ml (Appendix A). Then, linearized 5 µg DNA and 400 µl of parasites were mixed inside 0.2 cm gap electroporation cuvette (Biorad, U.S.A.). Parasites were immediately electroporated three times at 3750V/cm, 25 µF and 200 Ω; 3750V/cm, 25 µF and 100 Ω; and 3750V/cm, 25 µF and 50 Ω. After three pulses, the cuvettes were immediately incubated on ice for 10 minutes. Next, electroporated parasites were transferred to the *Leishmania* growth medium and were supplemented with selection antibiotics 24 hours after the initial inoculation. Enrichment of transgenic parasites was confirmed with fluorescence microscopy (for eGFP expression) for a period of at least three weeks. 50 µg/ml of Neomycin (Jena Biosciences, Germany) was used for the selection of EGFP-LUC expressing LRV- *L. major* strain.

### **2.3.2. Generation of LRV positive transgenic *L. major***

Aminoglycoside antibiotics like Hygromycin B were reported to be negative regulators of LRV survival via their effects on viral protein expression (Y T Ro, Scheffter, & Patterson, 1997a). Neomycin is a well-known aminoglycoside antibiotic similar to Hygromycin B. Therefore, selecting transgenic LRV + *L. major* with neomycin would cause the loss of LRV from parasites (Fourmy, Recht, & Puglisi, 1998). Blasticidin, on the other hand, can be utilized for selection since it is a peptidyl nucleoside antibiotic, which *Leishmania* is known to be sensitive to (Goyard & Beverley, 2000). Therefore, the neomycin resistant gene of pLEXSY-neo2.1 plasmid containing *EGFP-LUC*, was replaced with a blasticidin resistance gene by using the BlaF: 5'- CGCATGGATCCAATATGAAGACCTTCAACATCTCTCAGC-3' and BlaR: 5'- CGCATACTAGTTTAGTTCCTGGTGTACTTGAGGG-3' primer pair.

The pUNO1-hSTING-WT plasmid (Invivogen, France) (Appendix B) was used as a template to amplify the blasticidin resistance gene. PCR amplification was performed with the Q5® Hot Start High-Fidelity 2X Master Mix according to the manufacturer's instructions. The product was digested with the *Bam*HI and *Spe*I restriction enzymes and replaced with the neomycin resistance gene of the pLEXSY-neo2.1 plasmid that contains *EGFP-LUC*. *E. coli* DH5 $\alpha$  strain was used as the host organism for the cloning of the newly designed pLEXSY-bla2.1 plasmid (Bolhassani et al., 2011). Next, LRV+ *L. major* parasites were electroporated as described in section 2.3.1 with the linearized pLEXSY-bla2.1 plasmid that contains *EGFP-LUC*, followed by antibiotic selection using 10  $\mu$ g/ml blasticidin (Invivogen, France).

## **2.4. Generation of THP-1 Dual ISG15 Knock out cell line**

### **2.4.1. Oligo design and cloning**

*ISG15* knock-out in THP1-Dual™ cells (Invivogen, France) was performed using the LentiCRISPR v2 system that utilizes a single guide RNA (sgRNA) scaffold and nonhomologous end-joining (NHEJ) knock out strategy (Sanjana, Shalem, & Zhang, 2014; Shalem et al., 2014). The single oligo pair was designed according to the recommendations of Zhang lab for the *ISG15* gene (<https://crispr.mit.edu>).

The selected oligo pair was: 5'-CACCGGCTGGCGGGCAACGAATTCC-3' and 5'-AAACGGAATTCGTTGCCCGCCAGCC-3', which targets the second exon of the *ISG15* gene. According to the website software, the arbitrary success score of this oligo pair was 94% and off-targets were reported outside the coding region of the genome (<https://crispr.mit.edu>). The TLCV2 plasmid was used as a LentiCRISPR v2 transfer vector system to produce sgRNA (Barger, Branick, Chee, & Karpf, 2019). In order to clone this oligo pair inside the TLCV2 vector, 5  $\mu$ g TLCV2 plasmid was digested with FastDigest Esp3I and dephosphorylated with FastAP Thermosensitive Alkaline Phosphatase in the presence of 100 mM DTT and FastDigest buffer (Thermo Fisher Scientific, U.S.A.) for 30 minutes at 37°C. Agarose gel electrophoresis revealed a 10 kb fragment, which was subsequently purified from the gel with NucleoSpin® Gel

and PCR Clean-up kit (Macherey Nagel, Germany). Phosphorylation and annealing of the complementary oligo pair was performed by mixing 1  $\mu$ l of 100  $\mu$ M Oligo 1 and 1  $\mu$ l of 100  $\mu$ M Oligo 2 with 1  $\mu$ l of 10X T4 Ligation Buffer and 0.5  $\mu$ l of T4 PNK (New England BioLabs, U.S.A) which was completed to 10  $\mu$ l with ddH<sub>2</sub>O. The reaction was carried out in a thermocycler starting at 37°C for 30 minutes, then set to 95°C for 5 minutes but ramping down 5°C per minute to 25°C. Afterwards, the annealed oligo pair was 1:200 diluted and ligated to previously digested TLCV2 with Quick Ligase (New England BioLabs, U.S.A) for 10 minutes at RT and transformed into *E. coli* Stbl3 competent cells. After antibiotic selection with 100  $\mu$ g/ml Ampicillin (Sigma-Aldrich, Germany), plasmids were isolated from the growing colonies and send to sequencing to identify correct clones. THP-1 Dual lentivirus control (LVC) cell line was established via the self-ligation product of TLCV2.

#### **2.4.2. Lentiviral vector production**

In order to generate replication-deficient lentivirus that can produce *ISG15* specific sgRNA, the plasmids TLCV2, psPAX2 and pCMV-VSV-G were utilized for transfer, packaging and envelope protein expression, respectively (Stewart et al., 2003; Wei et al., 2010) (Appendix B).  $2.5 \times 10^5$  cell/ml HEK 293FT cells were cultured in 6-well plates (Sarstedt, Germany) containing 2 ml of seeding media (Appendix B) and incubated for 36 hours until 70-80% cell confluency. 2  $\mu$ g TLCV2, 1.59  $\mu$ g psPAX2 and 0.88  $\mu$ g pCMV-VSV-G per well were mixed in 250  $\mu$ l OptiMEM media (Thermo Fisher Scientific, U.S.A.) and incubated for 5 minutes at RT. Parallel to this, 10  $\mu$ l Lipofectamine 2000 (Thermo Fisher Scientific, U.S.A.) and 250  $\mu$ l OptiMEM media were mixed and incubated for 5 minutes at RT. Two mixtures were combined and incubated for 30 minutes for complexation. Next, the transfection mix (500  $\mu$ l) was added to HEK 293FT cells in seeding media. After incubation for 18 hours at 37°C, cells were checked for GFP expression via fluorescence microscopy to assess transfection efficiency. In order to remove the transfection reagent, seeding media was replaced with harvest media (Appendix B) at the end of the 18 hours incubation period.

Viruses were harvested every 24 hours for three days. Collected harvest media was centrifuged at 500g for 10 minutes to get rid of cell debris, filtered with 0.45 µm filter, and subsequently stored at -80°C.

#### **2.4.3. Lentiviral transduction of THP-1 Dual cells**

THP-1 Dual cells were inoculated on 6-well plates at a density of  $3 \times 10^5$  cells/well in 1 ml of LentiRPMI 1640 medium (Appendix A., Table A.5.) without any selective antibiotics. Then, 1 ml of harvest medium that contains replication-deficient lentivirus was added onto THP-1 Dual cells accompanied with 10 µg/ml polybrene (Merck, Germany) and 1.25 µg/ml doxycycline (Sigma Aldrich, Germany). Plates were spinoculated at 1000g for 1 hour at 32°C (Zeisig & Wai Eric So, 2009). Following a 24 hour incubation period at 37°C, cell culture media was replenished with 2 ml of LentiRPMI 1640 medium supplemented with 1.25 µg/ml puromycin (Invivogen, France). Once puromycin resistant THP-1 Dual cells reached a confluency of  $1 \times 10^6$  cells/ml, they were diluted and inoculated in 96 well plates (Sarstedt, Germany) at a density of 0.5 cells/well. Here, the aim was to obtain a single cell in each well of the plate which was assessed via phase-contrast microscopy. Single-cell colony formation was followed for at least 45 days.

#### **2.4.4. Confirmation of *ISG15* knock out clones**

At least 30 colonies were analyzed for the absence of ISG15 protein by western blot (Section 2.5.4.) using specific anti-ISG15 antibody (Santa Cruz, U.S.A.). Genomic DNA from one colony that proved to lack the ISG15 protein was isolated. The genomic region that should bear the mutation because of NHEJ was amplified with the primer pair of 5'- GTGCCAGCCAATTTTCGTCTC - 3' and 5'- TATTTCCGGCCCTTGATCCT - 3' via Q5® Hot Start High-Fidelity 2X Master Mix according to manufacturer's instructions. The amplified 907 base pair fragment was subjected to Sanger and next-generation sequencing by SeqStudio Genetic

Analyzer (Thermo Fisher Scientific, U.S.A.) via services of MedSanTek and Miseq System, respectively.

## **2.5. *In vitro* infection with transgenic EGFP-LUC expressing *L. major***

### **2.5.1. Cell culture**

THP1-Dual™, THP1-Dual™ KO-cGAS, THP1-Dual™ KO-STING, THP1-Dual™ KO-TBK1 (Invivogen, France), THP-1 Dual ISG15KO and THP-1 Dual LentiControl (LVC, this study) were infected with transgenic LRV+ and LRV- *L. major* strains at different conditions. THP1-Dual cell lines were maintained in 10% (v/v) FBS supplemented RPMI 1640 medium (Appendix A) containing 100 µg/ml zeocin and 10 µg/ml blasticidin (Invivogen, France), while THP-1 Dual ISG15KO and THP-1 Dual LVC were maintained in 10% (v/v) tetracycline free FBS supplemented RPMI 1640 (Appendix A). All mammalian cell lines used in this study were maintained at an initial concentration of  $5-7 \times 10^5$  cells/ml and sub-cultured before their density reached  $2 \times 10^6$  cells/ml. THP-1 Dual cells were counted using Novocyte 2060R flow cytometer (ACEA Biosciences, U.S.A.) based on forward and side scatter gated cell numbers per acquired volume.

As an *in vitro* infection model, THP-1 Dual monocytes were differentiated to macrophages with phorbol myristate acetate (PMA) (Invivogen, France) at high (50ng/ml) and low (5ng/ml) concentrations. THP-1 Dual cells treated with 50 ng/ml PMA were incubated for 24 hours, while cells treated with 5 ng/ml PMA were incubated for 48 hours at 37°C in a 5% CO<sub>2</sub> incubator. In order to achieve the same number of the cells in every infection study, cells were primarily inoculated in T75 tissue culture flasks (SPL, South Korea). Adherent macrophages were detached using accutase solution (Biolegend, U.S.A.). Differentiated THP-1 cell lines were then inoculated in 96-well plates and 6-well plates at a density of  $10 \times 10^5$ /well and  $1 \times 10^6$ /well, respectively, in 2% (v/v) FBS supplemented RPMI 1640 medium (Appendix A).

### **2.5.2. Metacyclic parasite preparation for *in vitro* infection studies**

Since the metacyclic stage of *Leishmania* parasites is more virulent than other procyclic stages (Sacks & Perkins, 1984), stationary phase parasites were incubated for an additional 2-3 days at this state to enrich metacyclic parasites. *In vitro* infection of THP-1 Dual cells were optimized to 1:10 multiplicity of infection (MOI), so that  $1 \times 10^6$  parasites/well and  $10 \times 10^6$  parasites/well were used to infect THP-1 cells in 96-well plates and 6-well plates, respectively. Opsonization of *Leishmania* parasites with human serum was performed by incubating parasites in null RPMI 1640 media supplemented with 1% human serum for 15 minutes at RT. In the process of infection, parasites and THP-1 cells were always incubated with 2% (v/v) FBS supplemented RPMI 1640 medium (Appendix A). Parasites were removed from the media, and THP-1 cells were washed with DPBS and cultured in 10% (v/v) FBS supplemented RPMI 1640 medium. The infection process includes the co-incubation of THP-1 cells with parasites, whereas the proliferation process of *Leishmania* parasites begins after their removal from the culture media.

### **2.5.3. Detection of infection rates of THP-1 cell lines**

Following the infection and proliferation incubations, THP-1 cells were detached from 96-well plates using cold DPBS and from 6-well plates with accutase solution. Supernatants of infected cells were discarded and cells from 96-well and 6-well plates were incubated either with 150  $\mu$ l DPBS on ice or 250  $\mu$ l accutase at RT, respectively. Detached and collected cells were analyzed via flow cytometry. Since parasites express GFP, infection levels were determined according to green fluorescence intensity on the BL1 channel of the flow cytometer.

Different drug treatments were tested to alter wild type infection rate as follows: 40  $\mu$ M chloroquine (Sigma-Aldrich, Germany) 2 hours prior to infection, 500 nM rapamycin (Invivogen, France) 18 hours prior to infection, 500nM bafilomycin A1 (Invivogen, France) 1 hour prior to infection and 64  $\mu$ g/ml amlexanox (Invivogen, France) at least 1 hour prior to infection.

#### **2.5.4. Western Blotting**

At the end of various infection time points, cells were pelleted at 300g for 5 minutes and lysed with M-PER™ mammalian protein extraction reagent (Thermo Fisher Scientific, U.S.A.) supplemented with 1X cOmplete Mini EDTA free protease inhibitor cocktail and PhosSTOP™ (Sigma-Aldrich, Germany).  $1 \times 10^6$  cells were lysed with 70  $\mu$ l M-PER mix and incubated on ice for 30 minutes. Next, cell lysates were centrifuged at 15000g for 15 minutes at 4°C and supernatants that contain the soluble proteins were transferred to new tubes and stored at -20°C.

40  $\mu$ g protein extracts were denatured in 6X Laemmli buffer (Appendix C) at 95°C for 5 minutes. Proteins were separated via 4–20% Mini-PROTEAN® TGX Stain-Free™ gels (Biorad, U.S.A.) and transferred onto a nitrocellulose membrane (Biorad, U.S.A.) at 250 mA for 1 hour using the XCell SureLock Mini-Cell transfer system (Thermo Fisher Scientific, U.S.A.). 5% non-fat milk in Tris Buffer Saline- Tween (TBS-T) was used to block membranes (Appendix C) for 1 hour and then washed with TBS-T, three times for 5 minutes. Membranes were then incubated with the primary antibody (Appendix C) for 16 hours at 4°C, washed and incubated with species-specific secondary anti-IgG antibody for 1 hour at RT. Following three washing steps with TBS-T, proteins were visualized with WesternBright Sirius Chemiluminescent Detection Kit (Advansta, U.S.A.) according to manufacturer's instructions. Image lab software (Biorad, U.S.A.) was used to quantify band intensities of the proteins.

#### **2.6. Comparison of infectivity of LRV+ versus LRV- *L. major* strains in *in vivo* mouse infection model**

6-10 weeks old adult, male BALB/c mice were used for *in vivo* experiments. Animal care and maintenance took place at the Animal Facility of Molecular Biology and Genetics Department at Bilkent University (Ankara, Turkey). 12 hours of light and dark cycles at 22°C, as well as ad libitum food and water, were provided at the animal

facility. All protocols and conditions were carried out under the supervision of the Bilkent University animal ethical committee.

### **2.6.1. LRV– and LRV+ *L. major* virulence comparison**

Metacyclic LRV- and LRV+ parasites were pelleted and adjusted to a density of  $1.8 \times 10^8$  parasites/ml in DPBS at 1500g for 10 minutes.  $9 \times 10^6$  parasites that were re-suspended in 50  $\mu$ l DPBS were injected to the left footpads of mice using a 1 ml syringe with a 26G needle (Ayset, Turkey). Lesion development was monitored for 40 days and footpad sizes were measured with a digital caliper on indicated day intervals. Luciferase-expressing parasite loads in footpads were assessed based on luciferase bioluminescence measured using the *in vivo* Imaging System (IVIS).

#### **2.6.1.1. IVIS measurements of parasite loads in footpads**

Isoflurane vaporizer (VetEquip, U.S.A.) was used to anesthetize mice before footpad imaging. 50  $\mu$ l of D-Luciferin (Perkin Elmer, U.S.A.) was intraperitoneally injected to all mice at a concentration of 0.75 mg/mouse. IVIS Lumina III (Perkin Elmer, U.S.A.) was utilized to measure footpad parasite loads (which correlate with luciferase luminescence) with a FOV24 lens. Mice were kept anesthetized during the imaging process by the integrated gas flow unit. Regions of interest (ROI) (left feet of mice) images were recorded 40 times at every 30 seconds, making the total time-lapse 20 minutes.

### **2.6.2. Amlexanox therapy for the LRV- *L. major* infected mice**

After virulence comparison of LRV- and LRV+ parasites, seven mice that were infected with the LRV- *L. major* parasites, were used for the amlexanox therapy study. Four mice were injected with 50  $\mu$ l of 10 mg/ml amlexanox 41 days post-infection (p.i) intraperitoneally every 24 hours for 14 days and three mice were injected with 50  $\mu$ l of DMSO as a control. Footpad sizes were measured with a digital caliper and IVIS measurements were recorded as described at 2.6.1.1.

## CHAPTER 3

### RESULTS & DISCUSSION

#### **3.1. Detection of the Leishmania RNA virus 2-1 (LRV 2-1) in LRV + *L. major* exosomes**

Leishmania RNA Virus-1 (LRV-1) is a non-enveloped dsRNA virus of *Totiviridae* family, which infects New World Leishmania species (Giovanni Widmer & Dooley, 1995). Presence of LRV-1 was associated with exacerbation of disease and the development of mucocutaneous leishmaniasis in infected organisms (Ives et al., 2011). Interestingly, a separate group of LRV, named as LRV2 was first isolated from the non-human *Leishmania* parasite (*hertigi*) (Molyneux, 1974). LRV 2-1 was then found (Tax: 39116) in Old World *Leishmania* field isolates, including species from *L. major*, *L. aethiopica* and *L. infantum* (Hajjarian et al., 2016; Kleschenko et al., 2019; Nalçacı et al., 2019). Whether LRV2 affects disease severity is not known. In mice, infections caused by LRV1 carrying *L. guyanensis* initiates metastasizing mucocutaneous leishmaniasis in a TLR3 and type I interferon dependent manner (Ives et al., 2011). Virus-activated type I interferon production induces autophagy and results in ATG5-mediated degradation of inflammasome components NLRP3 and ASC, contributing to increased parasite survival and disease progression (de Carvalho et al., 2019). However, the impact of LRV2-1 presence in infections caused by Old World *Leishmania* species remains to be determined. Furthermore, since LRV1 and LRV2 are unable to produce extracellular infectious particles, how the virus infects *Leishmania* is not known (G Widmer, 1995). Therefore, in this part of the thesis we aimed to determine i) whether LRV2-1 contributes to disease severity in *L. major* induced cutaneous leishmaniasis in mice and ii) how LRV2-1 infects the parasites as described in the following sections. For this, we first obtained an LRV+ strain of *L. major* from our collaborators (Ahmet Ozbilgin, Celal Bayar University, Medical

Faculty). To confirm that the parasite indeed harbored the virus, we analyzed the presence of the viral genome in parasite RNA extracts. The LRV 2-1 genome is 5241 base pairs long and can be detected via straightforward RNA isolation and agarose gel electrophoresis (Scheffter et al., 1995) (Figure 3.1.).

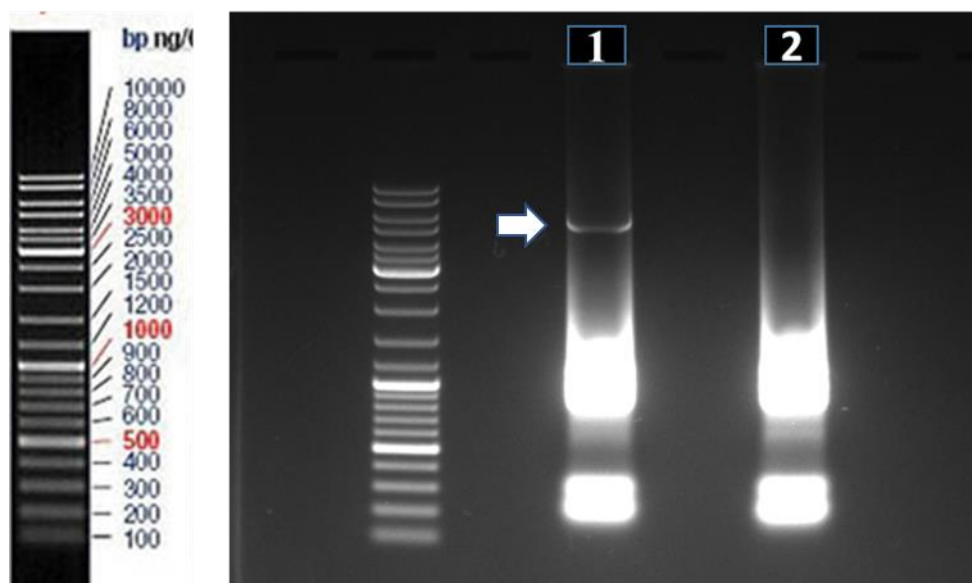


Figure 3.1. Presence of 5241 bp LRV dsRNA genome inside the *L. major* strain.

Total RNA of parasites were isolated as described in Section 2.2.1. and run at 100 V for 50 minutes on a 1% agarose gel.

Lane 1: Total RNA of LRV+ parasites, Lane 2: Total RNA of LRV- parasites

Figure 3.1. demonstrates that RNA isolated from the LRV+ strain of *L. major* displayed an additional band corresponding to the dsRNA virus genome of ~ 5000 bp in length (Lane 1; indicated by a white arrow), which was absent in RNA extracted from the LRV- *L. major* strain (Lane 2).

As mentioned above, since LRV does not produce extracellular infectious particles, how the virus spreads between parasites is unknown. *Leishmania* parasites can secrete exosomes enriched in parasitic proteins like gp63, elongation factor -1 $\alpha$ , and heat

shock proteins 90 and 70 which have immunomodulatory properties and are known to induce an indulgent environment for parasite infection *in vivo* (J. M. axwel. Silverman & Reiner, 2011). Exosomes have previously been shown to contribute to spread of viral infections (Ramakrishnaiah et al., 2013). Taken together, we hypothesized that LRV+ *L. major* exosomes may bear LRV2-1 and may serve as carriers of the virus which we addressed in the following *in vitro*. At the time when we initiated this study, evidence for exosome-mediated transfer of LRV between *Leishmania* was nonexistent. However, during the course of our experiments, an article was published demonstrating that exosomes derived from LRV1-infected *Leishmania* harbor viral particles and function in transfer of the virus to uninfected parasites (Atayde et al., 2019).

### **3.1.1. Analysis of LRV+ *L. major* exosomes for the presence of LRV2-1 specific RNA**

Isolated *Leishmania* exosomes (from LRV- strains) have previously been characterized and analyzed using atomic force microscopy (AFM) in our laboratory (Ayanoğlu, 2019); therefore, following exosome isolation, we first aimed to determine whether exosomes obtained from the LRV+ strain expressed the viral double stranded RNA or not. For this, we exploited two different approaches. In one approach, we probed the exosomes for the presence of dsRNA using the J2 monoclonal antibody specific to dsRNA as described previously (Zangger et al., 2013). For this, various concentrations of whole parasites, exosomes, poly I:C dsRNA positive control or poly U ssRNA negative control were spotted onto nitrocellulose membranes, dried and probed with mouse J2 anti-dsRNA antibody. Following incubation with anti-mouse IgG HRP conjugated secondary antibody, membranes were developed and imaged as shown in Figure 3.2.

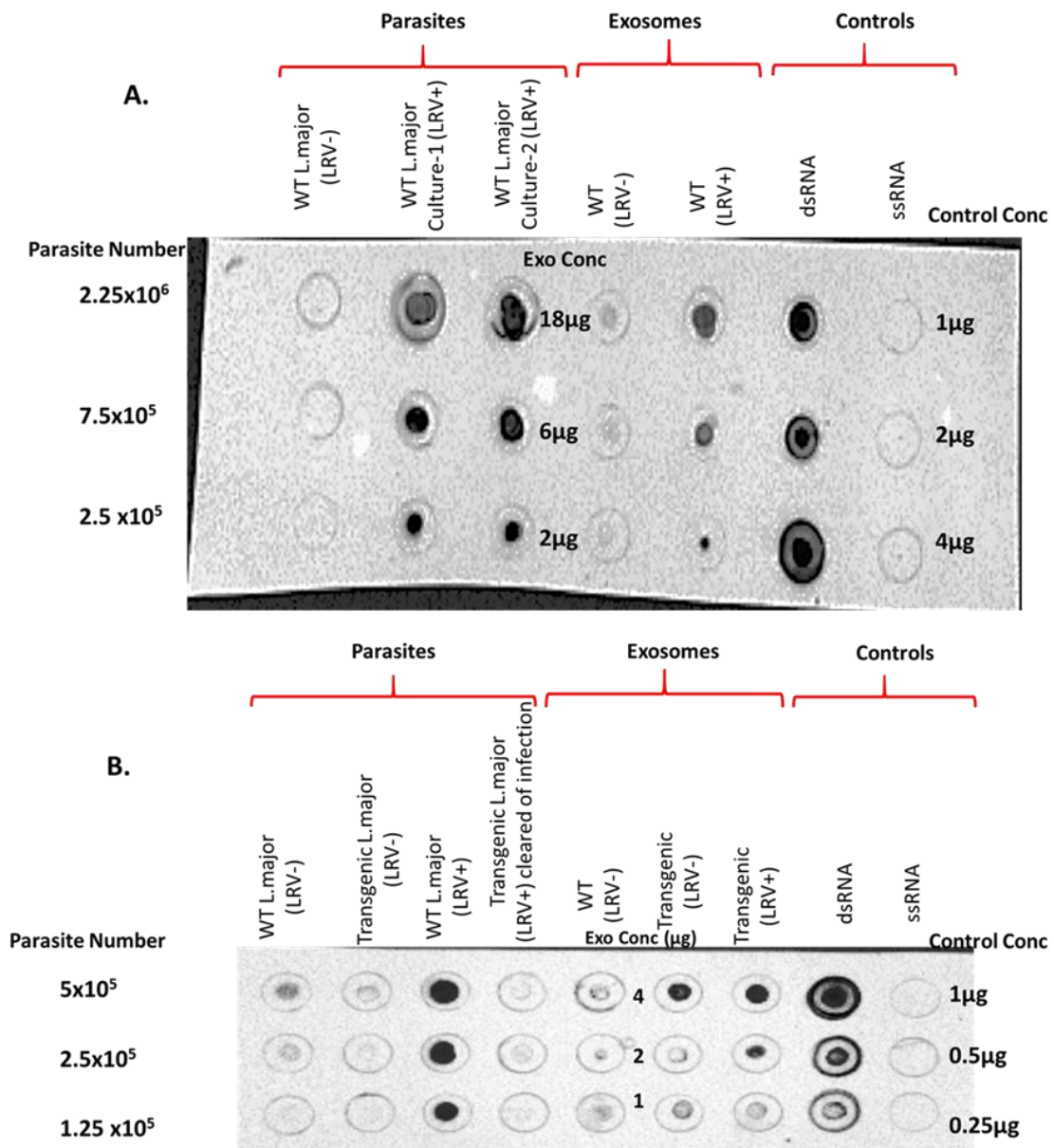


Figure 3.2. Use of J2 antibody on Dot Blot

LRV+ parasites and exosomes isolated from LRV+ strains specifically harbored higher concentrations of dsRNA than their LRV- counterparts

Based on these findings, we proceeded to utilize a more specific molecular approach to delineate the presence of the viral genome in the exosomal compartment as describe below.

Total RNA isolation from exosomes and conducting agarose gel electrophoresis to directly demonstrate the presence of viral dsRNA was not sensitive enough to understand whether exosomes carried LRV2-1 or not, since exosomal RNA yields remained low, precluding application of high concentrations to agarose gels. In order to overcome this problem, we performed cDNA synthesis from isolated RNA using random hexamer primers followed by LRV2-1 sequence-specific amplification. The products of this step were then sequenced to confirm the *bona fide* presence of LRV2-1 specific sequences in exosomes. Our PCR analysis was based on the fact that the LRV2-1 genome has two long open reading frames that encode capsid proteins and RNA-dependent RNA polymerase (RDRP) which reside between the 341-2485 bp and 2858-5191 bp of the total 5241 bp dsRNA genome, respectively (Figure 3.3.).

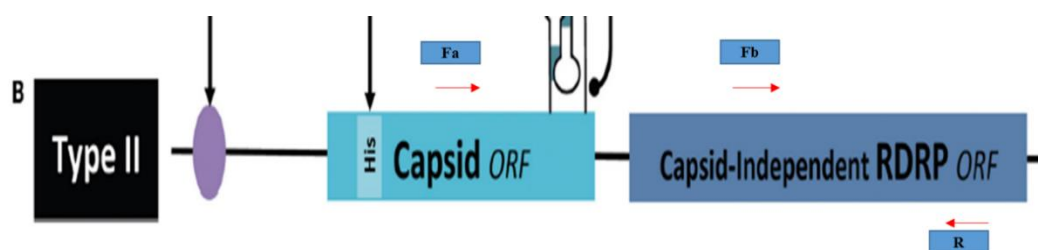


Figure 3.3. LRV2-1 dsRNA genomic organization.

Fa: LRV2-1\_Fa primer, Fb: LRV2-1\_Fb primer, R: LRV2-1\_R primer (Section 2.2.3.) (Hartley et al., 2012).

The LRV2-1\_Fa and LRV2-1\_R primer pair amplifies between 1381-4730 base pairs and forms a 3350bp long product, whereas the LRV2-1\_Fb and LRV2-1\_R pair amplifies the region between 3974-4730 base pairs, forming a 757 bp sized product.

Once we set our PCR based LRV2-1 dsRNA genome detection strategy using the primer pairs of LRV2-1\_Fa, Fb, R, and exosomal cDNA as template, we conducted PCR amplification using a Q5 polymerase (Figure 3.4. and Figure 3.5.).

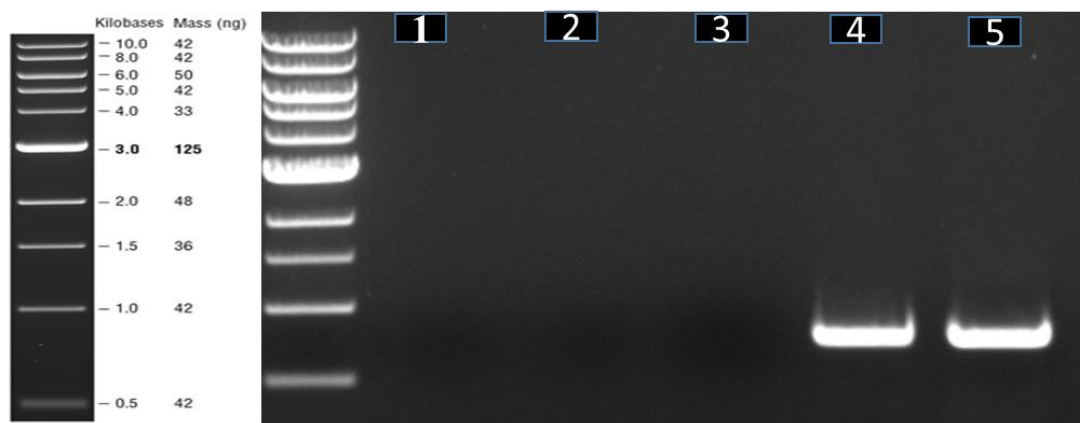


Figure 3.4. Detection of LRV2-1 specific sequence inside the exosomes by primer pair of LRV2-1\_Fb and LRV2-1\_R.

The 757 base pairs amplified region resides inside the RDRP.

Lane templates- Lane 1: No template, Lane 2: LRV- exosomal cDNA, Lane 3: LRV+ exosomal cDNA control, Lane 4: LRV+ exosomal cDNA, Lane 5: LRV+ *Leishmania* cDNA as positive control.

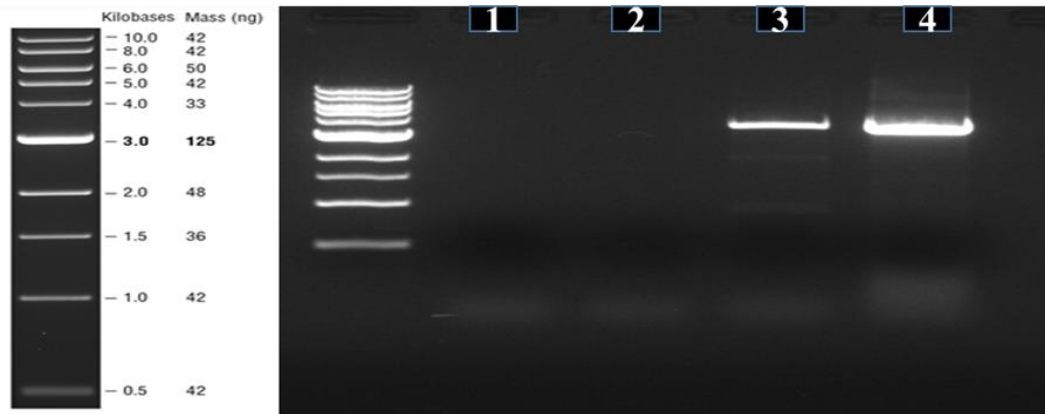


Figure 3.5. Detection of LRV2-1 specific sequence inside the exosomes by primer pair of LRV2-1\_Fb and LRV2-1\_R.

The 3350 base pairs amplified region resides inside the Capsid-RDRP.

Lane templates- Lane 1: No template, Lane 2: LRV+ exosomal cDNA control, Lane 3: LRV+ exosomal cDNA, Lane 4: LRV+ Leishmania cDNA as positive control.

Figures 3.4 and 3.5 collectively demonstrate that LRV+ *L. major* exosomes contain LRV specific sequences. LRV+ exosomal cDNA control contains all the cDNA synthesis ingredients except the enzyme mix that includes reverse transcriptase; therefore, any genomic DNA contamination that can cause non-specific amplification should be eliminated. Amplification of 757 and 3350 base pair regions from the template of LRV+ exosomal cDNA and its control but not the LRV- exosomal cDNA demonstrate that LRV2-1 specific sequences are present specifically inside the exosomes of LRV+ *L. major*. Of note, it was important to treat the exosomes with proteinase K and RNase prior to RNA isolation to ensure that the LRV specific sequences resided inside the exosomes and were not contaminants of cellular fractions less than 200nm in the final pellet (Théry et al., 2018).

To further demonstrate that the amplified 3350 base pair fragment was part of the LRV2-1 genome and not any non-specific amplification product, the 3350 base pair amplified fragment from LRV+ exosomal cDNA was eluted from the agarose gel and

sent to next-generation sequencing (NGS). Results were evaluated with Unipro UGENE v1.32.0 software and are demonstrated in Figure 3.6 (and Appendix B).

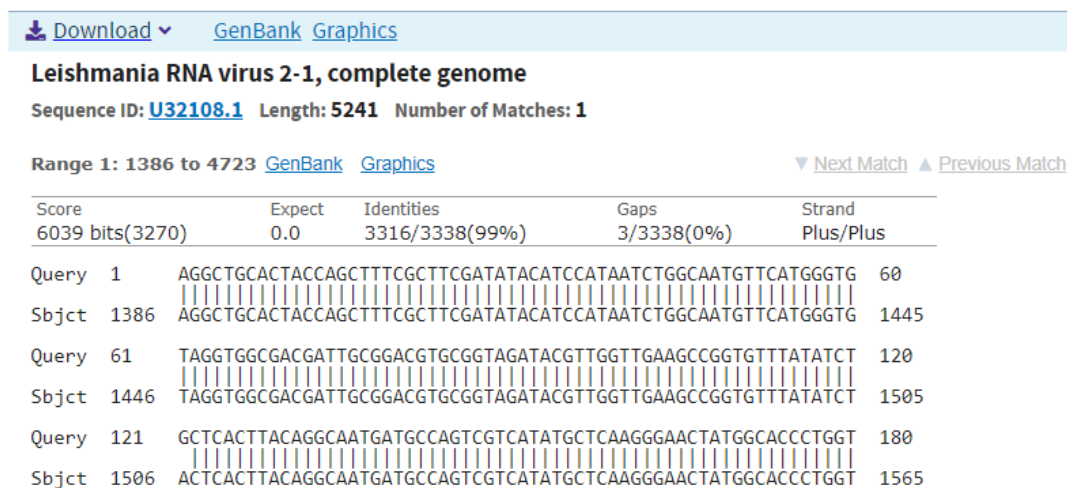


Figure 3.6. Next-generation sequencing result of 3350 base pair amplified region with the primer pair of LRV2-1\_Fa and LRV2-1\_R

As NGS result indicates, there is a 99% similarity between the database and our PCR amplified 3350 base pair fragment, which covers 64% of the total LRV2-1 genome. Of note, there is a 22 nucleotide difference along with a few gaps in our sequence compared to the database. These polymorphisms are mainly on the genetic code of the capsid protein and do not cause any frameshift for the expression of the capsid protein (Appendix B). Collectively, both PCR amplification studies and NGS of the amplified fragment demonstrate that the exosomal content of LRV+ *L. major* includes LRV specific sequences that cover at least 64% of the whole viral genome, suggesting that LRV2-1 can be released into the extra-parasitic space via exosomes.

### **3.1.2. Analysis of LRV+ *L. major* exosomes for the presence of LRV2-1 specific proteins**

Our next goal was to demonstrate the presence of LRV2-1 associated proteins in exosomes isolated from LRV+ *L. major*. However, commercially available antibodies for the LRV2-1 capsid protein and/or RDRP protein are nonexistent. Therefore, we attempted to express recombinant RDRP and capsid proteins of LRV2-1 but due to the codon bias and toxicity of these proteins (Young Tae Ro et al., 2004), we failed to achieve this goal. Only minor expression of RDRP protein (but no over-expression) was achieved by using the pET-22b vector system (Appendix D). Low yield and unsuccessful his-tag purification of recombinant RDRP protein hindered us from synthesizing an RDRP specific antibody. Therefore, our strategy to detect LRV2-1 specific protein on or within the LRV+ exosomes was changed from a specific immunoblotting based approach to a mass spectrometry-based strategy (MS).

#### **3.1.2.1. Mass spectrometric analysis of LRV+ *L. major* exosomes**

Exosomes of LRV+ *L. major* from two different batches were analyzed using MS for the presence of LRV2-1 specific proteins, Gene Ontology (GO) terms and Protein Analysis Through Evolutionary Relationships (PANTHER) tools (P. D. Thomas et al., 2003) (Figure 3.7 and Table 3.1).

	Leishmania major (REF)	upload 1 (▼ Hierarchy NEW! ?)				
PANTHER Protein Class	#	#	expected	Fold Enrichment	+/-	P value
Hsp90 family chaperone	4	3	.04	75.36	+	4.33E-03
tubulin	8	4	.08	50.24	+	5.63E-04
cell adhesion molecule	9	4	.09	44.66	+	8.07E-04
histone	10	3	.10	30.14	+	3.39E-02
annexin	20	6	.20	30.14	+	2.06E-05
↳ calcium-binding protein	66	8	.66	12.18	+	7.67E-05
calmodulin	38	8	.38	21.15	+	1.66E-06
↳ intracellular calcium-sensing protein	38	8	.38	21.15	+	1.66E-06
cysteine protease	72	6	.72	8.37	+	1.53E-02
↳ protease	175	11	1.74	6.32	+	2.48E-04
↳ hydrolase	426	16	4.24	3.77	+	6.71E-04

Figure 3.7. PANTHER Protein Class GO term Analysis classification of exosomal proteins

The full exosomal protein list with a significant mascot score is given in Table X (Appendix E). The most abundant LRV+ *L. major* exosomal proteins that were detected using MS are listed in Table 3.1. Mascot scores indicate significant matches and the average number of matches indicates protein abundance.

Table 3.1. Most Abundant Proteins of LRV+ *L. major* Exosomes based on MS Analysis

<b>Protein Name</b>	<b>Uniprot KB Accession Number</b>	<b>Average Mascot Score</b>	<b>Average number of significant matches</b>
Thiol specific antioxidant	Q4QF68	505	12
Tubulin beta chain	Q4Q4C4	283	7
GP63, leishmanolysin	Q4QHH1	259	8
Tubulin alpha chain	Q4QGC5	158	7
Putative heat-shock protein hsp70	Q4Q7Y4	151	7
Putative calpain-like cysteine peptidase	Q5SDH5	143	4
Heat shock protein 83-1	Q4Q4I0	139	4

As previously mentioned, GP63 and heat shock protein 70 are exosomal markers of the *Leishmania* parasite. Furthermore, the abundant presence of cytoskeletal proteins is also expected as the biogenesis of exosomes depends on cytoskeletal trafficking (Keller et al., 2006; Théry, Zitvogel, & Amigorena, 2002). The most common protein identified inside the LRV+ *Leishmania* exosomes was a thiol specific antioxidant known as tryparedoxin peroxidase, which catalyzes reactive oxygen species and was reported to have a pivotal role in the virulence and survival of the parasites (Lim et al., 1993). Since *Leishmania* exosomes possess immunomodulatory properties, the presence of stress proteins, virulence factors and cytoskeletal proteins inside the exosomes was not surprising. The exosomal content can be delivered inside the host where it can exert its immunomodulatory effect to set a permissive environment for

*Leishmania* infection (J. M. axwel. Silverman & Reiner, 2011). However, MS analysis failed to identify LRV2-1 specific proteins inside the exosomes (full list, Appendix E), suggesting that parasite-derived extracellular vesicles might harbor the viral genome, but not the whole virion. Whether this exosomal viral RNA is sufficient to initiate infection in uninfected *Leishmania* parasites upon delivery, remains to be determined.

During our ongoing studies, another group published results on LRV1 virus infection of parasites and demonstrated that the virus was transmitted through infected leishmanial exosomes (Atayde et al., 2019). According to their transwell infection study, *L. guyanensis* exosomes harboring the virus were released from LRV1-infected strain, passed into the lower chamber and triggered a transient infection in the LRV-strain. It is noteworthy that in the aforementioned study, the researchers used custom made LRV1 capsid protein-specific antibody which enabled them to support their claim using western blotting and electron microscopy. However, in our opinion, in this experimental setup, due to the lack of proper experimental controls (for example lack of isolated exosome controls to demonstrate their infectivity), it is not clear whether virions released from dead parasites or virus carrying exosomes themselves initiate the infection in the transwell chamber. To avoid this dilemma, we performed quantitative PCR-based analysis of the viral genome in LRV- *L. major* parasites following their co-incubation with LRV+ *L. major* exosomes. Our preliminary results failed to detect any transient infection in LRV- *L. major* by LRV2-1. However, we plan to repeat this experiment under different environmental conditions (increased temperature, lowered pH, etc) in the near future to confirm our results.

To our knowledge, there is no available data on the presence of LRV2-1 inside LRV+ *L. major* exosomes and their transmission through exosomes. Our results collectively suggest that LRV+ *L. major* exosomes explicitly contain LRV2-1 specific sequences, whereas the MS data does not support LRV2-1 specific protein expression inside exosomes. Therefore, we hypothesized that exosomal content may include a dsRNA viral genome or ssRNA transcripts of the dsRNA genome. We think that the template

of our amplified 3350 base pair fragment can be the transcribed portion of a hypothetical fusion protein of LRV2-1 capsid and RDRP. This fusion protein has already been shown to be commonly found in LRV1-4 but has yet to be detected in LRV2-1 (Lee et al., 1996; Y T Ro et al., 1997b). However, exosomal content may also include a dsRNA genome without the protein coat of the virus and this can be sufficient to transmit the LRV2-1 itself to other parasites as the dsRNA genome carries all the necessary genetic information of the complete virus (van Dongen, Masoumi, Witwer, & Pegtel, 2016). As an analogous phenomenon in mammalian cells, it was documented that hepatocyte derived carcinoma cells infected with the hepatitis C virus, transfer viral RNA to neighboring non-infectable plasmacytoid dendritic cells (pDC) through exosome secretion, resulting in the production of type I IFNs. Exosomal transfer of the hepatitis C virus is based on coordinated functions of the endosomal sorting complex and Annexin A2, membrane vesicle trafficking proteins and RNA binding proteins of the pDCs (Dreux et al., 2012). Similarly, LRV+ *L. major* exosomes may contain intact virions too, which can be investigated using immunoblotting with a custom made or commercial antibody specific to LRV2-1 proteins become available.

In order to identify the origin of LRV2-1 specific sequences inside LRV+ *L. major* exosomes, (i.e., whether they are ssRNA transcripts or a dsRNA genome), exonuclease T treatment assay was employed. Exonuclease T is a single strand specific nuclease that only trims single-stranded nucleic acids from their 3' ends (Cheng et al., 2019). Our purpose was to degrade possible ssRNA transcripts inside the exosomes after exosomal RNA isolation. If the PCR amplification product was resistant to exonuclease T mediated degradation, we could conclude that the PCR template of the 3350 base pair fragment stems from dsRNA. However, RNase contamination of isolated exosomal content, other than the applied exonuclease T treatment, could not be overcome (data not shown). Therefore, we are still not sure whether the LRV+ *L. major* exosomes contain dsRNA or ssRNA transcripts or both. However, it is clear that they contain virus-specific RNA sequences that comprise

64% of the whole dsRNA genome. Collectively, our MS and PCR amplification studies demonstrate that *L. major* exosomes do not contain viral proteins but they carry viral RNA from at least 64% of their whole genome. Further studies are needed to clarify whether exosomes contain the whole LRV2-1 virus or the *bona fide* absence of virus proteins inside of exosome and whether LRV2-1 transmission through exosomes occurs for *L. major* parasites or not. Of note, the concentration of isolated exosomes is always a limiting factor for current exosome studies in our lab, therefore, enrichment of the exosomal content would be a substantial improvement for further *Leishmania* exosome related studies.

### **3.2. Generation of EGFP-LUC Expressing Transgenic LRV- and LRV+ *L. major* Strains**

Recombinant EGFP-LUC fusion protein-expressing parasites would be beneficial for *in vitro* and *in vivo* quantification of infection rates and parasite loads, respectively (Bolhassani et al., 2011). To achieve this, a codon optimized EGFP-LUC protein expressing pLEXSY-neo vector for *L. major* was ordered. For *in vitro* infection studies of mammalian cells with EGFP expressing parasites, infection rates were quantified based on the fluorescence emission detected through the BL1 channel of the flow cytometry. Parasite loads in footpads of mice were quantified according to LUC expression using IVIS *in vivo* imaging system.

#### **3.2.1. Generation of EGFP-LUC expressing Transgenic LRV- *L. major***

In order to generate EGFP-LUC expressing LRV- transgenic *L. major*, pLEXSY-neo2.1 plasmid was electroporated to parasites and positive parasites were selected with neomycin (Section 2.3.1.). After electroporation, parasites were daily monitored with fluorescence microscopy and their culture media was replenished every four days. On average, after 4 weeks, the parasites were enriched and stored in liquid nitrogen (Figure 3.8.).

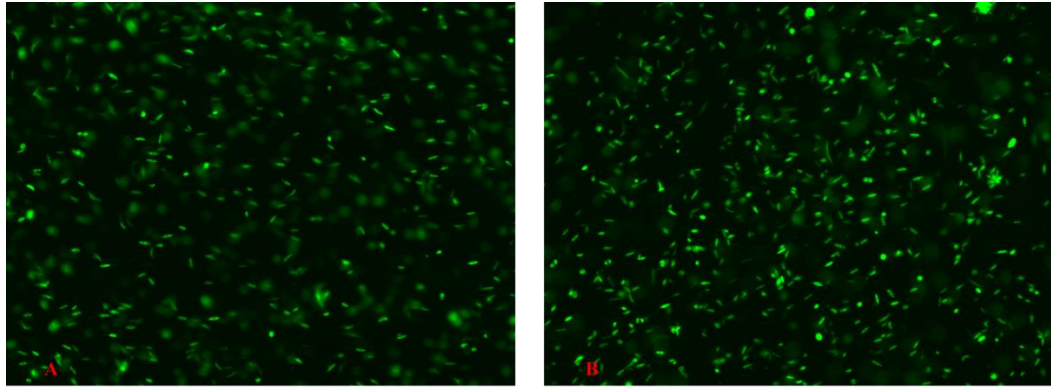


Figure 3.8. Fluorescence microscopy images of EGFP-LUC expressing LRV- (A) and LRV+ (B) *L. major*

### 3.2.2. Generation of EGFP-LUC expressing Transgenic LRV+ *L. major*

As it was mentioned before, selection of LRV bearing transgenic parasites with neomycin would cause the loss of LRV since neomycin is an aminoglycoside antibiotic like Hygromycin B which prevents proliferation of LRV. Therefore, neomycin expressing sequence of the pLEXSY-neo2.1 was replaced with blasticidin expression gene. *Leishmania* is sensitive to blasticidin antibiotic and blasticidin is a peptidyl nucleoside antibiotic and not an aminoglycoside antibiotic, therefore would not interfere with virus replication (Fourmy et al., 1998; Y T Ro et al., 1997a). Based on this knowledge, we also generated LRV+ transgenic *L. major* in the presence of neomycin using the original plasmid construct to develop a virus-cured isogenic strain which can be used in direct comparison with the parental LRV+ *L. major*. Establishment of these LRV- *L. major* parasites gave us an important advantage to compare the virulence of LRV- and LRV+ isogenic strains to better understand the impact of LRV2-1 on disease pathogenesis.

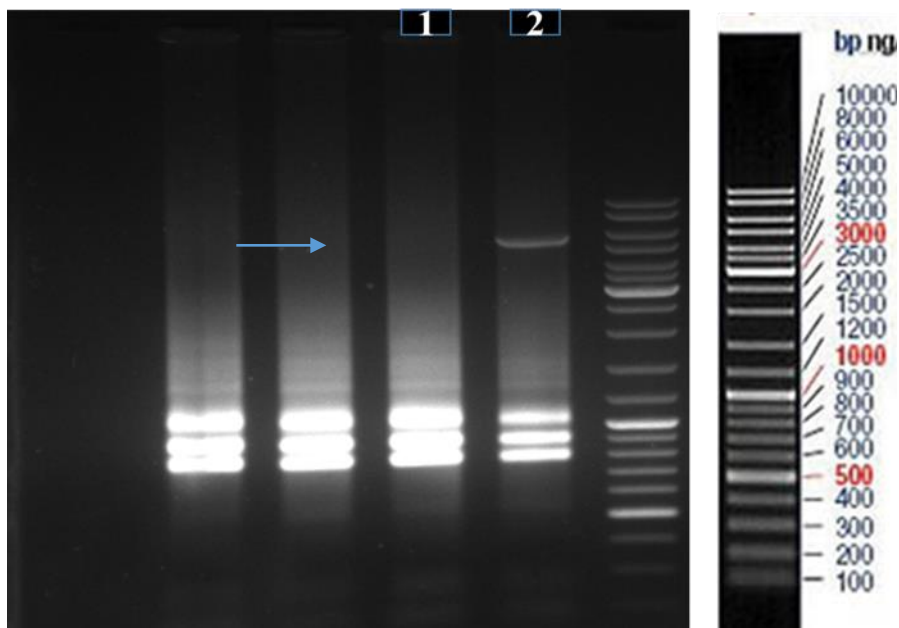


Figure 3.9. Neomycin depletion of LRV2-1 to generate transgenic LRV- *L. major* strain

Lane 1: Transgenic and neomycin selected LRV+ *L. major* total RNA, Lane 2: Non transgenic LRV+ *L. major* total RNA

To our knowledge, none of the previous studies comparing the virulence of LRV+ and LRV- parasites used isogenic strains of *L. major*. Since virulence of different *Leishmania* isolates of the same species may differ and this situation affects the course of the disease, how LRV impacts disease progression can only be assessed in an unbiased fashion through the use of isogenic strains only (Kébaïer, Louzir, Chenik, Ben Salah, & Dellagi, 2001). Comparison of virulence of LRV- *L. major* that is isolated from a patient and LRV+ *L. major* that is isolated from another patient, is in our view not ideal but this approach was nevertheless used in most previous published studies (de Carvalho et al., 2019; R. Kariyawasam et al., 2018; Zangger et al., 2013). To overcome this situation, we used LRV- *L. major* strain for *in vitro* and *in vivo* infection studies that was generated via the depletion of LRV2-1 by neomycin (Figure 3.9, lane 1). Neomycin resistance gene of pLEXXSY-neo2.1 was replaced with

blastocidin resistance gene and the new pLEXSY-bla2.1 plasmid was utilized to generate EFGP-LUC expressing LRV+ *L. major* (Figure 3.10.).

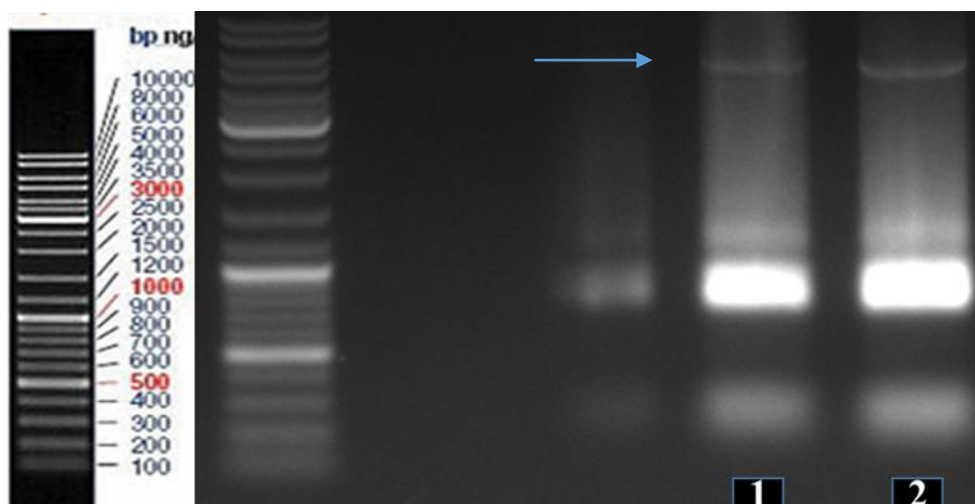


Figure 3.10. Blastocidin selected transgenic LRV+ *L. major*

Lane 1: Transgenic and blastocidin selected LRV+ *L. major* total RNA, Lane 2: non transgenic LRV+ *L. major*

After enriching transgenic LRV+ *L. major* strain (Figure 3.10., lane 1) that is selected by blastocidin that still retained its viral content, LRV- *L. major* and LRV+ *L. major* transgenic strains that expressed the EFGP-LUC recombinant protein can be used for *in vitro* and *in vivo* studies because they are isogenic and therefore their virulence is expected to differ only because of their viral inhabitance.

Luciferase expression in the transgenic parasites was confirmed by *in vivo* imaging (IVIS) in mice administered with different doses of the parasites (Section 2.6.1.1.) and luminescence intensities arising from the footpads correlated with the administered dose of parasites in BALB/c mice (Figure 3.11.).

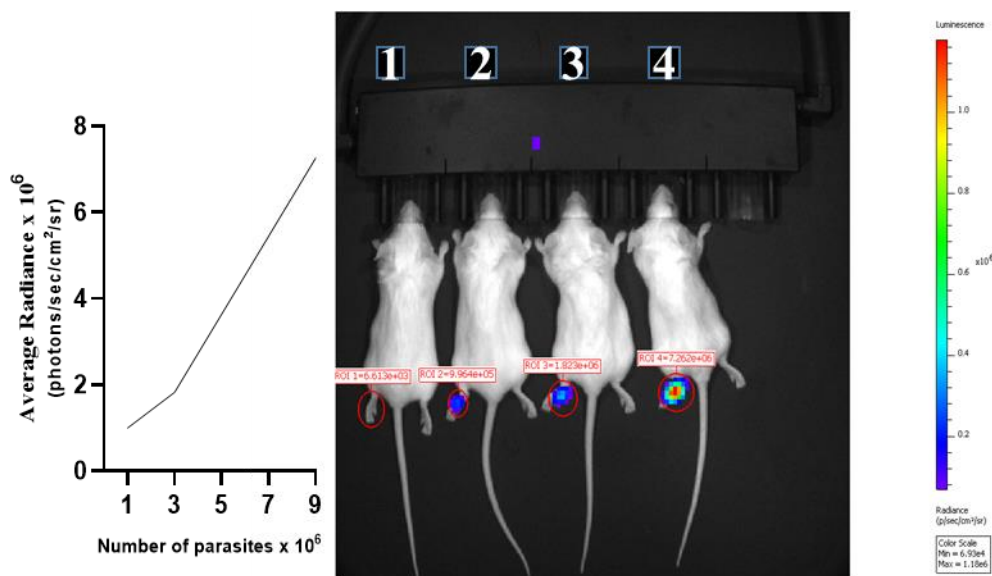


Figure 3.11. Confirmation of luciferase expression in transgenic parasites and optimization of injection dose of the *L. major* into the footpad of mice

Mouse 1: Injected with  $9 \times 10^6$  metacyclic wild type parasite, Mouse 2: Injected with  $1 \times 10^6$  metacyclic transgenic parasite, Mouse 3: Injected with  $3 \times 10^6$  metacyclic transgenic parasite, Mouse 4: Injected with  $9 \times 10^6$  metacyclic transgenic parasite, measurements were taken as stated at Section 2.6.1.1., Luciferase signal was recorded as radiance, ROI: Region of Interest

As it can be seen from the Figure 3.11, dose dependent increase of the injected transgenic parasites amplifies the radiance signal because of increasing parasite loads. Therefore, we can conclude that transgenic parasites expressing luciferase and this feature of the parasites can be utilized for challenge experiments and *in vivo* imaging system. The high signal intensity obtained from the fourth mouse (Figure 3.11.) encouraged us to use  $9 \times 10^6$  parasites per footpad for further studies.

### 3.3. Generation of THP-1 Dual ISG15 Knock out and THP-1 Dual Lentiviral Control (LVC) Cell lines by LentiCRISPR v2 System

ISG15 is a ubiquitin-like antiviral protein that is upregulated upon type I IFN stimulation, capable of covalently binding to cellular target proteins, thereby regulating their functions (Lenschow, 2010). There are very few reports on the relation

between ISG15 and *Leishmania* infection which makes it a neglected research area. Only one study reported that ISG15 was upregulated ~3.5 fold during *in vitro* infection of dendritic cells with *L. braziliensis* but not with *L. amazonensis* (Vargas-Inchaustegui et al., 2008). The ISG15 protein is ubiquitin-like in terms of its ability to covalently bind target proteins in a process termed as ISGylation. Over 150 target proteins including those involved in central immune signaling pathways like NFκB, JNK, and IRF-3 are ISGylated (Dos Santos & Mansur, 2017). However, unlike ubiquitylation, ISGylation does not result in protein degradation. Ubiquitin itself is a substrate of ISGylation (Fan et al., 2015). How ISGylation regulates cellular processes is not clear. Furthermore, free secreted form ISG15 exerts cytokine-like responses in target cells and is implicated as an important factor in anti-viral immunity (Owhashi et al., 2003; Padovan et al., 2002). Evidence suggests that type I interferon-mediated responses may modulate *Leishmania* pathogenesis. For instance, mice that were healed of *L. guyanensis* infection show relapsed disease pathology upon infection with the type I IFN inducer lymphocytic choriomeningitis virus (LCMV) (Rossi et al., 2017). Since ISG15 is among the 10 most expressed ISGs out of ~300 interferon stimulated genes (ISGs), we wanted to explore its role in immunity against *Leishmania* infection. To our knowledge, there are no published studies focusing on the relation of *L. major* infection and the ISG15 protein. Therefore, in this part of the thesis, we aimed to elaborate this relation by knocking ISG15 out in THP-1 dual WT cells using a LentiCRISPR v2 system based approach.

To enable this goal, the first step was to design an ISG15 specific oligo pair (Section 2.4.1.) that targets the second exon of *ISG15*, at the seventh amino acid. Next, this oligo pair was cloned into our transfer vector TLCV2 (Appendix B, the full coding region of ISG15). Besides the estimated software success score of the designed oligo pair, our strategy was to choose the oligo pair proximal to the start codon. After ligating the designed oligo pair into the TLCV2 transfer vector, we made sure with Sanger sequencing that only one oligo pair was inserted (Figure 3.12.).

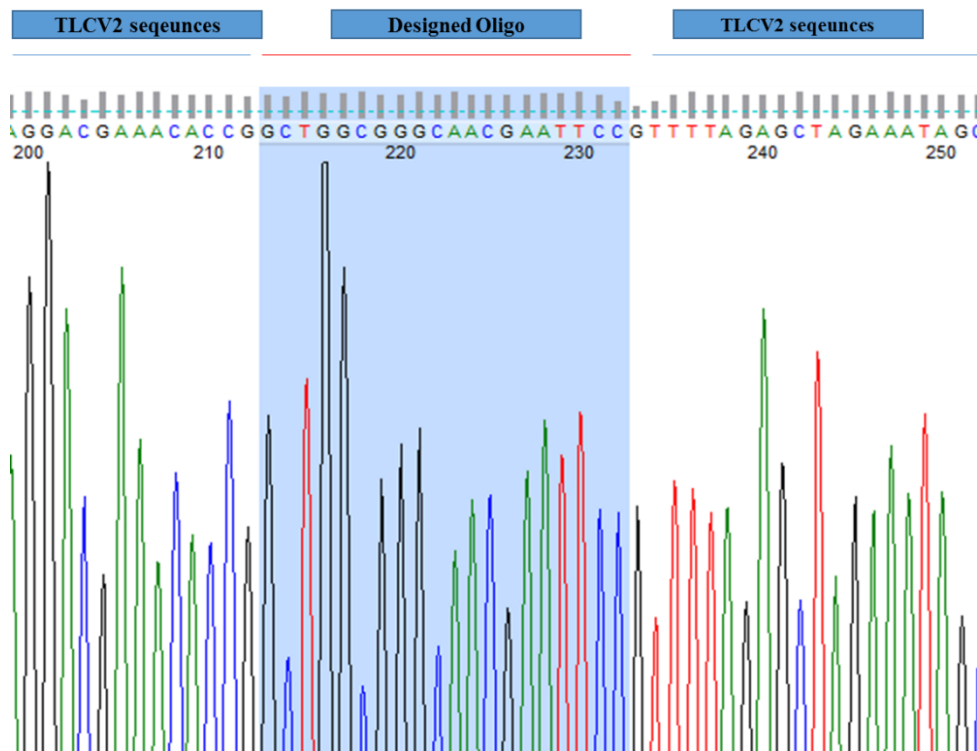


*Figure 3.12.* Sanger Sequencing of ISG15 oligo pair ligated into the TLCV2 transfer vector  
 Presence of one and only designed oligo in one strand flanked by TLCV2 sequences

Following this verification, we proceeded to the production of the lentivirus as mentioned in section 2.4.2. Then, we titered our lentivirus solution by re-infecting HEK 293FT cells to observe GFP expression. TLCV2 expresses doxycycline-inducible Cas9-P2A-GFP cassette (<https://www.addgene.org/87360/>), indicating the presence of lentivirus in our harvest (data not shown). Single-cell dilution of puromycin resistant cells was performed following the transduction of lentiviral harvest to the THP-1 Dual WT cell line (Section 2.4.3.). After the enrichment of 30 different puromycin resistant THP-1 Dual WT cell colonies, we observed that only one of them was ISG15 deficient (Figure 3.13.). Of note, all colonies were pretreated with recombinant recIFN $\beta$  (24 h) to upregulate ISG15, since otherwise, ISG15

expression would not be induced and the free protein or ISGylated targets would not be detected with western blotting.

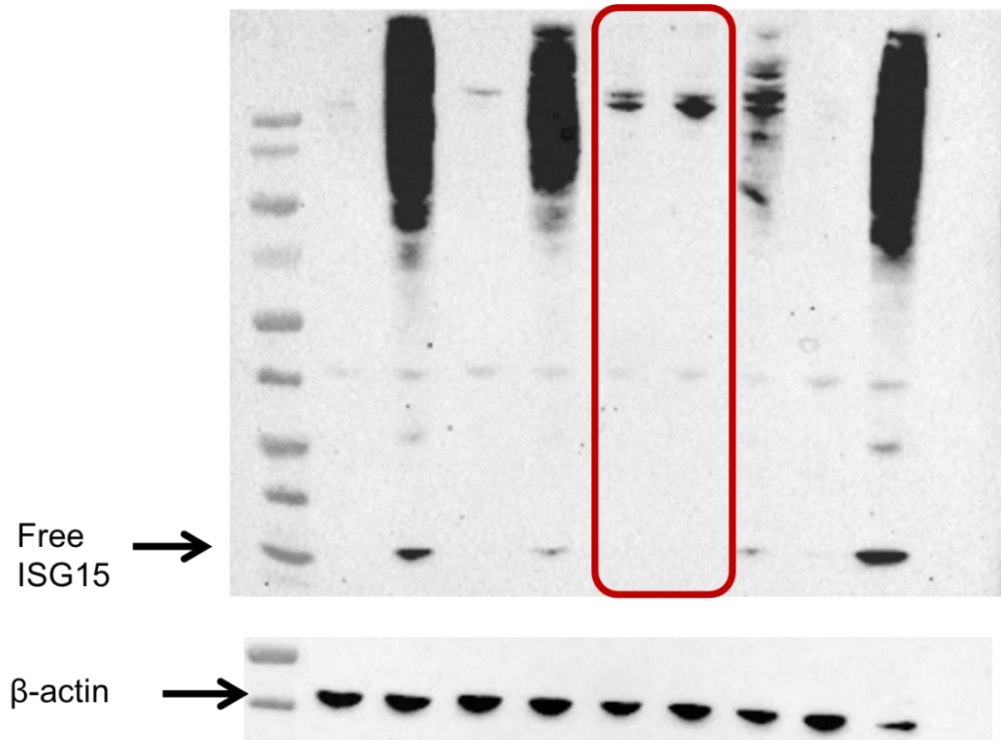


*Figure 3.13.* Monitoring of ISG15 deficient clones by Immunoblotting.

All wells were loaded with 25  $\mu$ g protein except for the seventh well, which was loaded with 30  $\mu$ g lysate. Long black smears are indicators of ISGylation. Arrows indicate the 15 kDa Free ISG15 and  $\beta$ -actin as loading control, respectively. Immunoblotting was performed by using ISG15 specific primary antibody followed by probing with HRP-conjugated secondary antibody.

Lane 1: Protein ladder, Lane 2: THP-1 LVC, Lane 3: THP-1 LVC pretreated with 50 ng/ml recIFN $\beta$ , Lane 4: THP-1 Dual WT, Lane 5: THP-1 Dual WT pretreated with 50 ng/ml recIFN $\beta$ , Lane 6: THP-1 ISG15KO, 25  $\mu$ g, pretreated with 50 ng/ml recIFN $\beta$ , Lane 7: THP-1 ISG15KO, 30  $\mu$ g pretreated with 50 ng/ml recIFN $\beta$ , Lane 8: Unsuccessful clone, Lane 9: THP-1 Dual WT, Lane 10: THP-1 Dual WT pretreated with 50 ng/ml recIFN $\beta$  as a second positive control

Immunoblotting revealed that out of 30 colonies tested, only one colony failed to express ISG15 in response to recIFN $\beta$  stimulation (Figure 3.13., Lane 5-6). Of note, in contrast to the THP-1 ISG15 KO cell line, the puromycin resistant

THP-1 LVC cell line did not produce sgRNA for *ISG15* which was generated and utilized as a control strain for the THP-1 *ISG15* KO cell line.

The next step was to sequence the NHEJ-induced mutated genomic region which should reside 3-4 nucleotide upstream of our PAM sequence and was at 5'-AGG-3' (Su et al., 2016) (Appendix B). The mutated genomic region was PCR amplified (Section 2.4.4.), and subjected to NGS and Sanger sequencing, demonstrating the presence of a mutation in the *ISG15* genomic region and confirming the generation of a stable THP-1 *ISG15* KO cell line (Figure 3.14.).

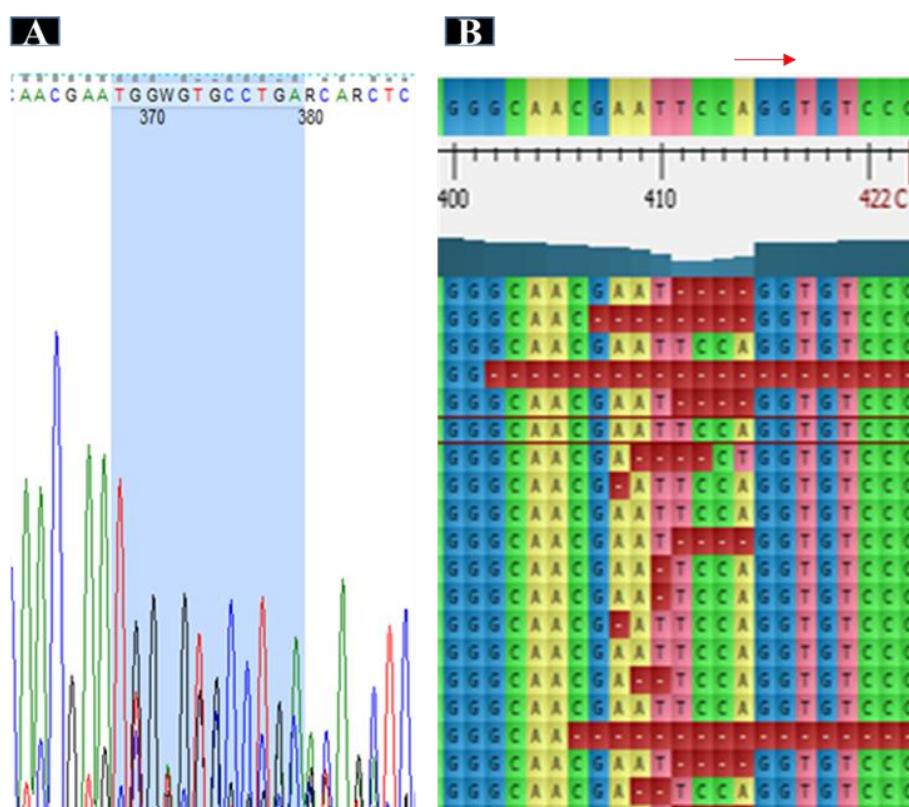
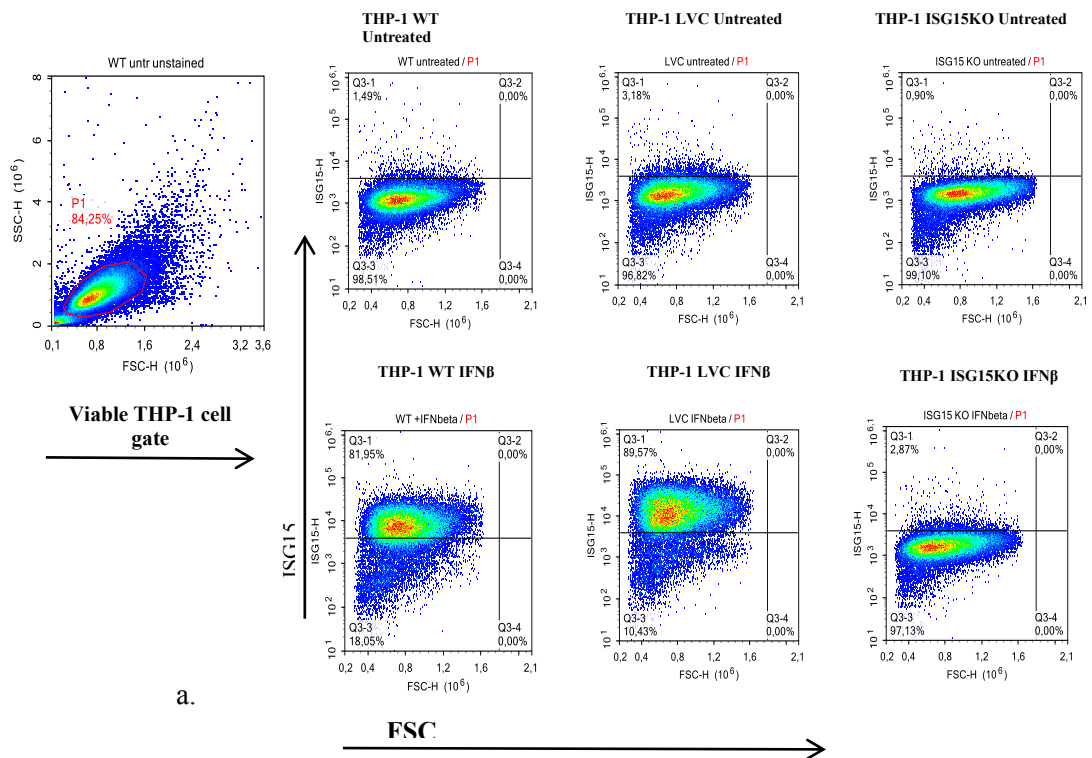


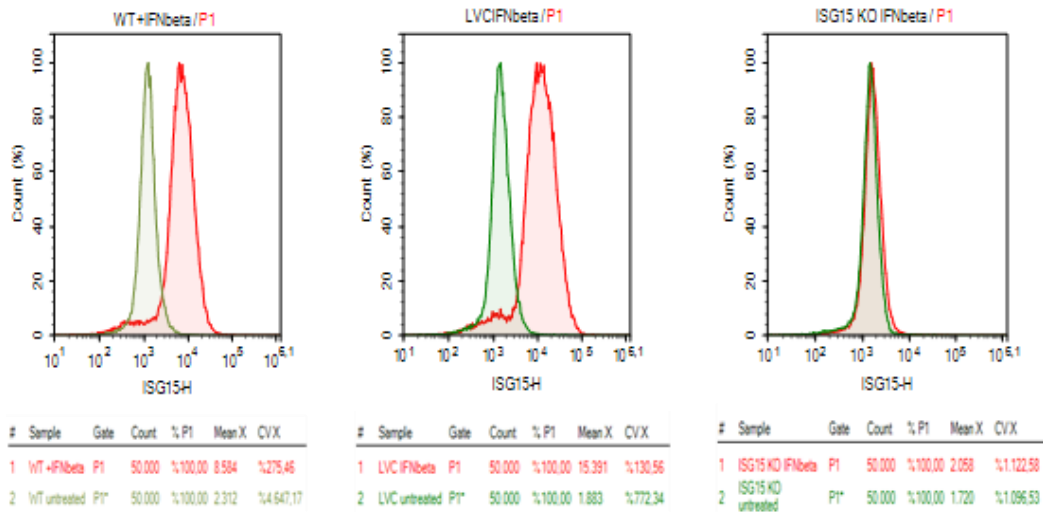
Figure 3.14. Sanger (A) and Next generation (B) sequencing of PAM sequence included region of THP-1 *ISG15* KO cell line genome

Red dash: PAM sequence 5'-AAG-3', Blue shadow: Upstream of PAM sequence on Sanger Sequencing (A) results, Red boxes: Unmatched reads of NGS to consensus sequence

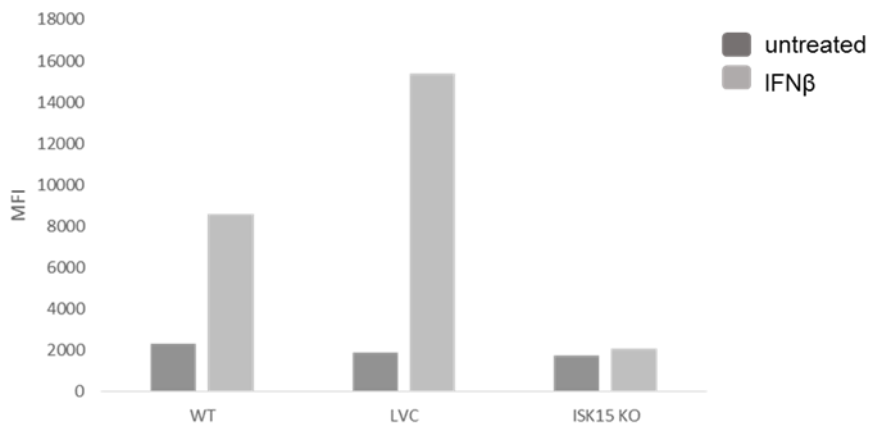
It is clear from our sequencing results that the genome of THP-1 Dual cell line was mutated with our LentiCRISPR v2 system specifically on *ISG15* gene near the PAM sequence, generating the THP-1 ISG15 KO cell line that failed to express the ISG15 protein in response to recIFN $\beta$  stimulation (Figure 3.13.). However, in order to provide further evidence for the lack of ISG15 expression, we performed intracellular staining of inducible protein expression using PE (phycoerythrin) conjugated human anti-ISG15/UCRP flow antibody. THP Dual WT, THP LVC, THP ISG15 KO cell lines were pretreated or not with 50 ng/ml recIFN $\beta$  to upregulate ISG15 expression and stained with PE-conjugated ISG15 antibody following fixation and permeabilization (Figure 3.15.).



a.



b.



c.

Figure 3.15. THP-1 ISG15 KO intracellular staining with PE-conjugated ISG15 flow cytometry antibody

Intracellular staining was performed as it mentioned in Section X. Viable cell gating strategy was indicated at section a and b. PE channel of flow cytometry was used to detect signal. All cell lines were pretreated with IFN $\beta$  parallel to their untreated versions as control.

a: Dot plots of intracellular ISG15 staining, b: Mean fluorescence intensity (MFI) histogram plots of intracellular ISG15 staining, c: Bar graph representation of MFI values

IFN $\beta$  treatment upregulated ISG15 expression in THP-1 WT cell line and THP-1 LVC cell line, whereas ISG15 KO cells could not produce ISG15. Even after pretreatment with recIFN $\beta$ , no ISG15 production could not be detected using either western blotting or intracellular ISG15 staining (Figure 3.13., 3.15.). Collectively, our results suggest that we successfully knocked ISG15 out in THP-1 Dual WT cells and named them as THP-1 ISG15 KO. This cell line was used in the following experiments together with THP-1 LVC in order to understand the impact of ISG15 on *Leishmania* infection and autophagy.

### **3.4. Assessment of *in vitro* infection rates of THP-1 cell lines**

We used the mammalian cell lines THP-1 Dual WT, THP-1 cGAS KO, THP-1 STING KO, THP-1 TBK-1 KO, THP-1 ISG15 KO and THP-1 LVC which were infected with LRV- and/or LRV+ *L. major* transgenic parasites. These cell lines were chosen based on the following results obtained in a previous study from our laboratory (PhD thesis of Ihsan Cihan Ayanoglu, 2019). Stimulation of immune cells with the unique mitochondrial DNA obtained from *Leishmania* (known as kinetoplast DNA), increased the parasite loads in *in vitro* and *in vivo* *L. major* infection models. Evidence also suggested that kDNA induced type I interferon signaling, possibly through activating the cGAS/STING/TBK1 nucleic acid sensing pathway (Das et al., 2019). Therefore, herein, we also wanted to assess the contribution of cGAS, STING and TBK1 to *L. major* infection through the use of the commercially available knockout cell lines in comparison to their WT counterpart. For this, PMA-differentiated THP-1 WT, LVC control and knockout cell lines were infected with transgenic *Leishmania* strains and infection rates were assessed based on EGFP fluorescence intensities recorded on the BL1 channel of the flow cytometer.

#### **3.4.1. Optimization of *in vitro* *Leishmania* infection model**

In our preliminary experiments, we used the THP-1 Dual WT cell line and determined the optimal multiplicity of infection (MOI) to be as 1:10 (10 parasites per each THP-1 cell (data not shown)). As macrophages represent the most important target cells in

*Leishmania* infections, THP-1 monocytes were differentiated into macrophages using two different concentrations of PMA (5 ng/ml for 48 hours or 50 ng/ml for 24 hours (Rittig & Bogdan, 2000)). Following 5 ng/ml 48 hours PMA differentiation, cells were rested for another 24 hours and then infected with transgenic *Leishmania*. If more than one cell line was infected with *Leishmania* for an experiment, they initially were PMA-differentiated in a T75 flask, then detached with accutase solution and counted with flow cytometry. The cells were inoculated on cell culture plates at similar concentrations to establish same MOI of 1:10 for every experimental well.

During the infection process, involving co-incubation of THP-1 cells with parasites, 2% FBS supplemented culture media was used in order to minimize extracellular parasitic growth (Tegazzini et al., 2016). In order to prevent serum starvation of cells, the 2% FBS supplemented medium was replaced with 10% FBS supplemented medium at the intracellular proliferation phase of the parasites, which is defined as the period following the withdrawal of the unattached extracellular parasites from the culture.

Flow cytometric assessment of infection rates (based on percentage of infected cells), viable cell gating strategy, and parasite load comparisons (based on mean fluorescence intensities (MFI)) of infected and uninfected cell populations are demonstrated in Figure 3.16. and the same strategy was applied for all *in vitro* infection studies.

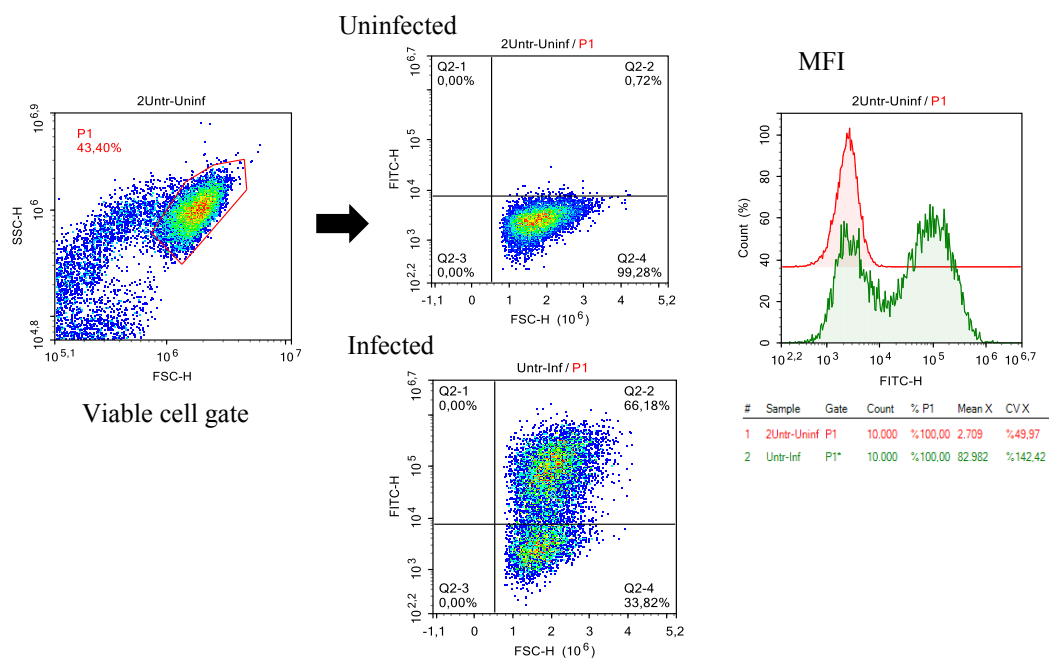


Figure 3.16. Assessment of *in vitro* infection rates and parasite loads of wild type THP-1 cells.

Viable cells were gated based on their forward and side scatter characteristics. Quadrants were placed according to the background green fluorescence cut-off of the uninfected cells and/or uninfected but drug treated cells

### 3.4.2. Comparison of *L. major* infection rates of WT versus STING or cGAS KO THP-1 cells

In order to investigate the role of cytosolic DNA sensing pathways on *Leishmania* infection rates, three different THP-1 cell lines were infected with transgenic parasites (Figure 3.17).

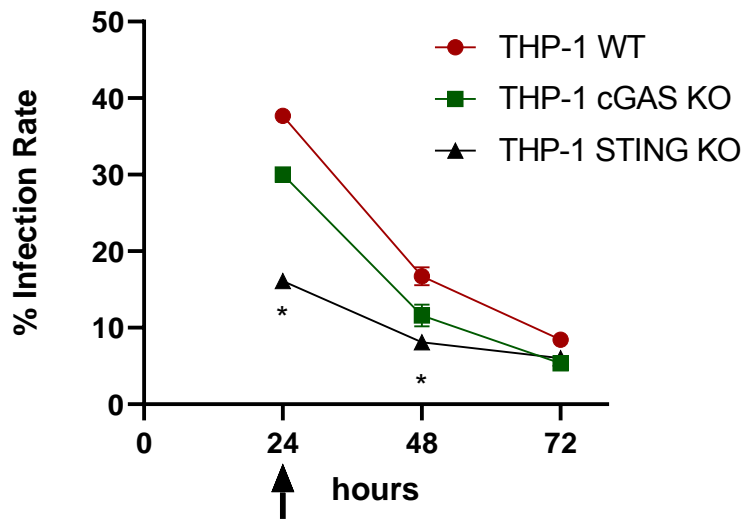


Figure 3.17. Transgenic *L. major* infection rate of THP-1 cell lines

$10^5$  THP-1 cells were infected with  $10^6$  parasites (MOI: 10:1) for 24 h and parasite proliferation was followed for a period of 72 h. Average % infection rates of three independent experiment using 3 biological replicates are shown. Parasites were not opsonized. THP-1 cells were differentiated with 50 ng/ml PMA for 24 hours before the infection process. Black arrow: Time point of parasite withdrawal.

All infection rates were compared to THP-1 WT group at each time point statistically by Kruskal-Wallis test followed by Dunn's multiple comparison test (\*.  $p < 0.05$ ).

Results demonstrated that percent infection rates decreased over time after parasite withdrawal in all cell lines, suggesting that in this *in vitro* infection model, the employed cell lines eliminated the internalized parasites. Interestingly, at early time points (24 and 48 h), infection rates were lower in cGAS and STING KO cells, and the results were statistically significant for the THP-1 STING KO cells (Figure 3.17.). There are only a handful of publications regarding the role of cGAS/STING signaling in parasitic infections and the conclusions derived from these studies are often conflicting. For example, in one study, STING KO mice were demonstrated to be more susceptible to *Toxoplasma gondii* (*T. gondii*) infection caused by impaired type I IFN and interferon-stimulated gene expression in the spleen (Wang et al., 2019). In contrast, another study also investigated the role of STING in a *T. gondii* infection

model and based on evidence showing reduced parasite proliferation in the absence of cGAS/STING signaling, concluded that STING exerted a pro-parasitic effect during *T. gondii* infections (Majumdar et al., 2015). To our knowledge, there is only one study that has investigated the relation between *L. donovani* infection and STING activation. This report claims that the activation of the cGAS-STING pathway, prior to parasitic *L. donovani* infection in mouse RAW264.7 leads to increased parasite loads in macrophages *in vitro* (Das et al., 2019). Our *in vitro* infection results (Figure 3.17) are in agreement with the findings of Das et al (2019) and implicate that *L. major* might use the cGAS/STING signaling pathway to its own advantage. Therefore, in order to verify this hypothesis, we next aimed to analyze the activation state of cGAS/STING signaling pathway in parasite infected cells. Various pathogen derived cytosolic DNA molecules have been shown to bind to and activate the enzyme cGAS, resulting in subsequent synthesis of a small second messenger, 2'3'-cGAMP. cGAMP then engages the adapter molecule STING, which recruits and activates TBK-1 and IKK (Chen et al., 2016). Activated TBK-1 then phosphorylates STING at several residues, including serine 366 (Ser366) (Liu et al., 2015). Based on this information, to understand whether *L. major* parasites hijack this signaling pathway to their advantage, we isolated total protein from the infected cells and performed western blotting using an anti-pSTING antibody (Ser366) (Figure 3.18.) as an indicator of activated STING.

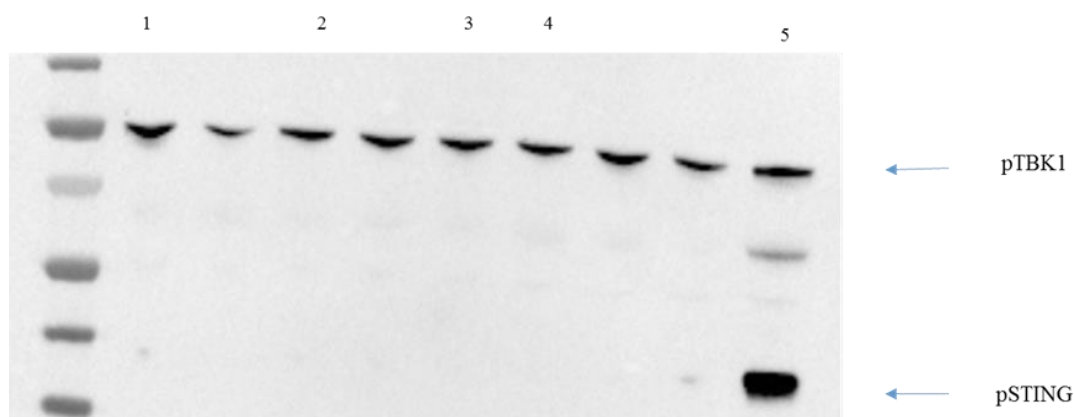


*Figure 3.18.* Western blot analysis of STING activation upon *in vitro* *L. major* infection of THP-1 WT cells.

All wells were loaded with 40 µg protein, western blot performed using anti pSTING Ser366 antibody. Representative immunoblotting result of three independent experiments with similar results is shown. pTBK1 demonstrated as a loading control.

Lane 1: Uninfected (24 hours) control, Lane 2: Uninfected (48 hours) control, Lane 3: *L. major* infected (24 hours), Lane 4: *L. major* infected (24 hours), Lane 5: cGAMP pretreated THP-1 WT (24 hours).

Based on the result shown in Figure 3.18, we concluded that *L. major* infection failed to induce detectable STING phosphorylation, whereas the positive control cGAMP strongly stimulated STING activation (blue arrow, Figure 3.18). This results suggests that infection with *Leishmania* parasites fail to activate the canonical STING signaling pathway. However, STING can also be activated non-canonically in a phosphorylation-independent manner through ubiquitination (Dunphy et al., 2018). We have not analyzed the role of this newly proposed pathway in *Leishmania* infected cells yet. Data presented in Figure 3.17. implicated that absence of STING somehow conferred resistance to infection. Yet, absence of pSTING in *L. major* infected cells suggested that this effect might be independent of STING signaling. Therefore, we hypothesized that the differences observed in infection rates of the THP-1 WT, THP-1 cGAS KO and THP-1 STING KO cells might stem from a generalized phagocytosis-related defect in the knockout cell lines, leading to decreased parasite uptake and hence lower infection rates. To test the validity of this hypothesis, we carried out

infection studies in wild type and knockout cells in parallel to parasite-related and unrelated phagocytosis assays as described in later sections of this thesis.

### **3.4.3. Comparison of *in vitro* infectivity of LRV- and LRV+ *L. major* transgenic strains**

As mentioned previously, LRV-1 infected new world *Leishmania* species cause exacerbated disease (Hartley et al., 2012; Ives et al., 2011; Ruwandi Kariyawasam et al., 2017). To our knowledge, the effect of LRV2-1 on disease severity has not yet been reported. We hypothesized that the *in vitro* infection model can be a useful tool to investigate this effect. Using LRV cured *L. major* for infection studies is advantageous because the genetic makeup of our LRV+ and LRV- parasites is identical. Therefore, any observable difference in virulence between these strains would be directly attributable to the LRV2-1 virus. However, in our THP-1 infection model, we found no significant differences in THP-1 infection rates following employment of LRV+ or LRV- *L. major* (Figure 3.19.).

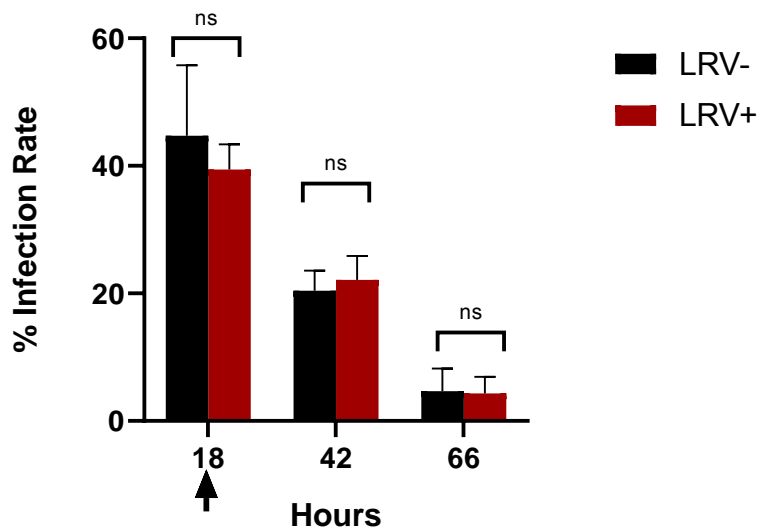


Figure 3.19. *In vitro* infection of THP-1 WT cells with LRV+ and LRV- parasites

$10^5$  THP-1 cells were infected with  $10^6$  parasites (MOI: 10:1) for 18 h and parasite proliferation was followed for a period of 66 h. Average % infection rates of two independent experiment using 2-3 biological replicates are shown. Parasites were not opsonized. THP-1 cells were differentiated with 5 ng/ml PMA for 48 hours and rested for another 24 hours before infection. Black arrow: Time point of parasite removal.

Infection rates of LRV+ versus LRV- strains at each time point were statistically compared with Mann-Whitney Unpaired test (ns, not significant;  $p > 0.05$ )

Next, we repeated the *in vitro* infection experiment in the knockout cell lines and still did not observe any significant differences between LRV+ and LRV- *L. major* strains (Figure 3.20.).

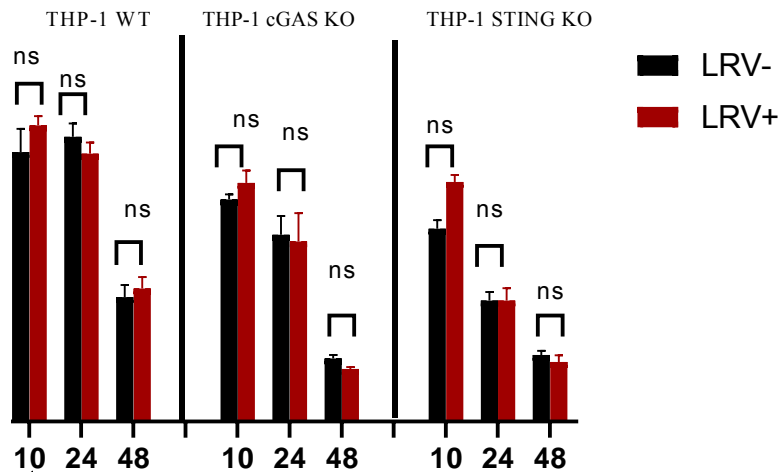


Figure 3.20. *In vitro* infection of THP-1 WT, cGAS KO and STING KO cells with LRV+ and LRV- parasites

$10^5$  THP-1 cells were infected with  $10^6$  parasites (MOI: 10:1) for 10 h and parasite proliferation was followed for a period of 48 h. Average % infection rates of two independent experiment using 2-3 biological replicates are shown. Parasites were not opsonized. THP-1 cells were differentiated with 50 ng/ml PMA for 24 hours before infection. Black arrow: Time point of parasite removal.

Infection rates of LRV+ versus LRV- strains of at each time point were compared with Mann-Whitney Unpaired test (ns, not significant;  $p > 0.05$ )

Collectively, our infection studies with the LRV+ and LRV- *L. major* strains demonstrate that presence of the LRV2-1 does not alter the virulence of *L. major* in our *in vitro* model. However, *in vitro* studies alone may not be conclusive since this system ignores the interaction between immune cells and remains ignorant of inflammation, which impacts disease progression *in vivo*. Furthermore, *Leishmania* parasites, upon entering the body, are first encountered and phagocytosed by neutrophils and are then transferred to macrophages (Peters & Sacks, 2009). Therefore, having an *in vivo* infection model is essential to compare the virulence of LRV+ and LRV- *L. major* strains. We performed an *in vivo* infection study to further investigate the effect of the LRV2-1 virus on *L. major* virulence which is presented in the following sections.

#### **3.4.4. Infection of THP-1 WT and THP-1 TBK-1 KO cells with transgenic *L. major* in the presence and absence of the TBK-1 inhibitor-Amlexanox**

As mentioned before, the cGAS-STING cytosolic DNA sensing pathway utilizes TBK-1 to phosphorylate STING and IRF3. Phosphorylated IRF3 then dimerizes and translocate to the nucleus, leading to type I interferon production (Chen et al., 2016). Since our results on *Leishmania*-induced STING activity remained inconclusive, we repeated the *in vitro* infection assays in the THP-1 Dual TBK-1 KO cell line and also employed the TBK-1 inhibitor, amlexanox in WT and KO cells (Figure 3.21.). The inhibition mechanism of amlexanox involves its competition with ATP on the ATP binding pocket of TBK-1. Nevertheless, it is also reported that this small molecule might increase pTBK-1 in a cell type dependent manner (Reilly et al., 2013).

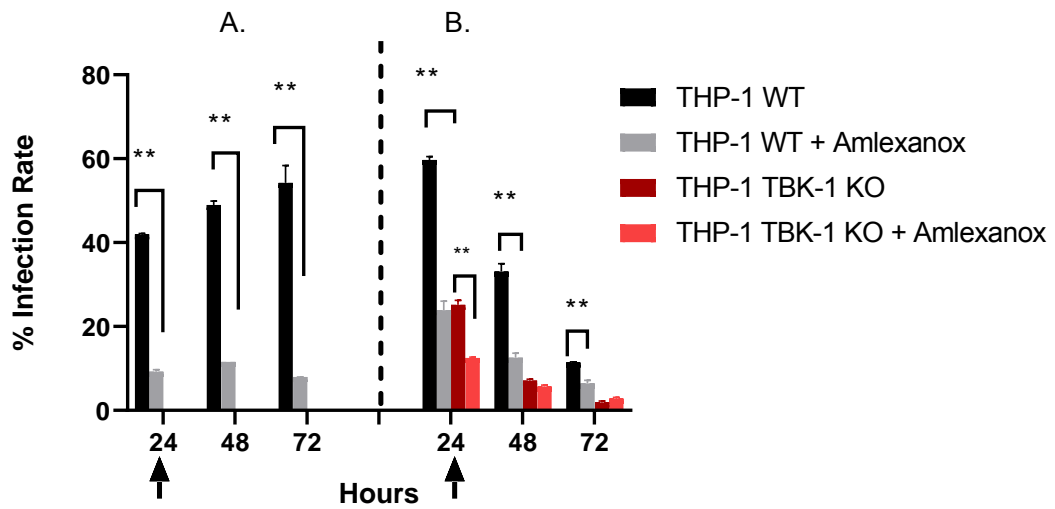


Figure 3.21. *In vitro* infection of THP-1 WT, TBK-1 KO cells with transgenic *L. major*.

$10^5$  THP-1 cells were infected with  $10^6$  parasites (MOI: 10:1) for 24 h and parasite proliferation was followed for a period of 72 h. Average % infection rates of two independent experiment using 2-3 biological replicates are shown. Parasites were not opsonized. THP-1 cells were differentiated with 5 ng/ml PMA for 48 hours and rested 24 hours before infection. When used, cells were pretreated with amlexanox for at least 1 hour before infection at a dose of 64  $\mu$ g/ml. Black arrow: Time point of parasite removal

A: Infection rates at all-time points were statistically compared with Mann-Whitney Unpaired test. B: Effect of amlexanox on TBK-1 KO infection rates were statistically compared with Mann-Whitney Unpaired test at 24 hours only due to the low infection rates of other time points. (\*.  $p < 0.05$ , \*\*.  $p < 0.01$ , \*\*\*.  $p < 0.001$ )

Our results demonstrate that amlexanox decreased *L. major* infection significantly in both THP-1 WT and THP-1 TBK-1 KO cell lines, suggesting that this effect might be independent of its TBK-1 inhibitory activity. Furthermore, similar to the results obtained in STING KO and cGAS KO cell lines, TBK-1 KO cells had significantly reduced infection rates when compared to THP-1 WT cells. However, as discussed before, this result might also be dependent on a generalized phagocytosis defect, requiring the use of a “phagocytosis control”, which will be addressed in the following sections. Of note, in our *in vitro* infection model, following parasite removal, the macrophages either became permissive or started to clear up the parasites over a period of 72 h (Figure 3.21. A versus B). Although we have employed identical THP-1

differentiation conditions and used the metacyclic form of the promastigotes in all our infection experiments at the same MOI, in some experiments we observed that parasites were cleared by macrophages over time, whereas in others, parasites proliferated successfully within the THP-1 macrophages. The reason for this inconsistent parasite behavior remains unclear but we suspect that the outcome of the infection is dependent on the PMA-differentiation state of the macrophages, which in turn depends on freshness of the PMA solution used in the experiments. We plan to repeat each experiment with a freshly opened PMA aliquot in the future and hope to standardize our *in vitro* infection model. The decreased infection rate after amlexanox pretreatment was encouraging to merit further investigation. The decreased infection rates of amlexanox treated THP-1 TBK-1 KO cells made us to think that there were unidentified targets of amlexanox other than TBK-1. It was previously reported that *L. donovani* internalization by host macrophages decreased upon destabilization of the actin cytoskeleton by cytochalasin D, which reflects as a reduction in intracellular amastigote load (Roy, Kumar, Jafurulla, Mandal, & Chattopadhyay, 2014). Similar to cytochalasin D, amlexanox, is a known pharmacological inhibitor of actin stress fibers and disrupts existing actin fibers (M. Kim, Song, Jin, & Sonn, 2012; Landriscina et al., 2000). As mentioned before, *Leishmania* uptake is phagocytosis dependent and actin polymerization is central to this process (Rougerie, Miskolci, & Cox, 2013). Moreover, promastigotes must be enclosed transiently with periphagosomal F-actin to avoid phagosome maturation and enable parasitophorous vacuole formation (Moradin & Descoteaux, 2012). Based on the above mentioned observations, we hypothesized that the infection reducing effect of amlexanox might be TBK-1 independent, but dependent on downregulation of actin stress fibers, leading to decreased phagocytosis of the parasites. We further elucidated the effect of amlexanox on phagocytosis rate and autophagy in the following sections. Furthermore, we planned to test our hypothesis related to amlexanox's effect on actin stress fiber formation during *Leishmania* infection using confocal microscopy in future studies.

### 3.4.5. Phagocytosis rates of THP-1 cell lines and the effects of drug treatments on phagocytosis rate

*Leishmania* parasites exploit the host serum opsonins to facilitate their phagocytosis-dependent entry into macrophages (N. Ueno & Wilson, 2012). To better compare the phagocytosis rates of *L. major* in the WT and KO cell lines, we first opsonized the parasites using human serum. Then, THP-1 cells were infected with serum-opsonized parasites for 1-2 hours, followed by removal of unattached parasites and observation for intracellularly proliferating parasites. We hypothesized that 1-2 hours' infection of cell lines with opsonized parasites is mostly dependent on their phagocytosis rate. To gain insight into *Leishmania*-independent general phagocytic capacity of the cell lines, we also performed a pHrodo labeled-zymosan phagocytosis assay (Simons, 2010) concomitantly, which was conducted by Emre Dünüröğlü, a member of our laboratory. In this assay, pHrodo labeled zymosan particles are not fluorescent but yield a fluorescence signal upon phagocytosis and entry into acidified phagosomes.

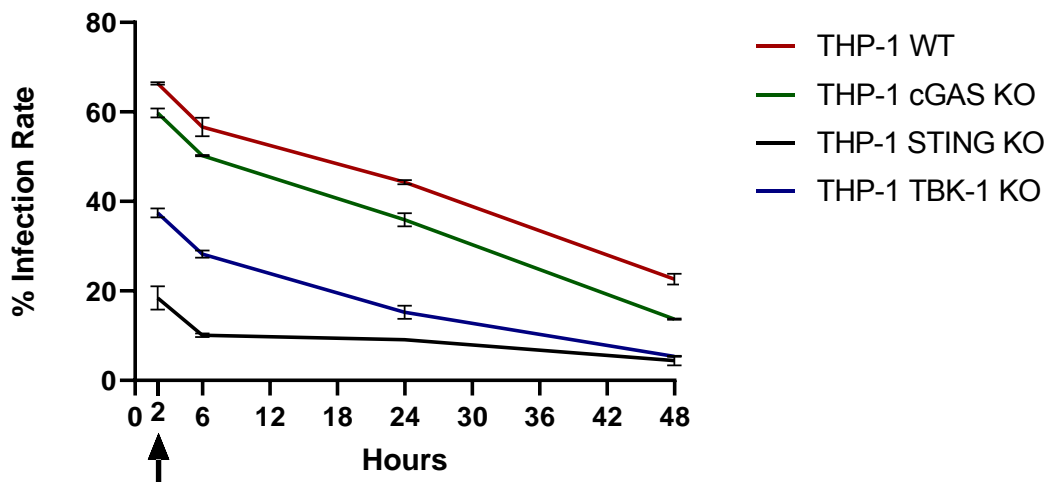


Figure 3.22. Infection of THP-1 cell lines with opsonized *L. major*

$10^5$  THP-1 cells were infected with  $10^6$  parasites (MOI: 10:1) for 2 h and parasite proliferation was followed for a period of 46 h. Parasites were opsonized prior to infection. THP-1 cells were differentiated with 5 ng/ml PMA for 48 hours and rested for another 24 hours before infection. Black arrow: Time point of parasite removal

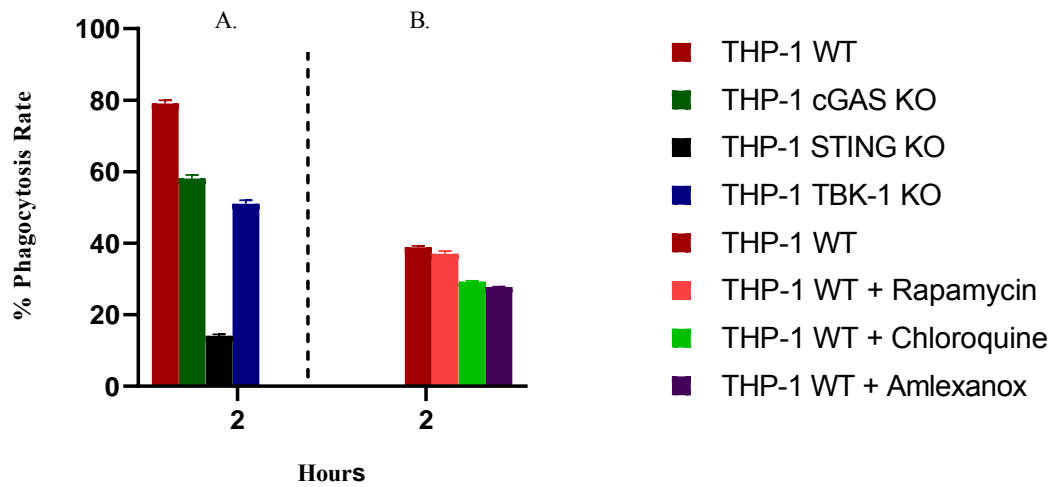


Figure 3.23. Phagocytosis assay with pHrodo green zymosan bioparticles

. THP-1 cells differentiated with 5 ng/ml PMA for 48 hours and rested for another 24 hours before experiment. Cells were incubated with pHrodo Green particles as described by the manufacturer. Rapamycin chloroquine and amlexanox treatments described in section 2.5.3. Data were generated by Emre Dünüroğlu

As can be seen in Figure 3.22. phagocytosis rates of THP-1 WT, cGAS KO, STING KO and TBK-1 KO cell lines very similar to infection rates of these cell lines with unopsonized parasites (Figure 3.17.) and followed the same internalization/parasite proliferation trend. These results suggested that the main differences in infection rates observed in KO THP-1 cell lines might be based on their phagocytosis capacity. Since previous publications claiming pro-parasitic effect of STING in infections lacked necessary phagocytosis controls (Majumdar et al., 2015), we wanted to assess the general phagocytic capacity of the cell lines using a parasite independent system (pHrodo-Zymosan).

Phagocytosis of zymosan particles is mediated by a variety of receptors, including the mannose, complement and  $\beta$ -glucan receptors (Underhill, 2003). *Leishmania* internalization is also mediated by different types of receptors, the most prominent,

being the third complement receptor (CR3), first complement receptor (CR1), Fc gamma receptors, mannose receptor (MR), and fibronectin receptors (N. Ueno & Wilson, 2012). Opsonization of *Leishmania* prior to infection converts the route of internalization towards a complement-opsonin dependent mechanism, which also serves as an entry route for zymosan particles (Domínguez & Toraño, 1999). Collectively, our data show that internalization rates of zymosan particles and opsonized parasites were similar in wild type versus KO cell lines, revealing a generalized phagocytosis deficiency in knockout cells which may account for their reduced infection rates (Figures 3.17., 3.21., 3.22., 3.23.).

In the B. part of Figure 3.23., the phagocytosis interfering effects of amlexanox, chloroquine and rapamycin pretreatment was investigated. Rapamycin, an autophagy inducer and chloroquine, a drug that prevents endolysosomal acidification were also used since these agents are employed in our autophagy studies (following sections) and it was important to analyze whether they impacted phagocytosis rates or not. Results demonstrated that pretreatment with amlexanox and chloroquine but not rapamycin, decreased zymosan phagocytosis rate, supporting our hypothesis presented in Section 3.4.4. Next, we also tested the effect of these drugs on phagocytosis rates in WT THP-1 cells infected with either unopsonized or opsonized *Leishmania* (Figure 3.24.).

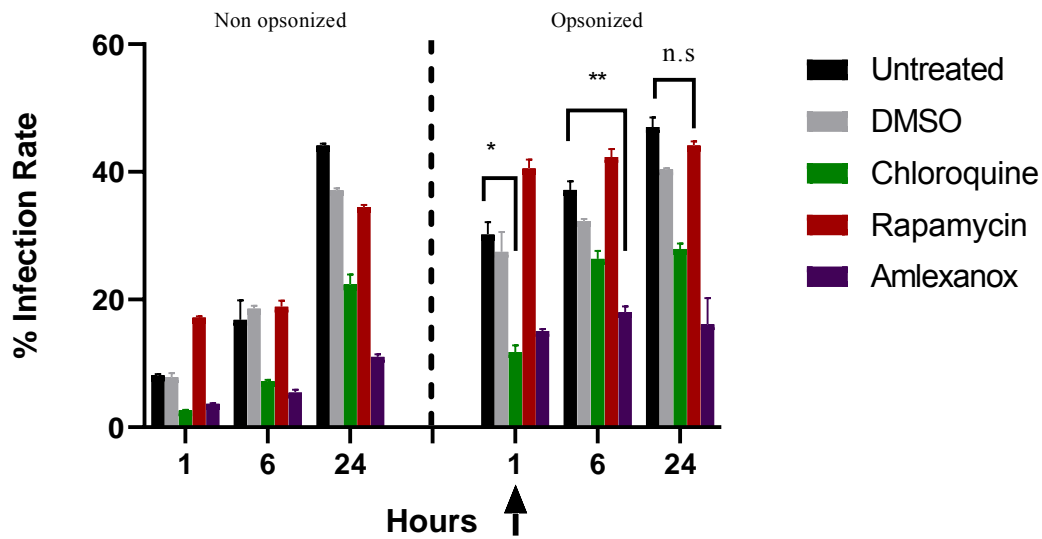


Figure 3.24. *In vitro* infection of THP-1 WT cells with opsonized and unopsonized transgenic *L. major*

$10^5$  THP-1 cells were infected with  $10^6$  parasites (MOI: 10:1). Average % infection rates of two independent experiment using 2-3 biological replicates are shown. THP-1 cells were differentiated with 5 ng/ml PMA for 48 hours and rested for another 24 hours before infection. Rapamycin chloroquine and amlexanox treatments were as described in Section 2.5.3. Black arrow: Time point of parasite removal.

A: Cells were infected with non-opsonized parasites but the parasites were not removed. Technical replicates from only one study is shown, precluding application of statistical analysis. B: Cells infected with opsonized parasites for 1h. All infection rates were compared to the untreated THP-1 WT group at all-time points statistically by Kruskal-Wallis test followed by Dunn's multiple comparison test (\*.  $p < 0.05$ , \*\*.  $p < 0.01$ ).

As it can be deduced from both zymosan (Figure 3.23.) and *Leishmania* phagocytosis assays (Figure 3.24.), amlexanox pretreatment suppressed phagocytosis of zymosan particles and significantly suppressed internalization of opsonized parasites. Moreover, this drug also significantly decreased the internalization of non-opsonized parasites in THP-1 WT and THP-1 TBK-1 KO cells (Figure 3.21.). Therefore, the phagocytosis inhibiting activity of amlexanox appears to be a generalized effect, possibly through interfering with actin stress fiber formation. In further studies, we aim to supply microscopic evidence for this phenomenon by labeling actin fibers during parasite infection with or without amlexanox pretreatment.

Chloroquine is a well-known anti-malarial drug and increases lysosomal pH, thereby inhibiting lysosomal degradation. Since chloroquine inhibits digestion of hemoglobin in malaria infected erythrocytes, parasite survival is compromised as a result of nutrient depletion (Homewood, Warhurst, Peters, & Baggaley, 1972). Interestingly, chloroquine also displayed an anti-parasitic activity in our *L. major* infection studies. When pretreated, chloroquine reduces the phagocytosis rate of zymosan particles (Figure 3.23.) and phagocytosis of non-opsonized and opsonized parasites (Figure 3.24.) in THP-1 WT cells. Chloroquine is a well-known autophagy inhibitor that blocks lysosomal degradation by increasing lysosomal pH and prevents autophagosome fusion with lysosomes (Mauthe et al., 2018). Rapamycin on the other hand, increases autophagy by binding fk506-binding protein (FKBP12) and inhibiting mTOR activity (Lin, Han, Weng, Wang, & Chen, 2018). Effect of rapamycin on phagocytosis rate of zymosan particles and opsonized parasites were not significantly different than those observed in THP-1 WT untreated cells (Figure 3.23., 3.24.). Therefore, chloroquine-mediated modification of phagocytosis appears to be an autophagy-independent process. The ability of this drug to inhibit both zymosan and opsonized *Leishmania* uptake, similar to the extent induced by amlexanox, indicates that both drugs might directly modulate pathways related to phagocytosis. Evidence suggests that chloroquine can suppress the internalization of serum opsonized bacteria (Antoni, Hrabák, & Csuka, 1986; Labro & Babin-Chevaye, 1988). Although how chloroquine interferes with phagocytosis is not clear, our data presented in Figure 3.25. using another lysosomal pH increasing agent (Bafilomycin A1), supports the notion that an increase in endolysosomal pH correlates with a general decrease in phagocytosis rates.

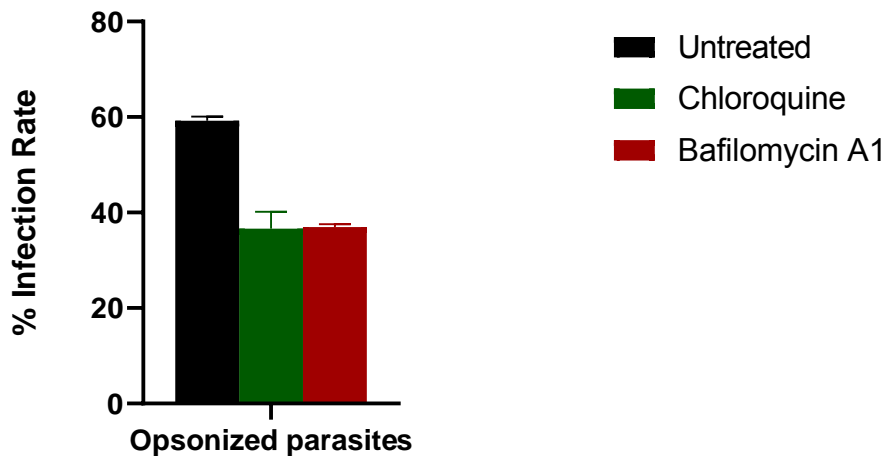


Figure 3.25. *In vitro* infection of THP-1 WT cells with opsonized transgenic *L. major* pretreated or not with Chloroquine or Bafilomycin A1.

THP-1 WT cells were infected with opsonized transgenic *L. major* following pretreatment with chloroquine or bafilomycin A1.  $10^5$  THP-1 cells were infected with  $10^6$  parasites (MOI: 10:1) for 1 h. THP-1 cells were differentiated with 5 ng/ml PMA for 48 hours and rested for another 24 hours before infection. Chloroquine and bafilomycin A1 treatments were as described in section 2.5.3.

Collectively, our results suggest that intrinsic differences in phagocytic capacity of THP-1 WT, STING KO, cGAS KO and TBK-1 KO cells impact the overall *L. major* parasite loads. Moreover, amlexanox, chloroquine and bafilomycin A1 decrease phagocytosis rate of both opsonized parasites and zymosan particles in WT cells to levels observed in STING and TBK1 knockout cells. We hope to unravel the detailed mechanism underlying these differences in future studies.

### 3.4.6. Comparison of *Leishmania* infection rates of THP-1 ISG15 KO and THP-1 LVC cells

As mentioned previously, type I interferon-mediated responses modulate disease severity in *Leishmania* infections. Since ISG15 is one of the most significantly upregulated genes in response to type I IFN signaling and is also expressed in *L. braziliensis* infected dendritic cells (Vargas-Inchaustegui et al., 2008), we wanted to investigate its role in immunity against *L. major* infection using our *in vitro* infection

model. For this, THP-1 ISG15 KO and THP-1 LVC cells were pretreated with 50 ng/ml recIFN $\beta$  or 5  $\mu$ g/ml cGAMP for 8 hours to induce expression of ISGs. Only one of our cell lines produces ISG15 in response to type I IFN or cGAMP stimulation (THP-1 LVC), whereas the other (THP-1 ISG15 KO) cannot. Phagocytosis assay using pHrodo labeled zymosan particles demonstrated similar zymosan phagocytosis rates in cGAMP pretreated THP-1 ISG15 KO and THP-1 LVC cell lines (Figure 3.26.). Therefore, differences observed in infection rates of cGAMP pretreated THP-1 ISG15 KO and THP-1 LVC cells might be attributed to the lack of ISG15 protein and not to a defect in phagocytosis.

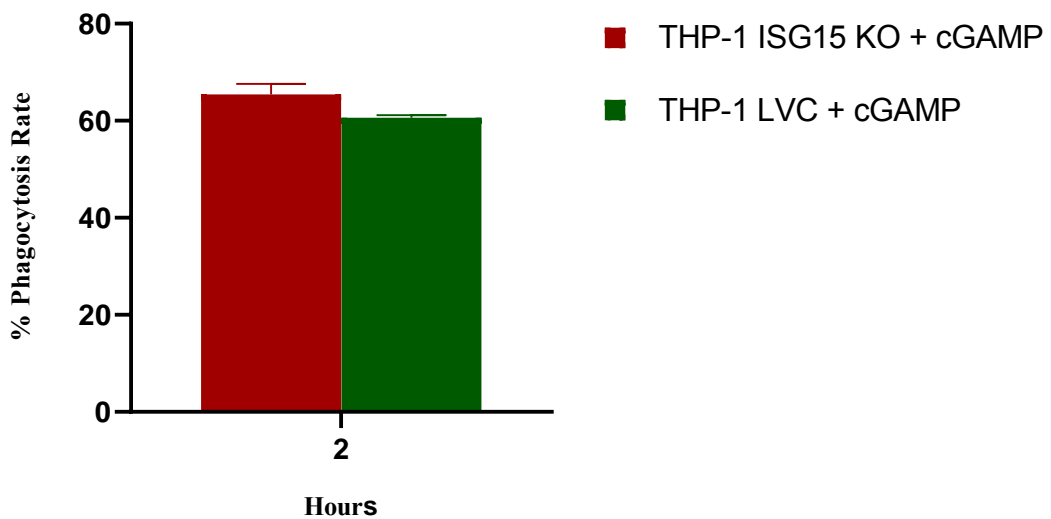


Figure 3.26. Phagocytosis assay with pHrodo green zymosan bioparticles

THP-1 cells differentiated with 5 ng/ml PMA for 48 hours and rested for another 24 hours before experiment. Cells were incubated with pHrodo Green particles as described by the manufacturer. Data were generated by Emre Dünüroğlu

THP-1 ISG15 KO infection studies with *L. major* indicated that this cell line was significantly resistant to infection whether pretreated with recIFN $\beta$  or not (Figure 3.27.).

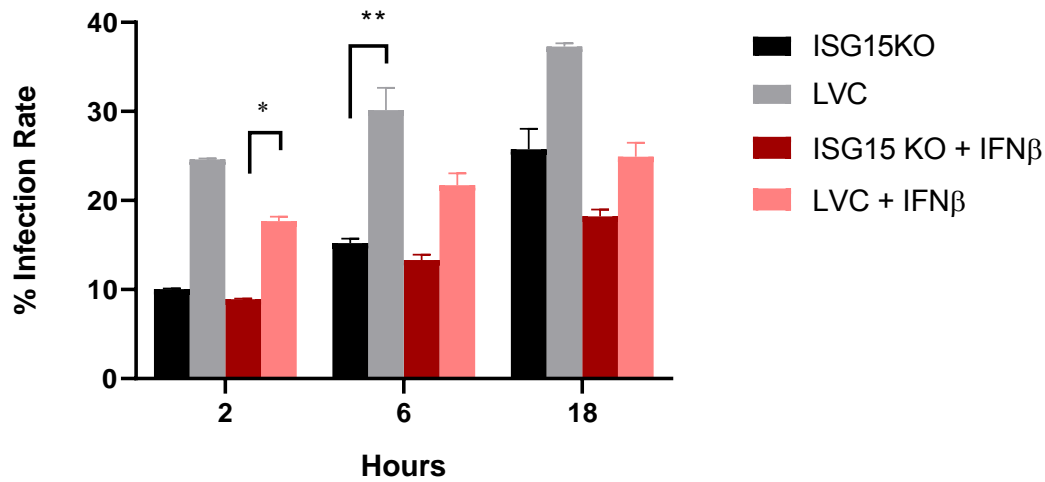


Figure 3.27. Comparison of *L. major* infection rates in THP-1 ISG15 KO and THP-1 LVC cells

18 hours of infection process.  $10^5$  THP-1 cells were infected with  $10^6$  parasites (MOI: 10:1) for 18 h. Parasites were not opsonized prior to infection. THP-1 cells were differentiated with 5 ng/ml PMA for 48 hours and rested for another 24 hours before infection. Average % infection rates of two independent experiment using 2-3 biological replicates are shown

Indicated groups were statistically compared with Mann-Whitney Unpaired test (\*.  $p < 0.05$ , \*\*.  $p < 0.01$ ).

Phagocytosis assay with zymosan particles on cGAMP pretreated THP-1 ISG15 KO and THP-1 LVC cell lines demonstrated that their phagocytosis rates were similar (Figure 3.26.). This result suggests that ISG15 might possess a pro-parasitic role and its absence limits *Leishmania* infectivity (Figure 3.27.). Infection of THP-1 ISG15 KO and LVC cell lines with opsonized parasites provided further evidence on the role of ISG15 in *L. major* infection (Figure 3.28.).

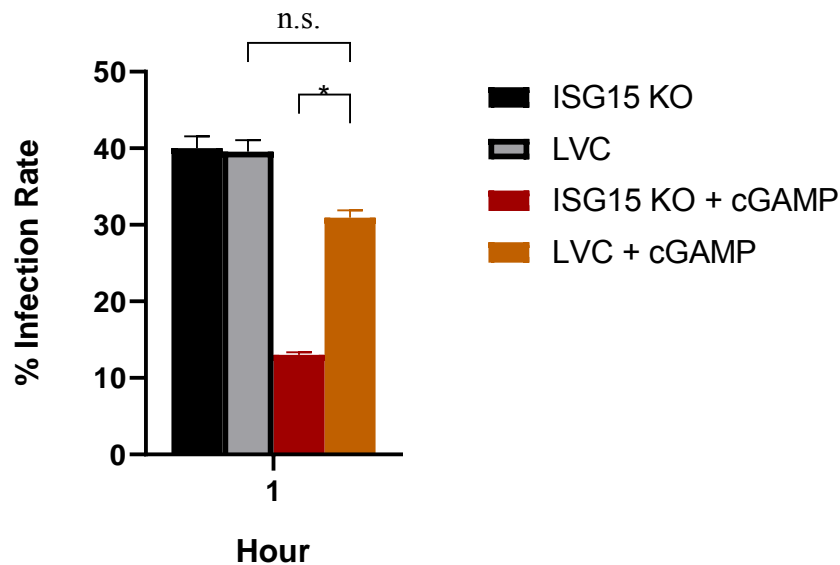


Figure 3.28. THP-1 ISG15 KO and THP-1 LVC infection rates with opsonized *L. major*

10<sup>5</sup> THP-1 cells were infected with 10<sup>6</sup> parasites (MOI: 10:1) for 1 h. Average % infection rates of two independent experiment using 2-3 biological replicates are shown. Parasites were opsonized with human serum prior to infection. THP-1 cells were differentiated with 5 ng/ml PMA for 48 hours and rested for another 24 hours before infection.

Indicated groups were statistically compared with Mann-Whitney Unpaired test (n.s, not significant; \*, p<0.05)

As mentioned before, cGAMP pretreated THP-1 ISG15 and THP-1 LVC zymosan uptake rates were not different (Figure 3.26.) whereas their infection rates differed significantly (Figure 3.27). Moreover, cGAMP pretreatment specifically reduced internalization rate of opsonized parasites in THP ISG15 KO cells but not the THP-1 LVC cells (Figure 3.28.). As mentioned before, very little is known about the function of ISG15 protein during *Leishmania* infection. Our results suggest that ISG15 might exert a pro-parasitic effect that is pronounced especially during the early infection (Figure 3.28.). Since absence of ISG15 was previously shown to influence the basal autophagy rates in certain cells (Y. Zhang et al., 2019) we assessed the autophagic

properties of THP-1 ISG15 KO cells to further elaborate the role of ISG15 in *Leishmania* infections (Section 3.5.2.).

### **3.5. Characterization of autophagic changes in *in vitro* *L. major* infection model**

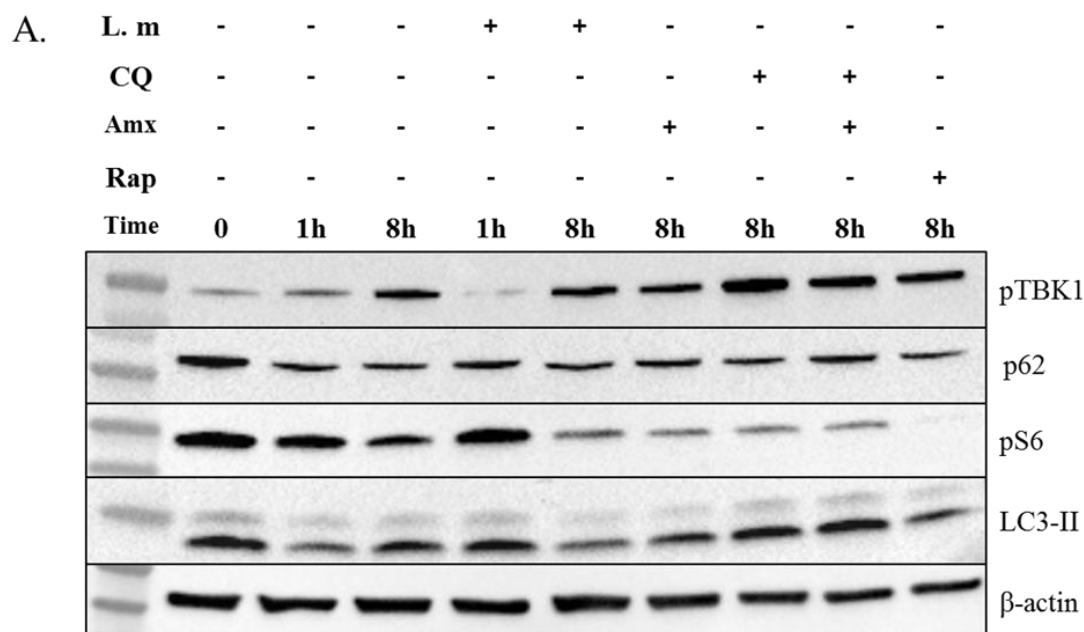
The role of autophagy in *Leishmania* infections remains not well understood, possibly due to conflicting published results (Veras, de Menezes, & Dias, 2019). The interplay between autophagy and the phagocytic pathway also remains unclear, complicating interpretation of results related to autophagy and *Leishmania* infection (Sanjuan et al., 2007). For example, one study reported that induction of autophagy with rapamycin prior to the initiation of phagocytosis, decreased the internalization rates of *L. amazonensis*, latex beads and zymosan particles in murine macrophages (Lima et al., 2011). A second study demonstrated that rapamycin pretreatment had no effect on dextran internalization (Haidinger et al., 2010). Our results are in agreement with this second study and revealed that rapamycin-induced autophagy did not change the phagocytosis rate of zymosan particles (Figure 3.23.) or the opsonized parasites (Figure 3.24., B.). However, rapamycin pretreatment specifically increased the infection rate of unopsonized parasites during the first hours of infection (Figure 3.24., A., 1-6 hours). Since opsonization broadens the receptor repertoire to which *Leishmania* parasites can attach to and use to trigger phagocytosis, it is conceivable that the effects of increased autophagy on phagocytosis and infection rates might be masked and became apparent only in the less efficient unopsonized parasite infection model.

Induction of autophagy during *L. amazonensis* infection on murine macrophages was previously reported. However, this particular study did not utilize the compounds that inhibit autophagosome maturation (Cyrino et al., 2012). Using BMDMs from BALB/c mice, one study demonstrated autophagic induction upon *L. major* infection, supported by data showing increased LC3-II to LC3-I ratio in infected cells (Frank et al., 2015). Recently, another work demonstrated that *L. major* infection induces autophagy in BMDMs of C57BL/6 mice in a toll-like receptor 3/7/9-dependent

manner (Franco et al., 2017). One other study also reported that autophagic pathway was activated in THP-1 cells upon infection with *L. donovani*, based on increased LC3-II/LC3-I ratios following immunoblotting of infected cell extracts (S. A. Thomas et al., 2018). Collectively, these previous studies indicate that *Leishmania* infection activates autophagy in different infected cell types. However, most of these studies employed a single time point to study autophagy and failed to address its role through the course of *Leishmania* infection (Veras et al., 2019).

There are some reports in which the impact of autophagy inducers were evaluated in *in vitro* infection experiments. For example, one study showed that starvation induced autophagy enhanced *L. amazonensis* intracellular viability in infection-susceptible BALB/c macrophages but not in the resistant C57BL/6 macrophages, whereas for *L. major*, intracellular viability remained unchanged following autophagy induction (Pinheiro et al., 2009). This is in support of our results, where rapamycin treatment did not change the parasite load upon infection of THP-1 cells with opsonized *L. major* (Figure 3.24., B.; later time points). However, when the earliest infection time point was analyzed, we saw that rapamycin augmented the infection rate (Figure 3.24., 1-hour data), suggesting that autophagy might contribute to establishment of *Leishmania* infection at early but not later time points. To assess the autophagic status of *L. major* infected THP-1 cells, we performed western blotting to investigate the alterations of autophagy related proteins during *in vitro* infection with *L. major*. Autophagy is a dynamic process and it is regulated at several steps. Therefore, assessment of LC3-II turnover by immunoblotting must be established in the presence and absence of lysosomal degradation (Z. Zhang, Singh, & Aschner, 2016). For this, we used chloroquine treatment to prevent lysosomal degradation and inhibit autophagic flux. In order to calculate LC3-II flux for a treatment, densitometric values of chloroquine treated and non-treated band intensities were subtracted ( $\delta$  value) and this approach was also used to calculate the flux of autophagy substrate SQSTM1/p62 (Z. Zhang et al., 2016).

Our preliminary efforts to observe autophagic changes upon *L. major* infection was to follow the LC3-II turnover in a time dependent manner without chloroquine addition. Contrary to previous findings (Pitale, Gendalur, Descoteaux, & Shaha, 2019), we did not observe a linear increase in LC3-II or p62 band intensities in parasite infected cells over time (Figure 3.29.).



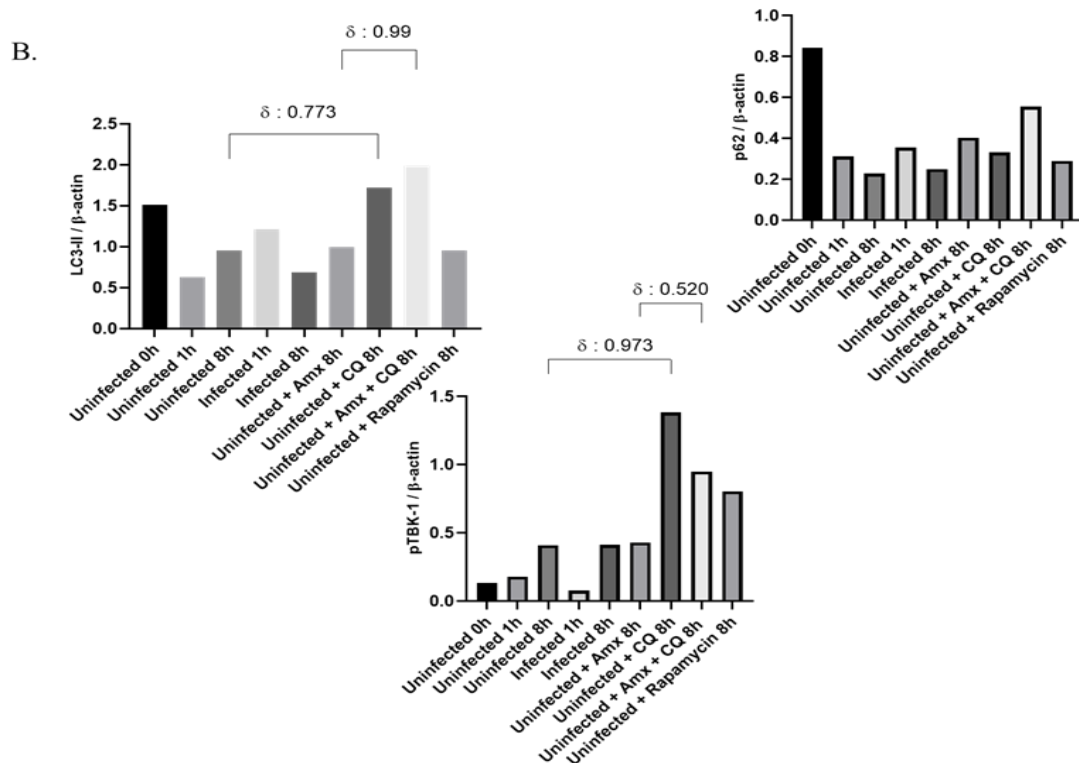


Figure 3.29. Western blot images (A) and densitometric analysis of band intensities (B) of THP-1 WT cells.

40  $\mu$ g total cell lysates were loaded to each well of a 4-20 % protein gradient gel. THP-1 cells were differentiated with 5 ng/ml PMA for 48 hours and rested for another 24 hours before infection. Chloroquine was added 2 hours before lysis. Rapamycin and amlexanox were introduced to cultures as described before (Section 2.5.2.).  $\delta$ : densitometric differences of indicated lanes. L. m: *L. major*, Amx: Amlexanox, CQ: Chloroquine, Rap: Rapamycin.

Untreated (8 hours) group and its chloroquine control demonstrated that autophagy was already upregulated in these PMA differentiated THP-1 WT cells (Densitometric difference in LC3-II/ $\beta$ actin,  $\delta$ : 0.773). This was as expected since PMA differentiation is a known inducer of autophagy (Y. Xu, Wang, Bai, Zhang, & Chen, 2015). Analysis of untreated sample (8 hours) and its chloroquine treated control, revealed the presence of spontaneously phosphorylated TBK1 were utilized by which undergoes lysosomal degradation (S. Yang et al., 2016) and therefore its flux can be monitored upon

chloroquine addition (Figure 3.29). As expected, TBK1 inhibitor amlexanox decreased pTBK1 flux from 0.973 to 0.520 in 8 hour uninfected cells.

Autophagy receptor sequestosome 1 (SQSTM1, p62) physically links autophagic cargo to the autophagic membrane and targets ubiquitinated cargos to autophagic degradation by binding to LC3 and is itself degraded in autolysosomes. Comparison of uninfected (8 hours) group with its chloroquine treated control demonstrated that p62 was also subjected to flux ( $\delta$ : 0.11). Collectively, based on the LC3-II and p62 densitometric results, we concluded that PMA differentiated THP-1 WT cells demonstrated spontaneous autophagy. To confirm this, we also monitored the phosphorylation status of the ribosomal S6 protein. S6 is phosphorylated by protein S6 kinase 1 (S6K1) which is a direct target of m-TORC1. Therefore, pS6 levels can be monitored as a marker for the catalytic activity of mTOR (Fingar et al., 2004). mTOR activity and hence pS6 levels should be down modulated in samples showing autophagic activity (Y. C. Kim & Guan, 2015). As expected, mTOR inhibitor rapamycin treated control revealed massive down regulation of pS6 level (Figure 3.29.). pS6 levels also decreased over time in untreated and uninfected groups, further supporting the upregulation of autophagy in PMA differentiated THP-1 WT cells (Figure 3.29.). Interestingly, pS6 levels were also down modulated in 8 h *Leishmania* infected, chloroquine and amlexanox treated samples. *Leishmania* gp63 protein targets and degrades mTOR protein (Jaramillo et al., 2011) and therefore would result in decreased S6 phosphorylation. Amlexanox inhibits pTBK1-mediated mTOR activation (Bodur et al., 2018) and hence prevents S6 phosphorylation (Figure 3.29). Finally, chloroquine interferes with mTORC1 activity by facilitating its release from lysosomal membranes (Zhitomirsky et al., 2018), resulting in reduced pS6 levels (Figure 3.29.).

Our western blot based approach to understand how *Leishmania* alters autophagy in host cells remained inconclusive, necessitating evaluation of our method. To better address this issue, we have ordered the THP1-Difluo™ hLC3 THP-1 reporter cells that are specifically designed to monitor the autophagic flux. These cells express the

acid-stable RFP::acid-sensitive GFP::LC3 fusion protein, enabling microscopic visualization of fluorescent puncta, degradation of the GFP, and accumulation of the RFP signal in autolysosomes. By measuring the number of fluorescent punctate autophagosomes per cell, and determining the percentages of RFP-GFP positive and RFP positive cells, we hope to assess autophagic flux more precisely and characterize the process in detail in *Leishmania* infected cells.

### 3.5.1. Characterization of autophagy related changes in THP-1 ISG15 KO cells and THP-1 LVC

Our preliminary studies demonstrated that without pretreatment with cGAMP, ISG15 was not detectable in parasite infected cells. However, *L. major* infection of cGAMP pretreated THP LVC cells demonstrated that ISG15 was transiently upregulated during early infection (1 hour), but not after 6 hour of infection (Figure 3.30.).

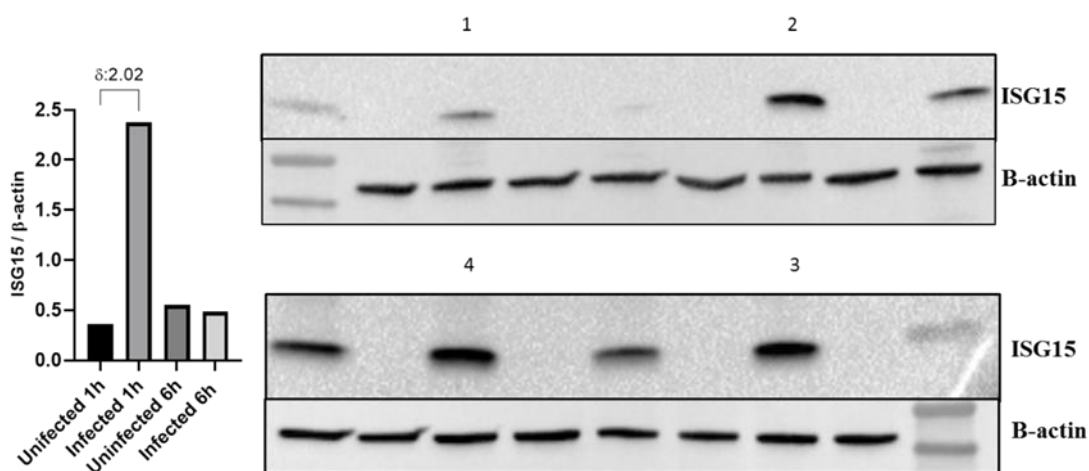


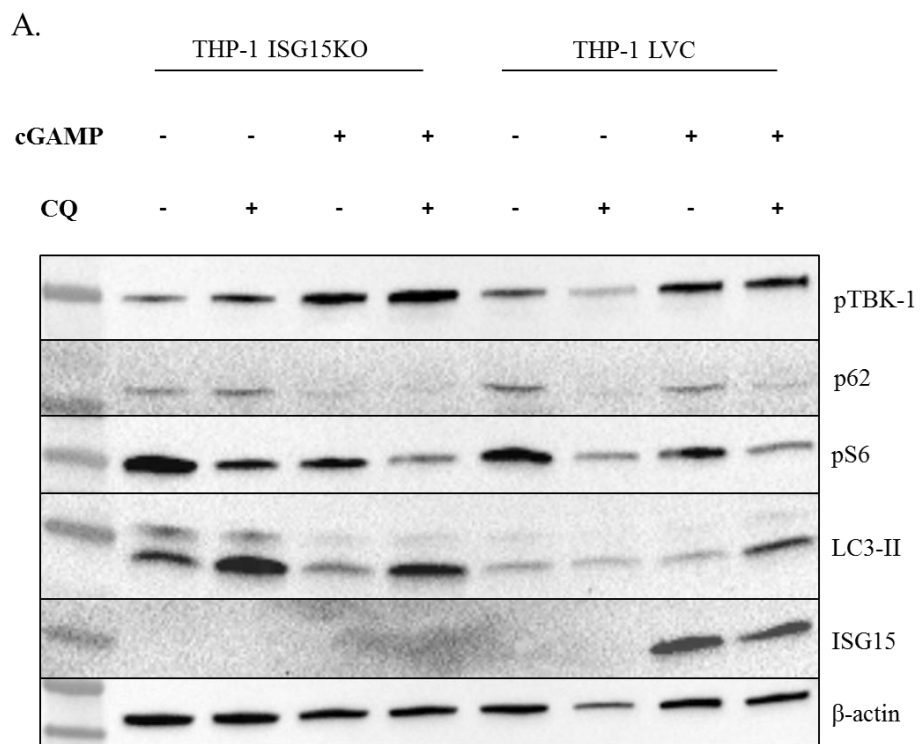
Figure 3.30. Western blot images and densitometric analysis of THP-1 LVC cells infected with *L. major* for 1 and 6 hours.

40  $\mu$ g protein was loaded onto each well of a 4-20 % protein gradient gel. THP-1 LVC cells were differentiated with 5 ng/ml PMA for 48 hours and rested for another 24 hours before infection. Cells were pretreated with 5  $\mu$ g/ml cGAMP for 12 hours to upregulate ISG15.  $\delta$ : densitometric differences of indicated lanes. Indicated antibodies were used (Appendix D).

Lane 1: Uninfected 1 hour, Lane 2: *L. major* infected for 1 hour, Lane 3: Uninfected 6 hour, Lane 4: *L. major* infected for 6 hours

This result indicates that ISG15 plays an important role during early infection, since its level was upregulated 6.62- fold (Figure 3.30.) within 1-hour of *L. major* infection. However, this difference was no longer observable at the later time point (6h). We plan to confirm these results in infected cells using intracellular staining and flow cytometric evaluation of ISG15 levels on an hourly basis to gain insight on how ISG15 is regulated in response to *Leishmania* infection. We also planned to use recombinant ISG15 to rescue the phenotype of THP-1 ISG15 KO to validate the pro-parasitic effect of ISG15 in our *L. major* infection model.

Autophagic status of THP-1 ISG15 KO cells were also determined through monitoring of LC3-II flux as mentioned before (Z. Zhang et al., 2016). Results presented in Figure 3.31 (LC3-II data) indicate that ISG15 deficient cells display enhanced autophagy. This result is consistent with the findings of previous studies that showed increased autophagy in the absence of ISG15 (D. Xu et al., 2015; Y. Zhang et al., 2019). Of note, one study proposed that ISGylation of BECN1 at Lys117 upon the type I interferon induction competed with its ubiquitination, which subsequently led to the inhibition of phosphatidylinositol 3-kinase catalytic subunit type 3 (PIK3C3) and suppression of autophagy (D. Xu et al., 2015). Our results are in support of a role of ISG15 in suppressing autophagy, since THP-1 ISG15 KO cells were highly autophagic in comparison to THP LVC cells (Figure 3.31.).



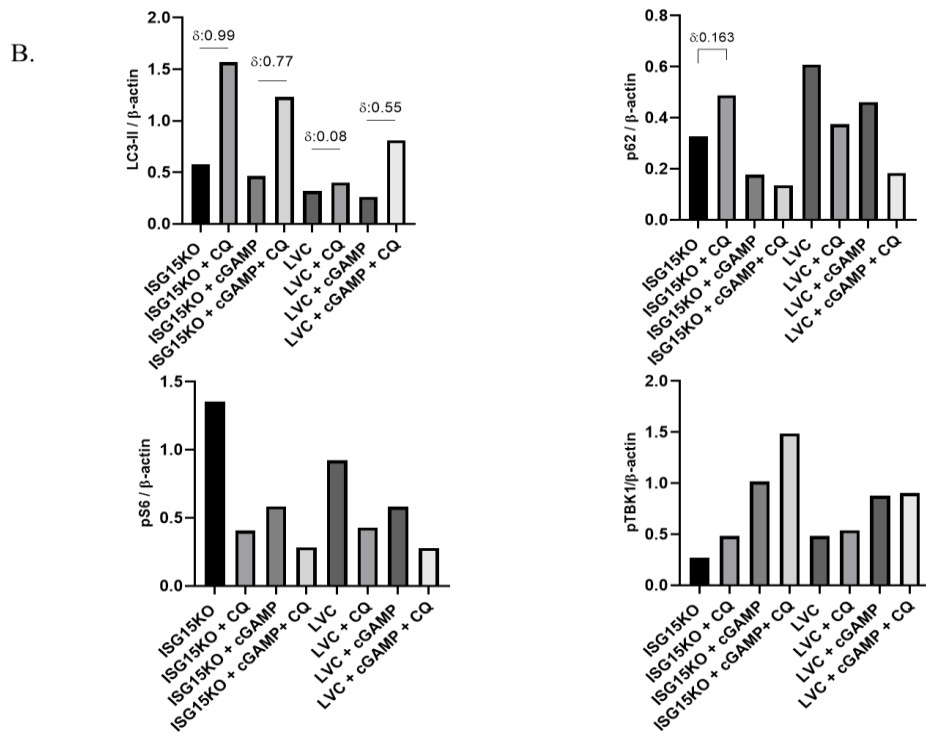


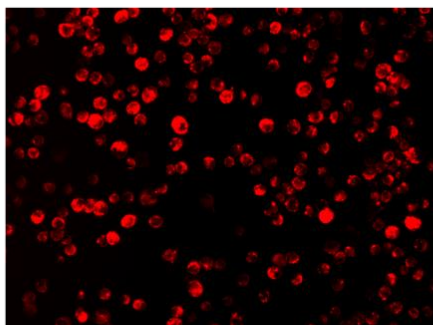
Figure 3.31. Western blot images (A) and densitometric analysis (B) of autophagy marker in THP-1 ISG15 KO and THP-1 LVC cells

40  $\mu$ g protein was loaded onto each well of a 4-20% protein gradient gel. THP-1 cells were differentiated with 5 ng/ml PMA for 48 hours and rested for another 24 hours. Chloroquine was added 2 hours before lysis of indicated groups  $\delta$ : densitometric differences of indicated lanes. Cells were pretreated with 5  $\mu$ g/ml cGAMP for 12 hours

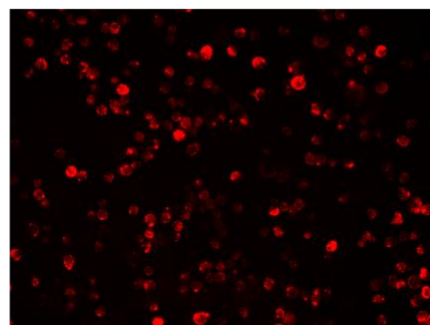
Densitometric difference for LC3-II flux between chloroquine treated and untreated of THP-1 ISG15 KO cells was  $\delta$ : 0.99, whereas this value was only  $\delta$ : 0.08 in THP-1 LVC cells (Figure 3.31., B.). As expected, pretreatment of THP-1 LVC cells with cGAMP increased the LC3-II flux ( $\delta$ : 0.08-0.55), since cGAMP depended activation of STING induces autophagy in a type I interferon-independent manner (Gui et al., 2019). Contrary to LVC controls, cGAMP pretreatment failed to further enhance autophagy in THP-1 ISG15 KO cells ( $\delta$ : 0.99 versus 0.77) (Figure 3.31., B.). Analysis of pS6 revealed decreased levels in cGAMP pretreated THP-1 ISG15 KO and LVC cells, compatible with their increased autophagic status. When p62 levels were assessed, in THP-1 ISG15 KO cells, chloroquine treated cells were found to

accumulate p62 ( $\delta$ : 0.163), whereas in THP-1 LVC, there was no p62 accumulation upon chloroquine treatment, suggesting absence of lysosomal degradation of p62 in steady state THP-1 LVC cells. Collectively, western blot analysis of autophagy markers demonstrated enhanced autophagy in both steady state and cGAMP pretreated THP-1 ISG15 KO cells compared to THP-LVC control cells. In addition to western blotting, we also used LysoTracker red stain to label the acidic compartments in ISG15 KO and LVC cells. LysoTracker dye stains acidic compartments inside the cell including lysosomes, autolysosomes, phagosomes and late endosome (Harrison, Bucci, Vieira, Schroer, & Grinstein, 2003). LysoTracker signal is enhanced during starvation or in the presence of pharmacological stimuli that induce autophagy (Devorkin & Gorski, 2014). Therefore, LysoTracker staining might be a complementary tool to analyze the autophagic status of the ISG15 KO and LVC control THP-1 cell lines. For this, cGAMP treated or untreated cell lines were loaded with the LysoTracker Red dye 30 min prior to the end of the incubation period. Images of the LysoTracker red signal were then collected on FLoid imaging station using the same brightness and contrast setting for all samples. Unprocessed images were transferred to Image J and LysoTracker Red signal of each sample was quantified following image conversion into gray scale and using the “Analyze” tab and “mean gray value” measurement.

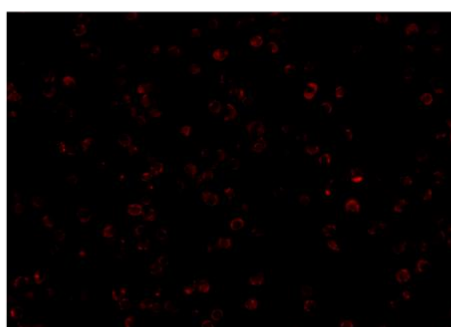
A.



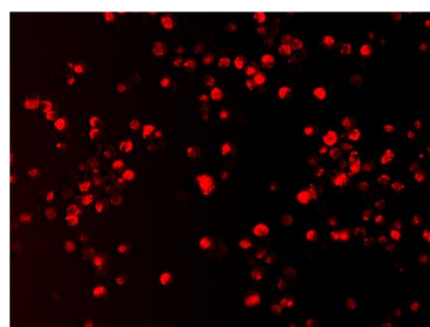
THP-1 ISG15 KO



THP-1 ISG15 KO + Rap

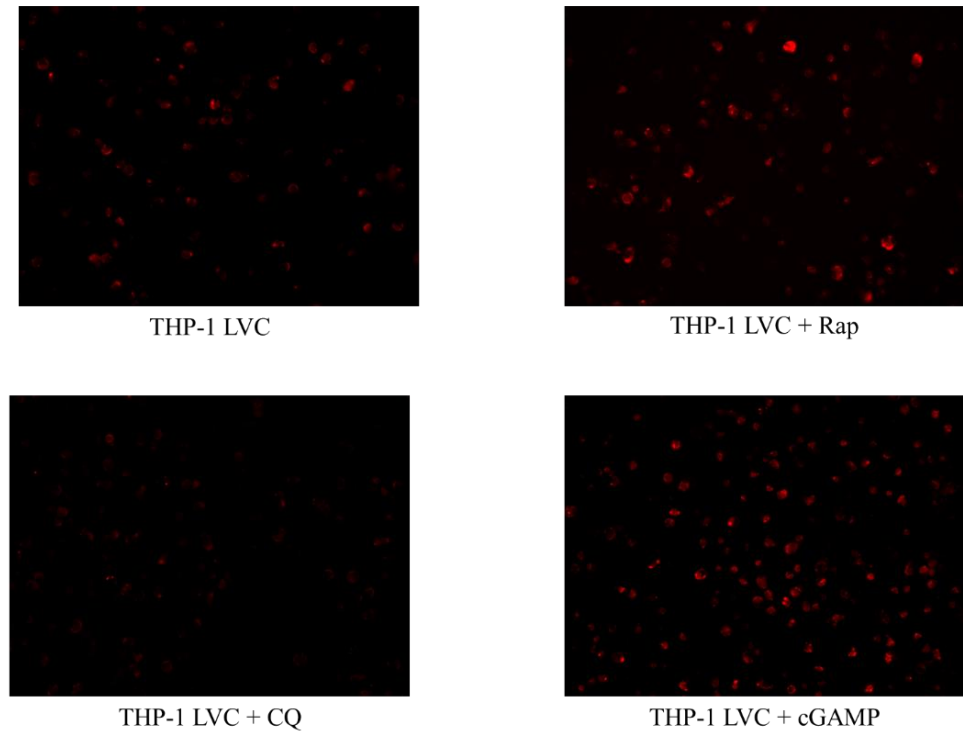


THP-1 ISG15 KO + CQ



THP-1 ISG15 KO + cGAMP

B.



C.

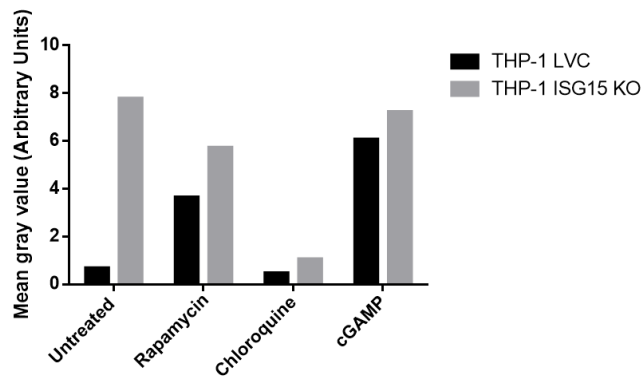


Figure 3.32. Fluorescence microscopy images of LysoTracker Red stained THP-1 ISG15 KO (A) and LVC (B) cells.

Cells were stained with 50 nM LysoTracker red for the last 30 minutes of incubation at 37°C. Same contrast and brightness settings used for all images. Cells were differentiated with 5 ng/ml PMA for 48 hours and rested for another 24 hours. Treatments included: pre incubation with 5 µg/ml cGAMP for 12 hours, 500 nM Rapamycin for 18 hours and 40 µM Chloroquine for 2 hours. C. LysoTracker Red signal of samples were quantified using the Image J software. CQ: Chloroquine, Rap: Rapamycin

LysoTracker results confirmed that rapamycin and cGAMP treatment increased the fluorescence signal significantly in LVC cells (Figure 3.32., B and C). In contrast, in ISG15 KO cells, in the absence of any stimulus, LysoTracker Red intensity was ~8-fold higher than LVC control and neither rapamycin, nor cGAMP failed to further enhance these levels (Figure 3.32., A and C). As expected, in the presence of chloroquine, LysoTracker signal was lost in both cell lines. Collectively, the LysoTracker staining results are in agreement with the western blot analysis (Figure 3.31.) and suggest increased autophagy in THP-1 ISG15 KO cells compared to THP-1 LVC cells. Further studies must elaborate the role of ISG15 in *L. major* infection and autophagy. Mechanistic explanations of pro-parasitic effect of ISG15 during early infection (Figure 3.28.), increased autophagic signaling in ISG15 KO cells (Figure 3.31, 3.32.) and whether these two phenomenon are related or not, will be investigated in future studies.

### **3.6. *In vivo* infection studies with LRV- and LRV+ *L. major* strains**

To assess whether the pathogenicity of the LRV+ and LRV- transgenic *L. major* strains differed, equal concentration of live parasites were injected into the left footpads of each mouse and footpad-associated parasite loads were determined using IVIS. Contrary to our expectations, mice that received the LRV positive parasites had very low parasite loads when compared to the group challenged with the virus negative strain (Figure 3.33).

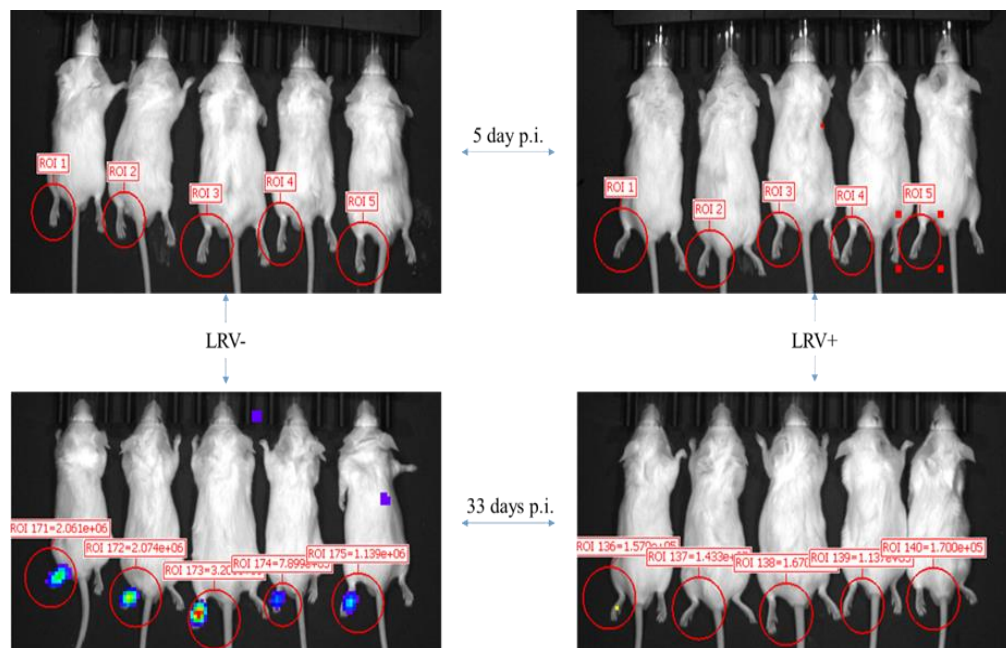


Figure 3.33. Monitoring of parasite loads in mice challenged with LRV- and LRV+ transgenic *L. major* using *in vivo* imaging

5 BALB/c mice were challenged with  $9 \times 10^6$  metacyclic LRV- or LRV+ parasites on day 0. Footpads were imaged for parasite loads on days 5 and 33 as described in section 2.6.1.1., p.i: post injection

33 days after challenge, LRV- *L. major* injected footpads displayed high parasite loads, whereas LRV+ *L. major* injected footpads yielded very low luminescence (Figure 3.33.). Therefore, LRV1 and LRV2-1 might affect disease progression differently. One interesting study showed that presence of LRV1, decreased the translation initiation rates in infected parasites (Atayde et al., 2019). Specifically, translation of parasite-associated *Gp63*, *Hsp70* and *Hsp83* was diminished in infected promastigotes. If this is the case, one would expect virally infected parasites to proliferate more slowly. Provided that LRV2-1 positive parasites also exhibit virus-induced diminished translation, it is conceivable that lower parasite counts (Figure 3.33.) might be related to slower growth of parasites. To test this hypothesis, future studies should perform comparative quantitative PCR of LRV2-1 +/- parasites.

However, in favor of this hypothesis, we did observe lower expression of EGFP in the metacyclic LRV+ *L. major* strain compared to the LRV- *L. major* strain. In summary, LRV2-1 infected *Leishmania* did not trigger severe/metastatic disease in our model.

### 3.7. *In vivo* amlexanox treatment of LRV- *L. major* infected BALB/c mice

Since our *in vitro* infection experiments revealed that amlexanox exhibited an anti-parasitic effect, we wanted to test its anti-leishmanial activity *in vivo*. For this, four out of seven mice that were infected with LRV- *L. major* (5 of them were presented in Figure 3.33.) were treated with amlexanox on day 41 post-challenge, as described in section 2.6.2. The drug was re-introduced to animals on a daily basis for 12 days and footpad swelling was assessed on the indicated days. The three mice in the control group received daily injections of an equivalent volume of DMSO only. Footpad size and parasite loads were determined through *in vivo* IVIS imaging on three different days and digital caliper on six different days (Figure 3.34., 3.35.). Days presented in Figures correspond to the initiation and continuation of amlexanox therapy.

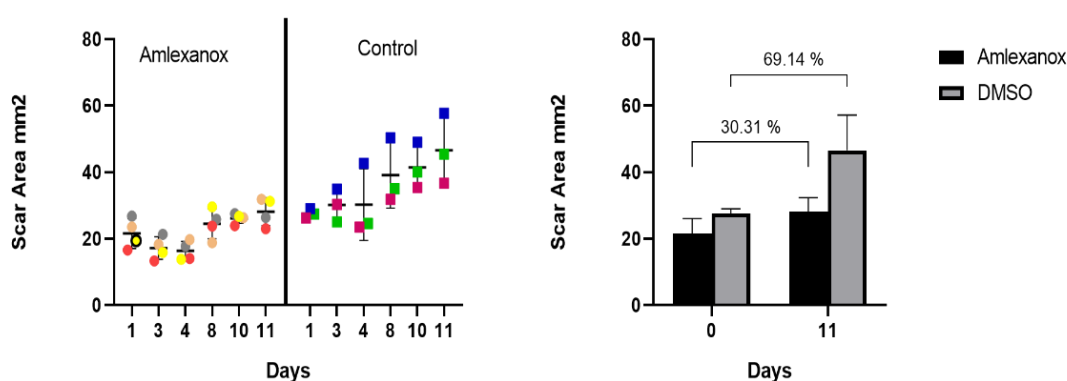


Figure 3.34. Monitoring of footpad swelling in LRV- *L. major* challenged mice during 12 days of amlexanox treatment

Results were based on digital caliper measurement of footpad depth and width of DMSO injected controls (n=3) and amlexanox injected (n=4) treatment groups. Colors represent individual mice.

Percent ratios indicate increase in scar area for amlexanox and DMSO treated groups

Footpad measurements demonstrated that amlexanox treatment delayed footpad swelling ~2-fold (30.31 % change), when compared to DMSO control group (69.14 % change) (Figure 3.34). Based on these results, we will repeat the *in vivo* amlexanox therapy assay using a larger sample size and intend to initiate amlexanox therapy earlier since the extent of footpad swelling in the above experiment was already too severe (~20 mm<sup>2</sup>), which may underestimate the therapeutic benefit of the drug. Starting *in vivo* amlexanox therapy when scar sizes are around 10 mm<sup>2</sup>, and administering amlexanox together with other anti-parasitic agents would improve the therapeutic outcome.

*In vivo* imaging-based parasite load measurement was more polymorphic than footpad area measurements, owing to the formation of scar tissues that masked the parasite associated luminescence signal especially on day 12. Therefore, IVIS measurements and footpad measurements do not complement each other (Figure 3.35.). As mentioned earlier, to circumvent scar tissue formation and assess parasite loads more precisely, amlexanox therapy will be initiated in mice with moderate parasitemia.

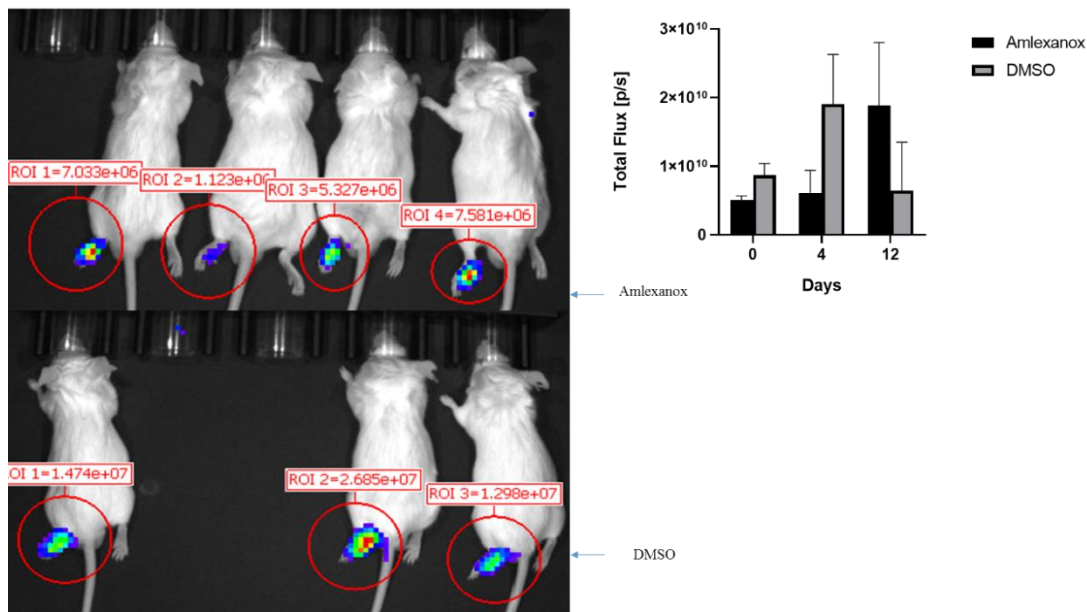


Figure 3.35. Monitoring of parasite loads in LRV- *L. major* challenged mice using IVIS *in vivo* imaging.

Representative IVIS imaging result from Day 4 is shown. Peak point of total flux was calculated and represented at top right panel.

To our knowledge, ours is the first study demonstrating an anti-leishmanial effect of amlexanox in already infected mice. Amlexanox decreased lesion development from 69.14% to 30.31% and on day 11, IVIS imaging results were in line with this observation (Figure 3.35). Since it was not safe to anesthetize the mice more than once per week, we could only perform three IVIS measurements within two weeks. Collectively, our preliminary therapeutic trial was encouraging, suggesting that amlexanox could be a new candidate drug for treatment of cutaneous leishmaniasis caused by *L. major*.

## CHAPTER 4

### CONCLUSION AND FUTURE PERSPECTIVES

Parasitic infectious diseases are a major health concern worldwide due to the difficulties in devising treatments to address the complexity of these microorganisms. Pharmacologic interventions remain limited due to the cost, general unavailability, and lack of efficiency of the drugs. Leishmaniasis is a neglected infectious disease that is commonly encountered in tropical and subtropical regions, including Turkey, Syria and Iran, where the incidence of *Leishmania* infections has increased in the last decades. Considering the negative impact of leishmaniasis to human health, the importance and necessity of developing alternative and/or effective treatments becomes apparent. Therefore, we sought to better understand and clarify the mechanisms contributing to immunity against leishmaniasis.

LRV carrying New World *Leishmania* parasites were reported to be more infectious than the ones lacking the virus. A different variant of the LRV virus (LRV2) is also found in the Old World *Leishmania* species. However, whether these virus carrying strains are more infectious or not is not known. To our knowledge, this study is the first to compare the pathogenicity of LRV2-1 proficient and deficient *L. major* strains. In order to make this comparison, unlike most studies reported on this topic, we cured the LRV2-1 infection in virus positive *L. major* parasites with neomycin treatment (Figure 3.9.). At the end, we obtained both LRV2-1 positive and negative isogenic and transgenic *L. major* strains (Figure 3.10.). We compared the infection rates of LRV2-1 positive and negative *L. major in vitro* and examined the differences in disease progression *in vivo*. We did not observe any significant differences between the infection rates of LRV2-1 bearing parasites and the ones devoid of LRV2-1 (Figure 3.19.). However, our *in vivo* results demonstrate that the LRV2-1 negative strain of *L. major* has a more severe disease progression based on the onset of cutaneous lesions

compared to the LRV2-1 positive strain (Figure 3.33). An earlier study suggests that LRV1 partially hinders the translational initiation of *Leishmania* virulence factors like gp63 (Atayde et al., 2019). In accordance with this study, we experienced that EGFP expression was lower in LRV2-1+ metacyclic transgenic parasites than in their LRV-counterparts. Therefore, we hypothesized that the decreased pathogenicity of LRV2-1 bearing parasites might be attributed to lower production of virulence factors. In order to validate or reject our hypothesis, using comparative quantitative PCR we plan to determine whether reduced translation of virulence factors explains the decreased pathogenicity of LRV2-1 carrying parasites. We intend to repeat our *in vivo* experiment to compare LRV2-1+ and LRV2-1- parasite virulence with metacyclic and late-log phase parasites.

*Leishmania* has been shown to secrete exosomes that have immunomodulatory effects on host cells, aiding parasite survival upon infection (J. M. axwel. Silverman & Reiner, 2011). Exosomes are 30-200nm sized, single-membraned organelles that are secreted to the environment to mediate intercellular communication through delivery of their molecular cargo to the target cell. Recent evidence also suggests that exosomal secretion can be exploited by viruses to initiate infection in other cells (van Dongen et al., 2016). Based on this observation and the fact that how LRV is maintained and transmitted in *Leishmania* remains unclear, we wanted to examine whether exosomes secreted from LRV2-1+ *L. major* contained LRV2-1 as well. For this, first, we did a dot blot with the dsRNA specific J2 antibody on exosomes purified from virus infected parasites and observed that the exosomal content of LRV2-1+ *L. major* was enriched in dsRNA amount compared to LRV2-1- parasite exosomes (Figure 3.2.). Next, we isolated RNA from LRV2-1+ *L. major* exosomes, synthesized cDNA, and performed conventional PCR with an LRV2-1 specific primer pair. Following sequencing of the PCR product, we detected that at least 64% of the LRV2-1 dsRNA genome was present in secreted exosomes (Figure 3.5., 3.6.). Since there are no commercially available antibodies against the LRV2-1 capsid or the RDRP proteins, we conducted mass spectroscopic analysis on LRV2-1+ *L. major* derived

exosomes. The results showed that the parasite exosomes were devoid of the viral capsid and RDRP proteins (Table 3.1.). In summary, our dot blot results showed presence of dsRNA in LRV2-1+ *L. major* exosomes and this observation was supported by our PCR and sequencing data, demonstrating that exosomes from LRV infected parasites harbored LRV2-1 specific RNA sequences. Taken together with the mass spectroscopy results refuting presence of viral proteins in LRV2-1+ *L. major* exosomes, our collective data suggests that viral RNAs but not proteins are disseminated in secreted exosomes. In the future, we intend to manually produce antibodies against the capsid or RDRP proteins and verify their *bona fide* absence or presence in LRV2-1+ *L. major* exosomes. Furthermore, we plan to perform *in vitro* translation studies to determine whether the exosomal content is sufficient to support virus infection in LRV- parasites.

A previous study conducted in our laboratory discovered that pretreatment with *Leishmania* kinetoplast DNA enhanced the parasitic load in macrophages upon *Leishmania* infection. Intracellular cytosolic DNA is recognized by the cGAS/STING nucleic acid sensing pathway and results in immune activation against various pathogens. To confirm whether or not this pathway also played a role in *Leishmania* infections, we used cGAS, STING and TBK1 KO THP-1 Dual monocytic cell lines in our *in vitro* infection model and assessed the effect of a TBK1 inhibitor (Amlexanox) on the infection rate. Our results demonstrated that the infection rates of STING KO and TBK-1 cell lines were significantly lower than wild type THP-1 cells (Figure 3.17., 3.21.). This result indicated a pro-parasitic role for cGAS-STING cytosolic DNA sensing pathway, confirming the findings of two previous studies (Das et al., 2019; Majumdar et al., 2015, 2019) contradicting the conclusion of another publication (Wang et al., 2019). To better understand the cause underlying the parasite resistant phenotype of the knockout cells, we repeated the infection studies with opsonized parasites and conducted phagocytosis assays with the parasites and zymosan particles. Results demonstrated that the rate of phagocytosis was the major determinant limiting the infection rate in the knockout but not the wild type cells

(Figure 3.22., 3.23.). Therefore, to correctly test the impact of cGAS-STING cytosolic initial infection rates of the KO and WT cells should be equalized. Our results on the effect of amlexanox in *Leishmania* infection revealed that significantly lower numbers of parasites were internalized in both THP-1 WT cells and THP-1 TBK KO cells (Figure 3.23.). Therefore, we hypothesized that the effect of amlexanox must be independent of its TBK-1 inhibitory function, but might be related to its actin stress fiber destabilizing ability (Roy et al., 2014), resulting in decrease in phagocytosis rates. We are planning to investigate the validity of this hypothesis using microscopic image analysis following labelling of actin fibers during the course of infection and in amlexanox treated samples in future studies.

Since autophagy can alter phagocytosis rates and is an important pathogen defense mechanism, we have also treated THP-1 cells prior to *Leishmania* infection and zymosan internalization assays with other pharmacological agents, including the autophagy inducer rapamycin, and the autophagy inhibitors chloroquine and bafilomycin A1. Results suggested that chloroquine and bafilomycin A1 reduced internalization of opsonized parasites significantly, whereas rapamycin did not exert any significant impact (Figure 3.23., 3.24.). However, rapamycin augmented the internalization of non-opsonized and opsonized parasites only at the very beginning of infection, suggesting that autophagy might contribute to *Leishmania* infection at the early but not the late phase of infection. Moreover, results of experiments where chloroquine and bafilomycin A were employed showed that these agents suppressed internalization of opsonized parasites. Data suggest that this effect might be independent of these agents' autophagy suppressive activity but rather depend on their capacity to elevate the pH of the endolysosome (Figure 3.25.). In future studies, we are planning to investigate the activity of the transcriptional factor EB (TFEB) in *Leishmania* infected cells, since this protein is the master regulator of autophagy, lysosomal biogenesis and phagocytosis (Zhitomirsky et al., 2018).

Type I interferon mediated responses modulate disease progression in *Leishmania* infections. ISG15 is an important interferon stimulated gene and plays a critical role

in immunity to various pathogens. To date, only one study examined the fate of ISG15 in *Leishmania* infection and concluded that ISG15 was upregulated in infected dendritic cells (Vargas-Inchaustegui et al., 2008). Therefore, we aimed to determine the role of ISG15 in *L. major* infection by mutating the *ISG15* inside the THP-1 genome. Using LentiCRISPRv2 system, we successfully knocked out the *ISG15* and verified the absence of ISG15 protein with western blot and intracellular staining in recIFN $\beta$  pretreated THP-1 ISG15 KO cells (Figure 3.13., 3.15.). Using our *in vitro* infection model, we detected reduced infection rates in both type I IFN stimulated or unstimulated THP-1 ISG15 KO cells compared to their LVC control (Figure 3.27.). Moreover, zymosan internalization assays with cGAMP pretreated THP-1 ISG15 KO and LVC strains demonstrated that these two cell lines had similar phagocytosis rates (Figure 3.26.), yet, parasite loads were reduced in ISG15 KO cells infected with opsonized and nonopsonized *L. major* (Figure 3.27., 3.28.). Collectively, these results suggest a pro-parasitic role for the ISG15 protein especially during the early infection. In support of this conclusion, our results demonstrated a 6.62-fold upregulation of ISG15 protein only during the first hour of infection, but not at 6 hours of infection (Figure 3.30.). Moreover, our LC3-II immunoblotting and LysoTracker results demonstrated enhanced autophagy in ISG15 KO cells compared to LVC (Figure 3.31., 3.32.). In future studies, we are planning to rescue the phenotype of ISG15 KO cells with recombinant ISG15 and transiently knockout ISG15 protein in primary cells with TRIM21-based trim-away technology to further support our claims.

Lastly, since amlexanox pretreatment exerted an anti-parasitic effect *in vitro*, we tested its anti-leishmanial activity in an established mouse infection model *in vivo* and observed delayed footpad swelling compared to DMSO treated controls (Figure 3.34.). However, we are planning to repeat this *in vivo* assay because we want to commence amlexanox administration at an earlier time point to better evaluate the therapeutic benefits of amlexanox treatment. Nevertheless, our preliminary results suggest that, amlexanox could be a new candidate drug for treatment of cutaneous leishmaniasis.



## REFERENCES

- Abu-Dayyeh, I., Hassani, K., Westra, E. R., Mottram, J. C., & Olivier, M. (2010). Comparative study of the ability of *Leishmania mexicana* promastigotes and amastigotes to alter macrophage signaling and functions. *Infection and Immunity*. <https://doi.org/10.1128/IAI.00812-09>
- Aga, E., Katschinski, D. M., van Zandbergen, G., Laufs, H., Hansen, B., Müller, K., ... Laskay, T. (2002). Inhibition of the Spontaneous Apoptosis of Neutrophil Granulocytes by the Intracellular Parasite *Leishmania major*. *The Journal of Immunology*. <https://doi.org/10.4049/jimmunol.169.2.898>
- Alvar, J., & Arana, B. (2018). I. Appraisal of Leishmaniasis Chemotherapy, Current Status and Pipeline Strategies Chapter 1: Leishmaniasis, Impact and Therapeutic Needs. In *RSC Drug Discovery Series*. <https://doi.org/10.1039/9781788010177-00001>
- Andrade-Narváez, F. J., Vargas-González, A., Canto-Lara, S. B., & Damián-Centeno, A. G. (2001). Clinical Picture of Cutaneous Leishmaniases Due to *Leishmania (Leishmania) Mexicana* in the Yucatan Peninsula, Mexico. *Memorias Do Instituto Oswaldo Cruz*. <https://doi.org/10.1590/S0074-02762001000200005>
- Antoine, J. C., Prina, E., Jouanne, C., & Bongrand, P. (1990). Parasitophorous vacuoles of *Leishmania amazonensis*-infected macrophages maintain an acidic pH. *Infection and Immunity*.
- Antoni, F., Hrabák, A., & Csuka, I. (1986). Effect of emetine and chloroquine on phagocytic processes of rat macrophages. *Biochemical Pharmacology*. [https://doi.org/10.1016/0006-2952\(86\)90478-8](https://doi.org/10.1016/0006-2952(86)90478-8)
- Arenas, R., Torres-Guerrero, E., Quintanilla-Cedillo, M. R., & Ruiz-Esmenjaud, J. (2017). Leishmaniasis: A review. *F1000Research*. <https://doi.org/10.12688/f1000research.11120.1>
- Armstrong, T. C., Keenan, M. C., Widmer, G., & Patterson, J. L. (1993). Successful transient introduction of *Leishmania* RNA virus into a virally infected and an uninfected strain of *Leishmania*. *Proceedings of the National Academy of Sciences of the United States of America*. <https://doi.org/10.1073/pnas.90.5.1736>
- Atayde, V. D., Aslan, H., Townsend, S., Hassani, K., Kamhawi, S., & Olivier, M. (2015). Exosome Secretion by the Parasitic Protozoan *Leishmania* within the Sand Fly Midgut. *Cell Reports*. <https://doi.org/10.1016/j.celrep.2015.09.058>
- Atayde, V. D., da Silva Lira Filho, A., Chaparro, V., Zimmermann, A., Martel, C., Jaramillo, M., & Olivier, M. (2019). Exploitation of the *Leishmania* exosomal pathway by *Leishmania* RNA virus 1. *Nature Microbiology*.

<https://doi.org/10.1038/s41564-018-0352-y>

- Bader, C. A., Shandala, T., Ng, Y. S., Johnson, I. R. D., & Brooks, D. A. (2015). Atg9 is required for intraluminal vesicles in amphisomes and autolysosomes. *Biology Open*. <https://doi.org/10.1242/bio.013979>
- Bailey, M. S., & Lockwood, D. N. J. (2007). Cutaneous leishmaniasis. *Clinics in Dermatology*. <https://doi.org/10.1016/j.clindermatol.2006.05.008>
- Bankoti, R., Gupta, K., Levchenko, A., & Stäger, S. (2012). Marginal Zone B Cells Regulate Antigen-Specific T Cell Responses during Infection. *The Journal of Immunology*. <https://doi.org/10.4049/jimmunol.1102880>
- Bañuls, A. L., Hide, M., & Prugnolle, F. (2007). Leishmania and the Leishmaniases: A Parasite Genetic Update and Advances in Taxonomy, Epidemiology and Pathogenicity in Humans. *Advances in Parasitology*. [https://doi.org/10.1016/S0065-308X\(06\)64001-3](https://doi.org/10.1016/S0065-308X(06)64001-3)
- Barbosa, F. M. C., Dupin, T. V., Toledo, M. dos S., Reis, N. F. dos C., Ribeiro, K., Cronemberger-Andrade, A., ... Xander, P. (2018). Extracellular Vesicles Released by Leishmania (Leishmania) amazonensis Promote Disease Progression and Induce the Production of Different Cytokines in Macrophages and B-1 Cells. *Frontiers in Microbiology*, 9(December), 1–14. <https://doi.org/10.3389/fmicb.2018.03056>
- Barger, C. J., Branick, C., Chee, L., & Karpf, A. R. (2019). Pan-cancer analyses reveal genomic features of FOXM1 overexpression in cancer. *Cancers*. <https://doi.org/10.3390/cancers11020251>
- Bee, A., Culley, F. J., Alkhalife, I. S., Bodman-Smith, K. B., Raynes, J. G., & Bates, P. A. (2001). Transformation of Leishmania mexicana metacyclic promastigotes to amastigote-like forms mediated by binding of human C-reactive protein. *Parasitology*. <https://doi.org/10.1017/S0031182001007612>
- Berman, J. D. (1997). Human leishmaniasis: Clinical, diagnostic, and chemotherapeutic developments in the last 10 years. *Clinical Infectious Diseases*. <https://doi.org/10.1093/clind/24.4.684>
- Bodur, C., Kazyken, D., Huang, K., Ekim Ustunel, B., Siroky, K. A., Tooley, A. S., ... Fingar, D. C. (2018). The IKK-related kinase TBK1 activates mTORC1 directly in response to growth factors and innate immune agonists. *The EMBO Journal*, 37(1), 19–38. <https://doi.org/10.15252/embj.201696164>
- Bogunovic, D., Byun, M., Durfee, L. A., Abhyankar, A., Sanal, O., Mansouri, D., Casanova, J. L. (2012). Mycobacterial disease and impaired IFN- $\gamma$  immunity in humans with inherited ISG15 deficiency. *Science*. <https://doi.org/10.1126/science.1224026>
- Bolhassani, A., Taheri, T., Taslimi, Y., Zamanilui, S., Zahedifard, F., Seyed, N., ...

- Rafati, S. (2011). Fluorescent Leishmania species: Development of stable GFP expression and its application for in vitro and in vivo studies. *Experimental Parasitology*, 127(3), 637–645. <https://doi.org/10.1016/j.exppara.2010.12.006>
- Borim, A., Wolf, I. R., Amorim, C., Augusto, G., Mota, F., Ma, A., ... Sartori, A. (2020). *Transcriptional analysis of THP-1 cells infected with Leishmania infantum indicates no activation of the inflammasome platform*. 1–24. <https://doi.org/10.1371/journal.pntd.0007949>
- Brittingham, A., Morrison, C. J., McMaster, W. R., McGwire, B. S., Chang, K.-P., & Mosser, D. M. (1995). Role of the Leishmania surface protease gp63 in complement fixation, cell adhesion, and resistance to complement-mediated lysis. *Parasitology Today*. [https://doi.org/10.1016/0169-4758\(95\)80054-9](https://doi.org/10.1016/0169-4758(95)80054-9)
- Campbell, P., Morris, H., & Schapira, A. (2018). Chaperone-mediated autophagy as a therapeutic target for Parkinson disease. *Expert Opinion on Therapeutic Targets*. <https://doi.org/10.1080/14728222.2018.1517156>
- Cecílio, P., Pérez-Cabezas, B., Santarém, N., Maciel, J., Rodrigues, V., & da Silva, A. C. (2014). Deception and manipulation: The arms of Leishmania, a successful parasite. *Frontiers in Immunology*. <https://doi.org/10.3389/fimmu.2014.00480>
- Chandel, H. S., Pandey, S. P., Shukla, D., Lalsare, K., Selvaraj, S. K., Jha, M. K., & Saha, B. (2014). Toll-like receptors and CD40 modulate each other's expression affecting Leishmania major infection. *Clinical and Experimental Immunology*. <https://doi.org/10.1111/cei.12264>
- Chappuis, F., Sundar, S., Hailu, A., Ghalib, H., Rijal, S., Peeling, R. W., ... Boelaert, M. (2007). Visceral leishmaniasis: What are the needs for diagnosis, treatment and control? *Nature Reviews Microbiology*. <https://doi.org/10.1038/nrmicro1748>
- Chen, Q., Sun, L., & Chen, Z. J. (2016). Regulation and function of the cGAS-STING pathway of cytosolic DNA sensing. *Nature Immunology*. <https://doi.org/10.1038/ni.3558>
- Cheng, K., An, R., Cui, Y., Zhang, Y., Han, X., Sui, Z., ... Komiyama, M. (2019). RNA ligation of very small pseudo nick structures by T4 RNA ligase 2, leading to efficient production of versatile RNA rings. *RSC Advances*. <https://doi.org/10.1039/c9ra01513b>
- Colombo, M., Raposo, G., & Théry, C. (2014). Biogenesis, Secretion, and Intercellular Interactions of Exosomes and Other Extracellular Vesicles. *Annual Review of Cell and Developmental Biology*. <https://doi.org/10.1146/annurev-cellbio-101512-122326>
- Cooper, K. F. (2018). Till death do us part: The marriage of autophagy and apoptosis. *Oxidative Medicine and Cellular Longevity*. <https://doi.org/10.1155/2018/4701275>

- Crauwels, P., Bohn, R., Thomas, M., Gottwalt, S., Jäckel, F., Krämer, S., ... Van Zandbergen, G. (2015). Apoptotic-like Leishmania exploit the host's autophagy machinery to reduce T-cell-mediated parasite elimination. *Autophagy*. <https://doi.org/10.1080/15548627.2014.998904>
- Croft, S. L., & Coombs, G. H. (2003). Leishmaniasis - Current chemotherapy and recent advances in the search for novel drugs. *Trends in Parasitology*. <https://doi.org/10.1016/j.pt.2003.09.008>
- Cyrino, L. T., Araújo, A. P., Joazeiro, P. P., Vicente, C. P., & Giorgio, S. (2012). In vivo and in vitro Leishmania amazonensis infection induces autophagy in macrophages. *Tissue and Cell*. <https://doi.org/10.1016/j.tice.2012.08.003>
- Dalzoto, P. R., Glienke-Blanco, C., Kava-Cordeiro, V., Ribeiro, J. Z., Kitajima, E. W., & Azevedo, J. L. (2006). Horizontal transfer and hypovirulence associated with double-stranded RNA in Beauveria bassiana. *Mycological Research*. <https://doi.org/10.1016/j.mycres.2006.08.009>
- Das, S., Kumar, A., Mandal, A., Abhishek, K., Verma, S., Kumar, A., & Das, P. (2019). Nucleic acid sensing activates the innate cytosolic surveillance pathway and promotes parasite survival in visceral leishmaniasis. *Scientific Reports*. <https://doi.org/10.1038/s41598-019-45800-0>
- Davies, C. R., Reithinger, R., Campbell-Lendrum, D., Feliciangeli, D., Borges, R., & Rodriguez, N. (2000). The epidemiology and control of leishmaniasis in Andean countries. *Cadernos de Saúde Pública / Ministério Da Saúde, Fundação Oswaldo Cruz, Escola Nacional de Saúde Pública*. <https://doi.org/10.1590/S0102-311X2000000400013>
- de Carvalho, R. V. H., Lima-Junior, D. S., da Silva, M. V. G., Dilucca, M., Rodrigues, T. S., Horta, C. V., ... Zamboni, D. S. (2019). Leishmania RNA virus exacerbates Leishmaniasis by subverting innate immunity via TLR3-mediated NLRP3 inflammasome inhibition. *Nature Communications*. <https://doi.org/10.1038/s41467-019-13356-2>
- de Veer, M. J., Curtis, J. M., Baldwin, T. M., DiDonato, J. A., Sexton, A., McConville, M. J., ... Schofield, L. (2003). MyD88 is essential for clearance of Leishmania major: Possible role for lipophosphoglycan and Toll-like receptor 2 signaling. *European Journal of Immunology*. <https://doi.org/10.1002/eji.200324128>
- Debus, A., Gläsner, J., Röllinghoff, M., & Gessner, A. (2003). High Levels of Susceptibility and T Helper 2 Response in MyD88-Deficient Mice Infected with Leishmania major Are Interleukin-4 Dependent. *Infection and Immunity*. <https://doi.org/10.1128/IAI.71.12.7215-7218.2003>
- Devorkin, L., & Gorski, S. M. (2014). LysoTracker staining to aid in monitoring autophagy in Drosophila. *Cold Spring Harbor Protocols*. <https://doi.org/10.1101/pdb.prot080325>

- Domínguez, M., & Toraño, A. (1999). Immune adherence-mediated opsonophagocytosis: The mechanism of Leishmania infection. *Journal of Experimental Medicine*. <https://doi.org/10.1084/jem.189.1.25>
- Dong, G., Filho, A. L., & Olivier, M. (2019). Modulation of host-pathogen communication by extracellular vesicles (EVs) of the protozoan parasite Leishmania. *Frontiers in Cellular and Infection Microbiology*. <https://doi.org/10.3389/fcimb.2019.00100>
- Dorlo, T. P. C., Rijal, S., Ostyn, B., De Vries, P. J., Singh, R., Bhattarai, N., Huitema, A. D. R. (2014). Failure of miltefosine in visceral leishmaniasis is associated with low drug exposure. *Journal of Infectious Diseases*. <https://doi.org/10.1093/infdis/jiu039>
- Dos Santos, P. F., & Mansur, D. S. (2017). Beyond ISGylation: Functions of Free Intracellular and Extracellular ISG15. *Journal of Interferon and Cytokine Research*. <https://doi.org/10.1089/jir.2016.0103>
- Dreux, M., Garaigorta, U., Boyd, B., Décembre, E., Chung, J., Whitten-Bauer, C., Chisari, F. V. (2012). Short-range exosomal transfer of viral RNA from infected cells to plasmacytoid dendritic cells triggers innate immunity. *Cell Host and Microbe*. <https://doi.org/10.1016/j.chom.2012.08.010>
- Dunkelberger, J. R., & Song, W. C. (2010). Complement and its role in innate and adaptive immune responses. *Cell Research*. <https://doi.org/10.1038/cr.2009.139>
- Dunphy, G., Flannery, S. M., Almine, J. F., Connolly, D. J., Paulus, C., Jønsson, K. L., ... Unterholzner, L. (2018). Non-canonical Activation of the DNA Sensing Adaptor STING by ATM and IFI16 Mediates NF-κB Signaling after Nuclear DNA Damage. *Molecular Cell*. <https://doi.org/10.1016/j.molcel.2018.07.034>
- Evavold, C. L., & Kagan, J. C. (2019). Inflammasomes: Threat-Assessment Organelles of the Innate Immune System. *Immunity*. <https://doi.org/10.1016/j.immuni.2019.08.005>
- Fan, J. B., Arimoto, K. L., Motamedchaboki, K., Yan, M., Wolf, D. A., & Zhang, D. E. (2015). Identification and characterization of a novel ISG15-ubiquitin mixed chain and its role in regulating protein homeostasis. *Scientific Reports*. <https://doi.org/10.1038/srep12704>
- Faria, M. S., Reis, F. C. G., Azevedo-Pereira, R. L., Morrison, L. S., Mottram, J. C., & Lima, A. P. C. A. (2011). Leishmania Inhibitor of Serine Peptidase 2 Prevents TLR4 Activation by Neutrophil Elastase Promoting Parasite Survival in Murine Macrophages. *The Journal of Immunology*. <https://doi.org/10.4049/jimmunol.1002175>
- Filardy, A. A., Pires, D. R., Nunes, M. P., Takiya, C. M., Freire-de-Lima, C. G., Ribeiro-Gomes, F. L., & DosReis, G. A. (2010). Proinflammatory Clearance of

Apoptotic Neutrophils Induces an IL-12 low IL-10 high Regulatory Phenotype in Macrophages . *The Journal of Immunology*. <https://doi.org/10.4049/jimmunol.1000017>

- Fingar, D. C., Richardson, C. J., Tee, A. R., Cheatham, L., Tsou, C., & Blenis, J. (2004). mTOR Controls Cell Cycle Progression through Its Cell Growth Effectors S6K1 and 4E-BP1/Eukaryotic Translation Initiation Factor 4E. *Molecular and Cellular Biology*. <https://doi.org/10.1128/mcb.24.1.200-216.2004>
- Flandin, J. F., Chano, F., & Descoteaux, A. (2006). RNA interference reveals a role for TLR2 and TLR3 in the recognition of *Leishmania donovani* promastigotes by interferon- $\gamma$ -primed macrophages. *European Journal of Immunology*. <https://doi.org/10.1002/eji.200535079>
- Fourmy, D., Recht, M. I., & Puglisi, J. D. (1998). Binding of neomycin-class aminoglycoside antibiotics to the A-site of 16 S rRNA. *Journal of Molecular Biology*, 277(2), 347–362. <https://doi.org/10.1006/jmbi.1997.1552>
- Franco, L. H., Fleuri, A. K. A., Pellison, N. C., Quirino, G. F. S., Horta, C. V., De Carvalho, R. V. H., ... Zamboni, D. S. (2017). Autophagy downstream of endosomal Toll-like receptor signaling in macrophages is a key mechanism for resistance to *Leishmania major* infection. *Journal of Biological Chemistry*. <https://doi.org/10.1074/jbc.M117.780981>
- Frank, B., Marcu, A., De Oliveira Almeida Petersen, A. L., Weber, H., Stigloher, C., Mottram, J. C., ... Schurigt, U. (2015). Autophagic digestion of *Leishmania major* by host macrophages is associated with differential expression of BNIP3, CTSE, and the miRNAs miR-101c, miR-129, and miR-210. *Parasites and Vectors*. <https://doi.org/10.1186/s13071-015-0974-3>
- Füllgrabe, J., Ghislat, G., Cho, D. H., & Rubinsztein, D. C. (2016). Transcriptional regulation of mammalian autophagy at a glance. *Journal of Cell Science*. <https://doi.org/10.1242/jcs.188920>
- Glick, D., Barth, S., & Macleod, K. F. (2010). Autophagy: Cellular and molecular mechanisms. *Journal of Pathology*. <https://doi.org/10.1002/path.2697>
- Gomez, M. A., Contreras, I., Hallé, M., Tremblay, M. L., McMaster, R. W., & Olivier, M. (2009). *Leishmania* GP63 alters host signaling through cleavage-activated protein tyrosine phosphatases. *Science Signaling*. <https://doi.org/10.1126/scisignal.2000213>
- Goyard, S., & Beverley, S. M. (2000). Blasticidin resistance: A new independent marker for stable transfection of *Leishmania*. *Molecular and Biochemical Parasitology*, 108(2), 249–252. [https://doi.org/10.1016/S0166-6851\(00\)00210-3](https://doi.org/10.1016/S0166-6851(00)00210-3)
- Guerra, C. S., Macedo Silva, R. M., Carvalho, L. O. P., Calabrese, K. da S., Bozza, P.

- T., & Côrte-Real, S. (2010). Histopathological analysis of initial cellular response in TLR-2 deficient mice experimentally infected by *Leishmania (L.) amazonensis*. *International Journal of Experimental Pathology*. <https://doi.org/10.1111/j.1365-2613.2010.00717.x>
- Gui, X., Yang, H., Li, T., Tan, X., Shi, P., Li, M., ... Chen, Z. J. (2019). Autophagy induction via STING trafficking is a primordial function of the cGAS pathway. *Nature*. <https://doi.org/10.1038/s41586-019-1006-9>
- Gupta, G., Oghumu, S., & Satoskar, A. R. (2013). Mechanisms of Immune Evasion in Leishmaniasis. In *Advances in Applied Microbiology*. <https://doi.org/10.1016/B978-0-12-407679-2.00005-3>
- Gupta, P., Giri, J., Srivastav, S., Chande, A. G., Mukhopadhyaya, R., Das, P. K., & Ukil, A. (2014). *Leishmania donovani* targets tumor necrosis factor receptor-associated factor (TRAF) 3 for impairing TLR4-mediated host response. *FASEB Journal*. <https://doi.org/10.1096/fj.13-238428>
- Gurung, P., & Kanneganti, T. D. (2015). Innate immunity against *Leishmania* infections. *Cellular Microbiology*. <https://doi.org/10.1111/cmi.12484>
- Haidinger, M., Poglitsch, M., Geyeregger, R., Kasturi, S., Zeyda, M., Zlabinger, G. J., ... Weichhart, T. (2010). A Versatile Role of Mammalian Target of Rapamycin in Human Dendritic Cell Function and Differentiation. *The Journal of Immunology*. <https://doi.org/10.4049/jimmunol.1000296>
- Hajjaran, H., Mahdi, M., Mohebbali, M., Samimi-Rad, K., Ataei-Pirkooh, A., Kazemi-Rad, E., ... Raoofian, R. (2016). Detection and molecular identification of leishmania RNA virus (LRV) in Iranian *Leishmania* species. *Archives of Virology*. <https://doi.org/10.1007/s00705-016-3044-z>
- Harrison, R. E., Bucci, C., Vieira, O. V., Schroer, T. A., & Grinstein, S. (2003). Phagosomes Fuse with Late Endosomes and/or Lysosomes by Extension of Membrane Protrusions along Microtubules: Role of Rab7 and RILP. *Molecular and Cellular Biology*. <https://doi.org/10.1128/mcb.23.18.6494-6506.2003>
- Hartley, M. A., Ronet, C., Zangger, H., Beverley, S. M., & Fasel, N. (2012). *Leishmania* RNA virus: when the host pays the toll. *Frontiers in Cellular and Infection Microbiology*. <https://doi.org/10.3389/fcimb.2012.00099>
- Hassani, K., Antoniak, E., Jardim, A., & Olivier, M. (2011). Temperature-induced protein secretion by *leishmania mexicana* modulates macrophage signalling and function. *PLoS ONE*, 6(5). <https://doi.org/10.1371/journal.pone.0018724>
- Herb, M., Gluschko, A., & Schramm, M. (2019). LC3-associated phagocytosis - The highway to hell for phagocytosed microbes. *Seminars in Cell and Developmental Biology*. <https://doi.org/10.1016/j.semcdb.2019.04.016>
- Homewood, C. A., Warhurst, D. C., Peters, W., & Baggaley, V. C. (1972). Lysosomes,

- pH and the anti-malarial action of chloroquine [9]. *Nature*. <https://doi.org/10.1038/235050a0>
- Hoover, D. L., Berger, M., Nacy, C. A., Hockmeyer, W. T., & Meltzer, M. S. (1984). Killing of *Leishmania tropica* amastigotes by factors in normal human serum. *Journal of Immunology (Baltimore, Md. : 1950)*.
- Hoover, D. L., & Nacy, C. A. (1984). Macrophage activation to kill *Leishmania tropica*: Defective intracellular killing of amastigotes by macrophages elicited with sterile inflammatory agents. *Journal of Immunology*.
- Hoyos, C. L., Cajal, S. P., Juarez, M., Marco, J. D., Alberti D'Amato, A. M., Cayo, M., ... Gil, J. F. (2016). Epidemiology of American Tegumentary Leishmaniasis and *Trypanosoma cruzi* Infection in the Northwestern Argentina. *BioMed Research International*. <https://doi.org/10.1155/2016/6456031>
- Huang, L., Hinchman, M., & Mendez, S. (2015). Coinjection with TLR2 Agonist Pam3CSK4 Reduces the Pathology of Leishmanization in Mice. *PLoS Neglected Tropical Diseases*. <https://doi.org/10.1371/journal.pntd.0003546>
- Ives, A., Ronet, C., Prevel, F., Ruzzante, G., Fuertes-Marraco, S., Schutz, F., ... Masina, S. (2011). *Leishmania* RNA virus controls the severity of mucocutaneous leishmaniasis. *Science*. <https://doi.org/10.1126/science.1199326>
- Jain, K., & Jain, N. K. (2015). Vaccines for visceral leishmaniasis: A review. *Journal of Immunological Methods*. <https://doi.org/10.1016/j.jim.2015.03.017>
- Jaramillo, M., Gomez, M. A., Larsson, O., Shio, M. T., Topisirovic, I., Contreras, I., Sonenberg, N. (2011). *Leishmania* repression of host translation through mTOR cleavage is required for parasite survival and infection. *Cell Host and Microbe*. <https://doi.org/10.1016/j.chom.2011.03.008>
- John, B., & Hunter, C. A. (2008). Immunology: Neutrophil soldiers or Trojan horses? *Science*. <https://doi.org/10.1126/science.1162914>
- Kanneganti, T. D., Özören, N., Body-Malapel, M., Amer, A., Park, J. H., Franchi, L., Núñez, G. (2006). Bacterial RNA and small antiviral compounds activate caspase-1 through cryopyrin/Nalp3. *Nature*. <https://doi.org/10.1038/nature04517>
- Kariyawasam, R., Mukkala, A., Lau, R., Valencia, B., Llanos-Cuentas, A., & Boggild, A. K. (2018). Influence of *Leishmania* RNA Virus-1 (LRV-1) on Virulence Factor RNA Transcript Expression of *Leishmania Viannia* spp. *International Journal of Infectious Diseases*. <https://doi.org/10.1016/j.ijid.2018.04.4145>
- Kariyawasam, Ruwandi, Grewal, J., Lau, R., Pursell, A., Valencia, B. M., Llanos-Cuentas, A., & Boggild, A. K. (2017). Influence of *Leishmania* RNA Virus 1 on Proinflammatory Biomarker Expression in a Human Macrophage Model of American Tegumentary Leishmaniasis. *Journal of Infectious Diseases*. <https://doi.org/10.1093/infdis/jix416>

- Karmakar, S., Bhaumik, S. K., Paul, J., & De, T. (2012). TLR4 and NKT cell synergy in immunotherapy against visceral leishmaniasis. *PLoS Pathogens*. <https://doi.org/10.1371/journal.ppat.1002646>
- Kaur, J., & Debnath, J. (2015). Autophagy at the crossroads of catabolism and anabolism. *Nature Reviews Molecular Cell Biology*. <https://doi.org/10.1038/nrm4024>
- Kébaïer, C., Louzir, H., Chenik, M., Ben Salah, A., & Dellagi, K. (2001). Heterogeneity of wild *Leishmania major* isolates in experimental murine pathogenicity and specific immune response. *Infection and Immunity*. <https://doi.org/10.1128/IAI.69.8.4906-4915.2001>
- Keller, S., Sanderson, M. P., Stoeck, A., & Altevogt, P. (2006). Exosomes: From biogenesis and secretion to biological function. *Immunology Letters*. <https://doi.org/10.1016/j.imlet.2006.09.005>
- Kevric, I., Cappel, M. A., & Keeling, J. H. (2015). New World and Old World *Leishmania* Infections: A Practical Review. *Dermatologic Clinics*. <https://doi.org/10.1016/j.det.2015.03.018>
- Khandia, R., Dadar, M., Munjal, A., Dhama, K., Karthik, K., Tiwari, R., ... Chaicumpa, W. (2019). A Comprehensive Review of Autophagy and Its Various Roles in Infectious, Non-Infectious, and Lifestyle Diseases: Current Knowledge and Prospects for Disease Prevention, Novel Drug Design, and Therapy. *Cells*. <https://doi.org/10.3390/cells8070674>
- Kim, M., Song, K., Jin, E. J., & Sonn, J. (2012). Staurosporine and cytochalasin d induce chondrogenesis by regulation of actin dynamics in different way. *Experimental and Molecular Medicine*. <https://doi.org/10.3858/emm.2012.44.9.059>
- Kim, Y. C., & Guan, K. L. (2015). mTOR: A pharmacologic target for autophagy regulation. *Journal of Clinical Investigation*. <https://doi.org/10.1172/JCI73939>
- Kiššova, I., Salin, B., Schaeffer, J., Bhatia, S., Manon, S., & Camougrand, N. (2007). Selective and non-selective autophagic degradation of mitochondria in yeast. *Autophagy*. <https://doi.org/10.4161/auto.4034>
- Kleschenko, Y., Grybchuk, D., Matveeva, N. S., Macedo, D. H., Ponirovsky, E. N., Lukashev, A. N., & Yurchenko, V. (2019). Molecular Characterization of *Leishmania RNA virus 2* in *Leishmaniamajor* from Uzbekistan. *Genes*. <https://doi.org/10.3390/genes10100830>
- Kopf, M., Brombacher, F., Köhler, G., Kienzle, G., Widmann, K. H., Lefrang, K., ... Solbad, W. (1996). IL-4-deficient Balb/c mice resist infection with *Leishmania major*. *Journal of Experimental Medicine*. <https://doi.org/10.1084/jem.184.3.1127>

- Kropf, P., Freudenberg, N., Kalis, C., Modolell, M., Herath, S., Galanos, C., ... Müller, I. (2004). Infection of C57BL/10ScCr and C57BL/10ScNCr mice with *Leishmania major* reveals a role for Toll-like receptor 4 in the control of parasite replication. *Journal of Leukocyte Biology*. <https://doi.org/10.1189/jlb.1003484>
- Kropf, Pascale, Freudenberg, M. A., Modolell, M., Price, H. P., Herath, S., Antoniazzi, S., ... Müller, I. (2004). Toll-Like Receptor 4 Contributes to Efficient Control of Infection with the Protozoan Parasite *Leishmania major*. *Infection and Immunity*. <https://doi.org/10.1128/IAI.72.4.1920-1928.2004>
- Kunzt, J. B., Schwarz, H., & Mayer, A. (2004). Determination of Four Sequential Stages during Microautophagy in Vitro. *Journal of Biological Chemistry*. <https://doi.org/10.1074/jbc.M307905200>
- Kushawaha, P. K., Gupta, R., Sundar, S., Sahasrabudhe, A. A., & Dube, A. (2011). Elongation Factor-2, a Th1 Stimulatory Protein of *Leishmania donovani*, Generates Strong IFN- $\gamma$  and IL-12 Response in Cured *Leishmania* -Infected Patients/Hamsters and Protects Hamsters against *Leishmania* Challenge. *The Journal of Immunology*. <https://doi.org/10.4049/jimmunol.1102081>
- Labro, M. T., & Babin-Chevaye, C. (1988). Effects of amodiaquine, chloroquine, and mefloquine on human polymorphonuclear neutrophil function in vitro. *Antimicrobial Agents and Chemotherapy*. <https://doi.org/10.1128/AAC.32.8.1124>
- Lambertz, U., Silverman, J. M., Nandan, D., McMaster, W. R., Clos, J., Foster, L. J., & Reiner, N. E. (2012). Secreted virulence factors and immune evasion in visceral leishmaniasis. *Journal of Leukocyte Biology*. <https://doi.org/10.1189/jlb.0611326>
- Landriscina, M., Prudovsky, I., Carreira, C. M., Soldi, R., Tarantini, F., & Maciag, T. (2000). Amlexanox reversibly inhibits cell migration and proliferation and induces the Src-dependent disassembly of actin stress fibers in vitro. *Journal of Biological Chemistry*. <https://doi.org/10.1074/jbc.M002336200>
- Lee, S. E., Suh, J. M., Scheffter, S., Patterson, J. L., & Chung, I. K. (1996). Identification of a ribosomal frameshift in *Leishmania* RNA virus 1-4. *Journal of Biochemistry*. <https://doi.org/10.1093/oxfordjournals.jbchem.a021387>
- Lenschow, D. J. (2010). Antiviral properties of ISG15. *Viruses*. <https://doi.org/10.3390/v2102154>
- Lessa, M. M., Lessa, H. A., Castro, T. W. N., Oliveira, A., Scherifer, A., Machado, P., & Carvalho, E. M. (2007). Mucosal leishmaniasis: Epidemiological and clinical aspects. *Brazilian Journal of Otorhinolaryngology*. [https://doi.org/10.1016/s1808-8694\(15\)31181-2](https://doi.org/10.1016/s1808-8694(15)31181-2)
- Li, W. W., Li, J., & Bao, J. K. (2012). Microautophagy: Lesser-known self-eating.

*Cellular and Molecular Life Sciences*. <https://doi.org/10.1007/s00018-011-0865-5>

- Lieberman, J., Wu, H., & Kagan, J. C. (2019). Gasdermin D activity in inflammation and host defense. *Science Immunology*. <https://doi.org/10.1126/sciimmunol.aav1447>
- Liese, J., Schleicher, U., & Bogdan, C. (2007). TLR9 signaling is essential for the innate NK cell response in murine cutaneous leishmaniasis. *European Journal of Immunology*. <https://doi.org/10.1002/eji.200737182>
- Lim, Y. S., Cha, M. K., Kim, H. K., Uhm, T. B., Park, J. W., Kim, K., & Kim, I. H. (1993). Removals of hydrogen peroxide and hydroxyl radical by thiol-specific antioxidant protein as a possible role in vivo. *Biochemical and Biophysical Research Communications*. <https://doi.org/10.1006/bbrc.1993.1410>
- Lima, J. G. B., de Freitas Vinhas, C., Gomes, I. N., Azevedo, C. M., dos Santos, R. R., Vannier-Santos, M. A., & Veras, P. S. T. (2011). Phagocytosis is inhibited by autophagic induction in murine macrophages. *Biochemical and Biophysical Research Communications*. <https://doi.org/10.1016/j.bbrc.2011.01.076>
- Lin, X., Han, L., Weng, J., Wang, K., & Chen, T. (2018). Rapamycin inhibits proliferation and induces autophagy in human neuroblastoma cells. *Bioscience Reports*. <https://doi.org/10.1042/BSR20181822>
- Liu, S., Cai, X., Wu, J., Cong, Q., Chen, X., Li, T., ... Chen, Z. J. (2015). Phosphorylation of innate immune adaptor proteins MAVS, STING, and TRIF induces IRF3 activation. *Science*. <https://doi.org/10.1126/science.aaa2630>
- Loeb, K. R., & Haas, A. L. (1992). The interferon-inducible 15-kDa ubiquitin homolog conjugates to intracellular proteins. *Journal of Biological Chemistry*.
- Maga, J. A., Widmer, G., & LeBowitz, J. H. (1995). Leishmania RNA virus 1-mediated cap-independent translation. *Molecular and Cellular Biology*. <https://doi.org/10.1128/mcb.15.9.4884>
- Majumdar, T., Chattopadhyay, S., Ozhegov, E., Dhar, J., Goswami, R., Sen, G. C., & Barik, S. (2015). Induction of Interferon-Stimulated Genes by IRF3 Promotes Replication of *Toxoplasma gondii*. *PLoS Pathogens*. <https://doi.org/10.1371/journal.ppat.1004779>
- Majumdar, T., Sharma, S., Kumar, M., Hussain, M. A., Chauhan, N., Kalia, I., ... Mazumder, S. (2019). Tryptophan-kynurenine pathway attenuates  $\beta$ -catenin-dependent pro-parasitic role of STING-TICAM2-IRF3-IDO1 signalosome in *Toxoplasma gondii* infection. *Cell Death and Disease*. <https://doi.org/10.1038/s41419-019-1420-9>
- Malakhov, M. P., Malakhova, O. A., Il Kim, K., Ritchie, K. J., & Zhang, D. E. (2002). UBP43 (USP18) specifically removes ISG15 from conjugated proteins. *Journal*

of *Biological Chemistry*. <https://doi.org/10.1074/jbc.M109078200>

- Malakhova, O. A., Kim, K. Il, Luo, J. K., Zou, W., Kumar, K. G. S., Fuchs, S. Y., ... Zhang, D. E. (2006). UBP43 is a novel regulator of interferon signaling independent of its ISG15 isopeptidase activity. *EMBO Journal*. <https://doi.org/10.1038/sj.emboj.7601149>
- Mariathasan, S., Weiss, D. S., Newton, K., McBride, J., O'Rourke, K., Roose-Girma, M., ... Dixit, V. M. (2006). Cryopyrin activates the inflammasome in response to toxins and ATP. *Nature*. <https://doi.org/10.1038/nature04515>
- Martinon, F., Burns, K., & Tschopp, J. (2002). The Inflammasome: A molecular platform triggering activation of inflammatory caspases and processing of proIL- $\beta$ . *Molecular Cell*. [https://doi.org/10.1016/S1097-2765\(02\)00599-3](https://doi.org/10.1016/S1097-2765(02)00599-3)
- Martinon, F., Pétrilli, V., Mayor, A., Tardivel, A., & Tschopp, J. (2006). Gout-associated uric acid crystals activate the NALP3 inflammasome. *Nature*. <https://doi.org/10.1038/nature04516>
- Mattner, F., Magram, J., Ferrante, J., Launois, P., Padova, K. Di, Behin, R., ... Alber, G. (1996). Genetically resistant mice lacking interleukin-12 are susceptible to infection with *Leishmania major* and mount a polarized Th2 cell response. *European Journal of Immunology*. <https://doi.org/10.1002/eji.1830260722>
- Mauthe, M., Orhon, I., Rocchi, C., Zhou, X., Luhr, M., Hijlkema, K. J., ... Reggiori, F. (2018). Chloroquine inhibits autophagic flux by decreasing autophagosome-lysosome fusion. *Autophagy*. <https://doi.org/10.1080/15548627.2018.1474314>
- Maxwell, M. J., Chan, S. K., Robinson, D. P., Dwyer, D. M., Nandan, D., Foster, L. J., & Reiner, N. E. (2008). Proteomic analysis of the secretome of *Leishmania donovani*. *Genome Biology*. <https://doi.org/10.1186/gb-2008-9-2-r35>
- McConville, M. J., & Blackwell, J. M. (1991). Developmental changes in the glycosylated phosphatidylinositols of *Leishmania donovani*. Characterization of the promastigote and amastigote glycolipids. *The Journal of Biological Chemistry*.
- McConville, M. J., Turco, S. J., Ferguson, M. A., & Sacks, D. L. (1992). Developmental modification of lipophosphoglycan during the differentiation of *Leishmania major* promastigotes to an infectious stage. *The EMBO Journal*. <https://doi.org/10.1002/j.1460-2075.1992.tb05443.x>
- Mercer, T. J., Gubas, A., & Tooze, S. A. (2018). A molecular perspective of mammalian autophagosome biogenesis. *Journal of Biological Chemistry*. <https://doi.org/10.1074/jbc.R117.810366>
- Mijatovic-Rustempasic, S., Tam, K. I., Kerin, T. K., Lewis, J. M., Gautam, R., Quaye, O., ... Bowen, M. D. (2013). Sensitive and specific quantitative detection of rotavirus a by one-step real-time reverse transcription-PCR assay without

- antecedent double-stranded-RNA denaturation. *Journal of Clinical Microbiology*, 51(9), 3047–3054. <https://doi.org/10.1128/JCM.01192-13>
- Mizushima, N. (2007). Autophagy: Process and function. *Genes and Development*. <https://doi.org/10.1101/gad.1599207>
- Mizushima, N., Levine, B., Cuervo, A. M., & Klionsky, D. J. (2008). Autophagy fights disease through cellular self-digestion. *Nature*. <https://doi.org/10.1038/nature06639>
- Molyneux, D. H. (1974). Virus-like particles in Leishmania parasites. *Nature*. <https://doi.org/10.1038/249588a0>
- Moore, K. J., & Matlashewski, G. (1994). Intracellular infection by Leishmania donovani inhibits macrophage apoptosis. *Journal of Immunology (Baltimore, Md. : 1950)*.
- Moradin, N., & Descoteaux, A. (2012). Leishmania promastigotes: building a safe niche within macrophages. *Frontiers in Cellular and Infection Microbiology*. <https://doi.org/10.3389/fcimb.2012.00121>
- Moreno, I., Molina, R., Toraño, A., Laurin, E., García, E., & Domínguez, M. (2007). Comparative real-time kinetic analysis of human complement killing of Leishmania infantum promastigotes derived from axenic culture or from Phlebotomus perniciosus. *Microbes and Infection*. <https://doi.org/10.1016/j.micinf.2007.09.009>
- Mosser, D. M., & Edelson, P. J. (1984). Activation of the alternative complement pathway by Leishmania promastigotes: parasite lysis and attachment to macrophages. *Journal of Immunology (Baltimore, Md. : 1950)*.
- Muraille, E., De Trez, C., Brait, M., De Baetselier, P., Leo, O., & Carlier, Y. (2003). Genetically Resistant Mice Lacking MyD88-Adapter Protein Display a High Susceptibility to Leishmania major Infection Associated with a Polarized Th2 Response. *The Journal of Immunology*. <https://doi.org/10.4049/jimmunol.170.8.4237>
- Nagar, R. (2017). Autophagy: A brief overview in perspective of dermatology. *Indian Journal of Dermatology, Venereology and Leprology*. <https://doi.org/10.4103/0378-6323.196320>
- Nalçacı, M., Karakuş, M., Yılmaz, B., Demir, S., Özbilgin, A., Özbel, Y., & Töz, S. (2019). Detection of Leishmania RNA virus 2 in Leishmania species from Turkey. *Transactions of the Royal Society of Tropical Medicine and Hygiene*. <https://doi.org/10.1093/trstmh/trz023>
- Okumura, A., Pitha, P. M., & Harty, R. N. (2008). ISG15 inhibits Ebola VP40 VLP budding in an L-domain-dependent manner by blocking Nedd4 ligase activity. *Proceedings of the National Academy of Sciences of the United States of*

America. <https://doi.org/10.1073/pnas.0710629105>

- Owhashi, M., Taoka, Y., Ishii, K., Nakazawa, S., Uemura, H., & Kambara, H. (2003). Identification of a ubiquitin family protein as a novel neutrophil chemotactic factor. *Biochemical and Biophysical Research Communications*. <https://doi.org/10.1016/j.bbrc.2003.08.038>
- Padovan, E., Terracciano, L., Certa, U., Jacobs, B., Reschner, A., Bolli, M., ... Heberer, M. (2002). Interferon stimulated gene 15 constitutively produced by melanoma cells induces E-cadherin expression on human dendritic cells. *Cancer Research*.
- Paludan, S. R., & Bowie, A. G. (2013). Immune Sensing of DNA. *Immunity*. <https://doi.org/10.1016/j.immuni.2013.05.004>
- Paolini, A., Omairi, S., Mitchell, R., Vaughan, D., Matsakas, A., Vaiyapuri, S., ... Patel, K. (2018). Attenuation of autophagy impacts on muscle fibre development, starvation induced stress and fibre regeneration following acute injury. *Scientific Reports*. <https://doi.org/10.1038/s41598-018-27429-7>
- Paul, J., Karmakar, S., & De, T. (2012). TLR-mediated distinct IFN- $\gamma$ /IL-10 pattern induces protective immunity against murine visceral leishmaniasis. *European Journal of Immunology*. <https://doi.org/10.1002/eji.201242428>
- Pérez-Cabezas, B., Santarém, N., Cecílio, P., Silva, C., Silvestre, R., A. M. Catita, J., & Cordeiro da Silva, A. (2019). More than just exosomes: distinct *Leishmania infantum* extracellular products potentiate the establishment of infection. *Journal of Extracellular Vesicles*. <https://doi.org/10.1080/20013078.2018.1541708>
- Perng, Y. C., & Lenschow, D. J. (2018). ISG15 in antiviral immunity and beyond. *Nature Reviews Microbiology*. <https://doi.org/10.1038/s41579-018-0020-5>
- Peters, N. C., Egen, J. G., Secundino, N., Debrabant, A., Kimblin, N., Kamhawi, S., ... Sacks, D. (2008). In vivo imaging reveals an essential role for neutrophils in leishmaniasis transmitted by sand flies. *Science*. <https://doi.org/10.1126/science.1159194>
- Peters, N. C., & Sacks, D. L. (2009). The impact of vector-mediated neutrophil recruitment on cutaneous leishmaniasis. *Cellular Microbiology*. <https://doi.org/10.1111/j.1462-5822.2009.01348.x>
- Pimenta, P. F. P., Saraiva, E. M. B., & Sacks, D. L. (1991). The comparative fine structure and surface glycoconjugate expression of three life stages of *Leishmania major*. *Experimental Parasitology*. [https://doi.org/10.1016/0014-4894\(91\)90137-L](https://doi.org/10.1016/0014-4894(91)90137-L)
- Pinheiro, R. O., Nunes, M. P., Pinheiro, C. S., D'Avila, H., Bozza, P. T., Takiya, C. M., ... DosReis, G. A. (2009). Induction of autophagy correlates with increased parasite load of *Leishmania amazonensis* in BALB/c but not C57BL/6

macrophages. *Microbes and Infection.*  
<https://doi.org/10.1016/j.micinf.2008.11.006>

- Pitale, D. M., Gendalur, N. S., Descoteaux, A., & Shaha, C. (2019). Leishmania donovani Induces Autophagy in Human Blood-Derived Neutrophils . *The Journal of Immunology.* <https://doi.org/10.4049/jimmunol.1801053>
- Platnich, J. M., & Muruve, D. A. (2019). NOD-like receptors and inflammasomes: A review of their canonical and non-canonical signaling pathways. *Archives of Biochemistry and Biophysics.* <https://doi.org/10.1016/j.abb.2019.02.008>
- Puentes, S M, Da Silva, R. P., Sacks, D. L., Hammer, C. H., & Joiner, K. A. (1990). Serum resistance of metacyclic stage Leishmania major promastigotes is due to release of C5b-9. *Journal of Immunology (Baltimore, Md. : 1950).*
- Puentes, Stephen M., Sacks, D. L., Da Silva, R. P., & Joiner, K. A. (1988). Complement binding by two developmental stages of leishmania major promastigotes varying in expression of a surface lipophosphoglycan. *Journal of Experimental Medicine.* <https://doi.org/10.1084/jem.167.3.887>
- Ramakrishnaiah, V., Thumann, C., Fofana, I., Habersetzer, F., Pan, Q., De Ruiter, P. E., ... Van Der Laan, L. J. W. (2013). Exosome-mediated transmission of hepatitis C virus between human hepatoma Huh7.5 cells. *Proceedings of the National Academy of Sciences of the United States of America.* <https://doi.org/10.1073/pnas.1221899110>
- Raman, V. S., Bhatia, A., Picone, A., Whittle, J., Bailor, H. R., O'Donnell, J., ... Reed, S. G. (2010). Applying TLR Synergy in Immunotherapy: Implications in Cutaneous Leishmaniasis. *The Journal of Immunology.* <https://doi.org/10.4049/jimmunol.1000238>
- Ravichandran, K. S. (2010). Find-me and eat-me signals in apoptotic cell clearance: Progress and conundrums. *Journal of Experimental Medicine.* <https://doi.org/10.1084/jem.20101157>
- Reilly, S. M., Chiang, S. H., Decker, S. J., Chang, L., Uhm, M., Larsen, M. J., ... Saltiel, A. R. (2013). An inhibitor of the protein kinases TBK1 and IKK-ε improves obesity-related metabolic dysfunctions in mice. *Nature Medicine.* <https://doi.org/10.1038/nm.3082>
- Ribeiro-Gomes, F. L., Peters, N. C., Debrabant, A., & Sacks, D. L. (2012). Efficient capture of infected neutrophils by dendritic cells in the skin inhibits the early anti-leishmania response. *PLoS Pathogens.* <https://doi.org/10.1371/journal.ppat.1002536>
- Rittig, M. G., & Bogdan, C. (2000). Leishmania-host-cell interaction: Complexities and alternative views. *Parasitology Today.* [https://doi.org/10.1016/S0169-4758\(00\)01692-6](https://doi.org/10.1016/S0169-4758(00)01692-6)

- Ro, Y T, Scheffter, S. M., & Patterson, J. L. (1997a). Hygromycin B resistance mediates elimination of Leishmania virus from persistently infected parasites. *Journal of Virology*, 71(12), 8991–8998. Retrieved from <http://www.ncbi.nlm.nih.gov/pubmed/9371555><http://www.pubmedcentral.nih.gov/articlerender.fcgi?artid=PMC230199>
- Ro, Y T, Scheffter, S. M., & Patterson, J. L. (1997b). Specific in vitro cleavage of a Leishmania virus capsid-RNA-dependent RNA polymerase polyprotein by a host cysteine-like protease. *Journal of Virology*.
- Ro, Young Tae, Kim, E. J., Lee, H. Il, Saiz, M., Carrion, R., & Patterson, J. L. (2004). Evidence that the fully assembled capsid of Leishmania RNA virus 1-4 possesses catalytically active endoribonuclease activity. *Experimental and Molecular Medicine*. <https://doi.org/10.1038/emm.2004.21>
- Ronet, C., Beverley, S. M., & Fasel, N. (2011). Muco-cutaneous leishmaniasis in the New World: The ultimate subversion. *Virulence*. <https://doi.org/10.4161/viru.2.6.17839>
- Rossi, M., Castiglioni, P., Hartley, M. A., Eren, R. O., Prével, F., Desponds, C., ... Fasel, N. (2017). Type I interferons induced by endogenous or exogenous viral infections promote metastasis and relapse of leishmaniasis. *Proceedings of the National Academy of Sciences of the United States of America*. <https://doi.org/10.1073/pnas.1621447114>
- Rostami, M. N., Keshavarz, H., Edalat, R., Sarrafnejad, A., Shahrestani, T., Mahboudi, F., & Khamesipour, A. (2010). CD8+ T cells as a source of IFN- $\gamma$  production in human cutaneous leishmaniasis. *PLoS Neglected Tropical Diseases*. <https://doi.org/10.1371/journal.pntd.0000845>
- Rougerie, P., Miskolci, V., & Cox, D. (2013). Generation of membrane structures during phagocytosis and chemotaxis of macrophages: Role and regulation of the actin cytoskeleton. *Immunological Reviews*. <https://doi.org/10.1111/imr.12118>
- Roy, S., Kumar, G. A., Jafurulla, M., Mandal, C., & Chattopadhyay, A. (2014). Integrity of the actin cytoskeleton of host macrophages is essential for Leishmania donovani infection. *Biochimica et Biophysica Acta - Biomembranes*. <https://doi.org/10.1016/j.bbamem.2014.04.017>
- Sacks, D. L., & Perkins, P. V. (1984). Identification of an infective stage of Leishmania promastigotes. *Science*. <https://doi.org/10.1126/science.6701528>
- Salinas, G., Zamora, M., Stuart, K., & Saravia, N. (1996). Leishmania RNA viruses in Leishmania of the Viannia subgenus. *American Journal of Tropical Medicine and Hygiene*. <https://doi.org/10.4269/ajtmh.1996.54.425>
- Sanjana, N. E., Shalem, O., & Zhang, F. (2014). Improved vectors and genome-wide libraries for CRISPR screening. *Nature Methods*.

<https://doi.org/10.1038/nmeth.3047>

- Sanjuan, M. A., Dillon, C. P., Tait, S. W. G., Moshiah, S., Dorsey, F., Connell, S., ... Green, D. R. (2007). Toll-like receptor signalling in macrophages links the autophagy pathway to phagocytosis. *Nature*. <https://doi.org/10.1038/nature06421>
- Satoh, T., & Akira, S. (2016). Toll-Like Receptor Signaling and Its Inducible Proteins. *Microbiology Spectrum*. <https://doi.org/10.1128/microbiolspec.mchd-0040-2016>
- Savoia, D. (2015). Recent updates and perspectives on leishmaniasis. *Journal of Infection in Developing Countries*. <https://doi.org/10.3855/jidc.6833>
- Schamber-Reis, B. L. F., Petritus, P. M., Caetano, B. C., Martinez, E. R., Okuda, K., Golenbock, D., ... Gazzinelli, R. T. (2013). UNC93B1 and nucleic acid-sensing toll-like receptors mediate host resistance to infection with leishmania major. *Journal of Biological Chemistry*. <https://doi.org/10.1074/jbc.M112.407684>
- Scheffter, S. M., Ro, Y. T., Chung, I. K., & Patterson, J. L. (1995). The Complete Sequence of Leishmania RNA Virus LRV2-1, a Virus of an Old World Parasite Strain. *Virology*. <https://doi.org/10.1006/viro.1995.1456>
- Schneider, P., Rosat, J. P., Bouvier, J., Louis, J., & Bordier, C. (1992). Leishmania major: Differential regulation of the surface metalloprotease in amastigote and promastigote stages. *Experimental Parasitology*. [https://doi.org/10.1016/0014-4894\(92\)90179-E](https://doi.org/10.1016/0014-4894(92)90179-E)
- Shalem, O., Sanjana, N. E., Hartenian, E., Shi, X., Scott, D. A., Mikkelsen, T. S., ... Zhang, F. (2014). Genome-scale CRISPR-Cas9 knockout screening in human cells. *Science*. <https://doi.org/10.1126/science.1247005>
- Silverman, J. M., axwel., & Reiner, N. E. (2011). Leishmania exosomes deliver preemptive strikes to create an environment permissive for early infection. *Frontiers in Cellular and Infection Microbiology*. <https://doi.org/10.3389/fcimb.2011.00026>
- Silverman, J. M., Clos, J., De'Oliveira, C. C., Shirvani, O., Fang, Y., Wang, C., ... Reiner, N. E. (2010). An exosome-based secretion pathway is responsible for protein export from Leishmania and communication with macrophages. *Journal of Cell Science*, 123(6), 842–852. <https://doi.org/10.1242/jcs.056465>
- Silverman, J. M., Clos, J., Horakova, E., Wang, A. Y., Wiesgigl, M., Kelly, I., ... Reiner, N. E. (2010). Leishmania Exosomes Modulate Innate and Adaptive Immune Responses through Effects on Monocytes and Dendritic Cells. *The Journal of Immunology*. <https://doi.org/10.4049/jimmunol.1000541>
- Simpson, R. J., Lim, J. W. E., Moritz, R. L., & Mathivanan, S. (2009). Exosomes: Proteomic insights and diagnostic potential. *Expert Review of Proteomics*. <https://doi.org/10.1586/epr.09.17>

- Smelt, S. C., Cotterell, S. E. J., Engwerda, C. R., & Kaye, P. M. (2000). B Cell-Deficient Mice Are Highly Resistant to *Leishmania donovani* Infection, but Develop Neutrophil-Mediated Tissue Pathology. *The Journal of Immunology*. <https://doi.org/10.4049/jimmunol.164.7.3681>
- Stewart, S. A., Dykxhoorn, D. M., Palliser, D., Mizuno, H., Yu, E. Y., An, D. S., ... Novina, C. D. (2003). Lentivirus-delivered stable gene silencing by RNAi in primary cells. *RNA*. <https://doi.org/10.1261/rna.2192803>
- Su, T., Liu, F., Gu, P., Jin, H., Chang, Y., Wang, Q., ... Qi, Q. (2016). A CRISPR-Cas9 assisted non-homologous end-joining strategy for one-step engineering of bacterial genome. *Scientific Reports*. <https://doi.org/10.1038/srep37895>
- Sun, Li, Wang, X., Zhou, Y., Zhou, R. H., Ho, W. Z., & Li, J. L. (2016). Exosomes contribute to the transmission of anti-HIV activity from TLR3-activated brain microvascular endothelial cells to macrophages. *Antiviral Research*. <https://doi.org/10.1016/j.antiviral.2016.07.013>
- Sun, Lijun, Wu, J., Du, F., Chen, X., & Chen, Z. J. (2013). Cyclic GMP-AMP synthase is a cytosolic DNA sensor that activates the type I interferon pathway. *Science*. <https://doi.org/10.1126/science.1232458>
- Sundar, S. (2001). Drug resistance in Indian visceral leishmaniasis. *Tropical Medicine and International Health*. <https://doi.org/10.1046/j.1365-3156.2001.00778.x>
- Sunter, J., & Gull, K. (2017). Shape, form, function and *Leishmania* pathogenicity: from textbook descriptions to biological understanding. *Open Biology*. <https://doi.org/10.1098/rsob.170165>
- Tanaka, Y., & Chen, Z. J. (2012). STING specifies IRF3 phosphorylation by TBK1 in the cytosolic DNA signaling pathway. *Science Signaling*. <https://doi.org/10.1126/scisignal.2002521>
- Tarr, P. I., Aline, R. F., Smiley, B. L., Scholler, J., Keithly, J., & Stuart, K. (1988). LR1: A candidate RNA virus of *Leishmania*. *Proceedings of the National Academy of Sciences of the United States of America*. <https://doi.org/10.1073/pnas.85.24.9572>
- Tegazzini, D., Díaz, R., Aguilar, F., Peña, I., Presa, J. L., Yardley, V., ... Cantizani, J. (2016). A Replicative In Vitro Assay for Drug Discovery against *Leishmania donovani*. *Antimicrobial Agents and Chemotherapy*. <https://doi.org/10.1128/AAC.01781-15>
- Théry, C., Witwer, K. W., Aikawa, E., Alcaraz, M. J., Anderson, J. D., Andriantsitohaina, R., ... Zuba-Surma, E. K. (2018). Minimal information for studies of extracellular vesicles 2018 (MISEV2018): a position statement of the International Society for Extracellular Vesicles and update of the MISEV2014 guidelines. *Journal of Extracellular Vesicles*.

<https://doi.org/10.1080/20013078.2018.1535750>

- Théry, C., Zitvogel, L., & Amigorena, S. (2002). Exosomes: Composition, biogenesis and function. *Nature Reviews Immunology*. <https://doi.org/10.1038/nri855>
- Thomas, P. D., Campbell, M. J., Kejariwal, A., Mi, H., Karlak, B., Daverman, R., ... Narechania, A. (2003). PANTHER: A library of protein families and subfamilies indexed by function. *Genome Research*. <https://doi.org/10.1101/gr.772403>
- Thomas, S. A., Nandan, D., Kass, J., & Reiner, N. E. (2018). Countervailing, time-dependent effects on host autophagy promotes intracellular survival of Leishmania. *Journal of Biological Chemistry*. <https://doi.org/10.1074/jbc.M117.808675>
- Ueno, N., Bratt, C. L., Rodriguez, N. E., & Wilson, M. E. (2009). Differences in human macrophage receptor usage, lysosomal fusion kinetics and survival between logarithmic and metacyclic *Leishmania infantum* chagasi promastigotes. *Cellular Microbiology*. <https://doi.org/10.1111/j.1462-5822.2009.01374.x>
- Ueno, N., & Wilson, M. E. (2012). Receptor-mediated phagocytosis of *Leishmania*: Implications for intracellular survival. *Trends in Parasitology*. <https://doi.org/10.1016/j.pt.2012.05.002>
- Ueno, T., & Komatsu, M. (2017). Autophagy in the liver: Functions in health and disease. *Nature Reviews Gastroenterology and Hepatology*. <https://doi.org/10.1038/nrgastro.2016.185>
- Underhill, D. M. (2003). Macrophage recognition of zymosan particles. *Journal of Endotoxin Research*. <https://doi.org/10.1179/096805103125001586>
- van Dongen, H. M., Masoumi, N., Witwer, K. W., & Pegtel, D. M. (2016). Extracellular Vesicles Exploit Viral Entry Routes for Cargo Delivery. *Microbiology and Molecular Biology Reviews*. <https://doi.org/10.1128/mnbr.00063-15>
- van Zandbergen, G., Klinger, M., Mueller, A., Dannenberg, S., Gebert, A., Solbach, W., & Laskay, T. (2004). Cutting Edge: Neutrophil Granulocyte Serves as a Vector for *Leishmania* Entry into Macrophages. *The Journal of Immunology*. <https://doi.org/10.4049/jimmunol.173.11.6521>
- Vargas-Inchaustegui, D. A., Tai, W., Xin, L., Hogg, A. E., Corry, D. B., & Soong, L. (2009). Distinct roles for MyD88 and toll-like receptor 2 during *Leishmania braziliensis* infection in mice. *Infection and Immunity*. <https://doi.org/10.1128/IAI.00154-09>
- Vargas-Inchaustegui, D. A., Xin, L., & Soong, L. (2008). *Leishmania braziliensis* Infection Induces Dendritic Cell Activation, ISG15 Transcription, and the Generation of Protective Immune Responses. *The Journal of Immunology*.

<https://doi.org/10.4049/jimmunol.180.11.7537>

- Veras, P. S. T., de Menezes, J. P. B., & Dias, B. R. S. (2019). Deciphering the Role Played by Autophagy in Leishmania Infection. *Frontiers in Immunology*. <https://doi.org/10.3389/fimmu.2019.02523>
- Wang, P., Li, S., Zhao, Y., Zhang, B., Li, Y., Liu, S., ... You, F. (2019). The GRA15 protein from *Toxoplasma gondii* enhances host defense responses by activating the interferon stimulator STING. *Journal of Biological Chemistry*. <https://doi.org/10.1074/jbc.RA119.009172>
- Weeks, R., Aline, R. F., Myler, P. J., & Stuart, K. (1992). LRV1 viral particles in *Leishmania guyanensis* contain double-stranded or single-stranded RNA. *Journal of Virology*.
- Wei, B., Feng, N., Zhou, F., Lu, C., Su, J., & Hua, L. (2010). Construction and identification of recombinant lentiviral vector containing HIV-1 Tat gene and its expression in 293T cells. *Journal of Biomedical Research*. [https://doi.org/10.1016/S1674-8301\(10\)60009-7](https://doi.org/10.1016/S1674-8301(10)60009-7)
- Weinkopff, T., Mariotto, A., Simon, G., Torre, Y. H. La, Auderset, F., Schuster, S., ... Tacchini-Cottier, F. (2013). Role of toll-like receptor 9 signaling in experimental leishmania braziliensis infection. *Infection and Immunity*. <https://doi.org/10.1128/IAI.01401-12>
- Werneke, S. W., Schilte, C., Rohatgi, A., Monte, K. J., Michault, A., Arenzana-Seisdedos, F., Lenschow, D. J. (2011). ISG15 is critical in the control of chikungunya virus infection independent of UbE11 mediated conjugation. *PLoS Pathogens*. <https://doi.org/10.1371/journal.ppat.1002322>
- Wheeler, R. J., Sunter, J. D., & Gull, K. (2016). Flagellar pocket restructuring through the *Leishmania* life cycle involves a discrete flagellum attachment zone. *Journal of Cell Science*. <https://doi.org/10.1242/jcs.183152>
- Widmer, G. (1995). Suppression of *Leishmania* RNA virus replication by capsid protein overexpression. *Journal of Virology*.
- Widmer, Giovanni, & Dooley, S. (1995). Phylogenetic analysis of *Leishmania* RNA virus and leishmania suggests ancient virus-parasite association. *Nucleic Acids Research*. <https://doi.org/10.1093/nar/23.12.2300>
- Woalder. (2017). HHS Public Access. *Physiology & Behavior*, 176(1), 139–148. <https://doi.org/10.1016/j.physbeh.2017.03.040>
- Xu, D., Zhang, T., Xiao, J., Zhu, K., Wei, R., Wu, Z., Yuan, J. (2015). Modification of BECN1 by ISG15 plays a crucial role in autophagy regulation by type I IFN/interferon. *Autophagy*. <https://doi.org/10.1080/15548627.2015.1023982>
- Xu, Y., Wang, L., Bai, R., Zhang, T., & Chen, C. (2015). Silver nanoparticles impede

- phorbol myristate acetate-induced monocyte-macrophage differentiation and autophagy. *Nanoscale*. <https://doi.org/10.1039/c5nr04200c>
- Yáñez-Mó, M., Siljander, P. R. M., Andreu, Z., Zavec, A. B., Borràs, F. E., Buzas, E. I., ... De Wever, O. (2015). Biological properties of extracellular vesicles and their physiological functions. *Journal of Extracellular Vesicles*. <https://doi.org/10.3402/jev.v4.27066>
- Yang, S., Imamura, Y., Jenkins, R. W., Canadas, I., Kitajima, S., Aref, A., ... Barbie, D. A. (2016). Autophagy inhibition dysregulates TBK1 signaling and promotes pancreatic inflammation. *Cancer Immunology Research*. <https://doi.org/10.1158/2326-6066.CIR-15-0235>
- Yang, Z. J., Chee, C. E., Huang, S., & Sinicrope, F. A. (2011). The role of autophagy in cancer: Therapeutic implications. *Molecular Cancer Therapeutics*. <https://doi.org/10.1158/1535-7163.MCT-11-0047>
- Yang, Z., & Klionsky, D. J. (2010). Mammalian autophagy: Core molecular machinery and signaling regulation. *Current Opinion in Cell Biology*. <https://doi.org/10.1016/j.ceb.2009.11.014>
- Yu, L., McPhee, C. K., Zheng, L., Mardones, G. A., Rong, Y., Peng, J., ... Lenardo, M. J. (2010). Termination of autophagy and reformation of lysosomes regulated by mTOR. *Nature*. <https://doi.org/10.1038/nature09076>
- Zaffagnini, G., & Martens, S. (2016). Mechanisms of Selective Autophagy. *Journal of Molecular Biology*. <https://doi.org/10.1016/j.jmb.2016.02.004>
- Zangger, H., Hailu, A., Desponds, C., Lye, L. F., Akopyants, N. S., Dobson, D. E., Fasel, N. (2014). Leishmania aethiops Field Isolates Bearing an Endosymbiotic dsRNA Virus Induce Pro-inflammatory Cytokine Response. *PLoS Neglected Tropical Diseases*. <https://doi.org/10.1371/journal.pntd.0002836>
- Zangger, H., Ronet, C., Desponds, C., Kuhlmann, F. M., Robinson, J., Hartley, M. A., ... Fasel, N. (2013). Detection of Leishmania RNA Virus in Leishmania Parasites. *PLoS Neglected Tropical Diseases*. <https://doi.org/10.1371/journal.pntd.0002006>
- Zeisig, B. B., & Wai Eric So, C. (2009). Retroviral/lentiviral transduction and transformation assay. *Methods in Molecular Biology*. [https://doi.org/10.1007/978-1-59745-418-6\\_10](https://doi.org/10.1007/978-1-59745-418-6_10)
- Zhang, Xianqin, Bogunovic, D., Payelle-Brogard, B., Francois-Newton, V., Speer, S. D., Yuan, C., ... Pellegrini, S. (2015). Human intracellular ISG15 prevents interferon- $\alpha/\beta$  over-amplification and auto-inflammation. *Nature*. <https://doi.org/10.1038/nature13801>
- Zhang, Xu, Shi, H., Wu, J., Zhang, X., Sun, L., Chen, C., & Chen, Z. J. (2013). Cyclic

GMP-AMP containing mixed Phosphodiester linkages is an endogenous high-affinity ligand for STING. *Molecular Cell*. <https://doi.org/10.1016/j.molcel.2013.05.022>

Zhang, Y., Thery, F., Wu, N. C., Luhmann, E. K., Dussurget, O., Foecke, M., ... Radoshevich, L. (2019). The in vivo ISGylome links ISG15 to metabolic pathways and autophagy upon *Listeria monocytogenes* infection. *Nature Communications*. <https://doi.org/10.1038/s41467-019-13393-x>

Zhang, Z., Singh, R., & Aschner, M. (2016). Methods for the detection of autophagy in mammalian cells. *Current Protocols in Toxicology*. <https://doi.org/10.1002/cptx.11>

Zhitomirsky, B., Yunaev, A., Kreiserman, R., Kaplan, A., Stark, M., & Assaraf, Y. G. (2018). Lysosomotropic drugs activate TFEB via lysosomal membrane fluidization and consequent inhibition of mTORC1 activity. *Cell Death and Disease*. <https://doi.org/10.1038/s41419-018-1227-0>

## APPENDICES

### A. Media Recipes

*Table A.1. Leishmania (LRV-) Growth Medium*

<b>Ingredient</b>	<b>Volume (ml)</b>	<b>Final Concentration</b>	<b>Company</b>	<b>Cat No:</b>
Heat Inactivated FBS	130	20 %	Biological Industries, Israel	04-127-1A
HEPES buffer 1M	13	20 mM	Biological Industries, Israel	03-025-1B
Penicillin/Streptomycin (Pen/Strep) Solution	6.5	Pen: 100 units/ml Strep: 100 µg/ml	Biological Industries, Israel	03-031-1B
RPMI 1640 Medium with L-glutamine and Phenol Red	500		Biological Industries, Israel	01-100-1A
<b>TOTAL</b>	649.5			

*Table A.2. Leishmania (LRV+) Growth Medium*

<b>Ingredient</b>	<b>Volume (ml)</b>	<b>Final Concentration</b>	<b>Company</b>	<b>Cat No:</b>
Heat Inactivated FBS	130	20 %	Biological Industries, Israel	04-127-1A
HEPES buffer 1M	13	20 mM	Biological Industries, Israel	03-025-1B
Penicillin/Streptomycin (Pen/Strep) Solution	6.5	Pen: 100 units/ml Strep: 100 µg/ml	Biological Industries, Israel	03-031-1B
RPMI 1640 Medium with L-glutamine and Phenol Red	250		Biological Industries, Israel	01-100-1A
Medium 199 With Hanks' salts	250		Merck KgaA, Germany	M7653
<b>TOTAL</b>	649.5			

Table A.3. Leishmania Freezing Medium

<b>Ingredient</b>	<b>Volume (ml)</b>	<b>Final Concentration</b>	<b>Company</b>	<b>Cat No:</b>
Heat Inactivated FBS	4	40 %	Biological Industries, Israel	04-127-1A
Dimethyl Sulfoxide (DMSO)	2	20%	Merck, Germany	D8418
RPMI 1640 Medium with L-glutamine and Phenol Red	4		Biological Industries, Israel	01-100-1A
<b>TOTAL</b>	<b>10</b>			

Table A.4. 20%, 10% and 2% Regular RPMI 1640 Medium

<b>Ingredient</b>	<b>Volume (ml)</b>	<b>Final Concentration</b>	<b>Company</b>	<b>Cat No:</b>
Heat Inactivated FBS	100,50,10	20 %, 10%, 2%	Biological Industries, Israel	04-127-1A
HEPES buffer 1M	10	20 mM	Biological Industries, Israel	03-025-1B
Penicillin/Streptomycin (Pen/Strep) Solution	5	Pen: 100 units/ml Strep: 100 µg/ml	Biological Industries, Israel	03-031-1B
MEM Non-Essential Amino Acids Solution (100X)	5	1X (100nm of each amino acid)	Biological Industries, Israel	01-340-1B
Sodium Pyruvate Solution	5	0.11 mg/ml	Biological Industries, Israel	03-042-1B
RPMI 1640 Medium with L-glutamine and Phenol Red	375,425,465		Biological Industries, Israel	01-100-1A
<b>TOTAL</b>	<b>500</b>			

Table A.5. LentiRPMI 1640 medium

<b>Ingredient</b>	<b>Volume (ml)</b>	<b>Final Concentration</b>	<b>Company</b>	<b>Cat No:</b>
Heat Inactivated tetracycline negative FBS	50,100	10 %, 20%	Biological Industries, Israel	04-127-1A
HEPES buffer 1M	10	20 mM	Biological Industries, Israel	03-025-1B
Penicillin/Streptomycin (Pen/Strep) Solution	5	Pen: 100 units/ml Strep: 100 µg/ml	Biological Industries, Israel	03-031-1B
MEM Non-Essential Amino Acids Solution (100X)	5	1X (100nm of each amino acid)	Biological Industries, Israel	01-340-1B
Sodium Pyruvate Solution	5	0.11 mg/ml	Biological Industries, Israel	03-042-1B
RPMI 1640 Medium with L-glutamine and Phenol Red	375,425		Biological Industries, Israel	01-100-1A
<b>TOTAL</b>	500			

**Electroporation Buffer pH: 7.5**

-137 mM NaCl

-21 mM HEPES

-6 mM Glucose

-5 mM KCl

-0.7 mM Na<sub>2</sub>HPO<sub>4</sub>

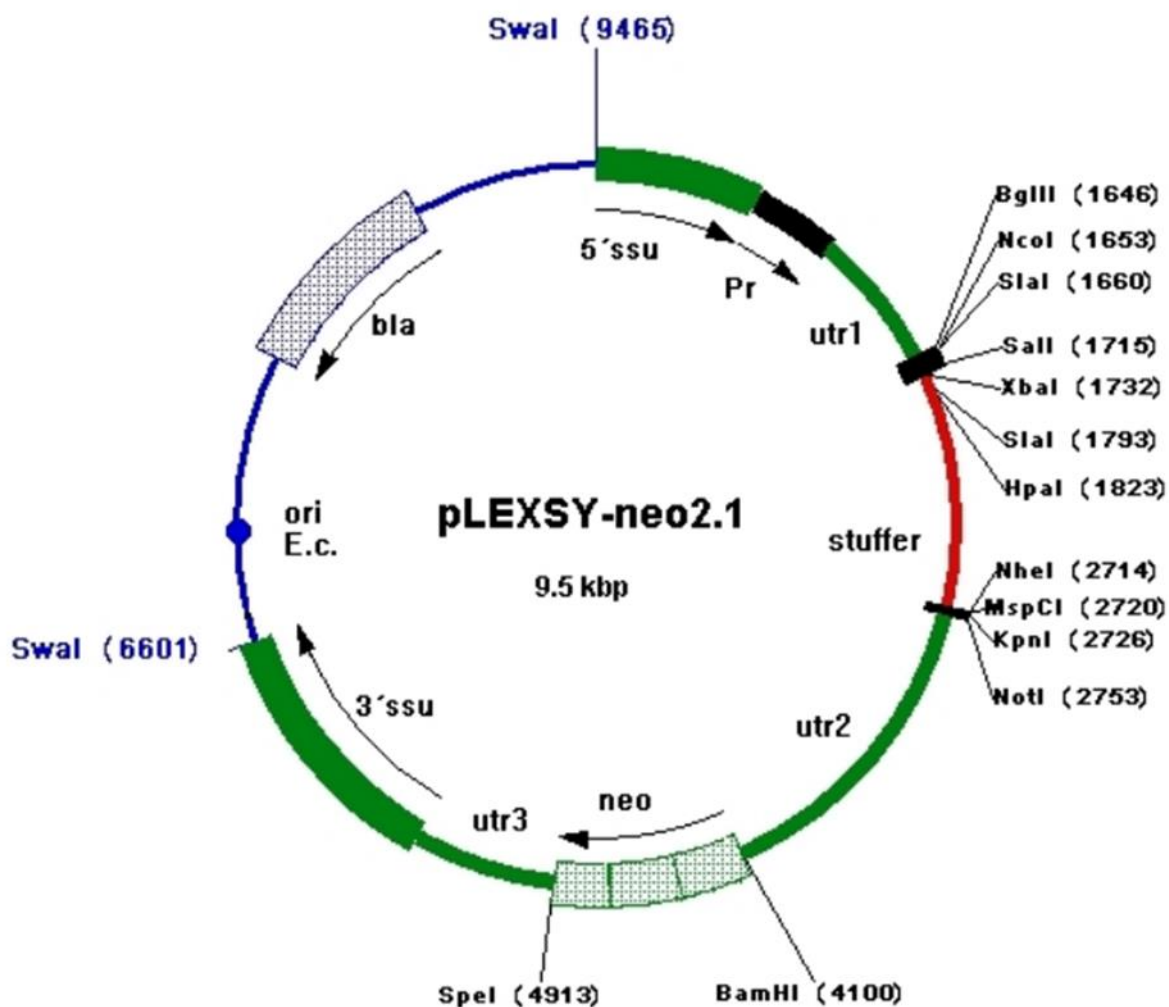
## B. Vector Maps and Sequences

### EGFP-LUC fusion protein codon optimized sequence:

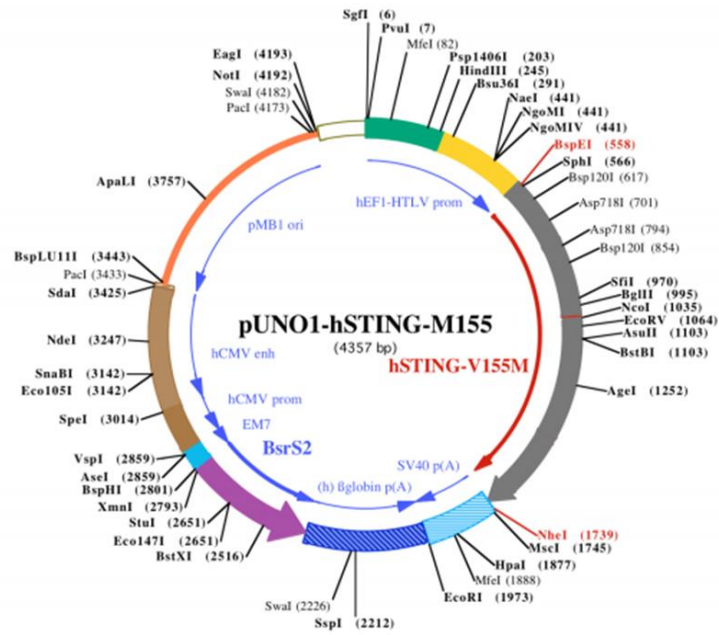
ATGGTGAGCAAGGGCGAGGAGCTGTTCACCGGGGTGGTGCCCATCCTGG  
TCGAGCTGGACGGCGACGTAAACGGCCACAAGTTCAGCGTGTCCGGCGA  
GGGCGAGGGCGATGCCACCTACGGCAAGCTGACCCTGAAGTTCATCTGC  
ACCACCGGCAAGCTGCCCGTGGCCCTGGCCCACCCTCGTGACCACCCTGAC  
CTACGGCGTGCAGTGCTTCAGCCGCTACCCCGACCACATGAAGCAGCAC  
GACTTCTTCAAGTCCGCCATGCCCGAAGGCTACGTCCAGGAGCGCACCA  
TCTTCTTCAAGGACGACGGCAACTACAAGACCCGCGCCGAGGTGAAGTT  
CGAGGGCGACACCCTGGTGAACCGCATCGAGCTGAAGGGCATCGACTTC  
AAGGAGGACGGCAACATCCTGGGGCACAAGCTGGAGTACAACACTACAAC  
AGCCACAACGTCTATATCATGGCCGACAAGCAGAAGAACGGCATCAAGG  
TGAACTTCAAGATCCGCCACAACATCGAGGACGGCAGCGTGCAGCTCGC  
CGACCACTACCAGCAGAACACCCCATCGGCGACGGCCCCGTGCTGCTG  
CCCGACAACCACTACCTGAGCACCCAGTCCGCCCTGAGCAAAGACCCCA  
ACGAGAAGCGCGATCACATGGTCTGCTGGAGTTCGTGACCGCCGCCGG  
GATCACTCTCGGCATGGACGAGCTGTACAAGTCCGGCCGGACTCAGATC  
TCGAGCTCAAGCTTCGAATTCGAAGACGCCAAAAACATAAAGAAAGGCC  
CGGCGCCATTCTATCCGCTGGAAGATGGAACCGCTGGAGAGCAACTGCA  
TAAGGCTATGAAGAGATACGCCCTGGTTCCTGGAACAATTGCTTTTACAG  
ATGCACATATCGAGGTGGACATCACTTACGCTGAGTACTTCGAAATGTCC  
GTTTCGGTTGGCAGAAGCTATGAAACGATATGGGCTGAATACAAATCACA  
GAATCGTCGTATGCAGTGAAAACCTCTCTTCAATTCTTTATGCCGGTGTTG  
GGCGCGTTATTTATCGGAGTTGCAGTTGCGCCCGCGAACGACATTTATAA  
TGAACGTGAATTGCTCAACAGTATGGGCATTTTCGCAGCCTACCGTGGTGT  
TCGTTTCCAAAAAGGGGTTGCAAAAAATTTTGAACGTGCAAAAAAGCT  
CCCAATCATCCAAAAAATTATTATCATGGATTCTAAAACGGATTACCAGG  
GATTCAGTCGATGTACACGTTTCGTACATCTCATCTACCTCCCGGTTTAA  
ATGAATACGATTTTGTGCCAGAGTCCTTCGATAGGGACAAGACAATTGC  
ACTGATCATGAACTCCTCTGGATCTACTGGTCTGCCTAAAGGTGTCGCTC  
TGCCTCATAGAACTGCCTGCGTGAGATTCTCGCATGCCAGAGATCCTATT  
TTTGGCAATCAAATCATTCCGGATACTGCGATTTTAAAGTGTTGTTCCATTC  
CATCACGGTTTTTGAATGTTTACTACACTCGGATATTTGATATGTGGATTT  
CGAGTCGTCTTAATGTATAGATTTGAAGAAGAGCTGTTTCTGAGGAGCCT  
TCAGGATTACAAGATTCAAAGTGCGCTGCTGGTGCCAACCCTATTCTCCT  
TCTTCGCCAAAAGCACTCTGATTGACAAATACGATTTATCTAATTTACAC  
GAAATTGCTTCTGGTGGCGCTCCCCTCTCTAAGGAAGTCGGGGAAGCGG  
TTGCCAAGAGGTTCCATCTGCCAGGTATCAGGCAAGGATATGGGCTCAC  
TGAGACTACATCAGCTATTCTGATTACACCCGAGGGGGATGATAAACCG  
GGCGCGGTCCGTAAGTTGTTCCATTTTTTGAAGCGAAGGTTGTGGATCT  
GGATAACCGGAAAACGCTGGGCGTTAATCAAAGAGGCGAACTGTGTGTG  
AGAGGTCCTATGATTATGTCCGGTTATGTAAACAATCCGGAAGCGACCA

ACGCCTTGATTGACAAGGATGGATGGCTACATTCTGGAGACATAGCTTA  
 CTGGGACGAAGACGAACACTTCTTCATCGTTGACCGCCTGAAGTCTCTGA  
 TTAAGTACAAAGGCTATCAGGTGGCTCCCGCTGAATTGGAATCCATCTTG  
 CTCCAACACCCCAACATCTTCGACGCAGGTGTCGCAGGTCTTCCCGACGA  
 TGACGCCGGTGAACCTTCCCGCCGCGTTGTTGTTTTGGAGCACGGAAAGA  
 CGATGACGGAAAAAGAGATCGTGGATTACGTCGCCAGTCAAGTAACAAC  
 CGCGAAAAAGTTGCGCGGAGGAGTTGTGTTTGTGGACGAAGTACCGAAA  
 GGTCTTACCGGAAAACCTCGACGCAAGAAAAATCAGAGAGATCCTCATAA  
 AGGCCAAGAAGGGCGGAAAGATCGCCGTGTA

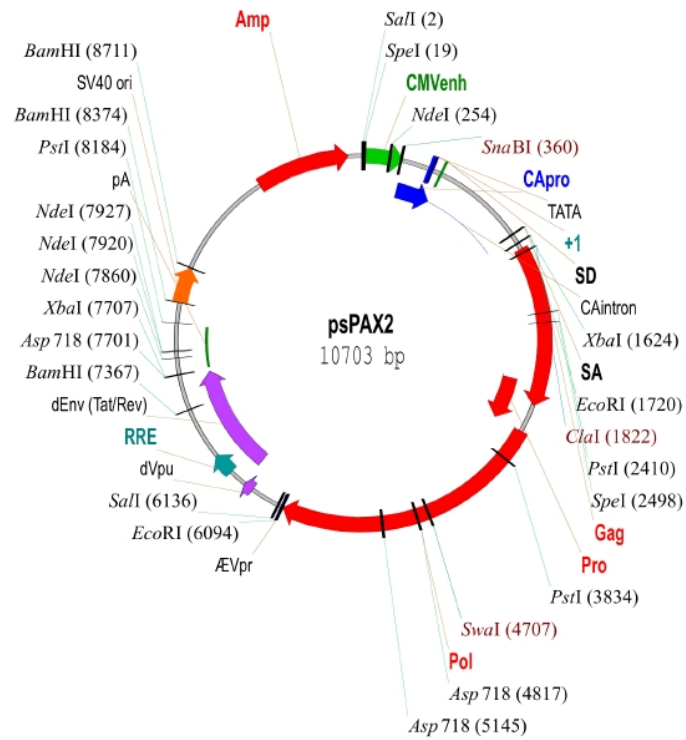
Vector Map of pLEXSY- neo2.1:



### Vector map of pUNO1-hSTING:

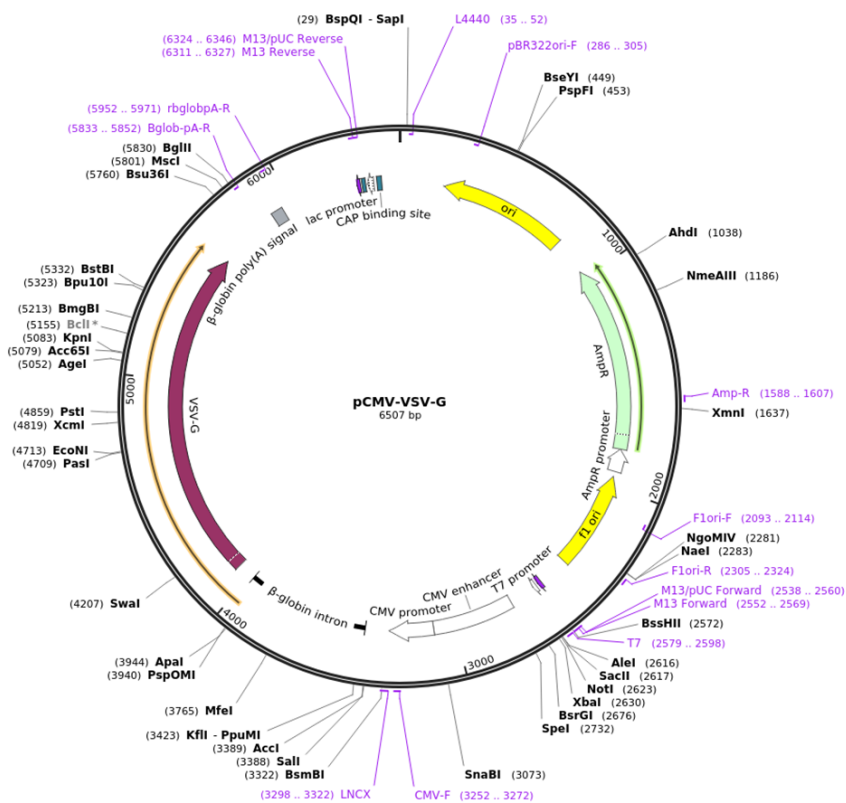


### Vector Map of PsPAX2:



## Vector Map of pCMV-VSV-G:

Created with SnapGene®



## LRV2-1 3350 bp NGS sequence from LRV+ exosome:

AGGCTGCACTACCAGCTTTTCGCTTCGATATACATCCATAATCTGGCAATG  
TTCATGGGTGTAGGTGGCGACGATTGCGGACGTGCGGTAGATACGTTGG  
TTGAAGCCGGTGTATATCTGCTCACTTACAGGCAATGATGCCAGTCGT  
CATATGCTCAAGGGAAGTATGGCACCCCTGGTTCTGGGTTGAGTCTACAGG  
CTTGTTCGGGACCTCACGTGCTTCAATATCCCTGGTTTGAGCGCTGGCT  
ATGGTCCTCAAGCGATATATGGCACAGCCATTACCCAGCCAGCCATGCA  
AGCTTGCGAATATACAGGTACTCGAGGATCATAACGATTATTACAATGTCG  
GGTGGACATCATTACGCAAGCACCCGCTTCTTGTCTTACAAACAACAGA  
GCTGGTGACGGCATTGCACATATGGAGGTAGGGCGTGATGCGGCCATAC  
CGTGGGTCTTGCCGGGACAACCACAAAGACGTGAGTGTACTGCGCAAGG  
TCACGGGACCCAGACTGCAACGTGTGGACACACAAAACACAATCGAGGG  
ACTTTGGATGAATATATCTGGGGTAGATTTTCCACGGGCCTATTCCATCC  
AGCCGAGCTAACAACTTTACTAACGTGGAGTTCGCGGTTAAGTGTGGGA  
CGGAAGACAATGACGGTAACGTACTCGAAACAGGTGCACCAGTCAAGG

ATATTGTGGAAGGGGGGGTTACTGTGAGTGTGAACGCAATACTACTTAC  
AAATTCCACCAATCACATACGTACGGTACCAGCAGTTCGACGTAGTTACC  
AAGCTGGCGCGAAGTATCTCGAAGAAGCACGAAGCCGTGGTACGATGTC  
TACACTTAATAGAATAATAGGAGGACAACCTTTTATAGGGATCTTCAACCTA  
TAAGCAAGCGAGGGGTGCCGCCACAGCCCAGCCTGTATGTGCAAGCAT  
GCCTGTTGAAACAACGAAAGAGGTTAGTCTGTCAAGGATCGGACCAATT  
CGTATCAACCAAAACGTTTTTCAGACCACGACCACAACCTACAGAAGAAG  
AGATGCATGAAGAACCAACGCCAGTAGCGCTCGAAGCAGAGCCACCAG  
GCGAAAATGTGTAAGTGACGGATTGGGAGTCTAAGTTCAAGAGTAGGTT  
GGCAAACGTGGTTGAACTGTTAAGGTATGATGCACTAACAGAGCCCTGT  
GGCGGGGAAACTAACCTTAGAGTGAGCGAAGAAACATGCTCCGGAATCC  
CAGTACTTCAGGAGGCGTGTATTTCGAAGATTTGTGGAGGAAAGGTTCAA  
TTTTATAGCAAGAATTACTGGAAAGAGTGATCGGCAGGGGCGGTGGAGA  
GCAGTTATTAATACGTGTTCTCAGTCCCTCATTATACAAACATACACGA  
CACCAAGATTTTTGGTGTAAACGATTACTAAGAATAATATTCACCGGATAT  
TATTCATATTTGCTTGTGTCTTGATATTTTGCACCTACGAAATGCGAGCGA  
AACTCACAAAAGTTGTTGAAGGTGATTTATCTGTATTTATGCCAAATGCA  
AGAATTAAGGTGAGTCACAAAATGCGAGCGATATACATCATTTTCTTG  
AATCAGTGGTTGAGGGCATCGATATACCACAGCCTGA--  
TCCTGATATTATCGCTGGAGGGAGTGTT-  
GGTCATAAGTACAACTTAAGCAACATATTGGTGCAAGTACAAAAGTTA  
ACATCCATGCTAGCGAGGTGATTGCAGGAAGTCGTAAATATGCTCGTAC  
GGTATATAGACAGTACGTGCAAATGAGTGGTCTTTTTTCGGGCATGTATG  
ATGATCACGTTGCTGGTATATTGTTGTACAGCGTATCAACGTTGAAGCAC  
TGTGATGTTTATGTGGCTATGGCCTATGGCATTGCAGCAGTCAGAGACTT  
AACACAAAGTGTGATCGCGGACTTAAGTGATGTACTCAAGCTGCGTGCA  
CTAGCAGCTTGGTGTCCCAATTATGTTGAGCTAAAGTGCCTACGTGGTCC  
AGGCATTGCTGAGCTTGATGTTATTGCTGAAGCAAAGCAGCGCCTAAAG  
AAACCAACACACCCATATGCTTATGCTGATAACGAAGAGCTACTACGTA  
ACGCTATTCGAAGAGTCTTTGATGAAGAGTTGCCAAGAGACAAAGTGGT  
GTTGAGGCCCAAAGATGACTTTTGGTTCGCTCGCTGGCTATGGGCGGCTA  
ATGGCGGTCATTCACGAGCACTAGAACATGCACACCCAGAAGTGCGAAC  
TCGAAAAGAAGTCCGAGCGTATCGTAAGTGTGTGCTCGAGCAGTGGCGG  
AATAACCCGATGGACGCGTGGGATGGTCAGGTATATGTTACACCCAGTC  
AGAAATTAGAGCATGGCAAGAGCAGACTCCTGCTGGCGTGTGACACTCT  
TTCTTACCTATGGTTTGGAGTATTACCTAAAGCCTGTTGAAACAGCGTGGT  
TGAATAAACGCACGCTGCTCAACCCCGGTGTTGTTAACCATTATTCAATG  
GCTAAGAAAGTTAAAGTGTATTGGCTGACGCAGAACACGATGAAACTA  
ATATTGAGCGCGGGACAAAGCTGTATAGCCTGGATTTTGAAGACTTCAA  
TTCACAGCACTCACTAGCTGCTCAGAAAATGGTGTGTTGAAGAGCTATTCA  
AACATGTTGGTATTGAAAACGAGGAAACACGAAAAGTAGTGAGCAGCTT  
CGAGCGAATGATAGTGTACAATGGGAAAGAGCCTCTAGGTGAGTACAT  
GGCACATTAATGAGCGGACACCGTGCTACAACCTTTTATTAACACCATATT  
AAACACTGCGTATCTATATGCTGCCGGGTTACACACCGTTTTTCTCATATC

ACGTTGGTGACGATGTCATATTCAGTACGGGCTGTGCTGAGGCTGCACGT  
TTGTATGATTGTCTAAAACATTATGGCGTGCGGTGTAACCCACATAAACA  
GTGTGCAAGTGAATATAGTGGTGAGTTCTTACGCGTTGCTCACACGAAAC  
ACTATAGTACTGGGTATGTCGCACGTGCTATTGCAAGCTGTGTCAGCGGT  
AATTGGGTGTCTGATCACGTCTTGGACCGACGAGAAGCATTGACAAATG  
CTATATCATGTGTCAGAACGATTATGAATCGTACACAATCTGATGAGGAC  
AATCCAATAGGTTCGTGTTGTAGCACTAAGCGTTGCGAAGCGATGTTGTGT  
CGAAGAAAAACACATACGCAAATTACTGTACGGTAAAGCTTGTGTTGGGC  
GAAGGCGTAATCTACGGGAAGCTGTGCAGCAGTGCAGGACGAAAGTTGATA  
TAAATGTCAATATGGATTATGACAAGACACGGACATTCAAATATGAAAT  
GTTTGCC

**ISG15 Coding sequence:**

5'-

ATGCTGGCGGGCAACGAATTC (position of mutation)  
CAGGTGTCCCTGAGCAGCTCCATGTTCGGTGTGTCAGAGCTGAAGGCGCAGA  
TCACCCAGAAGATCGGCGTGCACGCCTTCCAGCAGCGTCTGGCTGTCCAC  
CCGAGCGGTGTGGCGCTGCAGGACAGGGTCCCCCTTGCCAGCCAGGGCC  
TGGGCCCCGGCAGCACGGTCCCTGCTGGTGGTGGACAAATGCGACGAACC  
TCTGAGCATCCTGGTGAAGAATAACAAGGGCCGCAGCAGCACCTACGAG  
GTACGGCTGACGCAGACCGTGGCCACCTGAAGCAGCAAGTGAGCGGGC  
TGGAGGGTGTGCAGGACGACCTGTTCTGGCTGACCTTCGAGGGGAAGCC  
CCTGGAGGACCAGCTCCCGCTGGGGGAGTACGGCCTCAAGCCCCTGAGC  
ACCGTGTTTCATGAATCTGCGCCTGCGGGGAGGCGGCACAGAGCCTGGCG  
GGCGGAGCTAA-3'

**ISG15 aa sequence:**

MGWDLTV(position of mutation)  
KMLAGNEFQVSLSSMSVSELKAQITQKIGVHAFQQRLAVHPSGVALQDRV  
PLASQGLGPGSTVLLVVDKCDPLSILVRNNKGRSSTYEVRLTQVAHLKQQ  
VSGLEGVQDDLFWLTFEGKPLEDQLPLGEYGLKPLSTVFMNLRRLRGGGTEP  
GGRS

Seeding media: DMEM + 10%FBS without Pen/Strep

Harvest media: DMEMD + 30% FBS + 1X Pen/Strep

### C. Western blot buffers

#### **Lysis Buffer (180 $\mu$ L):**

18  $\mu$ l from 10xRipa buffer or M-PER

26  $\mu$ l from 10x stock solution of Roche complete mini EDTA free tablet solution

18  $\mu$ l from 10x stock solution of Roche PhosSTOP

118  $\mu$ l from MBG H<sub>2</sub>O

#### **Running Buffer(10X)**

30 g Tris base

144 g Glycine

10 g SDS

in 1L of filtered dH<sub>2</sub>O

#### **6X Laemmli Sample Loading Buffer (for non-reducing and reducing):**

1.2gr SDS (sodium dodecyl sulfate)

6mg bromophenol blue

4.7ml glycerol

1.2ml Tris 0.5M pH6.8

2.1ml dH<sub>2</sub>O

Completely dissolved.

2.5% v/v 2-Mercaptoethanol was added only for reducing SDS-PAGE.

**Transfer Buffer(1x):**

700 ml dH<sub>2</sub>O  
200ml absolute Methanol  
100 ml 10X Blotting Buffer

**Blotting Buffer(10x):**

30 g Tris  
144 g Glycine

pH is adjusted to 8.3 in 1 L dH<sub>2</sub>O. Stored at room temperature.

**TBST (1x, 1 L):**

100 ml of TBST(10x)

pH is adjusted to 7.4, then complete the volume with dH<sub>2</sub>O 1 L and add 0.1%

Tween 20

**Blocking Buffer (1x, 50 ml)**

2.5 g Skimmed Milk (5% w/v) with 50 ml TBST

**Wash Buffer**

1x TBST

**Mild Stripping Buffer(1L)**

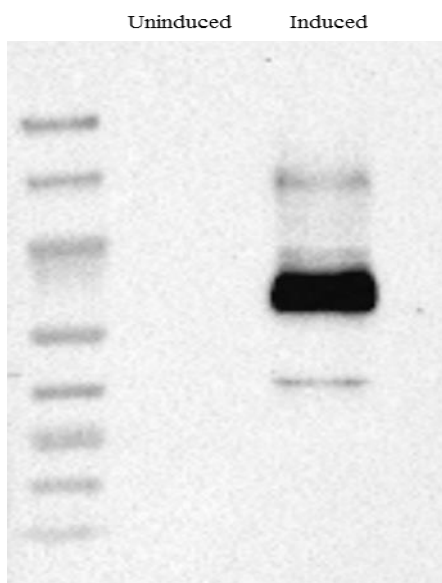
Glycine 15 g

SDS 1g

Tween20 10 ml

pH was adjusted to 2.2, then completed with dH<sub>2</sub>O to 1L.

**D. Western Blot images**



**RDRP expression, blotted with Anti-His6 antibody:**

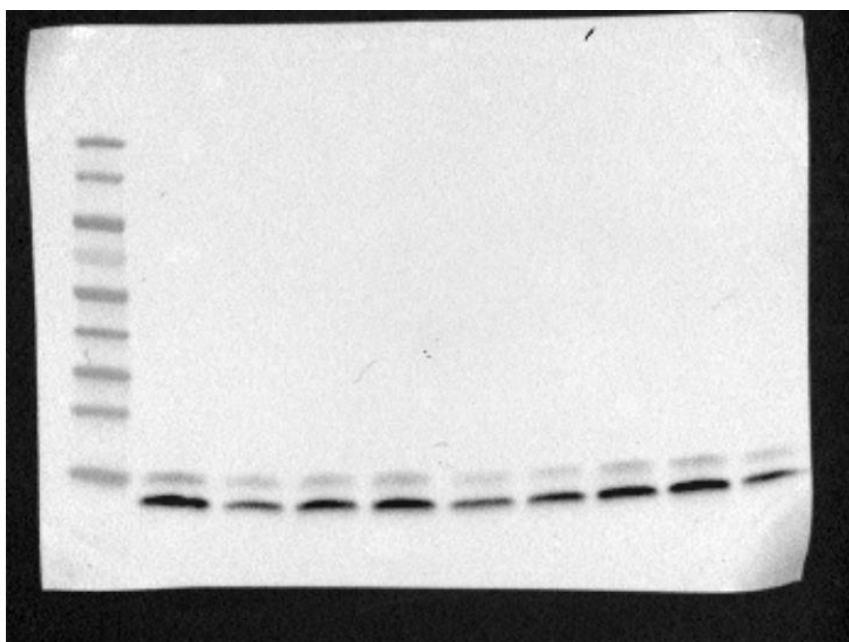


**Figure 3.29- LC3-II Blot**

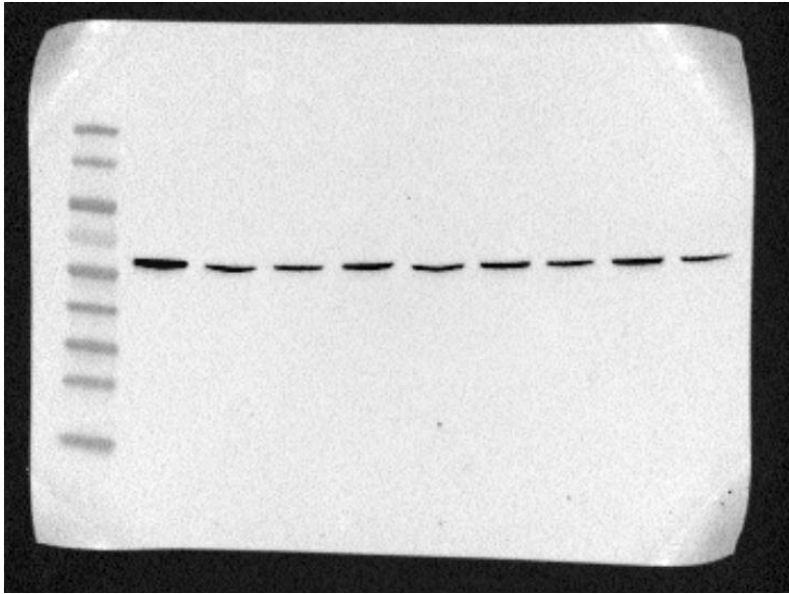


**Figure 3.29 p62 blot**

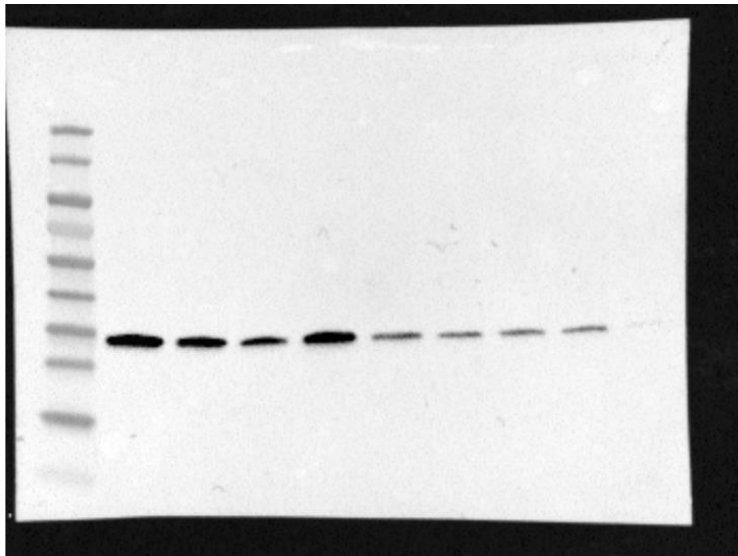


**Figure 3.29 pS6(Ser 240/244) Blot**

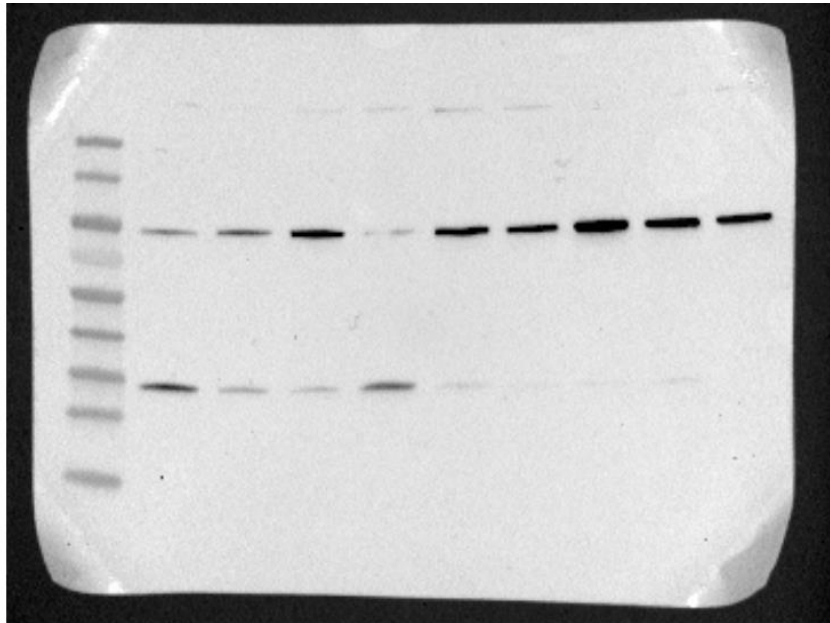


**Figure 3.29 pTBK-1 Blot**

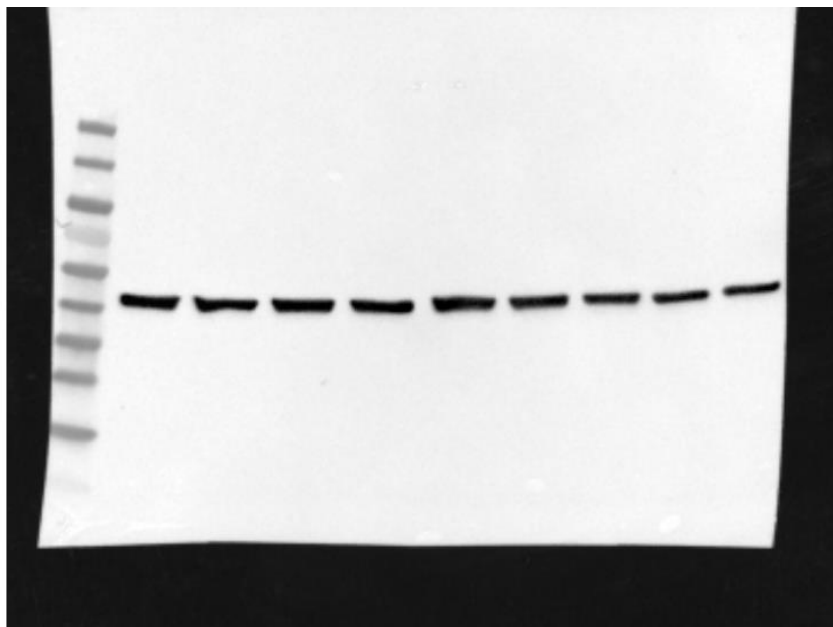


**Figure 3.29  $\beta$ -actin**

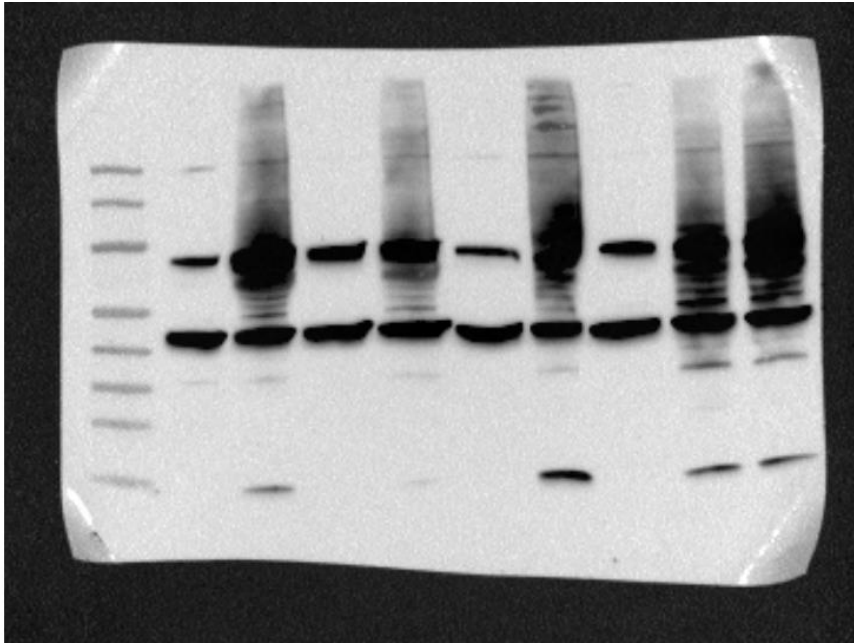


**Figure 3.30 ISG15 Blot 1-hour infection**

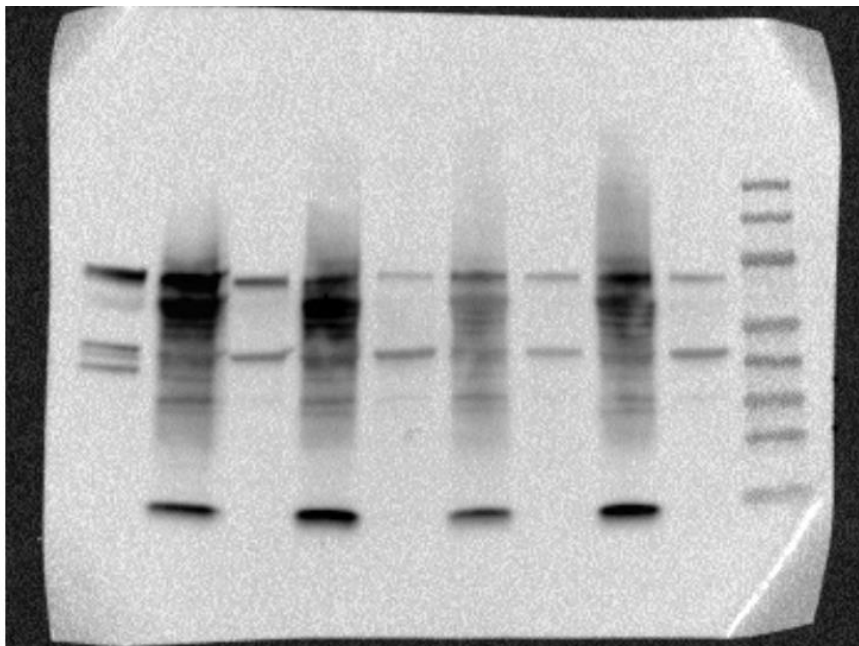


**Figure 3.30 ISG15 Blot 6 hours of infection**

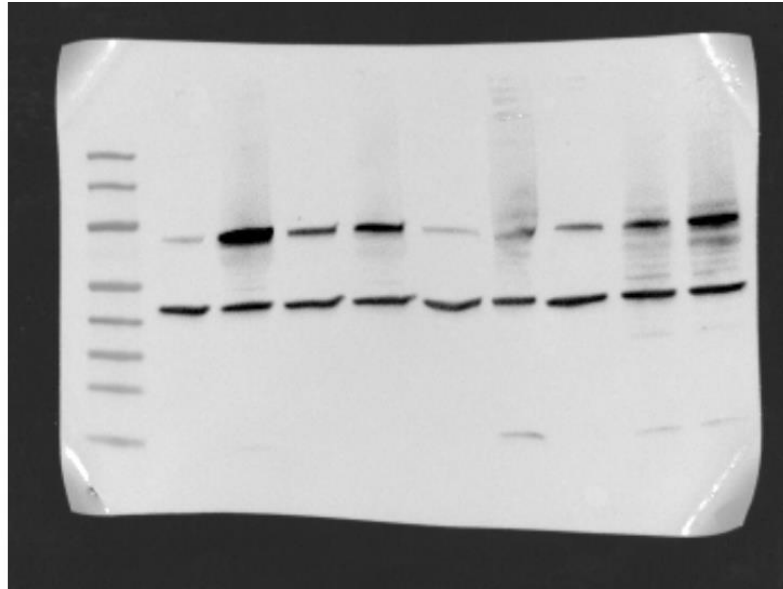


**Figure 3.30  $\beta$ -actin Blot 1 hours of infection**

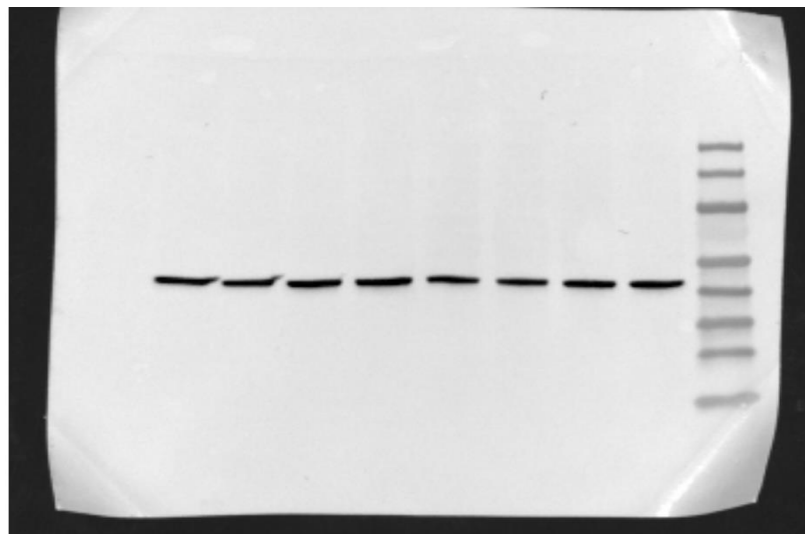


**Figure 3.30  $\beta$ -actin Blot 6 hours of infection**

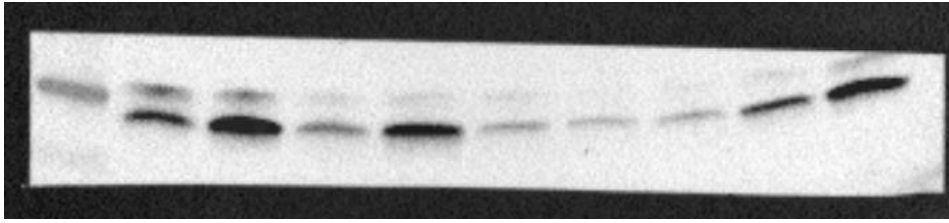


**Figure 3.31 LC3-II Blot**

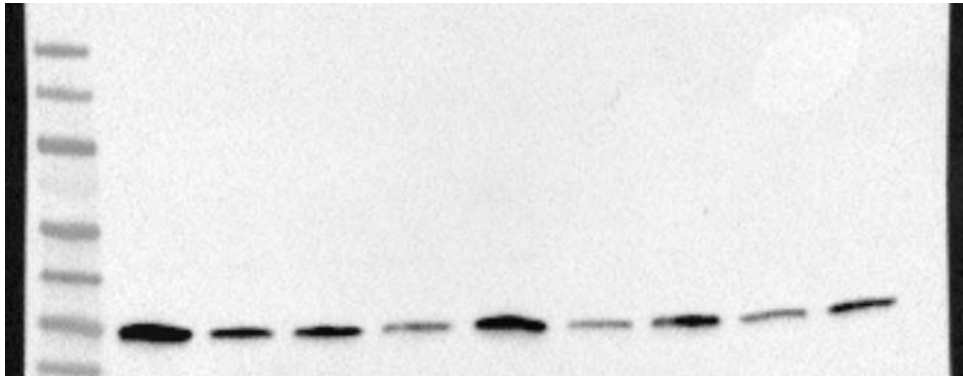


**Figure 3.31 pS6 (Ser 240/244) Blot**



**Figure 3.31 p62 Blot**

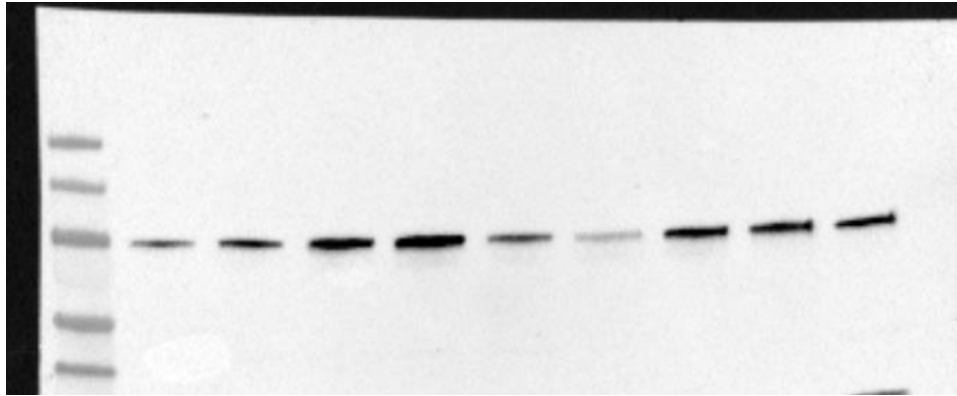


**Figure 3.31 pTBK1 Blot**

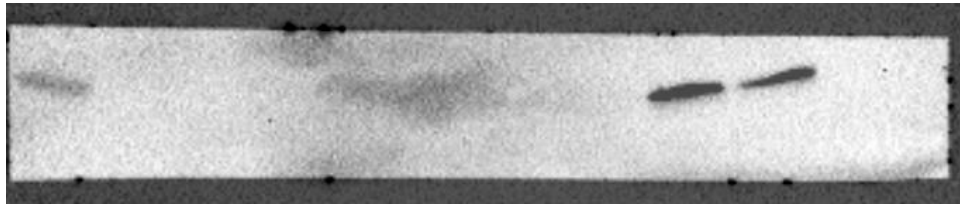


**Figure 3.31 ISG15 Blot**

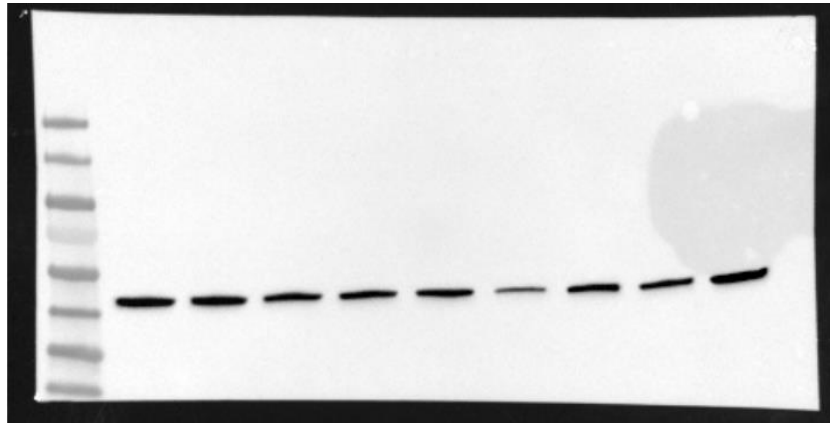


**Figure 3.31  $\beta$ -actin Blot**

### Primary Antibody list

<b>Name</b>	<b>Company</b>	<b>Cat no:</b>
ISG15 (F-9) mouse monoclonal IgG	Santa Cruz Biotechnology	sc-166755
LC3A/B (D3U4C) XP® Rabbit mAb	Cell Signaling Technology	12741S
SQSTM1 Antibody (D-3)	Santa Cruz Biotechnology	sc-28359
pTBK1/NAK rabbit mAb	Cell Signaling Technology	5483T
Phospho-S6 Ribosomal Protein (Ser240/244)	Cell Signaling Technology	2215S
β-Actin (13E5) Rabbit mAb	Cell Signaling Technology	4970S

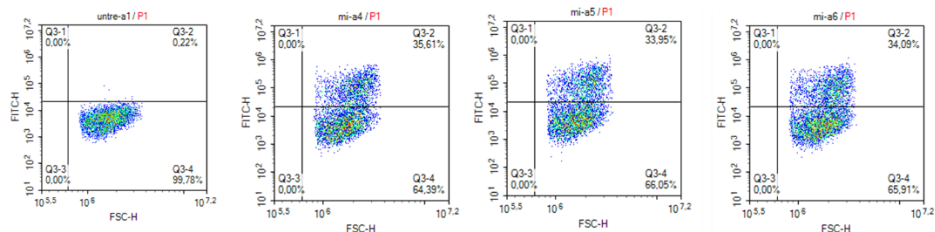
## E. MS full protein list

Family	Database	Accession	Score	Mass	Num.	Num.	Num.	Num.	Num.	Num.	Num.	Num.	Num.	Num.	Num.	Num.	Num.	Num.	Num.	Num.	Description
12	LMAJOR	E9ADW5	52	41109	1	1	1	1	1	0.08	Putative ribosomal prote in L1a OS=Leishmania major OX=5664 GN=LMJF_29_1070 PE=4 SV=1										
18	LMAJOR	P22045	24	32001	1	1	1	1	1	0.1	9,11-endoperoxide prostaglandin H2 reductase OS=Leishmania major OX=5664 GN=P100/11E PE=1 SV=3										
25	LMAJOR	Q4Q259	17	94928	1	1	1	1	1	0.03	Elongation factor 2 OS=Leishmania major OX=5664 GN=EF2-2 PE=4 SV=1										
14	LMAJOR	Q4Q277	37	11603	2	2	2	1	1	0.28	Histone H4 OS=Leishmania major OX=5664 GN=L7845_05 PE=3 SV=1										
20	LMAJOR	Q4Q2J8	23	54423	2	1	1	1	1	0.06	Uncharacterized prote in OS=Leishmania major OX=5664 GN=LMJF_34_3460 PE=4 SV=1										
15	LMAJOR	Q4Q3H7	29	78199	4	4	4	1	1	0.04	Uncharacterized prote in OS=Leishmania major OX=5664 GN=LMJF_34_0310 PE=4 SV=1										
24	LMAJOR	Q4Q3T3	17	57470	1	1	1	1	1	0.05	Metallo-peptidase, Clan MA(E), Family M32 OS=Leishmania major OX=5664 GN=LMJF_33_2540 PE=4 SV=1										
21	LMAJOR	Q4Q3V1	19	101902	2	2	2	1	1	0.03	Uncharacterized prote in OS=Leishmania major OX=5664 GN=LMJF_33_2360 PE=4 SV=1										
5	LMAJOR	Q4Q4C4	111	50335	5	5	5	5	5	0.35	Tubulin beta chain OS=Leishmania major OX=5664 GN=LMJF_33_0792 PE=3 SV=1										
7	LMAJOR	Q4Q4I0	91	80688	2	2	2	1	1	0.04	Heat shock protein 83-1 OS=Leishmania major OX=5664 GN=HSP83-8 PE=3 SV=1										
23	LMAJOR	Q4Q459	18	85882	1	1	1	1	1	0.04	Uncharacterized prote in OS=Leishmania major OX=5664 GN=LMJF_32_3430 PE=4 SV=1										
16	LMAJOR	Q4Q6L9	27	81042	1	1	1	1	1	0.04	Putative cytoskeleton-associated prote in CAPS 5 OS=Leishmania major OX=5664 GN=LMJF_31_0440 PE=3 SV=1										
22	LMAJOR	Q4Q6Z4	19	39397	1	1	1	1	1	0.08	Glyceraldehyde-3-phosphate dehydrogenase OS=Leishmania major OX=5664 GN=LMJF_30_2980 PE=3 SV=1										
19	LMAJOR	Q4Q7Y4	24	71893	1	1	1	1	1	0.04	Putative heat-shock prote in hsp70 OS=Leishmania major OX=5664 GN=LMJF_28_2770 PE=3 SV=1										
11	LMAJOR	Q4Q970	57	71001	2	2	2	1	1	0.04	Heat shock protein 70-related prote in OS=Leishmania major OX=5664 GN=HSP70_4 PE=3 SV=1										
2	LMAJOR	Q4Q861	267	16785	2	2	2	1	1	0.19	Uncharacterized prote in OS=Leishmania major OX=5664 GN=LMJF_23_1020 PE=4 SV=1										
8	LMAJOR	Q4QDU7	74	40471	5	5	5	1	1	0.08	Uncharacterized prote in OS=Leishmania major OX=5664 GN=LMJF_18_0950 PE=4 SV=1										
13	LMAJOR	Q4QEI8	39	49427	1	1	1	1	1	0.06	Elongation factor 1-alpha OS=Leishmania major OX=5664 GN=LMJF_17_0082 PE=2 SV=1										
10	LMAJOR	Q4QEX1	61	22582	1	1	1	1	1	0.14	Uncharacterized prote in OS=Leishmania major OX=5664 GN=LMJF_16_0490 PE=4 SV=1										
1	LMAJOR	Q4QF68	486	22385	13	13	6	6	6	1.2	Thiol specific antioxidant OS=Leishmania major OX=5664 GN=TRYP7 PE=2 SV=1										
6	LMAJOR	Q4QGC5	110	50526	4	4	3	3	3	0.2	Tubulin alpha chain OS=Leishmania major OX=5664 GN=LMJF_13_0280 PE=3 SV=1										
3	LMAJOR	Q4QH11	183	65069	6	6	3	3	3	0.15	GP63, leishmanolysin OS=Leishmania major OX=5664 GN=GP63-2 PE=4 SV=1										
17	LMAJOR	Q4QI85	25	22368	1	1	1	1	1	0.14	Amastin-like prote in OS=Leishmania major OX=5664 GN=LMJF_08_0800 PE=4 SV=1										
4	LMAJOR	Q5SDH5	180	15150	5	5	2	2	2	0.47	Putative calpain-like cysteine peptidase OS=Leishmania major OX=5664 GN=SMP-1 PE=1 SV=1										
9	LMAJOR	Q9U1E1	69	16801	1	1	1	1	1	0.19	Nucleoside diphosphate kinase OS=Leishmania major OX=5664 GN=L1648_07 PE=1 SV=1										

Family	Database	Accession	Score	Mass	Num.	Num.	Num.	Num.	Num.	Num.	Num.	Num.	Num.	Num.	Num.	Num.	Num.	Num.	Num.	Description
1	LMAJOR	E9ADP0	38	38204	2	1	2	1	0.08	Uncharacterized prote in OS=Leishmania major OX=5664 GN=LMJF_27_1730 PE=4 SV=1										
2	LMAJOR	E9ADN6	21	151883	1	1	1	1	0.02	Uncharacterized prote in OS=Leishmania major OX=5664 GN=LMJF_29_0350 PE=4 SV=1										
3	LMAJOR	E9ADW5	92	41109	2	2	1	1	0.08	Putative ribosomal prote in L1a OS=Leishmania major OX=5664 GN=LMJF_29_1070 PE=4 SV=1										
4	LMAJOR	E9ADX4	60	16647	3	2	3	2	0.42	Tryptaredoxin OS=Leishmania major OX=5664 GN=TXN1 PE=1 SV=1										
5	LMAJOR	P22045	38	32001	1	1	1	1	0.1	9,11-endoperoxide prostaglandin H2 reductase OS=Leishmania major OX=5664 GN=P100/11E PE=1 SV=3										
6	LMAJOR	Q4Q259	58	94928	1	1	1	1	0.03	Elongation factor 2 OS=Leishmania major OX=5664 GN=EF2-2 PE=4 SV=1										
7	LMAJOR	Q4Q2J8	18	54423	3	1	1	1	0.06	Uncharacterized prote in OS=Leishmania major OX=5664 GN=LMJF_34_3460 PE=4 SV=1										
8	LMAJOR	Q4Q3H7	17	78199	1	1	1	1	0.04	Uncharacterized prote in OS=Leishmania major OX=5664 GN=LMJF_34_0310 PE=4 SV=1										
9	LMAJOR	Q4Q3P6	16	290836	1	1	1	1	0.01	Uncharacterized prote in OS=Leishmania major OX=5664 GN=LMJF_33_2890 PE=3 SV=1										
10	LMAJOR	Q4Q4C4	283	50335	10	7	8	7	0.52	Tubulin beta chain OS=Leishmania major OX=5664 GN=LMJF_33_0792 PE=3 SV=1										
11	LMAJOR	Q4Q4I0	139	80688	5	4	3	3	0.12	Heat shock protein 83-1 OS=Leishmania major OX=5664 GN=HSP83-8 PE=3 SV=1										
12	LMAJOR	Q4Q4Y1	19	57468	1	1	1	1	0.05	Tubulin-tyrosine ligase-like prote in OS=Leishmania major OX=5664 GN=LMJF_32_2930 PE=4 SV=1										
13	LMAJOR	Q4Q5I5	16	69159	1	1	1	1	0.04	Uncharacterized prote in OS=Leishmania major OX=5664 GN=LMJF_32_2600 PE=4 SV=1										
14	LMAJOR	Q4Q5F4	22	70944	1	1	1	1	0.04	Uncharacterized prote in OS=Leishmania major OX=5664 GN=LMJF_32_1180 PE=4 SV=1										
15	LMAJOR	Q4Q5N4	49	22380	1	1	1	1	0.14	Putative ras-related rab-4 OS=Leishmania major OX=5664 GN=LMJF_32_0490 PE=4 SV=1										
16	LMAJOR	Q4Q6L9	55	81042	2	2	2	2	0.08	Putative cytoskeleton-associated prote in CAPS 5 OS=Leishmania major OX=5664 GN=LMJF_31_0440 PE=3 SV=1										
17	LMAJOR	Q4Q6R3	104	86627	4	3	4	3	0.11	S-methyltetrahydropteroyltrimethylglutamate-homocystein e S-methyltransferase OS=Leishmania major OX=5664 GN=LMJF_31_00										
18	LMAJOR	Q4Q6Z4	18	39397	1	1	1	1	0.08	Glyceraldehyde-3-phosphate dehydrogenase OS=Leishmania major OX=5664 GN=LMJF_30_2980 PE=3 SV=1										
19	LMAJOR	Q4Q7Y4	151	71893	8	7	4	4	0.18	Putative heat-shock prote in hsp70 OS=Leishmania major OX=5664 GN=LMJF_28_2770 PE=3 SV=1										
20	LMAJOR	Q4Q8Z6	23	90104	1	1	1	1	0.03	Uncharacterized prote in OS=Leishmania major OX=5664 GN=LMJF_26_1960 PE=4 SV=1										
21	LMAJOR	Q4Q970	135	71001	2	2	2	1	0.04	Heat shock protein 70-related prote in OS=Leishmania major OX=5664 GN=HSP70_4 PE=3 SV=1										
22	LMAJOR	Q4Q9H4	20	28940	1	1	1	1	0.11	Putative 60S ribosomal prote in L7 OS=Leishmania major OX=5664 GN=LMJF_26_0170 PE=4 SV=1										
23	LMAJOR	Q4QAI0	40	19578	1	1	1	1	0.16	Putative IgE-dependent histamine-releasing factor OS=Leishmania major OX=5664 GN=LMJF_24_1500 PE=3 SV=1										
24	LMAJOR	Q4QAV5	21	357708	2	2	1	1	0.01	Uncharacterized prote in OS=Leishmania major OX=5664 GN=LMJF_24_0260 PE=4 SV=1										
25	LMAJOR	Q4Q861	89	16785	2	2	1	1	0.19	Uncharacterized prote in OS=Leishmania major OX=5664 GN=LMJF_23_1020 PE=4 SV=1										
26	LMAJOR	Q4QDN7	22	107977	1	1	1	1	0.03	Plasma membrane ATPase OS=Leishmania major OX=5664 GN=H1A-2 PE=3 SV=1										
27	LMAJOR	Q4QDQ2	45	92715	1	1	1	1	0.03	Putative heat shock prote in OS=Leishmania major OX=5664 GN=LMJF_18_1370 PE=3 SV=1										
28	LMAJOR	Q4QDU7	55	40471	5	5	1	1	0.08	Uncharacterized prote in OS=Leishmania major OX=5664 GN=LMJF_18_0950 PE=4 SV=1										
29	LMAJOR	Q4QEK1	51	22582	1	1	1	1	0.14	Uncharacterized prote in OS=Leishmania major OX=5664 GN=LMJF_16_0900 PE=4 SV=1										
30	LMAJOR	Q4QEX3	21	20846	1	1	1	1	0.15	Uncharacterized prote in OS=Leishmania major OX=5664 GN=LMJF_16_0470 PE=4 SV=1										
31	LMAJOR	Q4QF68	505	22385	12	12	6	6	1.2	Thiol specific antioxidant OS=Leishmania major OX=5664 GN=TRYP7 PE=2 SV=1										
32	LMAJOR	Q4QFL8	22	46689	2	2	2	2	0.14	Enolase OS=Leishmania major OX=5664 GN=ENOL PE=3 SV=1										
33	LMAJOR	Q4QG33	30	55252	1	1	1	1	0.06	Nucleobase transporter OS=Leishmania major OX=5664 GN=NT3 PE=4 SV=1										
34	LMAJOR	Q4QGC5	158	50526	7	7	4	4	0.27	Tubulin alpha chain OS=Leishmania major OX=5664 GN=LMJF_13_0280 PE=3 SV=1										
35	LMAJOR	Q4QH70	55	53850	1	1	1	1	0.06	Putative seryl-tRNA synthetase OS=Leishmania major OX=5664 GN=LMJF_11_0100 PE=4 SV=1										
36	LMAJOR	Q4QH11	259	65069	9	8	5	4	0.2	GP63, leishmanolysin OS=Leishmania major OX=5664 GN=GP63-2 PE=4 SV=1										
37	LMAJOR	Q4QHT2	48	16814	1	1	1	1	0.19	Putative calmodulin OS=Leishmania major OX=5664 GN=LMJF_09_0910 PE=4 SV=1										
38	LMAJOR	Q4QI79	22	108293	2	2	1	1	0.03	AP-2 complex subunit alpha OS=Leishmania major OX=5664 GN=LMJF_07_0050 PE=3 SV=1										
39	LMAJOR	Q4QJ26	30	197627	6	4	1	1	0.02	Uncharacterized prote in OS=Leishmania major OX=5664 GN=LMJF_06_0520 PE=4 SV=1										
40	LMAJOR	Q4QJ68	59	66936	5	4	1	1	0.05	Uncharacterized prote in OS=Leishmania major OX=5664 GN=LMJF_06_0110 PE=4 SV=1										
41	LMAJOR	Q5SDH5	143	15150	5	4	3	2	0.47	Putative calpain-like cysteine peptidase OS=Leishmania major OX=5664 GN=SMP-1 PE=1 SV=1										
42	LMAJOR	Q66ND0	18	46548	1	1	1	1	0.07	Elongation factor 1B gamma OS=Leishmania major OX=5664 GN=EF1G PE=4 SV=1										
43	LMAJOR	Q9U1E1	125	16801	2	2	1	1	0.19	Nucleoside diphosphate kinase OS=Leishmania major OX=5664 GN=L1648_07 PE=1 SV=1										

## F. Representative *in vitro* infection raw data

THP-1 WT 24 hours



THP-1 WT 48 hours

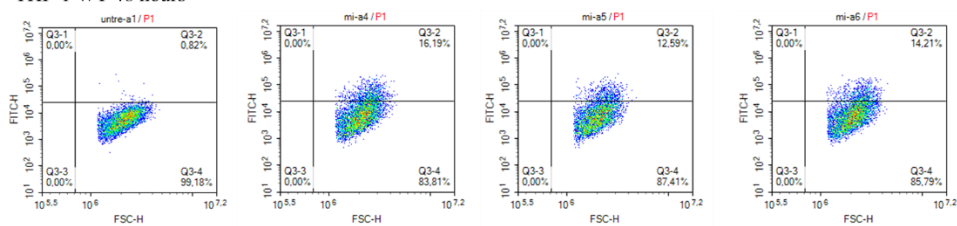
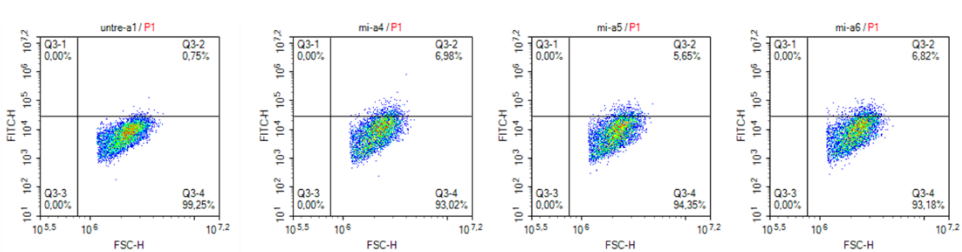


Figure 3.17 representative raw data of three biological replica

THP-1 WT 72 hours



THP-1 cGAS KO 24 hours

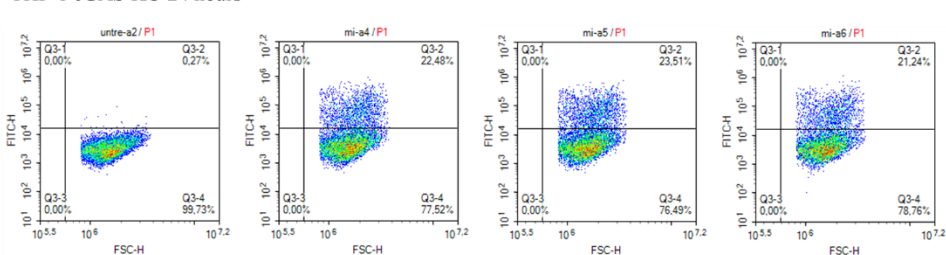
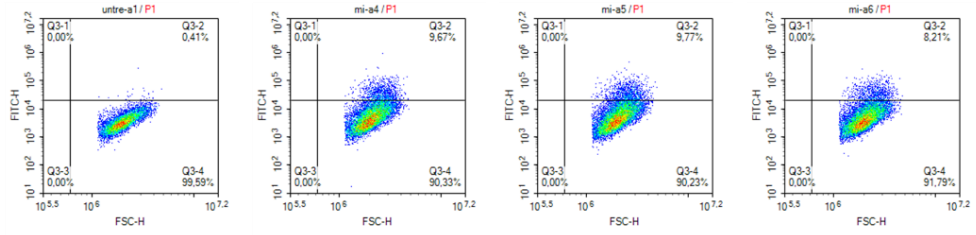


Figure 3.17 representative raw data of three biological replica

THP-1 cGAS KO 48 hours



THP-1 cGAS KO 72 hours

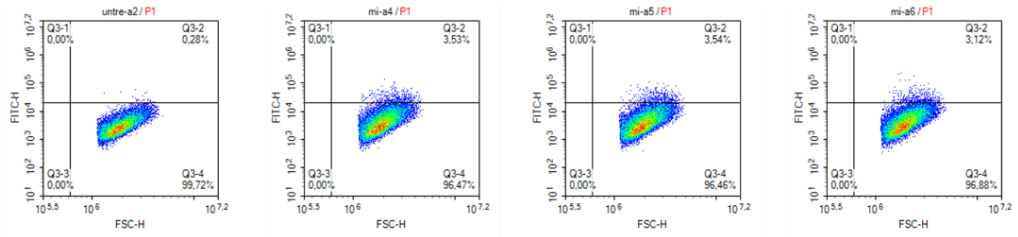
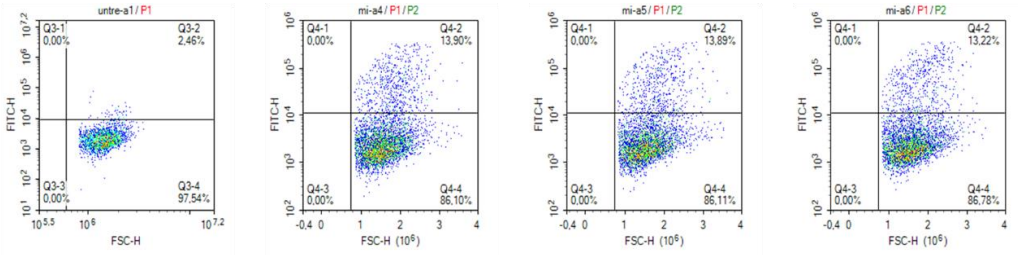


Figure 3.17 representative raw data of three biological replica

THP-1 STING KO 24 hours



THP-1 STING KO 48 hours

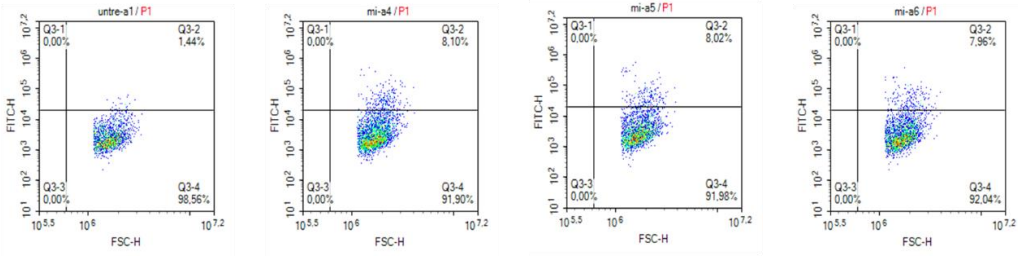


Figure 3.17 representative raw data of three biological replica

THP-1 STING KO 72 hours

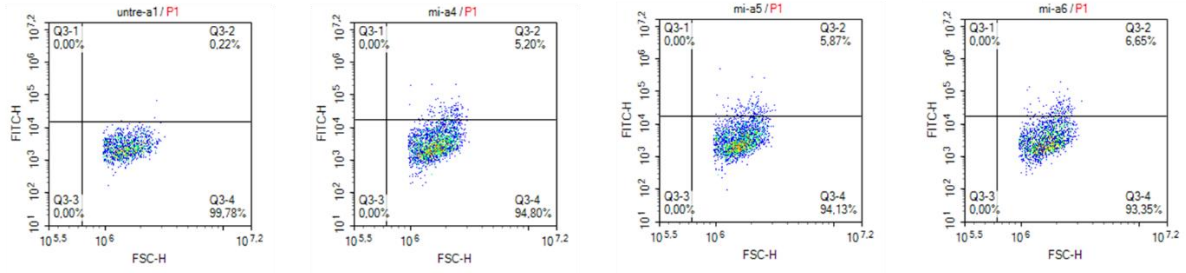
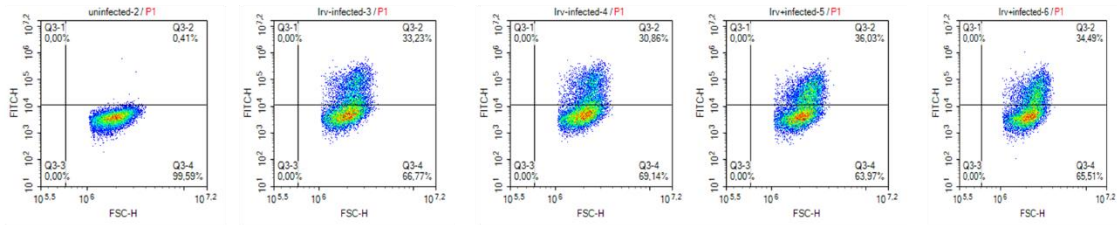
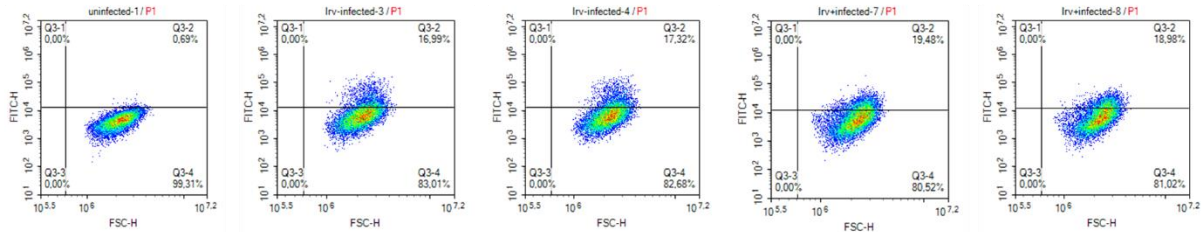


Figure 3.17 representative raw data of three biological replica

THP-1 WT 18 hours



THP-1 WT 42 hours



THP-1 WT 66 hours

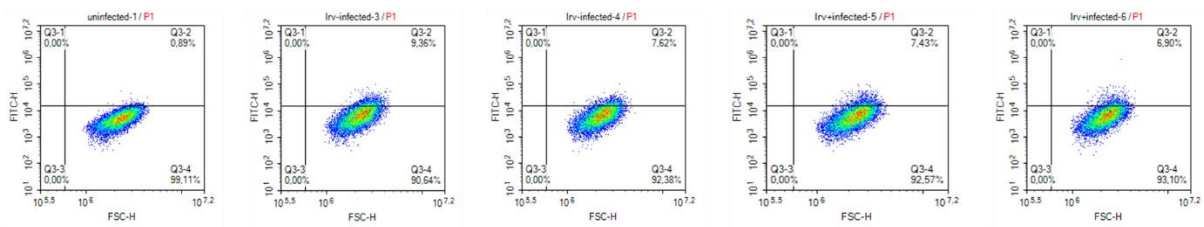
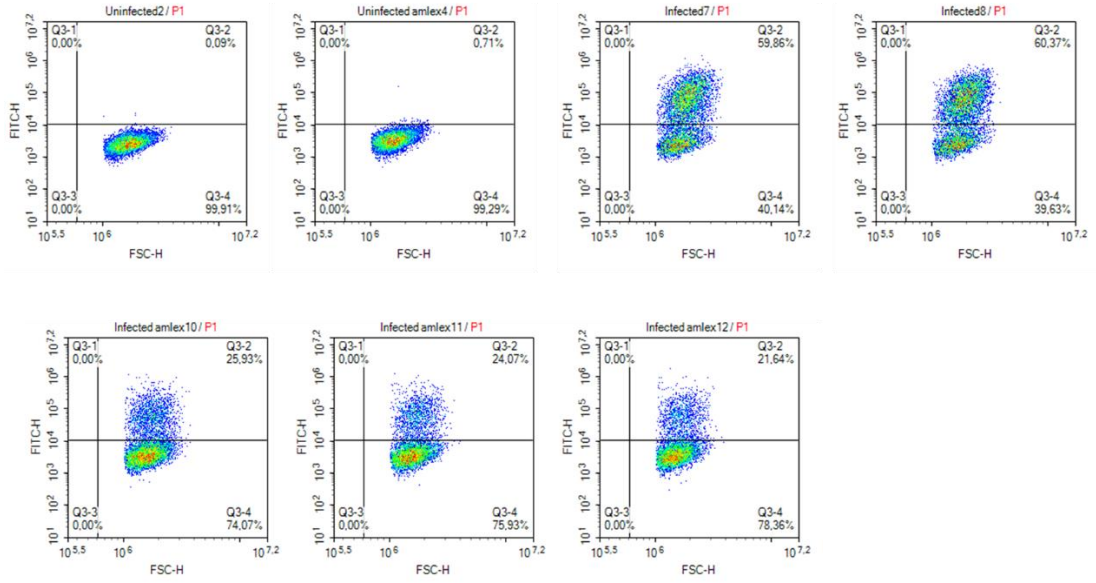


Figure 3.19 representative raw data of two biological replica

THP-1 WT 24 Hours



THP-1 TBK-1 KO 24 Hours

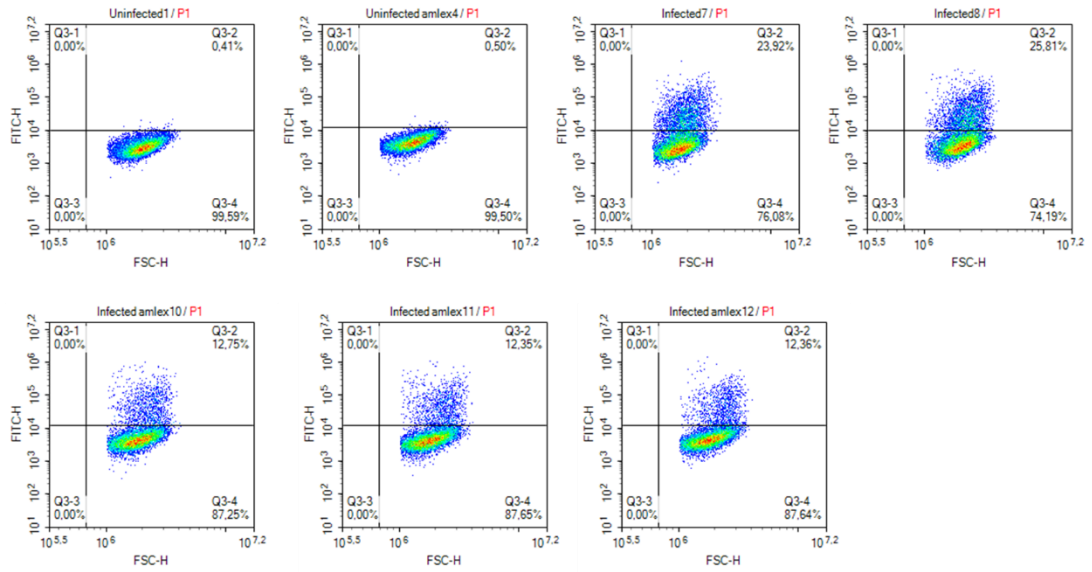
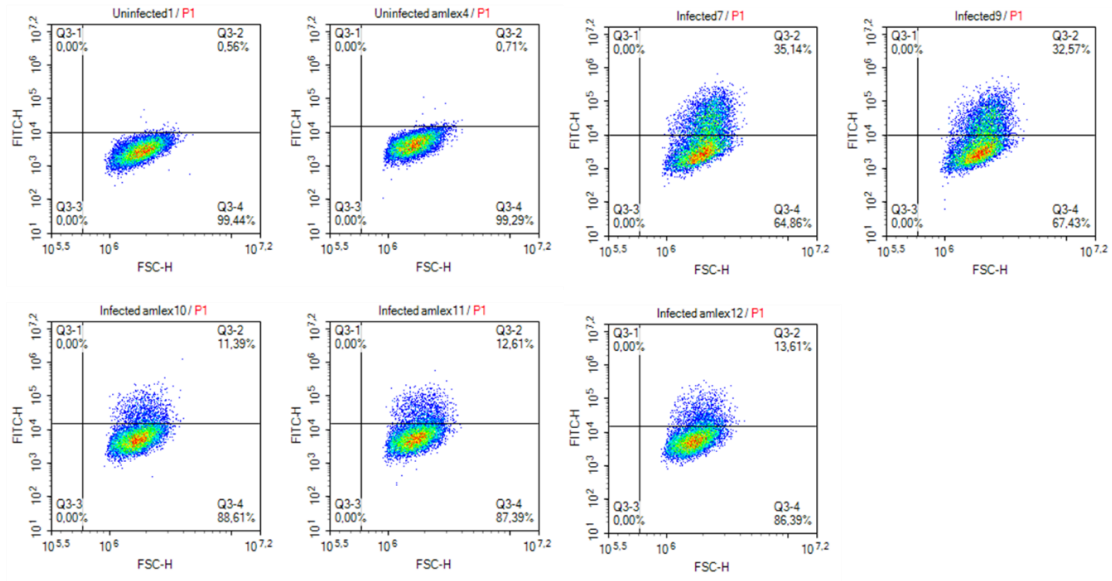


Figure 3.21 representative raw data of two biological replica

THP-1 WT 48 Hours



THP-1 TBK-1 KO 48 Hours

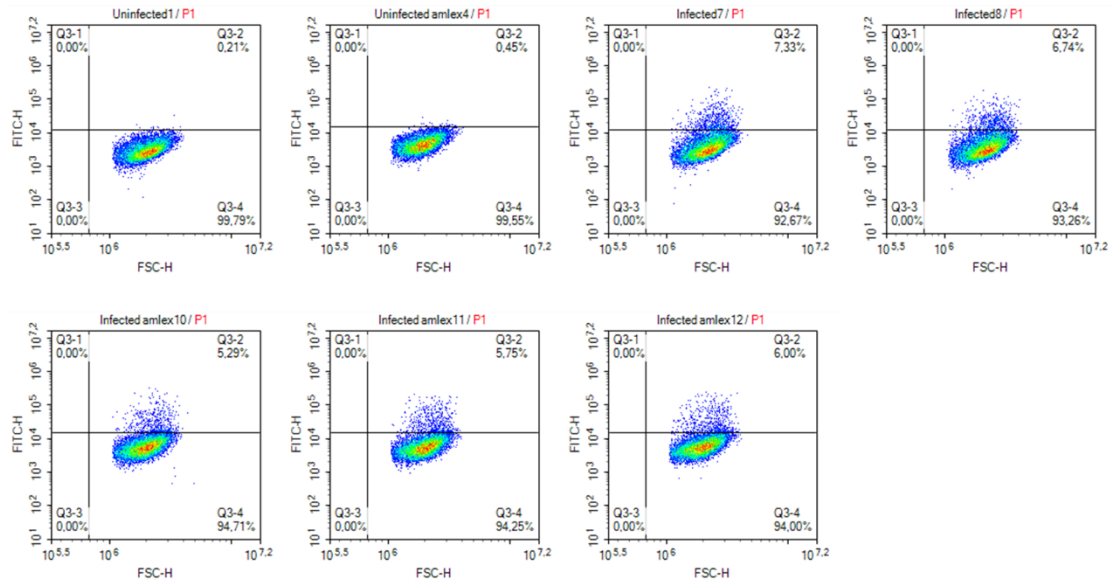
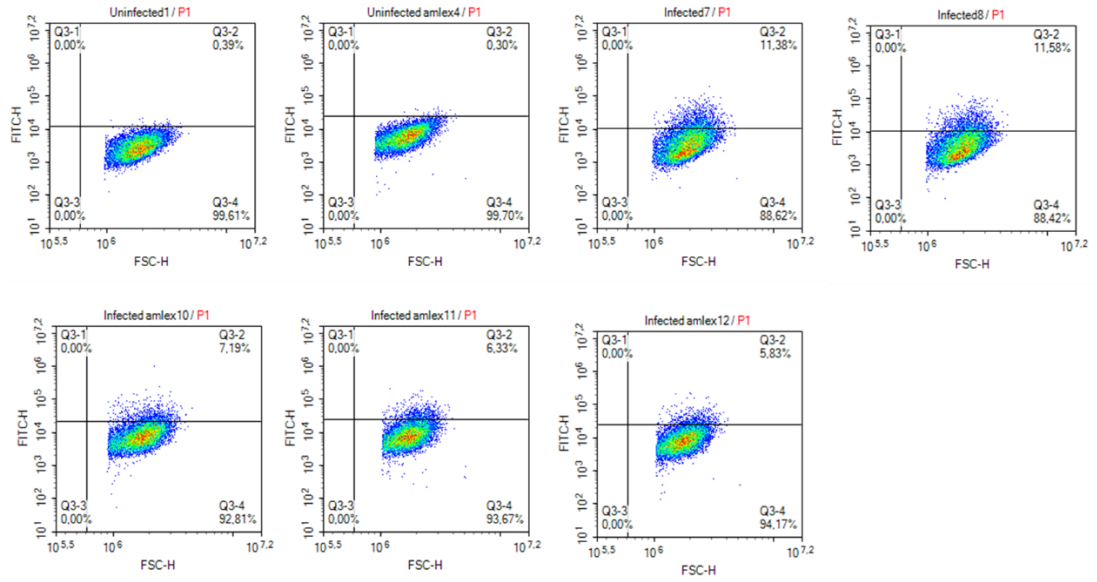


Figure 3.21 representative raw data of two biological replica

THP-1 WT 72 Hours



THP-1 TBK-1 KO 72 Hours

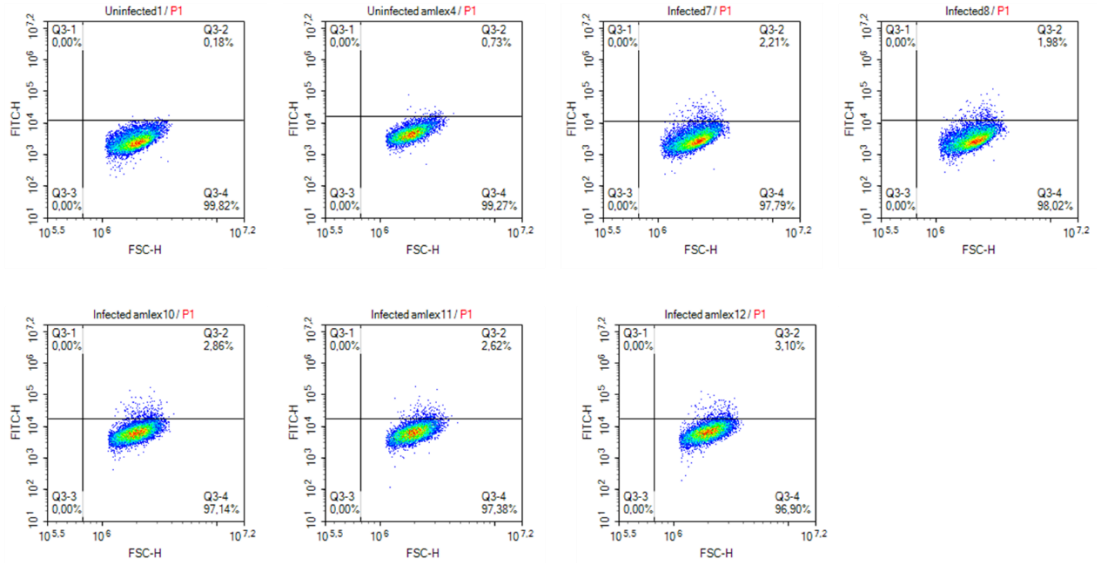


Figure 3.21 representative raw data of two biological replica

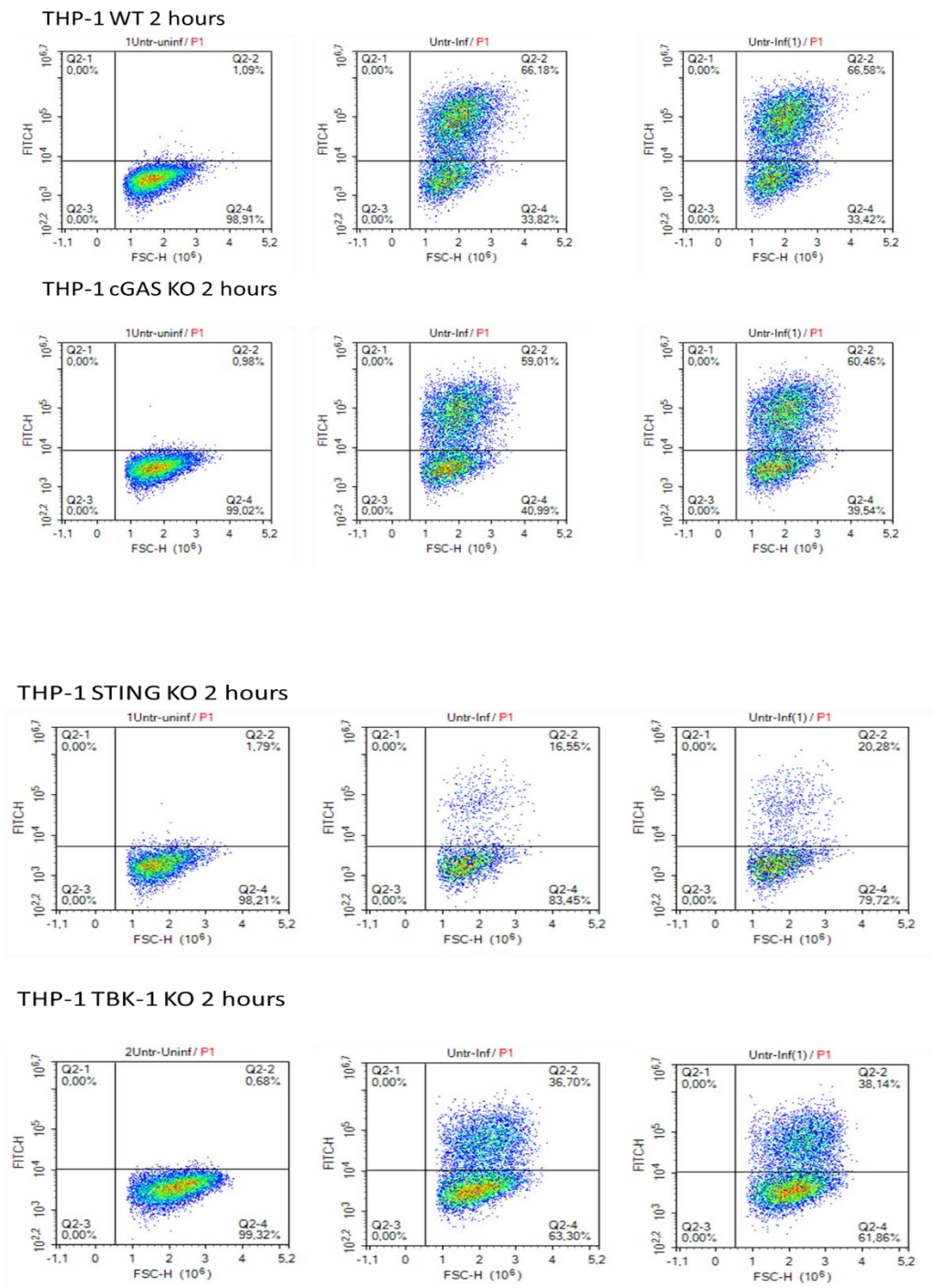
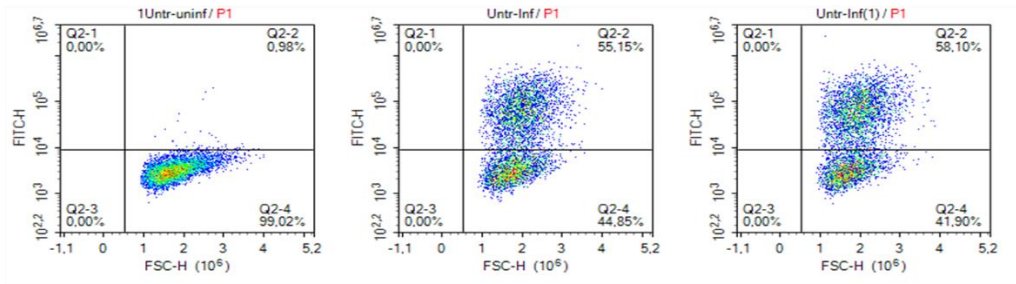
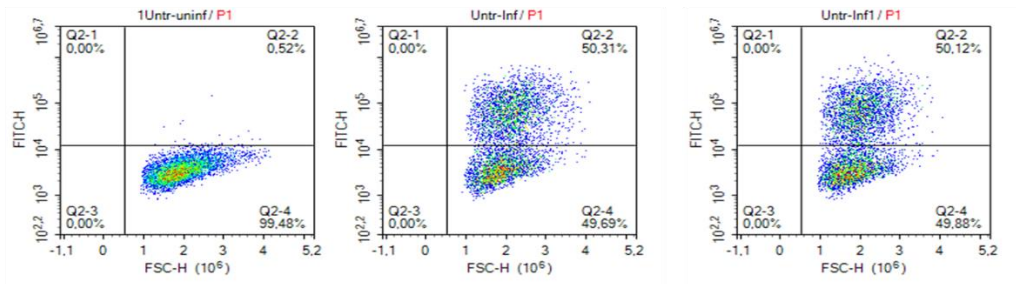


Figure 3.22 raw data

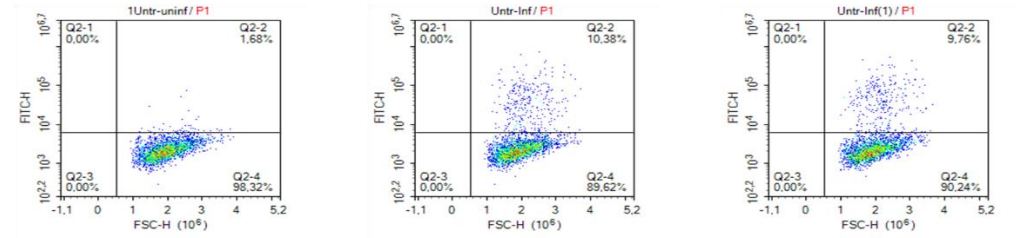
THP-1 WT 6 hours



THP-1 cGAS KO 6 hours



THP-1 STING KO 6 hours



THP-1 TBK-1 KO 6 hours

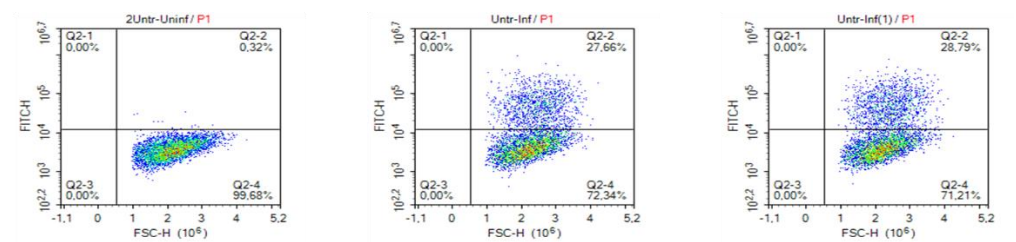
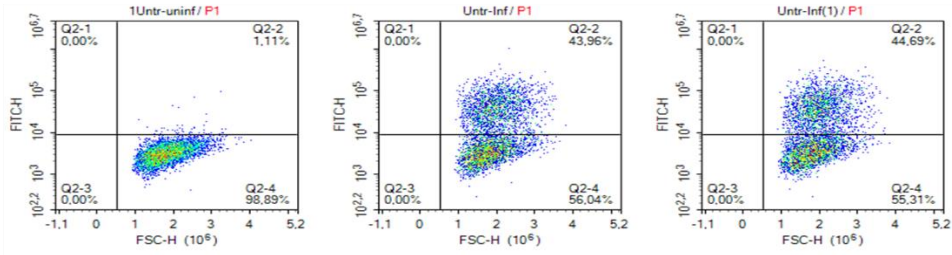
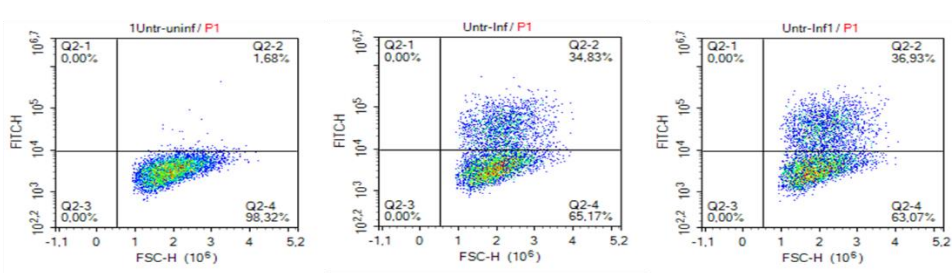


Figure 3.22 raw data

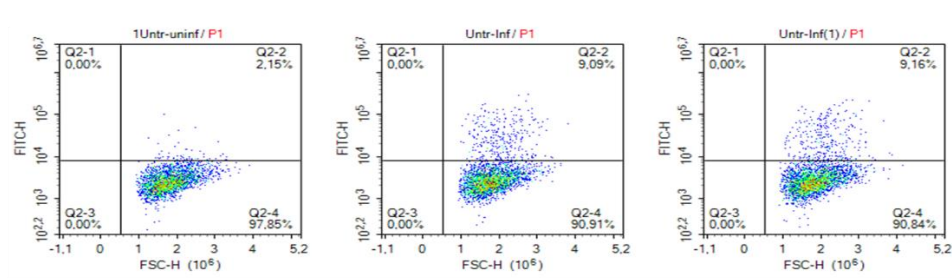
THP-1 WT 24 hours



THP-1 cGAS KO 24 hours



THP-1 STING KO 24 hours



THP-1 TBK-1 KO 24 hours

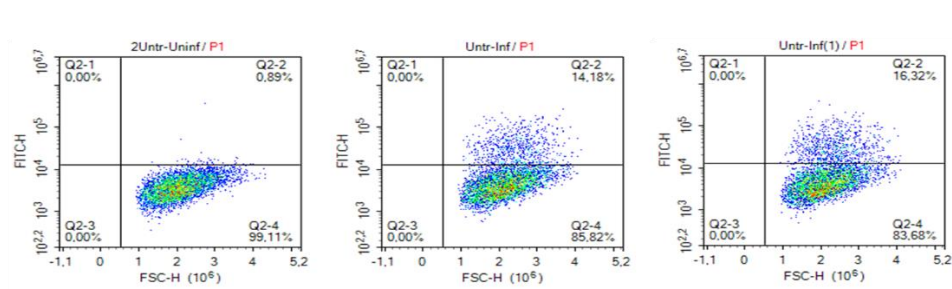
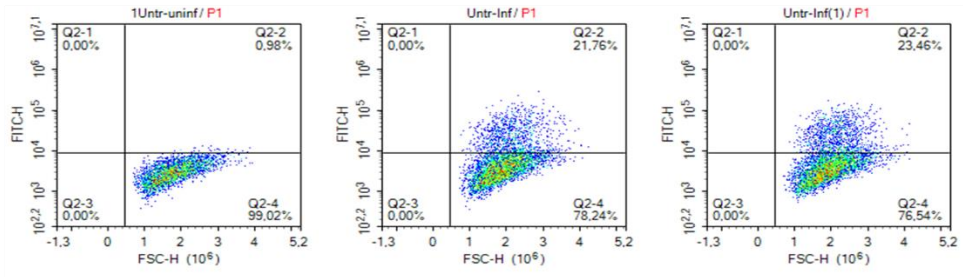
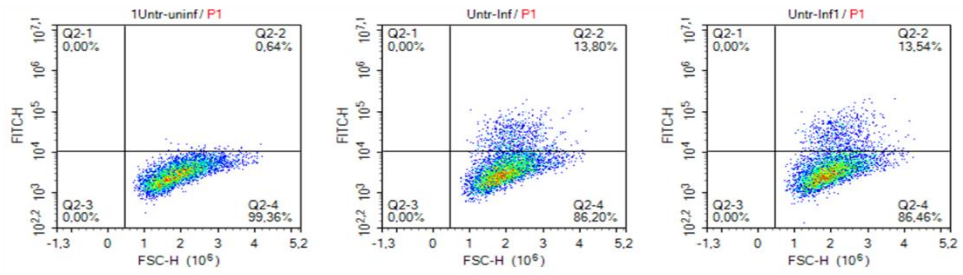


Figure 3.22 raw data

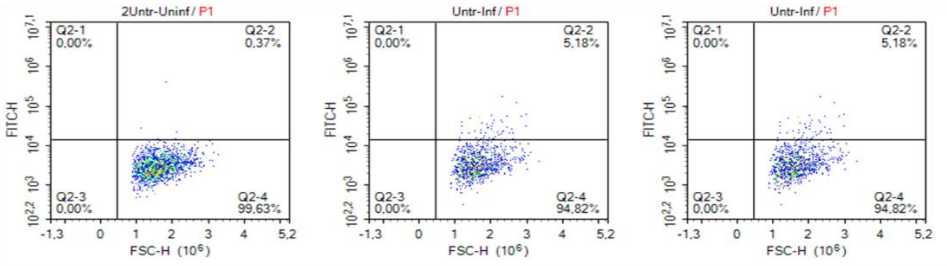
THP-1 WT 48 hours



THP-1 cGAS KO 48 hours



THP-1 STING KO 48 hours



THP-1 TBK-1 KO 48 hours

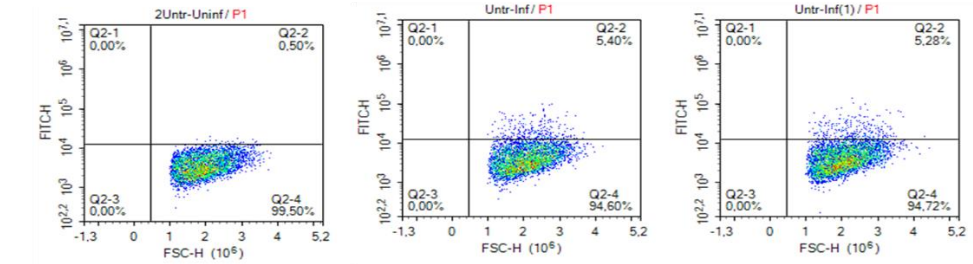
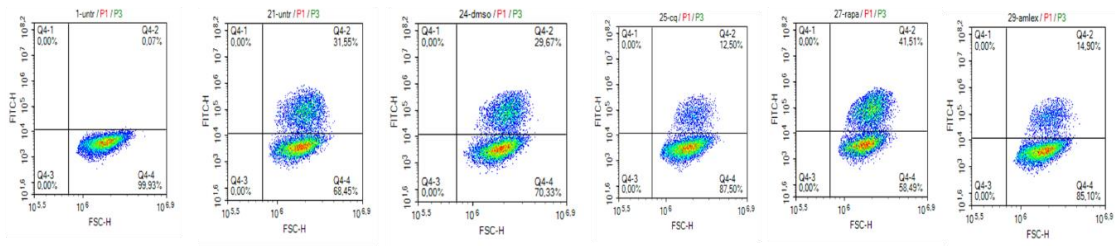
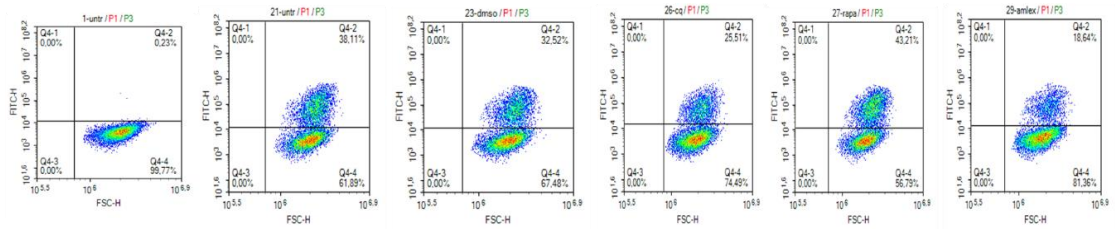


Figure 3.22 raw data

THP-1 WT 1 hour



THP-1 WT 6 hours



THP-1 WT 24 hours

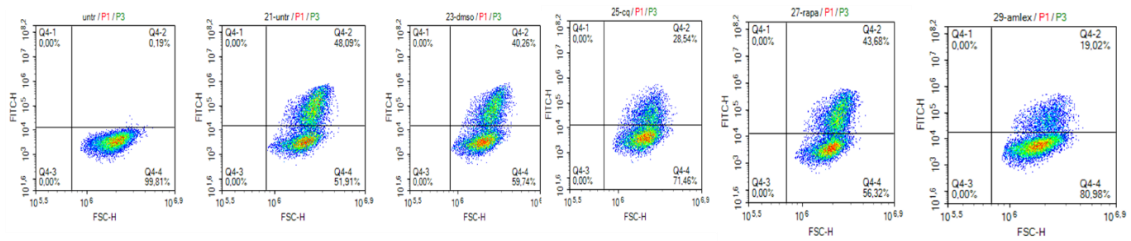
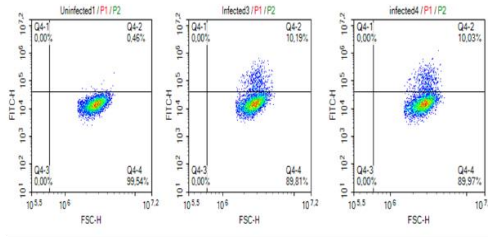
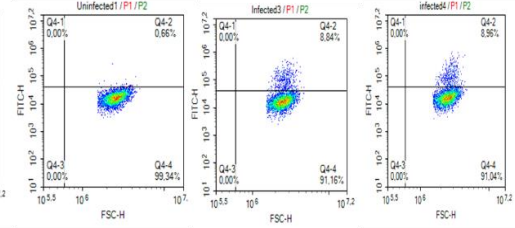


Figure 3.24 representative raw data of two biological replica

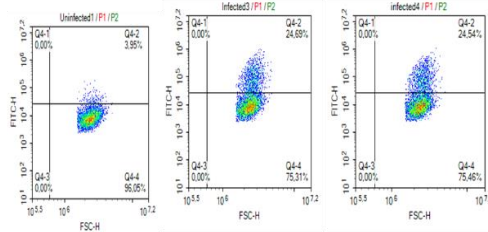
THP-1 ISG15 KO 2 hours



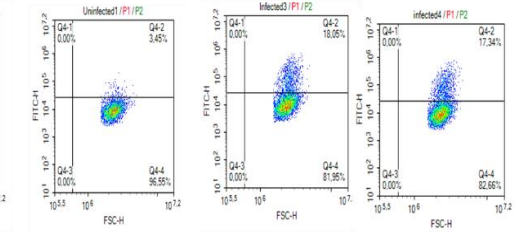
THP-1 ISG15 KO + IFN $\beta$  2 hours



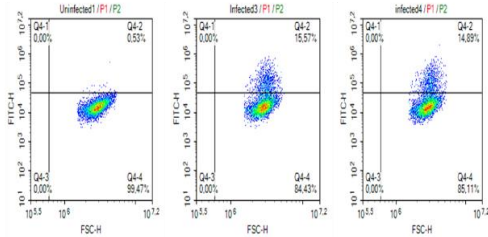
THP-1 LVC 2 hours



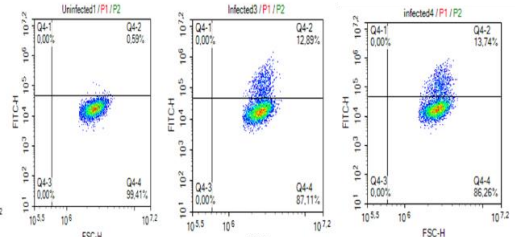
THP-1 LVC + IFN $\beta$  2 hours



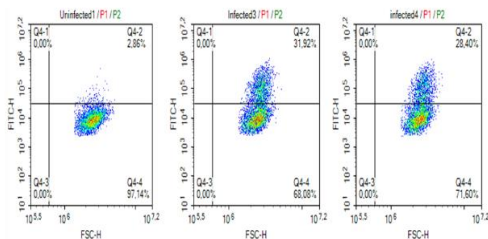
THP-1 ISG15 KO 6 hours



THP-1 ISG15 KO + IFN $\beta$  6 hours



THP-1 LVC 6 hours



THP-1 LVC + IFN $\beta$  2 hours

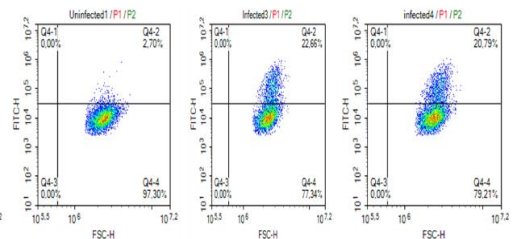
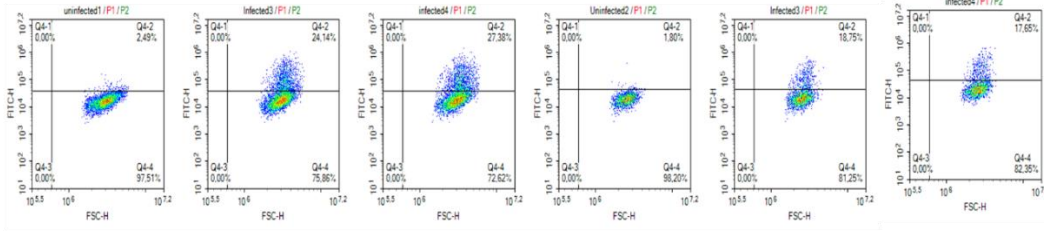


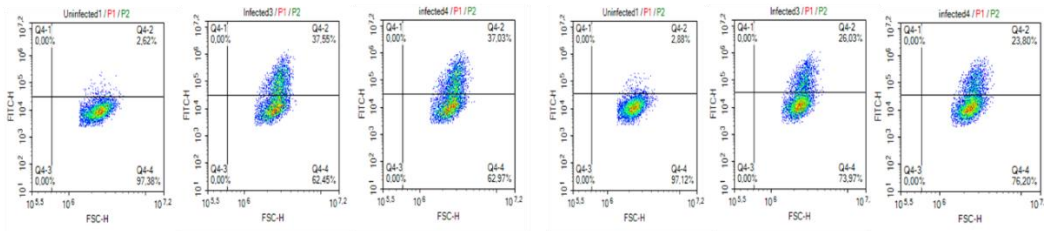
Figure 3.27 representative raw data of two biological replica

THP-1 ISG15 KO 18 hours



THP-1 ISG15 KO + IFN $\beta$  18 hours

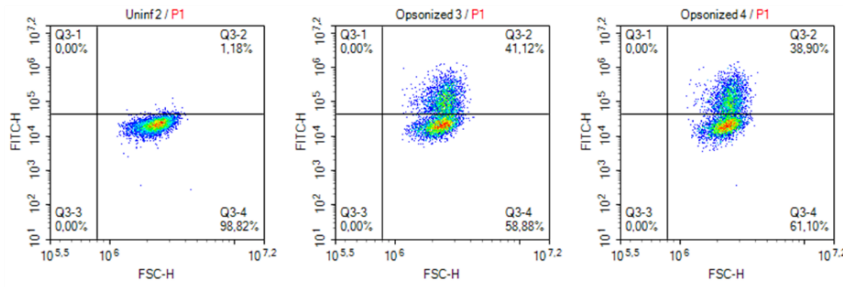
THP-1 LVC 18 hours



THP-1 LVC + IFN $\beta$  18 hours

Figure 3.27 representative raw data of two biological replica

THP-1 ISG15 KO 1 hour



THP-1 ISG15 KO + cGAMP 1 hour

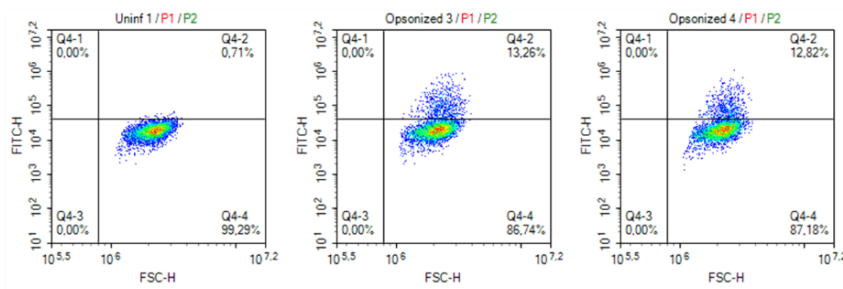
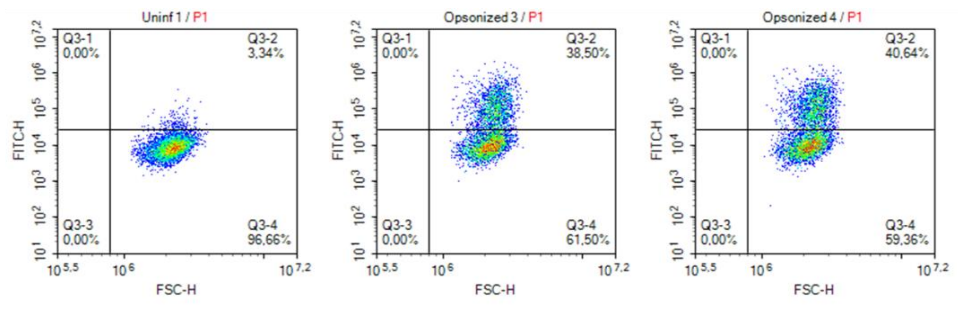


Figure 3.28 representative raw data of two biological replica

THP-1 LVC 1 hour



THP-1 LVC + cGAMP 1 hour

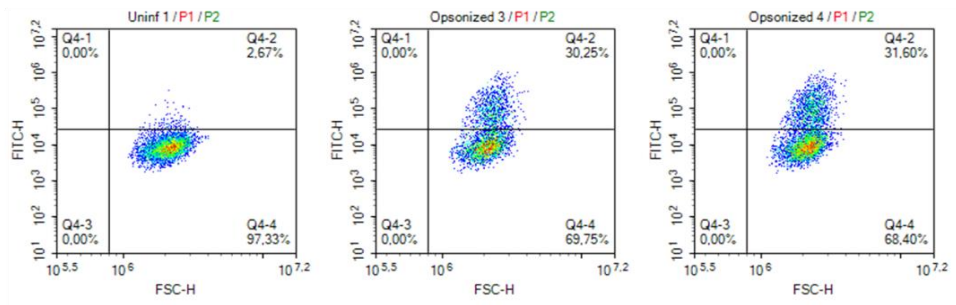


Figure 3.28 representative raw data of two biological replica



## CURRICULUM VITAE

### PERSONAL INFORMATION

Surname, Name : Yılmaz, İsmail Cem  
Nationality : Turkish (TC)  
Date and Place of Birth : 9 August 1987, Trabzon  
Phone : +90 312 210 7627  
E-mail : e147691@metu.edu.tr

### EDUCATION

<b>Degree</b>	<b>Institution</b>	<b>Year of Graduation</b>
MS	METU Biology	2014
BS	METU Molecular Biology and Genetics	2010
High School	Trabzon Kanuni Anatolian High School	2005

### WORK EXPERIENCE

<b>Year</b>	<b>Place</b>	<b>Enrollment</b>
2011-2020	METU Biology	Research Assistant

### FOREIGN LANGUAGES

Advanced English,

### PUBLICATIONS

### HOBBIES

Guitar player, vocal and composer